



Universitat Autònoma de Barcelona

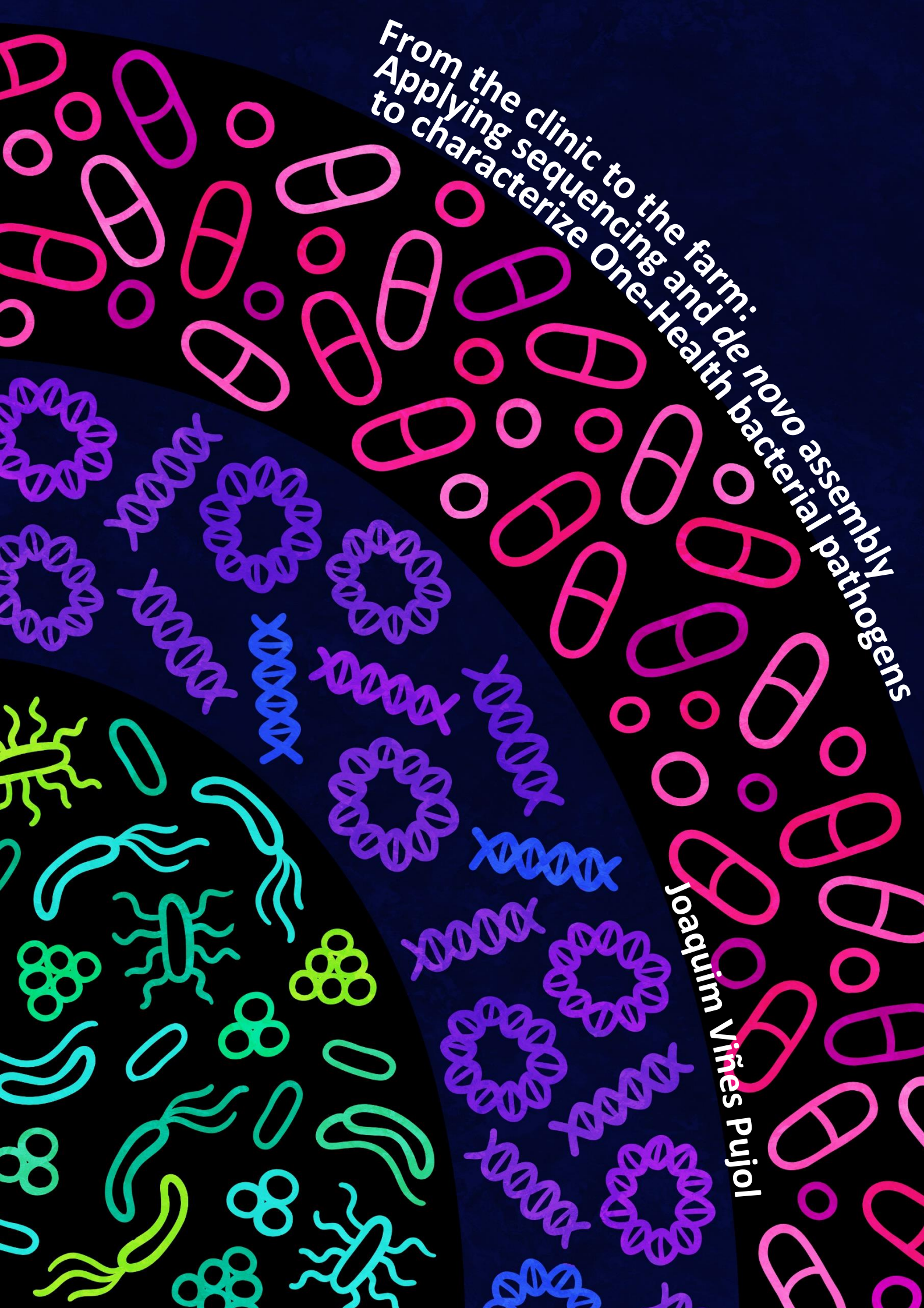
ADVERTIMENT. L'accés als continguts d'aquesta tesi queda condicionat a l'acceptació de les condicions d'ús establertes per la següent llicència Creative Commons:  http://cat.creativecommons.org/?page_id=184

ADVERTENCIA. El acceso a los contenidos de esta tesis queda condicionado a la aceptación de las condiciones de uso establecidas por la siguiente licencia Creative Commons:  <http://es.creativecommons.org/blog/licencias/>

WARNING. The access to the contents of this doctoral thesis it is limited to the acceptance of the use conditions set by the following Creative Commons license:  <https://creativecommons.org/licenses/?lang=en>

From the clinic to the farm:
Applying sequencing and de novo assembly
to characterize One-Health bacterial pathogens

Joachim Viñes Pujol



Cover illustration by Rik Schlimbach (@rikdrawsthings). Bacteria protected from antibiotics by DNA molecules.

From the clinic to the farm:
Applying sequencing and *de novo*
assembly to characterize One-Health
bacterial pathogens



Joaquim Viñes Pujol

Departament de Ciència Animal i dels Aliments

Facultat de Veterinària, Universitat Autònoma de Barcelona

A thesis submitted for the degree of Doctor (PhD)

Directors: Dr. Olga Francino Martí

Dr. Anna Maria Cuscó Martí

Tutor: Dr. Armand Sánchez Bonastre

June 2021

La **Dra. Olga Francino Martí**, investigadora del Departament de Ciència Animal i dels Aliments de la Universitat Autònoma de Barcelona, i la **Dra. Anna Maria Cuscó Martí**, investigadora de Vetgenomics SL,

Certifiquen que Joaquim Viñes Pujol ha dut a terme sota la nostra direcció el treball de recerca realitzat al Departament de Ciència Animal i dels Aliments de la Facultat de Veterinària de la Universitat Autònoma de Barcelona, que ha portat a l'elaboració d'aquesta Tesi Doctoral, titulada "From the clinic to the farm: Applying sequencing and *de novo* assembly to characterize One-Health bacterial pathogens".

Bellaterra, 3 de Juny de 2021

Dra. Olga Francino Martí

Dra. Anna Maria Cuscó Martí

Joaquim Viñes Pujol

This work was supported by a grant awarded by **Pla de Doctorats Industrial** (2017 DI 37) provided by the Agència de Gestió d'Ajuts Universitaris i de Recerca (AGAUR); Secretaria d'Universitats i Recerca del Departament d'Economia i Coneixement de la Generalitat de Catalunya

This Industrial PhD project was performed in collaboration with **Vetgenomics, SL**

Joaquim Viñes Pujol was funded by Vetgenomics, SL.



“Los árboles no dejan ver el bosque”

SUMMARY

Multi-drug resistant bacteria infections are a threat to animal and human health due to the limitation in treatment, which can lead to severe clinical complications, longer hospital stays, or even death. Multi-drug resistant bacteria can be transmitted to the environment, other animals, or humans via different ways, such as fecal contamination or food-chain. In this scenario, One-Health is an approach that considers health as a global entity, including human, animal, and the environment.

The aim of this thesis is to optimize the use of long reads in whole-genome sequencing approaches for characterizing the bacterial genome and plasmids, including the presence of antibiotic resistance genes, mobile genetic elements, and virulence factors.

By using long-read whole-genome sequencing, we *de novo* assembled complete chromosomes and plasmids as single contigs for *Staphylococcus pseudintermedius* from dogs, *Escherichia coli* from livestock and the farmer, and *Klebsiella pneumoniae* from humans. This approach located the antibiotic resistance genes in plasmids or chromosomes and spanned mobile genetic elements, thus overcoming the pitfalls associated with short reads. Moreover, we unraveled the transmission of similar plasmids harboring antibiotic resistance genes for colistin-resistant *Escherichia coli* in a mixed farm and for carbapenem-resistant *Klebsiella pneumoniae* in an inter-hospital outbreak.

The antibiotic resistance and virulence factor genes profiles of *Staphylococcus pseudintermedius* from dogs and *Escherichia coli* from livestock highlight the role of domestic animals as a reservoir of pathogens with highly zoonotic potential.

RESUM

Les infeccions causades per bacteris resistents a múltiples antibiòtics son una amenaça tant per a la salut animal com la humana degut a la limitació en el tractament, la qual pot portar a complicacions clíniques severes, estades hospitalàries més llargues o, fins i tot, a la mort. Els bacteris resistents a múltiples antibiòtics poden ser transmesos al medi ambient, a altres animals o a humans a través de diferents vies, tals com la contaminació fecal o per la cadena alimentària. En aquest escenari, l'aproximació *One-Health* considera la salut com una entitat global, incloent la humana, l'animal i la mediambiental.

L'objectiu d'aquesta tesis és optimitzar l'ús de *reads* llargs en la seqüenciació de genoma complet (*whole-genome sequencing*) per a la caracterització del cromosoma i plasmidis bacterians, incloent la presència de gens de resistència a antibiòtics, elements genètics mòbils, i factors de virulència.

Mitjançant l'ús de seqüenciació de genoma complet amb *reads* llargs hem muntat *de novo* cromosomes i plasmidis en *contigs* únics per a *Staphylococcus pseudintermedius* aïllats en gossos, *Escherichia coli* d'animals de producció i el granger, i *Klebsiella pneumoniae* d'humans. Aquesta aproximació ha permès localitzar els gens de resistència a antibiòtics en plasmidis o cromosoma, i ha permès seqüenciar elements genètics mòbils sencers, superant així els desavantatges associats al *reads* curts. A més, hem pogut descriure la transmissió de plasmidis similars que duïen gens de resistència a antibiòtics per a *Escherichia coli* resistent a colistina en una granja mixta, i per a *Klebsiella pneumoniae* resistent a carbapenems en un brot interhospitalari.

Els perfils de resistència a antibiòtics i factors de virulència d'*Staphylococcus pseudintermedius* aïllats de gossos i *Escherichia coli* d'animals de producció ressalten el rol dels animals domèstics com a un reservori de patògens amb alt potencial zoonòtic.

RESUMEN

Las infecciones causadas por bacterias resistentes a múltiples antibióticos son una amenaza tanto para la salud animal como la humana debido a la limitación en el tratamiento, la cual puede conllevar complicaciones clínicas severas, estancias hospitalarias más largas o incluso la muerte. Las bacterias resistentes a múltiples antibióticos pueden ser transmitidas al medio ambiente, otros animales o humanos mediante diferentes vías, tales como la contaminación fecal o a través de la cadena alimentaria. En este escenario, la aproximación One-Health considera la salud como una entidad global, incluyendo la humana, la animal y la medioambiental.

El objetivo de esta tesis es optimizar el uso de *reads* largos en la secuenciación de genoma completo (*whole-genome sequencing*) para la caracterización del cromosoma y plásmidos bacterianos, incluyendo la presencia de genes de resistencia a antibióticos, elementos genéticos móviles, y factores de virulencia.

Mediante el uso de secuenciación de genoma completo con *reads* largos hemos montado *de novo* cromosomas y plásmidos en *contigs* únicos para *Staphylococcus pseudintermedius* aislados de perros, *Escherichia coli* de animales de producción y el granjero, i *Klebsiella pneumoniae* de humanos. Esta aproximación ha permitido localizar los genes de resistencia a antibióticos en plásmidos o el cromosoma, y ha permitido secuenciar elementos genéticos móviles completos, superando así las desventajas asociadas a *reads* cortos. Además, hemos podido describir la transmisión de plásmidos similares que llevaban genes de resistencia a antibióticos para *Escherichia coli* resistente a colistina en una granja mixta, y para *Klebsiella pneumoniae* resistente a carbapenems en un brote interhospitalario.

Los perfiles de resistencia a antibióticos y factores de virulencia de *Staphylococcus pseudintermedius* aislados de perros y *Escherichia coli* de animales de producción resaltan el rol de los animales domésticos como reservorio de patógenos con alto potencial zoonótico.

CONTENTS

1. Introduction	1
1.1. One-Health approach and the antibiotic resistance threat.....	2
1.1.1. One-Health and zoonosis	2
1.1.2. Antibiotics mode of action and resistance.	4
1.1.3. Mobile genetic elements and antibiotic resistance transmission	8
1.2. Identification of bacteria and antibiotic resistance: whole-genome sequencing	11
1.3. <i>Staphylococcus pseudintermedius</i>	16
Ecology and antibiotic resistance	16
Virulence	25
1.4. <i>Escherichia coli</i>	26
Ecology and antibiotic resistance.....	26
Virulence.....	29
1.5. <i>Klebsiella pneumoniae</i>	32
Ecology and antibiotic resistance	32
Virulence	33
2. Objectives	35
3. Materials and methods	37
3.1. Bacterial isolates	38
3.2. Whole-genome sequencing: read pre-processing, <i>de novo</i> assembly, and polishing	39
3.3. Genomic characterization	42
3.4. Data availability	44
4. Results	45
4.1. Whole-genome sequencing and <i>de novo</i> assembly of a methicillin-resistant <i>Staphylococcus pseudintermedius</i> (MRSP) isolate	47
4.2. Whole-genome sequencing and <i>de novo</i> assembly of <i>Staphylococcus pseudintermedius</i> isolated from dogs with pyoderma and healthy dogs	51
Analyses of antibiotic resistance genes, prophages, and virulence factors .	54
Pangenome analysis of <i>Staphylococcus pseudintermedius</i> isolates	60
4.3. Transmission of similar <i>mcr-1</i> carrying plasmids among different <i>Escherichia coli</i> lineages in a mixed farm	67
Hybrid assemblies of the chromosomes and plasmids harboring antibiotic resistance genes	69
Analyses of antibiotic resistance genes	74
Analyses of virulence factor genes.....	80
4.4. Dissemination of carbapenem-resistant <i>Klebsiella pneumoniae</i> in healthcare institutions	83
Hybrid assembly of <i>Klebsiella pneumoniae</i> isolates from Hospital B.....	90
5. Discussion	93
5.1. Harnessing long-read whole-genome sequencing to characterize One-Health pathogens	93

5.2. Long-read whole-genome sequencing to unravel antimicrobial resistance and its transmission patterns	96
5.3. <i>Staphylococcus pseudintermedius</i> in dogs with pyoderma and healthy dogs	99
5.4. Future steps	101
6. Conclusions	103
7. References	105
8. Acknowledgements	131
9. Annexes	133

List of boxes

Box 1. A brief history of antibiotic discovery.....	4
Box 2. Mechanisms of DNA transmission among bacteria	9
Box 3. A brief retrospective view of sequencing technologies.	14
Box 4. Timeline of the discovery of the SIG members	18

List of Tables

Table 1. Overview of phenotypical and molecular methods used to identify bacterial isolates	12
Table 2. Overview of some studies regarding <i>S. pseudintermedius</i> isolated from human and animal clinical cases	23
Table 3 Antibiotic resistance gene profiles in European lineages ST71, ST258, and ST496; and North American lineage ST68.....	24
Table 4. <i>nuc</i> and <i>mecA</i> primers.....	39
Table 5. Software used for basecalling, demultiplexing, assembly, and polishing.....	40
Table 6. Software used for characterizing the genome and plasmid assemblies.	42
Table 7. Summary of the antibiotic resistance determined by disk diffusion testing and its correspondence to sequencing results	49
Table 8. Characteristics of the genome assemblies from the 33 <i>S. pseudintermedius</i> isolated from pyoderma	53
Table 9. Characteristics of the genome assemblies from the 22 <i>S. pseudintermedius</i> isolated from healthy dogs	54
Table 10. Antibiotic resistance genes and plasmid replicons associated to the 55 <i>S. pseudintermedius</i> (33 from disease dogs, and 22 from healthy dogs).....	55
Table 11. NCBI BLAST results of the contigs that are putative plasmids	57
Table 12. Virulence factor genes with a variable distribution between isolates	58
Table 13. Enriched functions in <i>S. pseudintermedius</i> isolated from pyoderma	63
Table 14. Enriched functions in <i>S. pseudintermedius</i> from isolates of healthy dogs.	64
Table 15. Chromosomal genome assembly and location and genomic context of <i>mcr-1</i> gene	70
Table 16. Plasmids bearing ARGs retrieved from the 18 isolates	72
Table 17. Comparison of coverage (COV) and identity (ID) of the <i>mcr-1</i> -IncX4 plasmid from the farmer versus the bovine and porcine isolates	77

Table 18. IncF-family plasmids harboring virulence factor (VF) genes and antibiotic resistance genes (ARGs)	81
Table 19. <i>K. pneumoniae</i> isolates main characteristics: MLST, antibiotic resistance genes, plasmids' incompatibility groups, and plasmids' size	84
Table 20. Whole-genome sequencing and assembly of plasmids harboring genes encoding for carbapenemases and ESBLs (genes in bold)	85
Table 21. Genome characteristics and other plasmids bearing antibiotic resistances genes rather than β -lactamases in the three isolates from Hospital B	90
Table 22. Genome CDS number retrieved by Prokka, and genome completeness from Hospital B isolates by means of BUSCO.....	92

List of Figures

Figure 1. Deaths attributable to different causes.	3
Figure 2. A generic overview of the mode of action of antibiotics	5
Figure 3. Antibiotic resistance mechanisms	7
Figure 4. Schematic review of mobile genetic elements (MGEs) and their mobilization mechanisms	8
Figure 5. Main pros and cons of Nanopore and Illumina sequencing	15
Figure 6. Scheme of the <i>mecA</i> -mediated resistance to methicillin.	19
Figure 7. Schematic representation of the basic structure of SCC <i>mec</i>	20
Figure 8. Principal virulence regulation systems in <i>Staphylococcus</i> spp	26
Figure 9. Colistin mechanism of action and resistance mediated by MCR-1.....	28
Figure 10. Scheme of some virulence mechanisms from <i>E. coli</i>	30
Figure 11. <i>K. pneumoniae</i> infection sites.....	33
Figure 12. Workflow used for the hybrid assembly and polishing of <i>E. coli</i> and <i>K. pneumoniae</i> genomes and plasmids.....	41
Figure 13. Whole-genome sequencing and <i>de novo</i> hybrid assembly of <i>S. pseudintermedius</i> isolated from canine otitis.....	47
Figure 14. <i>mecA</i> and <i>nuc</i> genes PCRs results viewed using electrophoresis.....	48
Figure 15. Representation of G3C4 <i>S. pseudintermedius</i> genome, and location of the antibiotic resistance genes retrieved by Abricate.....	50
Figure 16. Whole-genome sequencing and <i>de novo</i> assembly of 55 genomes of <i>S. pseudintermedius</i> isolated from dogs with pyoderma and healthy dogs.....	51
Figure 17. Pangenome visualization of the 22 isolates from healthy dogs.....	60
Figure 18. Pangenome visualization of the 33 isolates from dogs with pyoderma	61
Figure 19. <i>S. pseudintermedius</i> isolated from pyoderma (darker blue) presented significant larger genomes when compared with isolates from healthy dogs (turquoise)	65
Figure 20. Methodology applied to characterize the colistin-resistant <i>E. coli</i> isolated from bovine, porcine, and human fecal samples from a mixed farm	68
Figure 21. Chromosome phylogeny based on	71
Figure 22. Schematic visualization of the genetic context surrounding <i>mcr-1</i> gene	75
Figure 23. Venn diagram of the Antibiotic Resistance Genes described in the 18 colistin-resistant <i>E. coli</i> isolated from a mixed farm	76

Figure 24. <i>bla</i> _{CTX-M-15} genetic context in bovine 15A_11 isolate.....	76
Figure 25. Annotation of the IncX4 plasmid from the Farmer.....	78
Figure 26. BLAST Ring Image Generator (BRIG) visualization of the 14 IncX4 plasmids from this study and three IncX4 plasmids from NCBI	79
Figure 27. Venn diagram representing the virulence factor genes described in the 18 colistin-resistant <i>E. coli</i> isolated from a mixed farm by VirulenceFinder.....	80
Figure 28. Methodology approach to characterize the <i>K. pneumoniae</i> isolated from human clinical cases	83
Figure 29. Schematic visualization of the plasmid harboring <i>bla</i> _{NDM-1} gene in HA-3 isolate	86
Figure 30. Comparison of plasmids IncN + IncR from isolates HUB-3 and HA-3.....	87
Figure 31. Schematic visualization of the plasmid harboring <i>bla</i> _{OXA-48} gene in HA-4 isolate	88
Figure 32. Visualization of genetic context of <i>bla</i> _{NDM-1} , <i>bla</i> _{NDM-7} , and <i>bla</i> _{OXA-48}	89
Figure 33. <i>bla</i> _{CTX-M-15} was present in the genome of three carbapenem-resistant <i>K. pneumoniae</i> , HUB-1, HUB-2, and HUB-3	91
Figure 34. Clonal transmission of plasmids within a mixed farm and between hospitals ..	97

Abbreviations

ANI, Average Nucleotide Identity	MRSP, methicillin-resistant <i>Staphylococcus pseudintermedius</i>
AqP, aquaporin	MSSA, methicillin-susceptible <i>Staphylococcus aureus</i>
ARGs, antibiotic resistance genes	MSSP, methicillin-susceptible <i>Staphylococcus pseudintermedius</i>
β -LAC, β -lactams	NHE3, Na ⁺ -H ⁺ exchanger
Ccr, cassette chromosome recombinase	NMEC, neonatal meningitis-associated <i>Escherichia coli</i>
CDS, coding sequences	ONT, Oxford Nanopore Technologies
CDT, cytolethal distending toxin	<i>ori</i> , origin of replication
CHL, chloramphenicol	<i>oriT</i> , origin of transmission
CNVs, copy number variants	PABA, para-aminobenzoic acid
CRE, carbapenem-resistant Enterobacteriaceae	PBD, penicillin-binding domain
DDH, DNA-DNA Hybridization	PBPs, penicillin-binding proteins
DHF, dihydrofolic acid	PEN, penicillin
ERY, erythromycin	PFGE, pulse-field gel electrophoresis
EHEC, enterohemorrhagic <i>Escherichia coli</i>	PSMs, phenol-soluble modulins
EIEC, enteroinvasive <i>Escherichia coli</i>	SCC _{mec} , Staphylococcal chromosomal cassette
EPEC, enteropathogenic <i>Escherichia coli</i>	SEPEC, sepsis-associated <i>Escherichia coli</i>
ESKAPE, <i>Enterococcus faecium</i> , <i>Staphylococcus aureus</i> , <i>Klebsiella pneumoniae</i> , <i>Acinetobacter baumannii</i> , <i>Pseudomonas aeruginosa</i> , and <i>Enterobacter</i>	SGLT-1, Na ⁺ -glucose transporter
ETEC, enterotoxigenic <i>Escherichia coli</i>	SIG, <i>Staphylococcus intermedius</i> group
ExPEC, extra-intestinal pathogenic <i>Escherichia coli</i>	SNPs, single nucleotide polymorphisms
FQ, fluoroquinolones	Ssr, site-specific recombination
GEN, gentamicin (aminoglycoside)	STEC, Shiga toxin-producing <i>Escherichia coli</i>
HGT, horizontal gene transfer	STH, streptothricin
ICE, integrative conjugative element	STR, streptomycin
In, integron	SXT, trimethoprim-sulfamethoxazole or co-trimoxazole
Indels, insertions and deletions	T4SS, type 4 secretion system
IPEC, intestinal pathogenic <i>Escherichia coli</i>	TET, tetracycline
IS, insertion sequence	THF, tetrahydrofolic acid
KAN, kanamycin	tn, transposon
LEE, locus for enterocyte effacement	tnp, transposase
LIN, lincosamides	TOB, tobramycin
MALDI-TOF MS, Matrix-Assisted Laser Desorption/Ionization Time of Flight Mass Spectrometry	UPEC, uropathogenic <i>Escherichia coli</i>
MDR, multi-drug resistant	VFs, virulence factors
MGEs, mobile genetic elements	WGS, Whole-Genome Sequencing
ML(ST), multilocus (sequence type)	
MRSA, methicillin-resistant <i>Staphylococcus aureus</i>	

1. INTRODUCTION

In this section, we introduce the well-known threat of antibiotic resistance on bacteria and its transmission. We cover key concepts such as One-Health and zoonosis.

We provide an overview of the main identification techniques for multi-drug resistant bacteria. Specifically, we focus on whole-genome sequencing using Illumina and Nanopore platforms.

Finally, we focus on the three specific pathogens characterized in this Ph.D. thesis: *Staphylococcus pseudintermedius*, *Escherichia coli*, and *Klebsiella pneumoniae*. We describe their ecology, antibiotic resistance genes, and virulence factors.

1.1. One-Health approach and the antibiotic resistance threat

1.1.1. One-Health and zoonosis

One-Health is an approach that considers health as a global entity, including human, animal, and the environment. According to the Center for Disease Control and Prevention (CDC) One-Health is “*a collaborative, multisectoral, and transdisciplinary approach – working at the local, regional, national, and global levels – with the goal of achieving optimal health outcomes recognizing the interconnection between people, animals, plants, and their shared environment*” (fragment extracted from (CDC, 2018)).

Many infectious diseases are caused by pathogens transmitted from animals to humans, a process known as zoonosis. About 60% of the pathogens affecting humans have a zoonotic origin (Bueno-Marí et al., 2015). Some of these zoonotic pathogens include microorganisms like the Ebola virus, *Yersinia pestis*, or the human immunodeficiency virus. The main reason for zoonosis is the anthropological alteration of the ecology of the host, the pathogen, or both, including livestock farming, biodiversity depletion, human travel, or interaction with wildlife, among others (Daszak, 2000; Cunningham et al., 2017; Gibb et al., 2020). Because of their social, political, and economic impacts (Evans and Leighton, 2014), it is necessary to adopt a One-Health approach to prevent them.

Zoonotic bacteria can present resistance to the antibiotics licensed for human and veterinary medicine. Through the 20th century, the intensification of livestock production was accompanied by higher use of antibiotics as a prophylactic, to enhance growth rates, improve feeding efficiency, and decrease waste production (Karesh et al., 2012; Evans and Leighton, 2014). The indiscriminate use of antibiotics exerts selective pressure, allowing resistant bacteria to survive over susceptible bacteria, which can then be transmitted to the environment, other animals, or humans via different ways, such as fecal contamination or the food chain.

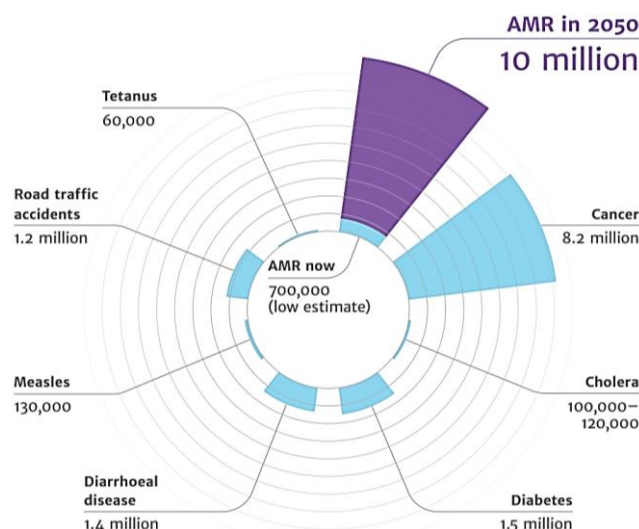


Figure 1. Deaths attributable to different causes. By 2050, deaths attributable to infections caused by antibiotic-resistant pathogens will surpass the deaths attributable to cancer. Figure excerpted from (O’Neil, 2016).

If we continue with this trend of antibiotic use, by the year 2050 deaths attributable to infections caused by resistant pathogens will surpass the deaths caused by cancer and traffic road accidents together (**Figure 1**) (<https://amr-review.org/>). What’s more, someone could die every three seconds due to this kind of infection (O’Neil, 2016).

Among all the antibiotic-resistant bacteria, the ESKAPE group –*Enterococcus faecium*, *Staphylococcus aureus*, *Klebsiella pneumoniae*, *Acinetobacter baumannii*, *Pseudomonas aeruginosa*, and *Enterobacter*– present a wide range of antibiotic resistance and can “escape” the effect of the antimicrobial agents. ESKAPE includes the most commonly identified bacterial pathogens among life-threatening nosocomial infections –also known as healthcare-associated infection (HAI)–, which are those infections acquired during the stay at the healthcare settings that were not present pre-admission (Sikora and Zahra, 2021). Infections by ESKAPE pathogens cause an estimated amount of 29,000 deaths in the United States, costing approximately 4.7 billion \$, and 33,000 deaths in Europe costing 1.5 billion \$ (Santajit and Indrawattana, 2016; Mulani et al., 2019; De Oliveira et al., 2020). As a specific example, infections caused by methicillin-resistant *Staphylococcus aureus* (MRSA) compared to methicillin-susceptible (MSSA) one present a much higher mortality rate (24% MRSA *vs.* 11.4% MSSA), are more expensive to treat (35,000\$ to treat MRSA infection *vs.* 16,000\$ to treat MSSA infection) and have fewer treatment options (Filice et al., 2010).

Thus, researchers’ main objective is to find alternatives to avoid the current dependence on antibiotics. Some of the options include limiting the use of antibiotics as a last resort, using

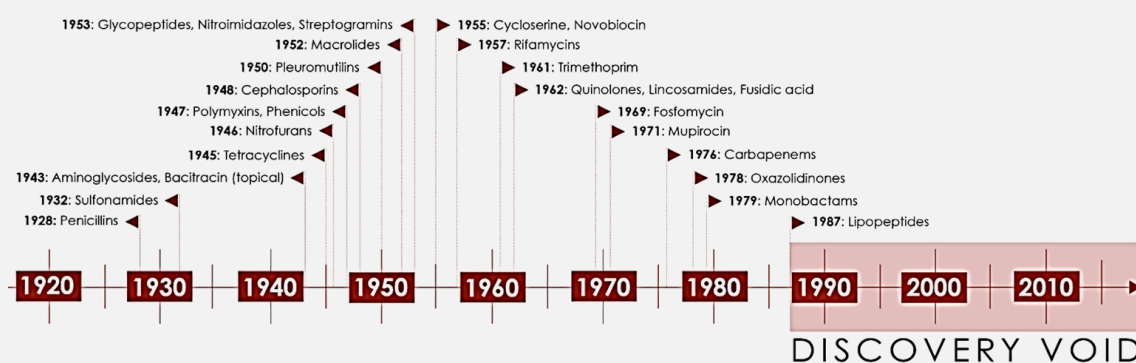
bacteriophages or antimicrobial peptides as a therapy, developing vaccines, and complementing livestock diet with probiotics rather than antibiotics to promote growth (Karesh et al., 2012; O’Neil, 2016; World Health Organization, 2019).

1.1.2. Antibiotics mode of action and resistance

Antibiotics are natural or synthetic compounds used to treat bacterial infections. They present a bacteriostatic effect by stopping bacterial growth or a bactericidal one, by causing bacterial death (Pankey and Sabath, 2004). Since the discovery of penicillin (**Box 1**), other classes of antibiotics have been discovered over the years, such as sulfonamides, tetracyclines, macrolides, trimethoprim, or quinolones.

Box 1. A brief history of antibiotic discovery. During the 40s and the beginning of the 60s, there was a boom in antibiotics discovery (golden age). However, since the 90s, there has been a lack of discovery of new antibacterial molecules (discovery void). Figure excerpted and modified from <https://www.reactgroup.org/wp-content/uploads/2016/09/ab-discovery-timeline.png>

Alexander Fleming, a British physician and microbiologist, discovered penicillin, a β -lactam antibiotic. Fleming described that some *Staphylococcus* colonies’ growth was inhibited after exposure to air contamination. This phenomenon was due to the presence of colonies of a contaminating mold (*Penicillium*), which released an inhibitory compound for the bacteria, penicillin (Fleming, 1929).



However, the idea of antibiosis was present before Fleming’s discovery. After analyzing bones discovered in Nubia (an ancient region between the south of Egypt and north of Sudan, 1,600 years ago), scientists realized that the osteons possessed alternating layers with and without tetracycline, a broad-spectrum antibiotic that started to be used in medicine about the 1950s. Tetracycline is a compound that binds to calcium and phosphorus. The mystery comes when, as mentioned before, tetracycline was first used in medicine not long ago, so which was the source? They concluded that the antibiotic ended accumulating in the bones after people drinking fermented brew that contained *Streptomyces* spores, a known group of bacteria that produces tetracycline (Bassett et al., 1980; Hummert and Van Gerven, 1982). Thus, although antibiotics were discovered and used consciously during the 20th century, they were already being used years ago without knowing it.

In general, antibiotics act at different levels (**Figure 2**):

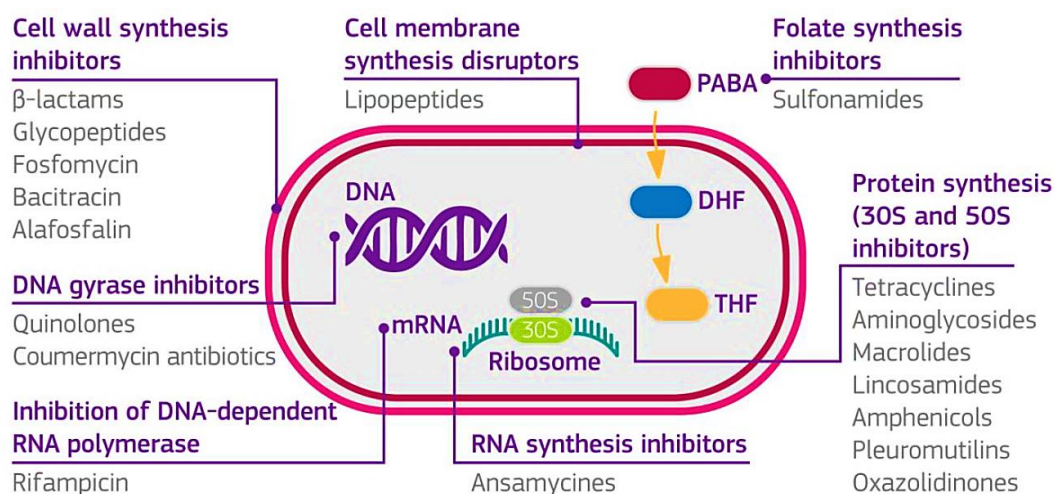


Figure 2. A generic overview of the mode of action of antibiotics. Antibiotics can act at different points, causing bacteriostatic or bactericidal effects. The actions include cell wall synthesis inhibition, DNA gyrase and DNA-dependent RNA polymerase inhibition, RNA, protein and folate inhibition, or cell membrane disruption. PABA, para-aminobenzoic acid; DHF, dihydrofolic acid; THF, tetrahydrofolic acid. Figure excerpted from (Sanseverino et al., 2018).

Inhibiting cell wall synthesis. β -lactam antibiotics –such as penicillin, cephalosporines, or carbapenems– bind to penicillin-binding proteins (PBPs), the transpeptidases involved in the cell wall biosynthesis of peptidoglycan, inhibiting the enzyme function. The imperfections in the cell wall lead to the cell death (Codjoe and Donkor, 2017).

Inhibiting DNA gyrase. Once fluoroquinolones are internalized, they inhibit type II DNA topoisomerases such as gyrase GyrA, which play a role in DNA replication by creating strand breaks and resolving them. Fluoroquinolones bind to the topoisomerase-DNA complex and prevent the strands from resealing, causing cell death (Zhanel et al., 2002).

Inhibiting DNA-dependent RNA polymerase. Rifampicin interacts with the DNA-dependent RNA polymerase –an enzyme that transcribes DNA to mRNA– causing its inactivation and stopping cellular growth (Wehrli, 1983).

Inhibiting protein synthesis by interacting with the small (30S) and large (50S) ribosome subunits. Aminoglycosides interact with the A-site of the 30S subunit, causing misreading of the codons and incorrect protein production (Krause et al., 2016).

Tetracyclines impede the aminoacyl-tRNA-ribosome connection, preventing protein production (Chopra and Roberts, 2001).

Inhibiting folate synthesis. Trimethoprim acts as a competitive inhibitor of the dihydrofolate reductase, which catalyzes the reduction of dihydrofolate to tetrahydrofolate, thus inhibiting thymine and DNA synthesis (Gleckman et al., 1981).

Disrupting cell membrane. Colistin is a polycationic peptide composed of a hydrophilic positive end and a fatty-acid hydrophobic non-polar end. The positive part of the antibiotic can replace the divalent cations present in the outer membrane. Then, the cationic part and the non-polar end interact with the negative charges and lipids, causing the destabilization of the membrane, increasing permeability, and provoking cell death (Loho and Dharmayanti, 2015; Xu et al., 2018a).

We use antibiotics to treat bacterial infections, but bacteria can defend themselves against these compounds, limiting the treatment efficacies. The antimicrobial resistance can be caused by **point mutations** in essential genes involved in cellular processes, such as mutations in the *gyrA* gene, causing resistance to fluoroquinolones; or by **acquired resistance genes**. Overall, the resistance mechanisms can be classified into different groups (van Hoek et al., 2011; C Reygaert, 2018; Sanseverino et al., 2018; Yelin and Kishony, 2018; CDC, 2020) (**Figure 3**):

- Resistance due to changes in the antibiotic's target
- Resistance due to enhanced cell permeability
- Resistance due to alteration of the antibiotic (modification or degradation)
- Resistance due to efflux pumps getting rid of internalized antibiotics
- Resistance due to bypass via metabolic shunts (new enzymes that can perform the same action as the antibiotic's target)
- Resistance due to overproduction of the target

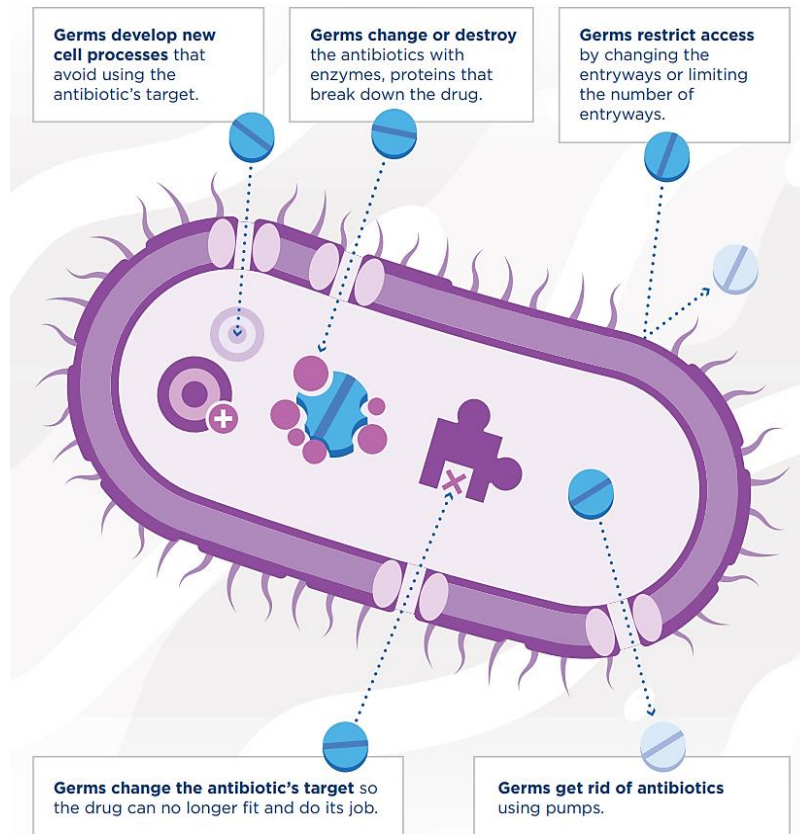


Figure 3. Antibiotic resistance mechanisms. Bacteria present different mechanisms to defend themselves in front of the action of antibiotics. These defenses encompass (1) using pumps to get rid of antibiotics, (2) changing the antibiotic's target, (3) restricting access, (4) breaking down, and (5) creating new cellular processes to avoid the use of the antibiotic's targets. Figure available at <https://www.cdc.gov/drugresistance/about/how-resistance-happens.html>

1.1.3. Mobile genetic elements and antibiotic resistance transmission

Antibiotic resistance genes (ARGs) are not only threatening for the defense against antibiotics they provide, but also for their capability of transmission among bacteria, even between different species. Acquired resistance genes can be transmitted vertically (from parent cell to its progeny) or by horizontal gene transfer (HGT), implying the presence of mobile genetic elements (MGEs) (**Figure 4**). For example, methicillin-resistance caused by *mecA* was transferred from coagulase-negative staphylococci to *S. aureus*, and then to *S. pseudintermedius* (Jamale, 2011; Xu et al., 2018b).

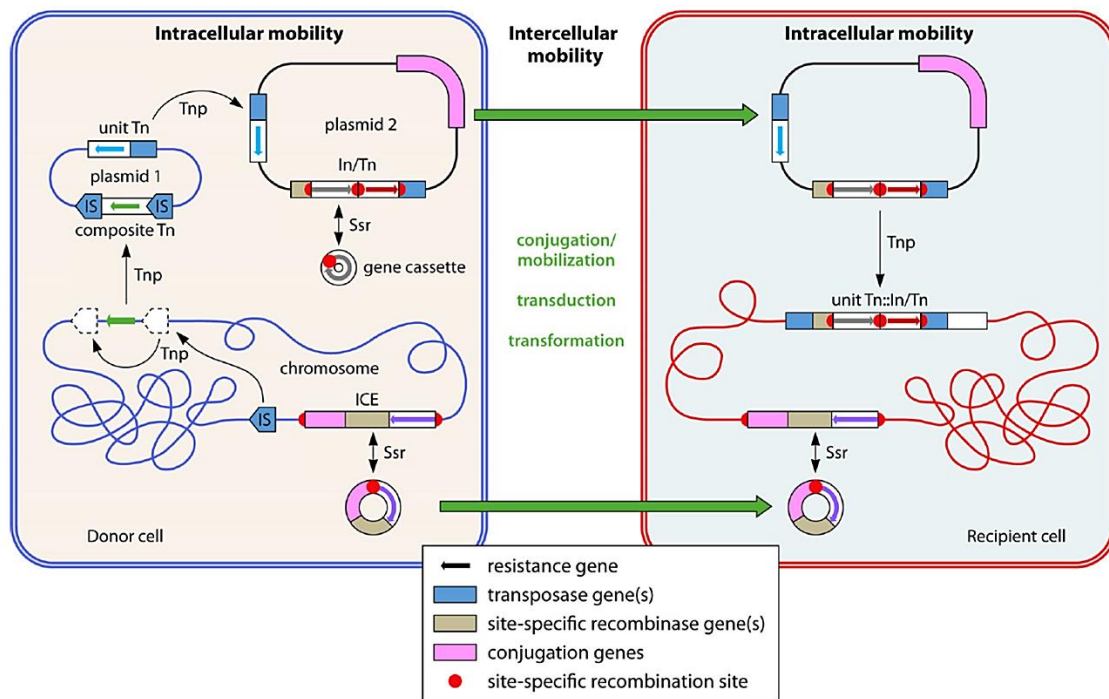


Figure 4. Schematic review of mobile genetic elements (MGEs) and their mobilization mechanisms. MGEs can jump and move among bigger DNA molecules, and typically, MGE acquisition supposes the gain of advantageous traits, such as antibiotic resistance. ICE, integrative conjugative element; In, integron; IS, insertion sequence; Ssr, site-specific recombination; tn, transposon; tnp, transposase. Figure excerpted from (Partridge et al., 2018).

MGEs are DNA structures that promote intra- and intercellular DNA mobilization through transformation, conjugation, or transduction (**Box 2**). These DNA structures code the necessary machinery to perform its mobilization, such as transposases or type 4 secretion system (T4SS), and can harbor other extra features such as antibiotic resistances or virulence

factors (Frost et al., 2005; Partridge et al., 2018). These elements may represent a relatively significant portion of the bacterial genome. For example, in *S. aureus*, MGEs can represent approximately 15% of the genome (Alibayov et al., 2014), and in *Staphylococcus pseudintermedius*, 8% of the genome (McCarthy et al., 2014).

Box 2. Mechanisms of DNA transmission among bacteria.

Among bacteria, there are different mechanisms to get new DNA via horizontal transfer: transformation, transduction, and conjugation.

Transformation occurs when competent bacteria –cells that can retrieve DNA from the environment– internalize and add foreign DNA by different cellular processes such as homologous recombination into the host chromosome; or in the case that a MGE is internalized, it can be autonomous (e.g., plasmid), or transpose to a bigger DNA molecule (e.g., transposon, insertion sequences).

Transduction is based on the principle that bacteriophages must pack their DNA to infect other cells. In the packaging process, the capsid may pack DNA from the host (bacterial DNA in this case), then this phage infects another cell, mobilizing DNA from the donor cell to the receptor.

Conjugation is performed by cells that harbor DNA molecules (such as conjugative plasmids or integrative conjugative elements) that present the genes for the conjugative machinery and an origin of transmission (*oriT*). In this process, the donor cell creates a syringe-like structure, which contacts the receptor cell and inoculates the mobilizable element.

Finally, in **vesiduction** specialized vesicles disseminate DNA among bacteria in biofilms (van Hoek et al., 2011; Rodríguez-Beltrán et al., 2021).

Some examples of MGEs are insertion sequences (IS), transposons (Tn), integrative conjugative elements (ICEs), integrons (In), cassettes, plasmids, as well as bacteriophages:

Insertion sequences (IS) are the simplest MGEs that contain a gene coding for a transposase –the enzyme responsible for their mobilization– flanked by inverted repeats. In some cases, accessory genes (like antibiotic resistance genes) can be flanked by two copies of an insertion sequence, a structure known as a **transposon (Tn)**. Sometimes, upstream insertion sequences provide a strong promoter region that controls the expression of the accessory gene present in the transposon.

The **integrative conjugative elements (ICE)**, or **conjugative transposons**, harbor an *oriT* (origin of transmission) and the genes to code the conjugation machinery. However, as ICEs do not present an origin of replication (*ori*), its multiplication and maintenance rely on

integrating into a replicative molecule, like the bacterial chromosome (van Hoek et al., 2011; Partridge et al., 2018).

Integrans (In) are MGEs that code for the integrase enzyme and provide a promoter region for other genes. Moreover, integrans present a site (*attI*) in which other elements can integrate by site-specific recombination mediated by the integrase enzyme.

Cassettes can exist in a free form that do not possess the capacity of autonomous replication; cassettes are usually found inserted in the integrans. They possess a sequence that allows their integration by specific recombination, and usually carry an antibiotic resistance gene that lacks the promoter region (Bennett, 1999).

Plasmids are usually closed DNA structures (supercoiled circular DNA) that coexist as an extra-chromosomal element inside the bacterial cell. The conjugative plasmids present at least the *ori* for replication and the *oriT* for transmission, plus the conjugation machinery genes (e.g., type 4 secretion system, T4SS), and other traits. The mobilizable plasmids are plasmids that present the *oriT* but do not harbor the T4SS. So, it could mobilize only if the cell containing this kind of plasmid also harbors a conjugative element.

Since the presence of plasmids usually supposes a fitness cost to the bacteria, plasmids present functions that help in their maintenance and confer an advantage to the cell, such as antibiotic resistance or virulence (Partridge et al., 2018). For example, plasmids can code for toxin-antitoxin systems, which consist of producing the toxin (long life) and the antitoxin (short life). If the plasmid is eliminated from the cell, the antitoxin will no longer inhibit the long-life toxin, which will ultimately kill the cell (van Hoek et al., 2011; Partridge et al., 2018; Rodríguez-Beltrán et al., 2021).

Bacteriophages are viruses that infect bacteria. Lytic (or virulent) phages lyse the cell after generating new viral particles using the host's machinery. Lisogenic (or temperate) phages insert their genetic material inside the cell and, with the help of self-encoded integrases, they integrate their genome into the host's DNA. When the virus is integrated in the genome it is known as a prophage. Moreover, when the prophage splits from the genome, it can take host's genetic material, encapsulate it in the viral particle, and spread it to other bacteria (process known as transduction, **Box 2**) (Frost et al., 2005; Brooks et al., 2020).

1.2. Identification of bacteria and antibiotic resistance: whole-genome sequencing

The identification of microorganism at diagnostic laboratory level is usually performed by phenotypic assays like bacterial cultures. Bacterial cultures have been largely used to grow microorganisms from different sources. The culture medium, whether liquid or solid, has the necessary elements for the bacteria to grow. Selective media contain extra elements, such as antibiotics, specific salts, or other substances, to further differentiate specific microbes.

These identification methods can sometimes be complemented by molecular genetic techniques for an increased resolution (**Table 1**). The most commonly used molecular typing techniques are multilocus sequence type (MLST) and 16S rRNA gene sequencing. MLST typing assesses the specific allelic profiles of seven loci of housekeeping genes, while 16S rRNA gene sequencing provides taxonomic information through its nine hypervariable regions. These approaches have been widely used to infer taxonomy and classify microorganisms; however, they may lack discriminative power regarding complex studies such as outbreaks and food-chain contamination infections (Uelze et al., 2020).

Thus, we need high-resolution methods to unravel the close phylogenetic relations in, for example, complex outbreaks. One of the most powerful techniques for identifying and characterizing bacteria (including antibiotic resistance and other traits such as virulence) is whole-genome sequencing.

Table 1. Overview of phenotypical and molecular methods used to identify bacterial isolates. ANI, Average Nucleotide Identity; DDH, DNA-DNA Hybridization; MALDI-TOF MS, Matrix-Assisted Laser Desorption/Ionization Time of Flight Mass Spectrometry; WGS, Whole-Genome Sequencing.

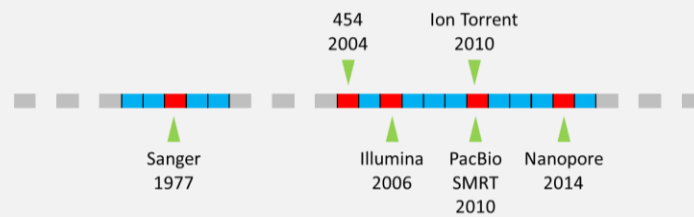
Technique	Description	References
Bacterial cultures	The use of culture media to grow bacteria has been largely used since their development in the 19 th century. Solid cultures contain agar, nutrients, growth factors, and can contain selective and differential components such as antibiotics, salts, or dyes.	(Bonnet et al., 2020)
Mannitol-salt agar	A selective and differential medium. NaCl inhibits the growth of most bacteria. Moreover, it contains mannitol and a pH indicator (phenol red). <i>S. aureus</i> tolerates high NaCl concentration and ferments mannitol, resulting in the growth of yellow colonies, while non-fermenting <i>Staphylococcus</i> produce red colonies.	(Horstmann et al., 2012; Lainhart et al., 2018)
MacConkey agar	A selective and differential medium. Crystal violet and bile salts are used to inhibit gram-positive bacteria. Moreover, it contains lactose and neutral red as a pH indicator. <i>E. coli</i> and <i>Klebsiella</i> ferment lactose strongly and weakly, respectively, and the colonies turn pink.	(MacConkey, 1905; UC, 2021)
Kirby-Bauer test	Once you have grown a microorganism throughout all the plate's surface, different circular disks soaked in specific antibiotic concentrations are placed on the culture. The zones of inhibition appear based on the diffusion of the antibiotic and the resistance of the microorganisms. Depending on the size of these zones, the bacteria is classified as resistant, susceptible, or intermediate according to CLSI rules.	(Patel et al., 2021)
DDH	DNA-DNA hybridization was the gold standard methodology for prokaryote taxonomy, which is based on the hybridization of the entire genomes from different organisms to calculate their genomic similitude. The generally accepted similarity value for establishing different species is 70%.	(Rosselló-Móra et al., 2011; Arahal, 2014; Chun et al., 2018)
16S rRNA gene sequencing	<i>16S rRNA</i> gene (~1,500 bp) encodes for the RNA from the small subunit of bacterial and archaeal ribosomes. It is widely used in taxonomic studies because it presents nine hypervariable regions and other conserved regions. The conserved regions allow the creation of primers that amplify the hypervariable regions and have taxonomic power. Its main pitfall is that it lacks phylogenetic power at lower levels (species level and some genera), even though there have been attempts to try to define thresholds (>98.7% for species and >95% for genera).	(Chakravorty et al., 2007; Janda and Abbott, 2007; Yarza et al., 2014; Jain et al., 2018)
ANI	Average nucleotide identity (ANI) has demonstrated the potential to replace DDH as the gold standard: it is easier to estimate, portable, low cost, and reproducible. This technique is more robust and decisive when compared with <i>16S rRNA</i> gene sequencing as it considers all the common genes among the studied genomes, not only one.	(Arahal, 2014; Chun et al., 2018; Jain et al., 2018)
Whole-genome sequencing (WGS)	Sequencing techniques are becoming more available and affordable. Once you have sequenced a genome, you can obtain the DNA sequences of the most used marker genes mentioned before; you can perform ANI calculations with other genomes; find single nucleotide polymorphisms (SNPs) to calculate phylogeny, among others.	(Quainoo et al., 2017; Perreten et al., 2020)
MALDI-TOF MS	The sample is mixed with an organic compound (the matrix) which after crystalizing liberates protonated ions from the sample when a laser impacts. These ions travel inside the light tube based on their mass-to-charge ratio and are finally detected using mass analyzers. This is a fast and accurate methodology that has already been applied in microbial detection in clinical microbiology.	(Singhal et al., 2015; Schubert and Kostrzewa, 2017)

WGS uses DNA sequencing reads to assemble the genome of the organism of interest and further characterize it. It began to be applied broadly with the advent of massive DNA sequencing techniques and the continuous appearance of new technologies and affordable platforms (**Box 3**). When compared to phenotypic methods and classical molecular genetics approaches like 16S rRNA sequencing, WGS offers higher resolution.

WGS allows phylogenomics, pangenomics, and characterization of specific genes of interest. Phylogenomics analysis can be used to assess the transmission of pathogens through time and space in different environments, such as clinical outbreaks or food-chain contamination (Krawczyk and Kur, 2018; Yin et al., 2018; Uelze et al., 2020). Pangenomics studies the collection of genes within a group of organisms (the pangenome) that encompasses the core genome –the genes shared by all the organisms– and the accessory, variable, or dispensable genome –the genes absent in at least one of the organisms–. Reference genomes can lack information from the accessory genome, thus using pangenomes as reference can give a wider look within the genomic content of a species (Golicz et al., 2020). Finally, the characterization of genes of interest includes describing point mutations (single nucleotide polymorphisms, SNPs), insertions and deletions (indels), structural variations, or copy number variants (CNVs), among other modifications. Moreover, especially long-read WGS can characterize easily the genetic context and location of the genes of interest –such as antimicrobial resistance genes or virulence factors–, including the presence of regulatory genetic elements that control their expression (e.g. promotor regions, enhancers, or silencers) or the presence of MGEs that can participate in their mobilization (Krawczyk and Kur, 2018; Yin et al., 2018; Uelze et al., 2020).

The application of WGS in clinical outbreaks and foodborne illnesses provides a rapid approach for resolving these situations. The analysis of clinical, environmental, and food samples is crucial to reduce the impact of these infections on human and animal health, as well as on the economy, since, for example, foodborne infections can lead to the elimination of good part of the affected product (Pightling et al., 2018). However, one of the main pitfalls is that WGS relies on the bacterium's growth in cultures, which adds a handicap in time (Schürch et al., 2018).

Box 3. A brief retrospective view of sequencing technologies. Timeline of the emergence of sequencing technologies: Sanger sequencing, massive parallel sequencing (454, Illumina, Ion Torrent), and single-molecule sequencing (PacBio, Nanopore). Figure adapted from (Mardis, 2017).



In 1977, Frederick Sanger and his colleagues developed one of the first DNA sequencing technologies based on dideoxynucleotides, radiation, or fluorescence-labeled nucleotides that, once incorporated by the polymerase, avoid further elongation. Even though Sanger sequencing is highly precise, read length is below 1,000 bp, and expensive (Sanger et al., 1977; Minakshi et al., 2014; Heather and Chain, 2016).

Massive parallel sequencers (also known as second-generation sequencers or next-generation sequencing) such as Roche 454, Thermo Fisher’s Ion Torrent, or Illumina, are based on the parallelization of a high number of sequencing reactions. Each sequencer is based on specific chemistry, such as pyrosequencing for 454 or pH variation for Ion Torrent. In the case of Illumina, sequencing is performed on a solid surface that is covered with oligonucleotides complementary to the adapter sequence. The subsequent PCR process is performed using a mix of the four types of nucleotides labeled with a different fluorophore. Once a labeled nucleotide is incorporated, the elongation is blocked. However, unlike Sanger sequencing, this blockage is reversible once the fluorophore is excised (Minakshi et al., 2014; Goodwin et al., 2016; Heather and Chain, 2016; Mardis, 2017).

Finally, single-molecule sequencers (also known as third-generation sequencers), such as those from Pacific Biosciences (PacBio) or Oxford Nanopore Technologies (ONT), are based on the sequencing of unique molecules of DNA without the need for prior PCR. PacBio is based on the use of individual wells with transparent bottoms in which a polymerase is fixed. Once the polymerase adds a fluorophore-labeled nucleotide, a laser hits the nucleotide and excites the fluorophore, which light is captured by a sensor. The polymerase can excise the fluorophore and continue elongating. On the other hand, Nanopore sequencing relies on the use of proteins (nanopores) embedded in a synthetic membrane. An ionic current is generated through the pores. Once a DNA molecule passes through the pore, the ionic current is altered, and depending on which nucleotide is passing and its biochemical structure, a different signal (squiggle) is generated (Minakshi et al., 2014; Oxford Nanopore Technologies, 2014; Laver et al., 2015; Goodwin et al., 2016; Heather and Chain, 2016; Mardis, 2017).

Specifically in this PhD thesis, we have assessed the use of long-read sequencing (Nanopore) in WGS. In some studies, we have combined it with short-read sequencing (Illumina). Illumina produces massive quantities of short reads (less than 750 bp) using a clonal PCR producing much more information than Sanger sequencing (more information in **Box 3**). Massive sequencing possesses a high accuracy, and the price per base pair is cheaper (Minakshi et al., 2014; Goodwin et al., 2016; Heather and Chain, 2016; Mardis, 2017). Nanopore sequencing produces long-reads –length limited by experimental procedures– and overcomes the need for clonal PCR amplification avoiding the associated PCR bias. Another

advantage when compared to any previous DNA sequencers is that it can provide results in real-time. The first Nanopore sequencing platform (launched in 2014) was the MinION. This device supposes a cost-efficient alternative compared to other DNA sequencers since it is portable (smartphone-sized), affordable (both the device and its consumables) and user-friendly (Quainoo et al., 2017). The main pitfall of Nanopore sequencing has been its lower accuracy with error-prone reads on homopolymeric regions (Goodwin et al., 2016) (**Figure 5**). However, continuous developments in sequencing pores, chemistries and bioinformatics analyses are improving accuracy to the desired level.

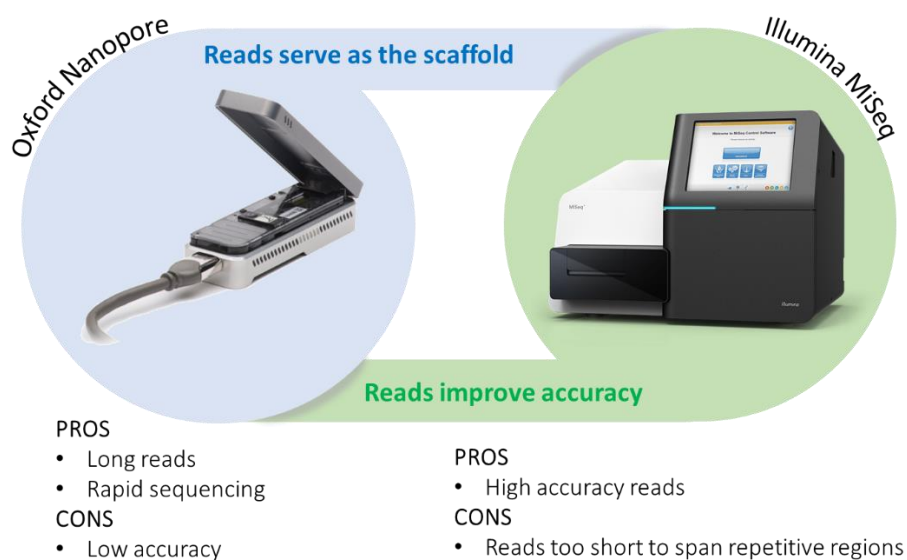


Figure 5. Main pros and cons of Nanopore and Illumina sequencing. Illumina offers short but highly accurate reads. However, the reads' size does not span repetitive regions. On the other hand, Nanopore's long reads can cover the repetitive regions, facilitating the assembly of complicated genetic regions. The main pitfall of Nanopore sequencing is its accuracy.

Thus, Illumina and Nanopore present their pros and cons, mainly regarding read length and accuracy (**Figure 5**). On one hand, Illumina's short reads do not allow spanning repetitive regions, which makes it challenging to perform *de novo* genome assembly. These repetitive regions include MGEs such as transposons and insertion sequences, which play an essential role in mobilization of antibiotic resistance genes and virulence factors genes. On the other hand, Nanopore's long reads can cover repetitive regions and provide genomic context allowing to close circular chromosomes, plasmids, or bacteriophages when performing WGS.

Nanopore sequencing is a rapidly evolving technology and this is reflected in the continuous improvements in raw read accuracy (the current guppy version, v5.0.7, presents an accuracy of 95.8% in its fast model, 97.8% in its high accuracy model, and 98.3% in its super-accurate model, for R9.4.1 chemistry Flow Cells (Oxford Nanopore Technologies, 2021)). These improvements are at the technological level through the development of better pores and sequencing chemistries and at the bioinformatic analysis level through new basecallers and polishing software. Basecallers are the software that convert the squiggles (electric signals) to nucleotide sequences, such as Albacore (2017-2019, discontinued), Guppy (Oxford Nanopore Technologies, 2020), or the newest Bonito (NanoporeTech, 2021). Polishing software corrects error-prone reads by overlapping them to get a consensus sequence, and the most commonly used are Racon (Vaser et al., 2017) and Medaka (Oxford Nanopore Technologies, 2018).

A hybrid sequencing approach combines the strengths from both error-prone long reads and high-accuracy short reads sequencing to assemble complete and high-quality bacterial genomes with software like Unicycler (Wick et al., 2017), which performs the hybrid assembling of the bacterial chromosome and plasmids and the polishing steps. The main idea is to sequence the same sample with both technologies and first perform *de novo* assembly with Nanopore sequencing data to generate complete and closed chromosomes and plasmids, and then polish the error-prone long-read assemblies using accurate Illumina data. The final assembly possesses both technologies' advantages: it spans repetitive regions and structural variations thanks to Nanopore long reads and presents high accuracy thanks to Illumina short reads. This hybrid sequencing strategy is considered a gold standard nowadays for bacterial genomes assembly, as reported for extraintestinal pathogenic *Escherichia coli* (Matrasingh et al., 2021), *S. aureus* isolated from a case of sepsis (Ono et al., 2021), or a hypervirulent *K. pneumoniae* (Kochan et al., 2020), among other examples.

1.3. *Staphylococcus pseudintermedius*

Ecology and antibiotic resistance

S. pseudintermedius is a commensal bacterium that colonizes approximately 90% of dogs (read **Box 4** for a historical overview). It can also be found in other animals such as cats and foxes. It forms part of the microbiota of the skin and mucocutaneous sites (mostly soft tissues) such as fur, mouth, nares, pharynx, rectum, perineum, groin, and urogenital tract (Bannoehr and Guardabassi, 2012; Grönthal et al., 2014; Iverson et al., 2015; Kjellman et al., 2015; Dmitrenko et al., 2016; Somayaji et al., 2016; Kmiecik and Szewczyk, 2018; Menandro et

al., 2019). Despite being a commensal, it can also present an opportunistic behavior triggered by preexistent skin lesions, decreased host immunity, antibiotic treatment, or an extended hospital stay (Bannoehr and Guardabassi, 2012; Grönthal et al., 2014; Loeffler and Lloyd, 2018). It has been associated with skin and soft tissue infections in dogs such as pyoderma, otitis externa, urinary tract infections, postoperative infections, conjunctivitis, or even fatal infections (Descloux et al., 2008; Kjellman et al., 2015; Damborg et al., 2016; Dmitrenko et al., 2016; Somayaji et al., 2016; Menandro et al., 2019; Zakošek Pipan et al., 2019).

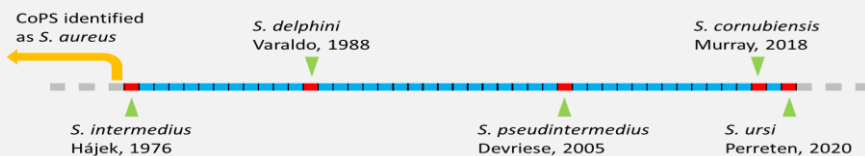
Since 1999 in the USA and 2005 in Europe, *mecA* gene conferring resistance to methicillin has been detected in isolates identified as *S. pseudintermedius* (Gortel et al., 1999; Kjellman et al., 2015; Dmitrenko et al., 2016; Bergot et al., 2018; Loeffler and Lloyd, 2018), previously detected in *S. aureus* and other Staphylococci. These bacteria are called Methicillin-Resistant *S. pseudintermedius* (MRSP) and have emerged from veterinary hospitals (Grönthal et al., 2014); in contrast, the rest are named Methicillin-Susceptible *S. pseudintermedius* (MSSP). MRSP prevalence varies by geography: for example, while Europe has a prevalence of around 30%, China and Japan present a prevalence of 50% and 70%, respectively (Loeffler and Lloyd, 2018). As previously mentioned, the mortality and economic impact of the infections caused by the ESKAPE bacterium MRSA suppose a big concern for human health, asymptomatic MRSP carriers can act as a reservoir spreading the methicillin resistance either to other pet animals or to humans (zoonotic transmission) (Kjellman et al., 2015).

Box 4. Timeline of the discovery of the SIG members.

Until 1976, most positive results from coagulase tests of *Staphylococcus* isolates were identified as *S. aureus* (Devriese et al., 2009; Murray et al., 2018) and classified into different biotypes considering their specific biochemical properties. This led to misidentification and underestimated incidence of some of the coagulase-positive staphylococci species (Hajek, 1976; Van Hoovels et al., 2006; Sasaki et al., 2007b; Sasaki et al., 2007a; Bannoehr et al., 2009; Devriese et al., 2009; Sasaki et al., 2010; van Duijkeren et al., 2011; Riegel et al., 2011; Lee et al., 2015; Murray et al., 2018; Perreten et al., 2020). In 1976, a group of CoPS isolated from pigeons, dogs, mink, and horses, with specific biochemical properties and cell wall structures previously called biotype E or F, became a unique species: *Staphylococcus intermedius* (Hajek, 1976). Twelve years later (1988), two strains isolated from dolphins were assigned to the *Staphylococcus* genus, and their biochemical properties were similar to those of *S. intermedius*. Even so, some of the properties differed from *S. intermedius*, such as acid production from carbohydrates, G+C content, or optimal NaCl concentration for bacteriolytic activity. Furthermore, DNA-DNA hybridization of these two isolates against *S. intermedius* indicated they were a new species: *Staphylococcus delphini* (Varaldo et al., 1988).

In 2005, four strains isolated from the lung of a cat, a skin lesion in a horse, an ear lesion in a dog, and the liver of a parrot, were analyzed because they shared a similar electrophoretic pattern that was different from the staphylococci known to date. The four strains shared 100% 16S rRNA gene similarity and were classified within the *S. intermedius* group. DNA-DNA hybridization levels among the four strains were high (96%) but decreased to 16-18% when compared with *S. intermedius* and 38-46% *S. delphini*. These four strains constituted a new species: *S. pseudintermedius* (Devriese et al., 2005).

Since the *S. pseudintermedius* two new species have been identified. In 2018, *Staphylococcus cornubiensis*, was isolated from human skin. It could not be differentiated from *S. pseudintermedius* by phenotypic characteristics and biochemical properties. When applying molecular techniques, the ANI value was not sufficient to determine that this strain belonged to an already existent species, so it was established as a new species (Murray et al., 2018). In 2020, *Staphylococcus ursi* strains were isolated from the skin of black bears. Employing different molecular methods, and some differences in the biochemical properties of the strains (e.g., absence of acid production from sucrose), the strains were differentiated into this new species of *Staphylococcus* (Perreten et al., 2020).



The *mecA* gene is located in the Staphylococcal chromosomal cassette (*SCC_{mec}*) (**Figure 6a**) and encodes for a different penicillin-binding protein, PBP2a, with low affinity for β -lactam antibiotics due to a narrower active site and an allosteric control site that opens when it interacts with the nascent peptidoglycan. The *SCC_{mec}* cassette can also harbor other related genes, such as *mecI*, *mecR1* and *mecR2* (**Figure 6b**). The *mecI* gene encodes for a transcriptional repressor that binds to the promoter region regulating *mecA* and *mecR1* genes. *mecR1* product is an integral-membrane sensor with peptidase activity. It presents a penicillin-binding domain (PBD) that can detect the presence of β -lactams. *mecR2* encodes for an antirepressor (Peacock and Paterson, 2015; Aguayo-Reyes et al., 2018).

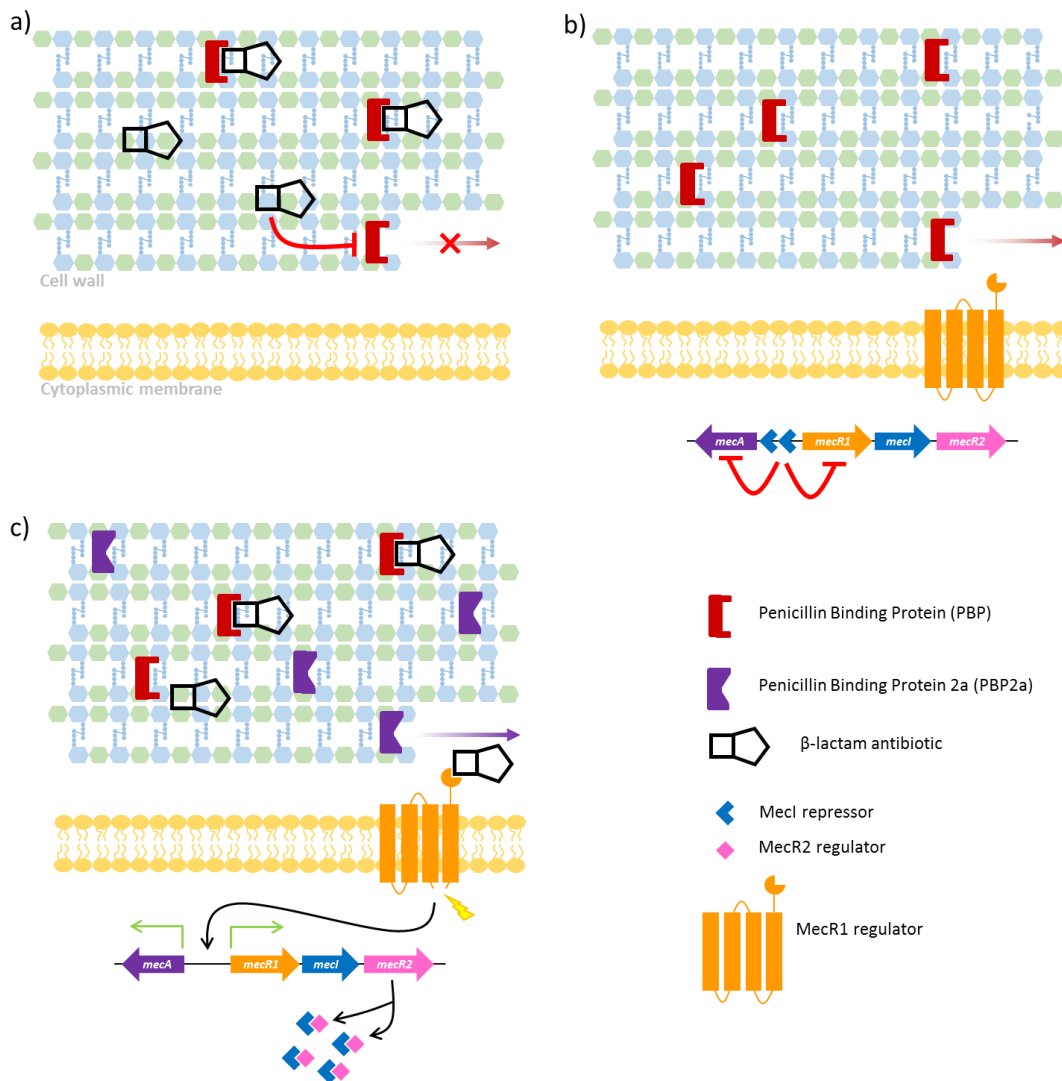


Figure 6. Scheme of the *mecA*-mediated resistance to methicillin. a) With the presence of a β -lactam antibiotic, the PBP is inhibited, leading to wall destabilization, and eventually, to cell death. b) In a strain carrying the *mecA* cassette, in the absence of the antibiotic, the wall production is performed as expected by the cell's PBP; c) however when a β -lactam is present, the genes are freed, and the transcription and translation of *mecA* start, overcoming the power of the β -lactam and allowing the cell to continue existing. Figure adapted from (Peacock and Paterson, 2015) and (Aguayo-Reyes et al., 2018).

If a bacterium harboring SCC*mec* is in contact with a β -lactam antibiotic (Figure 6c), the PBD of MecR1 detects it, and a subsequent conformational change leads to an autocatalytic cleavage of an intracellular sensor domain, followed by the cleavage of the repressor MecI. Once the promoter is freed from MecI, the expression of *mecA* takes place. Moreover, MecR2 binds to MecI, disrupting its union with the promoter and promoting its proteolysis through cytosolic proteases. Finally, the intrinsic PBPs are inhibited by the antibiotic, but PBP2a resists the action of the β -lactams and continues creating cell wall (Peacock and Paterson, 2015; Aguayo-Reyes et al., 2018).

There are different SCC mec types, but they all have three common structural elements: 1) ***mec* gene complex**: *mec* gene, its regulatory system (*mecI*, *mecR1*, and *mecR2*), and associated insertion sequences; 2) ***ccr* gene complex**: (cassette chromosome recombinase gene complex), these genes code for recombinases, responsible for the excision and integration of the genetic element into the chromosome (**Figure 7**); 3) **J regions**: joining regions code for nonessential elements, for example, other antimicrobial resistance genes (Hanssen and Ericson Sollid, 2006; Lakhundi and Zhang, 2018; Miragaia, 2018). These 3 elements present variants. According to the combination of these variants, several SCC mec types have been described. For example, SCC mec II-III was first described in *S. pseudintermedius*, and it is a combination of SCC mec II from *S. epidermidis* and SCC mec III from *S. aureus* (Descloux et al., 2008).

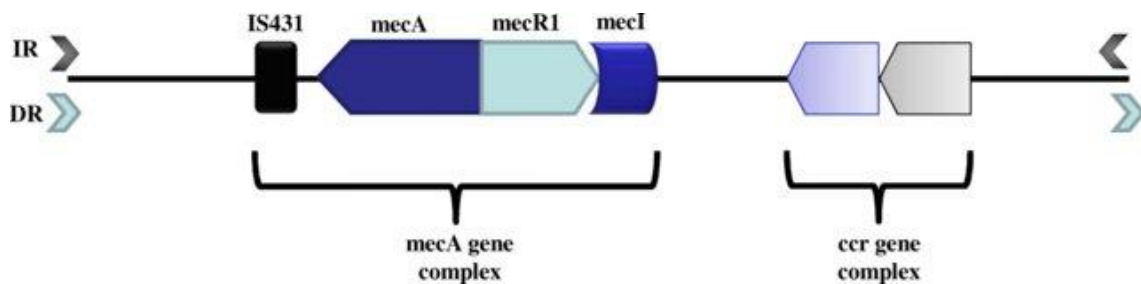


Figure 7. Schematic representation of the basic structure of SCC mec . Two gene complexes form the basic structure of the SCC mec : 1) the *mecA* gene complex that encodes for methicillin resistance (*mecA* gene) and its regulation system (*mecR1* and *mecI* genes), and 2) the *ccr* gene complex that codes for the machinery in charge of SCC mec 's mobilization. Figure excerpted from (Gill et al., 2019)

mecA confers resistance to methicillin and most of the other β -lactams, but the problem does not end here since a significant part of MRSP isolates are Multi-Drug Resistant (MDR, resistant to three or more different antimicrobials). One of the processes that *S. pseudintermedius* follows to become MDR involve three steps of accumulation of resistance elements (McCarthy et al., 2014): 1) acquisition of a SCC mec element, which possesses the *mecA* gene; 2) acquisition of a Tn5405-like element, which harbors different antibiotic resistance genes such as *ant(6')-Ia* and *aph(3')-III*, that confer resistance to aminoglycosides; *sat4*, that confers resistance to streptothricin; *dfr(G)*, that confers resistance to trimethoprim-sulfamethoxazole (also known as co-trimoxazole); and *erm(B)*, that confers resistance to erythromycin; and 3) presence of point mutations in the genes encoding for DNA topoisomerases (*gyrA*, *gyrB*, *grlA*, and *grlB*), which confer resistance to fluoroquinolones. Finally, *S. pseudintermedius* can form biofilms (*icaA* to *icaD* genes), in which the bacteria are embedded within a matrix. These biofilms do not allow the proper administration of

treatment, making it difficult to eliminate them (Bannoehr and Guardabassi, 2012; Grönthal et al., 2014; Dmitrenko et al., 2016; Kmiecik and Szewczyk, 2018; Loeffler and Lloyd, 2018).

Thus, MDR MRSP infections are challenging to treat through veterinary licensed antibiotics (Grönthal et al., 2014; McCarthy et al., 2014; Kjellman et al., 2015; Damborg et al., 2016; Loeffler and Lloyd, 2018; Menandro et al., 2019). Moreover, commensal MRSP may act as a reservoir for antibiotic resistance (Kjellman et al., 2015). It is worth considering that MRSP infections have already been described in humans (Iverson et al., 2015; Kjellman et al., 2015; Somayaji et al., 2016; Kmiecik and Szewczyk, 2018), which raises the concern for *S. pseudintermedius* from a One Health approach.

MDR *S. pseudintermedius* is present worldwide; however, antibiotic use by country can determine the higher or lower presence of the microorganism. For example, Romania is the 6th country in the world in consuming daily doses of antibiotics per inhabitant and has the highest rate in Europe of non-prescript use of antibiotics. A study comparing MRSP and MSSP of Romania and the UK found that Romanian MSSP exhibited more variety of resistances compared to the UK MSSP, but all the Romanian isolates were susceptible to β -lactams. In contrast, in the UK one of the first-line treatments for canine skin infections are β -lactams (cephalexin or amoxicillin/clavulanic acid), which is translated in higher rates of β -lactam resistance in UK MSSP compared to Romanian MSSP. This could be indicative of geographical variations on resistance patterns (Hritcu et al., 2020).

MRSP and other *S. pseudintermedius* causing pathology in dogs such as pyoderma or atopic dermatitis present a clonal distribution (Bannoehr and Guardabassi, 2012; Kjellman et al., 2015), whereas MSSP isolates present higher genetic variability (**Table 2**). *S. pseudintermedius* in pets is often the primary pathogen isolated (Somayaji et al., 2016; Ference et al., 2019).

One of the most used methods to classify clinical isolates is by multi-locus sequence types (MLSTs), defined by the genetic variants of seven loci: *tuf*, *cpn60*, *pta*, *purA*, *fdh*, *sar*, and *ack*. STs that are closely related form clonal complexes (Solyman et al., 2013). Regarding clonal distribution, the main lineage of *S. pseudintermedius* is MRSP ST71 in Europe and MRSP ST68 in North America (Bannoehr and Guardabassi, 2012; Grönthal et al., 2014; McCarthy et al., 2014; Kjellman et al., 2015; Damborg et al., 2016; Dmitrenko et al., 2016; Dos Santos et al., 2016; Bergot et al., 2018). ST71 has also spread worldwide and can be found in other continents like America or Asia (Dos Santos et al., 2016). In France, ST496 is a new emerging lineage that shows resistance to all veterinary licensed antibiotics (Bergot et al., 2018). In

Asia, ST45 and ST112 are the predominant MLST (Bergot et al., 2018), whereas ST45 is in Australia, Thailand, and Israel (Damborg et al., 2016).

ST71 isolates are associated with the highest amount carry-over of antibiotic resistances, including all veterinary licensed antibiotics (**Table 3**) (McCarthy et al., 2014; Kjellman et al., 2015; Damborg et al., 2016; Somayaji et al., 2016; Bergot et al., 2018; Wegener et al., 2018). ST258 is an emerging lineage in Europe that may be replacing ST71 (Kjellman et al., 2015; Damborg et al., 2016; Dos Santos et al., 2016; Bergot et al., 2018). ST258 is more susceptible to antibiotics than other lineages, and it has a lower tendency to form biofilm and adhere less to corneocytes (a type of skin cell) (Damborg et al., 2016; Bergot et al., 2018; Wegener et al., 2018; Menandro et al., 2019).

Table 2. Overview of some studies regarding *S. pseudintermedius* isolated from human and animal clinical cases.

Reference	Study
Human infections caused by <i>S. pseudintermedius</i>	
(Van Hoovels et al., 2006)	1 st documented human clinical case caused by <i>S. pseudintermedius</i> (60-year-old man with an infection in the pocket of his cardiac pacemaker).
(Somayaji et al., 2016)	Study of 24 cases causing skin and soft tissue infections, bacteremia, fistula wound infection, otitis externa, or prosthetic joint infection. 21 of the patients owned a dog. Six isolates obtained were MRSP isolates.
(Lozano et al., 2017)	Four clinical skin cases. All were MSSP and encoded for leukocidin and exfoliative toxin. Resistance to tetracycline, macrolides, or trimethoprim in some isolates.
(FERENCE et al., 2019)	<i>S. pseudintermedius</i> isolates from sinonasal infections. 45% of the patients presented polymicrobial infections, such as <i>Pseudomonas</i> , <i>E. coli</i> , <i>Serratia</i> , <i>Enterobacter</i> , <i>Klebsiella</i> , or <i>S. aureus</i> . 96% of the patients owned a dog.
Veterinary studies	
(Grönthal et al., 2014)	MRSP outbreak in a Finnish veterinary teaching school, caused by a clonal MRSP ST71 harboring SCC _{mec} type II-III.
(Kjellman et al., 2015)	54 MRSP (49 from infected and 5 from healthy dogs). 17/54 were ST258 and 12/54, ST71. ST258 exhibited resistance to a maximum of five antibiotics, ST71 exhibited resistance to five to seven of the antibiotics tested.
(Damborg et al., 2016)	46 clinical MRSP isolated from canine skin and mucosal infections. ST71 (13/46) and ST258 (7/46) were the most prevalent. ST71 harbored SCC _{mec} II-III and ST258 SCC _{mec} IV. Moreover, ST258 exhibited more susceptibilities to antibiotic than ST71.
(Menandro et al., 2019)	60 <i>S. pseudintermedius</i> , 19 of which corresponded to MRSP (18 from dog, and one from cat). All MRSP were MDR and isolated from otitis, pyoderma, conjunctivitis, and cutaneous fistula (among others). Fourteen MRSP belonged to ST71. While all ST71 isolates harbored SCC _{mec} II-III, ST258 encoded for SCC _{mec} IV. ST71 presented a wider range of antibiotic resistance than ST258.
(Meroni et al., 2019)	73 <i>S. pseudintermedius</i> isolates from dogs with clinical deep pyoderma, of which 56/73 belonged to ST71, 12/73 to ST258, and 5/73 to ST106. 35 isolates were MRSP: 24 ST71 SCC _{mec} II-III, 9 ST258 SCC _{mec} IV, and 2 ST106 SCC _{mec} IV. 42/73 of the isolates were MDR; while ST71 showed multiple resistances against typical veterinary-licensed antibiotics, ST258 were more susceptibilities to antibiotics. 69/73 of all isolates were biofilm producers.

Table 3 Antibiotic resistance gene profile in European lineages ST71, ST258, and ST496; and North American lineage ST68. Abbreviations: β -LAC, β -lactams; CHL, chloramphenicol; ERY, erythromycin; FQ, fluoroquinolones; GEN, gentamicin (aminoglycoside); KAN, kanamycin (aminoglycoside); LIN, lincosamides; PEN, penicillin; STH, streptothricin; STR, streptomycin (aminoglycoside); SXT, trimethoprim-sulfamethoxazole or co-trimoxazole; TET, tetracycline; TOB, tobramycin (aminoglycoside).

Gene	ST71	ST68	ST496	ST258	Resistance	Comments	References
<i>ant(6')-Ia/aadE</i>	X	X			STR	On Tn5405-like elements	1-6
<i>aph(3')-III</i>	X	X	X	X	KAN	On Tn5405-like elements	1-7
<i>aac(6')-Ie-aph(2')-Ia</i>	X	X	X		GEN, KAN, TOB	On IS2566 or IS1272 elements	1, 3-7
<i>blaZ</i>	X	X	X	X	PEN	On Tn552 or Tn55-like elements	1-5, 7
<i>mecA</i>	X	X	X	X	β -LAC	On SCCmec II-III (ST71) On SCCmec V (ST258 and ST68)	1-5, 7
<i>sat4</i>	X	X	X	X	STH	On Tn5405-like elements	1-5, 7
<i>dfr(G)</i>	X	X			STX	On Tn5405-like elements	2-6
<i>catpC221</i>	X		X		CHL		1-3, 5, 7
<i>tet(K)</i>	X				TET		1-3, 5-7
<i>tet(M)</i>		X	X	X	TET		1, 5
<i>gyrA / grlA</i> SNPs	X		X		FQ		1, 2, 4
<i>erm(A)</i>	X				ERY		7
<i>erm(B)</i>	X		X	X	ERY	On Tn5405-like elements	1, 3-7
<i>lnu(A)</i>		X			LIN		5

References: 1, (Bergot et al., 2018); 2, (Descloux et al., 2008); 3, (Ishihara et al., 2016); 4, (McCarthy et al., 2014); 5, (Perreten et al., 2010); 6, (Wegener et al., 2018); 7, (Menandro et al., 2019).

In relation to the SCC*mec* cassettes, ST68 and ST258 share SCC*mec* type V and ST71 is associated with SCC*mec* II-III (Descloux et al., 2008; Perreten et al., 2010; Ishihara et al., 2016; Dos Santos et al., 2016). Moreover, while ST71 and ST68 resistance to tetracycline is associated with *tet(K)* gene, ST258 is associated with *tet(M)* (Perreten et al., 2010; Bergot et al., 2018; Wegener et al., 2018)(Bergot et al., 2018). ST71 carries the *aac(6')-Ie-aph(2')-Ia* gene conferring resistance to different aminoglycoside antibiotics (**Table 3**), but ST258 isolates do not present it (Perreten et al., 2010; McCarthy et al., 2014; Ishihara et al., 2016; Bergot et al., 2018; Wegener et al., 2018; Menandro et al., 2019). As seen in **Table 3**, several genes are found in MGEs, and 8% of the genome is thought to be MGEs acquired by HGT in *S. pseudintermedius* (McCarthy et al., 2014; Dos Santos et al., 2016; Wegener et al., 2018). Finally, ST71 and ST68 have the major content of prophages (McCarthy et al., 2014).

Virulence

S. pseudintermedius harbors virulence factors that help the bacterium set an ideal environment for colonization and survival (Rigoulay et al., 2005; Hu et al., 2012; Kmiecik and Szewczyk, 2018; Moreno-Cinos et al., 2019).

Proteases (*clpP* and *htrA* genes) can degrade defective proteins produced under stress conditions (such as nutrient starvation or heat-stress situations); thermonucleases (*nuc* gene) can degrade host's nucleic acids; and lipases (*lip* gene) can degrade the sebum protective layer of the host skin.

Microbial surface components recognize adhesive matrix molecules from the host and help in colonization. SpsE, SpsD, SpsL, and SpsO are adhesive proteins that adhere to fibrinogen, fibronectin, and cytokeratin 10 present in human and canine corneocytes, and EbpS binds to elastin, which is present in the skin, lungs, or blood vessels. SpsP and SpsQ bind to the immunoglobulins, which inhibit opsonization and allow the bacterium to evade the host's immune system (Downer et al., 2002; Bannoehr et al., 2011; Bannoehr and Guardabassi, 2012; Latronico et al., 2014; Phumthanakorn et al., 2017; Balachandran et al., 2018; Kmiecik and Szewczyk, 2018).

S. pseudintermedius can also produce several toxins causing clinical symptoms on the infected host: enterotoxins, exfoliative toxins, and cytotoxins. Enterotoxins (*se_{int}* and *sec_{canine}* genes) cause vomiting. Exfoliative toxins (e.g., *siet*, *exi*, and *expB* genes) cause disaggregation of the skin layers, leading to exfoliation, erythema, crusting, erosive lesions, and intradermal splitting –symptoms related to pyoderma–, otitis, and staphylococcal scalded skin syndrome (among other diseases). Finally, cytotoxins such as hemolysins (*hla* and *hllb* genes) and leukotoxins (*lukS* and *lukF* genes) lyse erythrocytes and leukocytes, respectively.

Phenol-soluble modulins (PSMs) create pores in lipidic membranes. Furthermore, PSMs can polymerize to form structures that help stabilize biofilms (Bannoehr and Guardabassi, 2012; Cheung et al., 2014; Maali et al., 2018; González-Martín et al., 2020).

Different regulatory systems control the production of virulence factors, most of them two-component systems that have one element that detects environmental changes (the detector) and transmits them into the second element (the regulator), that regulates the expression of virulence factors (**Figure 8**). For example, the accessory gene regulator system (*agr* genes) is a quorum-sensing system formed by four elements (AgrA to AgrD). AgrA is the regulator, and AgrC the detector in the two-component system. AgrB matures and exports AgrD, also

called auto-inducing peptide. When AgrC detects high concentrations of AgrD, it activates AgrA, which induce the transcription of two RNAs that positively regulate some virulence factors, such as PSMs (Malone et al., 2007; Bannoehr and Guardabassi, 2012; Jenul and Horswill, 2019).

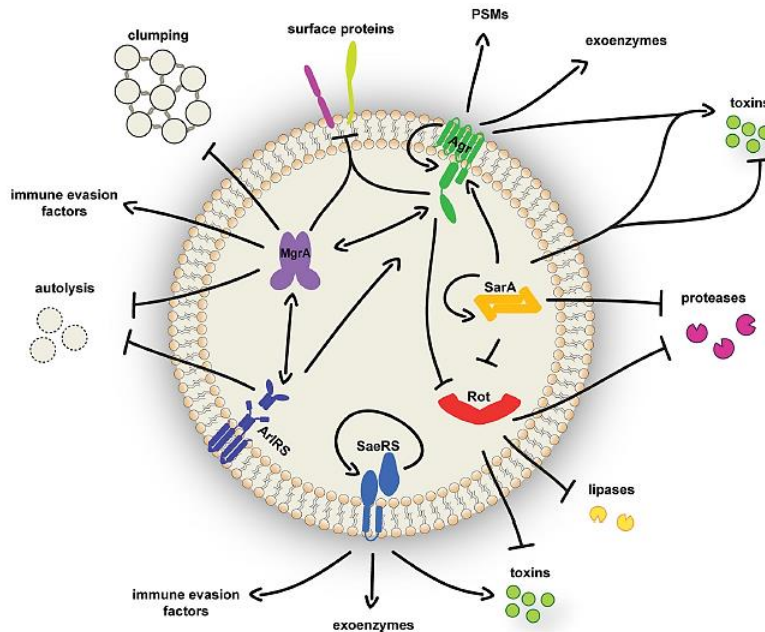


Figure 8. Principal virulence regulation systems in *Staphylococcus* spp. This figure corresponds to *S. aureus* since *S. pseudintermedius* and *S. aureus* share several regulation systems. Figure excerpted from (Jenul and Horswill, 2019).

1.4. *Escherichia coli*

Ecology and antibiotic resistances

E. coli is a well-known commensal of the Enterobacteriaceae family that inhabits the gut of vertebrate animals. However, it can also present an opportunistic behavior, causing either intestinal pathologies, from mild to hemorrhagic diarrheas (IPEC, intestinal pathogenic *E. coli*) or extra-intestinal pathologies, such as urinary tract infections, bacteremia, or meningitis (ExPEC, extra-intestinal pathogenic *E. coli*) (Thomas et al., 2016; Denamur et al., 2021). *E. coli* can be classified by pathotypes, which are groups that share pathogenic characteristics such as virulence factors and disease development. Several pathotypes have been described throughout the years inside the IPEC and ExPEC groups, such as Enterotoxigenic *E. coli* (ETEC), enteropathogenic (EPEC), enteroinvasive (EIEC), enterohemorrhagic (EHEC),

Shiga toxin-producing (STEC) for IPEC; and uropathogenic *E. coli* (UPEC), neonatal meningitis-associated (NMEC), and sepsis-associated (SEPEC) for ExPEC. MLST is also a widely used way to classify the microorganism. For *E. coli*, seven genes are considered: *adhE*, *fumC*, *gyrB*, *icd*, *mdh*, *purA*, and *recA* (Thomas et al., 2016; Poirel et al., 2018).

As a component of the fecal microbiota of mammals and birds, pathogenic *E. coli* can be transmitted via contact with animal feces, direct contact, or by the food chain. As an aggravating factor, it is usually a reservoir of several antibiotic resistance genes and virulence factors that threatens the treatment of its infections. Apart from the clinical concern, infection by *E. coli* in production animals provokes an economic impact. For example, diarrhea is a significant concern in livestock due to its easy propagation among the herd. Another important infection in dairy cattle is mastitis, which can be caused by an *E. coli* infection, reducing milk production (Poirel et al., 2018).

As probably the most studied bacterium, it has been thoroughly reported that *E. coli* presents a wide range of antibiotic resistance genes to most antibiotic families. It presents resistance to:

- β -lactams, either by narrow-spectrum β -lactamases such as *bla*_{TEM-1}, or extended-spectrum β -lactamases and carbapenemases, such as *bla*_{CTX-M-15} or *bla*_{NDM-1}.
- Fluoroquinolones, by punctual mutations on genes such as *gyrA* (which codes for the DNA gyrase) or acquired genes such as *qnrA1* or *aac(6')-Ib-cr*.
- Aminoglycosides, by enzymatic inactivation, mainly modifying the antibiotic by acetyltransferases (*aac* genes), nucleotidyltransferases (*ant* genes), and phosphotransferases (*aph* genes).
- Tetracyclines, either by efflux pumps (such as the one encoded by *tetA*) or by ribosome protective proteins (such as the one encoded by *tetM*).
- Phenicols can be inactivated by acetyltransferases (*cat* gene), pumped out the cell by efflux pumps (*cmlA* or *floR*), or resisted by punctual methylations. Resistance to sulfonamides and trimethoprim are mediated by *sul1* to *sul3* genes and *dfr* genes, respectively.

- Polymyxins, by mutations in the genes that code for the lipopolysaccharide-modifying enzymes (PmrA and PmrB); or by acquired genes, mostly plasmid-mediated, *mcr* (Poirel et al., 2018).

Among these antimicrobial resistances, colistin (polymyxin) is of special concern since it was categorized as a last resort antibiotic in human health to combat infections of extensively resistant gram-negative bacteria (Catry et al., 2015). The outer membrane of gram-negatives such as *E. coli* is composed of lipopolysaccharides in a double lipid layer conformation. The polysaccharide part of the lipids is negatively charged and stabilized by divalent cations such as Ca^{2+} and Mg^{2+} . *mcr-1* (mobilized colistin resistance) gene codes for the phosphatidylethanolamine transferase MCR-1, which transfers phosphoethanolamine (PPEA) to the lipid A part of the lipopolysaccharides. The final product (PPEA-4'-Lipid A) is charged positively, lowering the affinity of colistin to the outer membrane and making the bacteria resistant (Loho and Dharmayanti, 2015; Xu et al., 2018a) (**Figure 9**).

In livestock, colistin has been used to treat infections caused by enteric bacteria, and also as a prophylactic and metaphylactic against enteric diarrheas (Catry et al., 2015; Rennings et al., 2015). However, an abusive use of colistin can select for colistin-resistant bacteria. It has already been described the presence of *mcr-1*-harboring *E. coli* in street food, chicken, pork, and beef meat, water, and even the healthy human gut (Monte et al., 2017; Elbediwi et al., 2019; Johura et al., 2020).

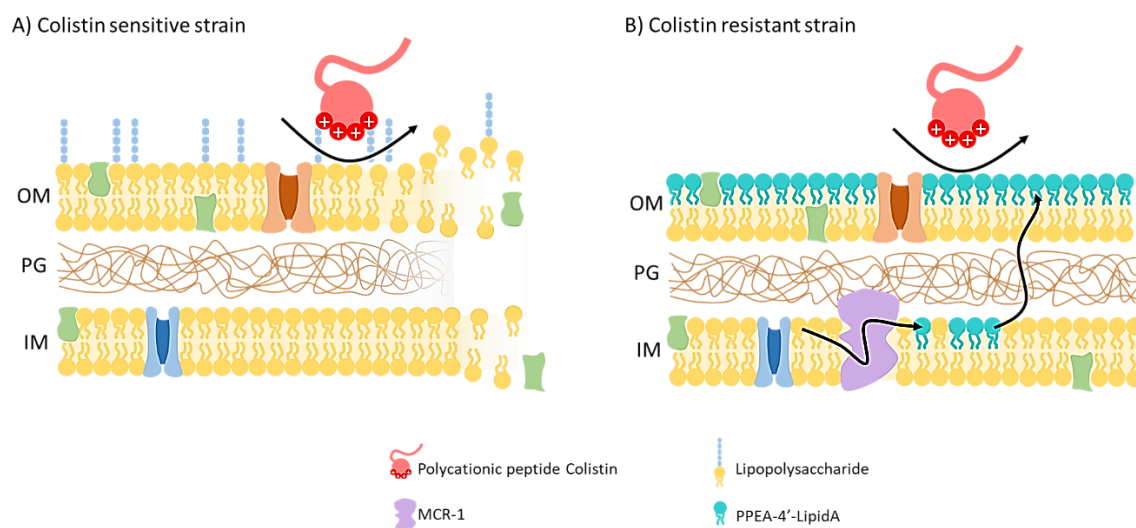


Figure 9. Colistin mechanism of action and resistance mediated by MCR-1. These figures represent the wall of a Gram-negative bacterium of a A) colistin sensitive and of a B) colistin-resistant strain. OM, Outer Membrane; PG, peptidoglycan; IM, Inner membrane; MCR-1, mobilized colistin resistance-1; PEA, 4'-phosphoethanolamine. Figure adapted from (Loho and Dharmayanti, 2015; Xu et al., 2018a).

Virulence

E. coli can produce a wide range of virulence factors that play a significant role during its infection (**Figure 10, Box 5**), intervening in its successful colonization and survival inside the host at the cost of causing damage that can turn to be fatal. Some *E. coli* virulence factors (EspF, Tir, EspB, NleA, among others) can cause exacerbation of diarrhea via different ways, such as altering transporters involved in the fluid homeostasis by inhibiting the Na⁺-glucose transporter (SGLT-1), reducing the expression of the Na⁺-H⁺ exchanger (NHE3), or inducing mislocalization of aquaporins (AqP); disrupting tight junctions that increase intestinal permeability; or inducing microvilli effacement that translates into a minor absorptive surface. Moreover, other *E. coli* virulence factors (Tir, NleA, NleB, EspJ, EspF, EspB, among others) can modulate the immunity of the host by stopping cytokine production that would then activate pro-inflammatory pathways (NF-κB and MAPK9) or lymphocyte proliferation; disrupting inflammasome activation; inhibiting extrinsic and intrinsic apoptosis; or preventing macrophage phagocytosis (Cepeda-Molero et al., 2020). Apart from these, *E. coli* can present virulence factors with cytotoxic activity adherence activity or enzymatic activity, among others (**Box 5** for more information and references).

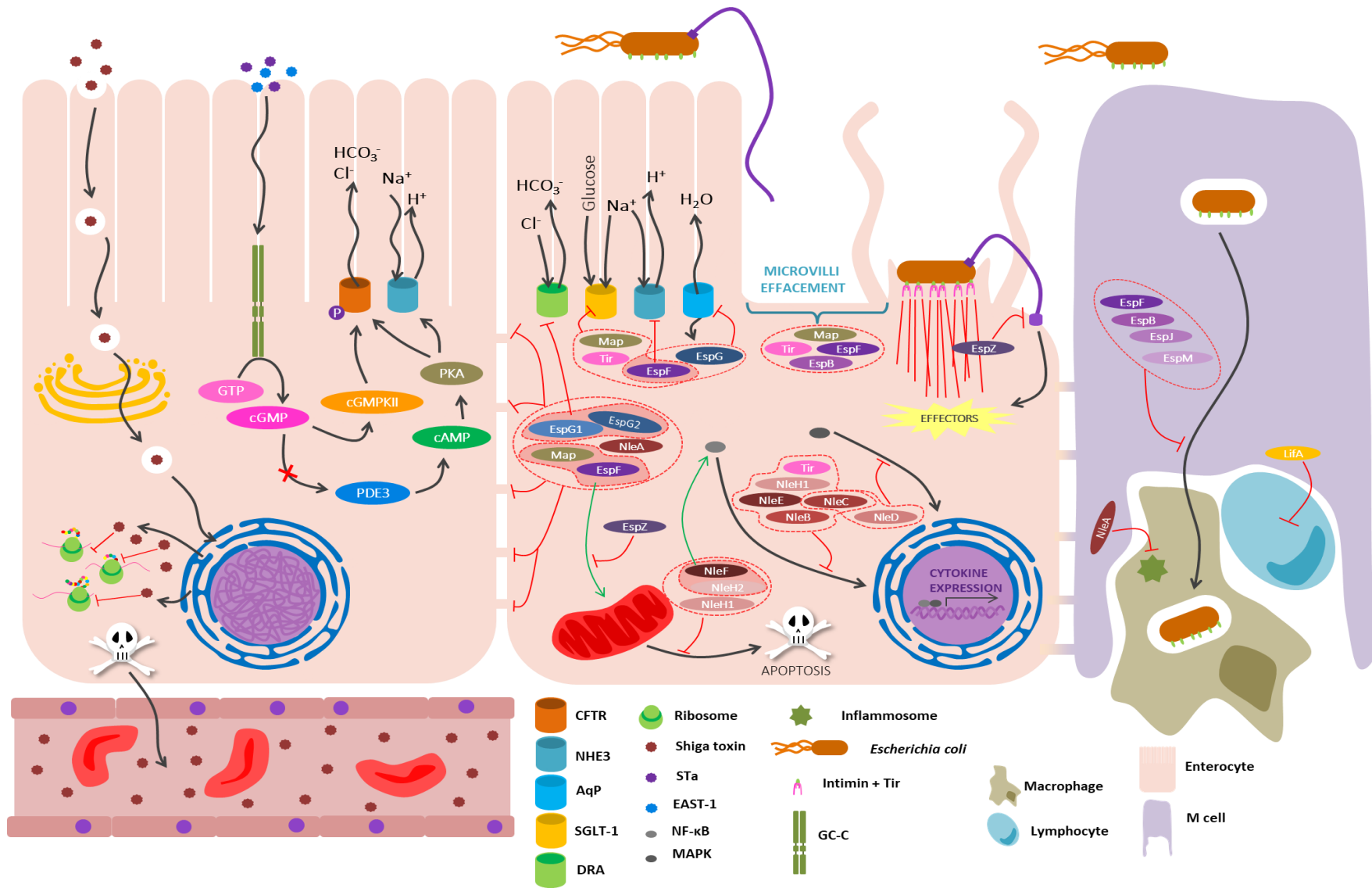


Figure 10. Scheme of some virulence mechanisms from *E. coli*. Virulence factors act at different levels, causing inhibition of protein production, leading to cell death, watery diarrhea, tight junction disruption, or microvilli effacement, among others. Figure based on figures from (Castro et al., 2017; Cepeda-Molero et al., 2020).

Box 5. Review of some virulence factors reported in *E. coli* and their mechanism of action.

Virulence factors	Action	References
Locus for Enterocyte Effacement (LEE pathogenicity island)	EspA interacts with the enterocyte, then EspB and EspD form the type III secretion system (T3SS, or injectisome). Different virulence factors are translocated through T3SS, like Tir, which reaches the enterocyte's membrane and integrate. Tir-intimin interaction allows the bacterium to adhere to the enterocyte surface and modulates the enterocyte's cytoskeleton, leading to the polymerization of actin underneath the <i>E. coli</i> (pedestal), and effacement of the brush border microvilli.	(Cepeda-Molero et al., 2017)
Enterohemolysin (<i>ehxA</i>)	It is a membrane pore-forming cytotoxin active against human and bovine cells. Moreover, it increases human mononuclear cells' IL-1 β production, a pro-inflammatory cytokine, which exacerbates tissue damage during disease.	(Lopez-Castejon and Brough, 2011; Cáceres et al., 2017; Noll et al., 2018; Shridhar et al., 2018; Fan et al., 2019)
Extracellular serine protease (<i>espP</i>)	Participates in the adhesion and colonization to bovine intestinal cells, and cleaves pepsin A and human coagulation factor V, leading from mild bleeding to severe gastrointestinal hemorrhages (hemorrhagic colitis).	(Etcheverría and Padola, 2013; Cáceres et al., 2017; Noll et al., 2018; Shridhar et al., 2018; Paraboschi et al., 2019)
EAST-1 heat-stable toxin (<i>astA</i>) Heat-stable enterotoxin ST-Ia (<i>stx1</i>)	Causes diarrhea by increasing cyclic guanosine monophosphate (cGMP) production, which inhibits Na ⁺ /Cl ⁻ co-transport, and consequently, water and electrolyte absorption from the intestine, thus altering fluid homeostasis.	(Mirzarazi et al., 2015; Dubreuil et al., 2016; Joffré et al., 2016)
Fimbriae (<i>f17A</i>, <i>C</i>, <i>D</i>, and <i>G</i>)	Colonization virulence factor associated with diarrhea in neonates.	(Dubreuil et al., 2016)
Cytotoxic distending toxin (<i>ctdA</i> to <i>C</i>)	It is a genotoxin due to the DNase activity of CdtB subunit. CDT can modulate the host physiology by modulating the immune system, modulating cell apoptosis or senescence, making lose control of bacterial proliferation and tissue regeneration. These effects lead to tissue lesions, slow healing, chronic wounds, and even carcinogenesis.	(Elwell et al., 2001; Pandey et al., 2003; Gargi et al., 2012; Faïs et al., 2016; Scuron et al., 2016)
Catalase-peroxidase (<i>katP</i>)	It is an enzyme that helps the bacterium to defend against oxidative stress created by phagocytes and other cells during the infection.	(Brunder et al., 1996; Etcheverría and Padola, 2013; Cáceres et al., 2017)
Shiga-toxin (<i>stx2</i>)	<i>stx2</i> gene can be carried by lysogenic prophages that integrate at tRNA regions (arginine, leucine, serine, and threonine are the most popular). Once this toxin is internalized, it modifies the 28S rRNA, inhibiting protein synthesis, leading to cell death. Then, Shiga-toxin could reach the bloodstream, reaching other organs.	(Fouts, 2006; Bugarel et al., 2011; Etcheverría and Padola, 2013; Saha et al., 2013; Thomas et al., 2016; Noll et al., 2018; Greig et al., 2019; Sharma et al., 2019)

1.5. *Klebsiella pneumoniae*

Ecology and antibiotic resistances

K. pneumoniae is a resilient bacterium that colonizes mucosa, such as the gastrointestinal tract and the oropharynx. Its resiliency is based on its survival strategy, which relies on a good defense against the host immune system. *K. pneumoniae* isolates have been typically classified into two main groups according to their virulence: classical and hypervirulent *K. pneumoniae*. Other classifications consider the antimicrobial resistances, such as carbapenem-resistant *K. pneumoniae* (named CRE for carbapenem-resistant Enterobacteriaceae); or the MLST types defined by 7 loci (*mdh*, *infB*, *tonB*, *gapA*, *pboE*, *pgi*, and *rpoB*) (Paczosa and Mecsas, 2016; Gonzalez-Ferrer et al., 2021).

Both classical and hypervirulent *K. pneumoniae* can be the etiological agent of severe diseases like urinary tract infections, pneumonia or even bacteremia (**Figure 11**). On one hand, classical *K. pneumoniae* usually causes infections in immunocompromised hosts in a nosocomial way. So, a patient comes to the hospital with another infection and is treated with antibiotics: resistant *K. pneumoniae* inhabiting on the gastrointestinal tract can be selected and can cause an opportunistic infection. If this infection reaches the bladder, the treatment and hospital stay may prolong and if it reaches the bloodstream (bacteremia), the fatality rate increases from 27.4 to 37% (Paczosa and Mecsas, 2016; Effah et al., 2020; Gonzalez-Ferrer et al., 2021; Lan et al., 2021). On the other hand, the hypervirulent *K. pneumoniae* can cause infections in both healthy and immunocompromised hosts, either nosocomial- or community-acquired. Infections caused by hypervirulent *K. pneumoniae* commonly evolve to systemic infections, reaching other body sites and causing pyogenic liver abscess, meningitis, or endophthalmitis, among others (**Figure 11**) (Paczosa and Mecsas, 2016; Effah et al., 2020; Gonzalez-Ferrer et al., 2021).

The most concerning isolates are those that harbor extended-spectrum β -lactamases and carbapenemases. Carbapenems are last-resort antibiotics for human medicine and rarely prescribed in veterinary medicine, except some third and fourth-generation cephalosporines. These concerning isolates are also resistant to fluoroquinolones and aminoglycosides, which are widely used in both human and veterinary medicine against many infections. The presence of all these resistances in *K. pneumoniae* may result in no antibiotic treatment available to tackle the infection since all licensed antibiotics are inhibited by bacterial mechanisms (Poirel et al., 2018; Effah et al., 2020).

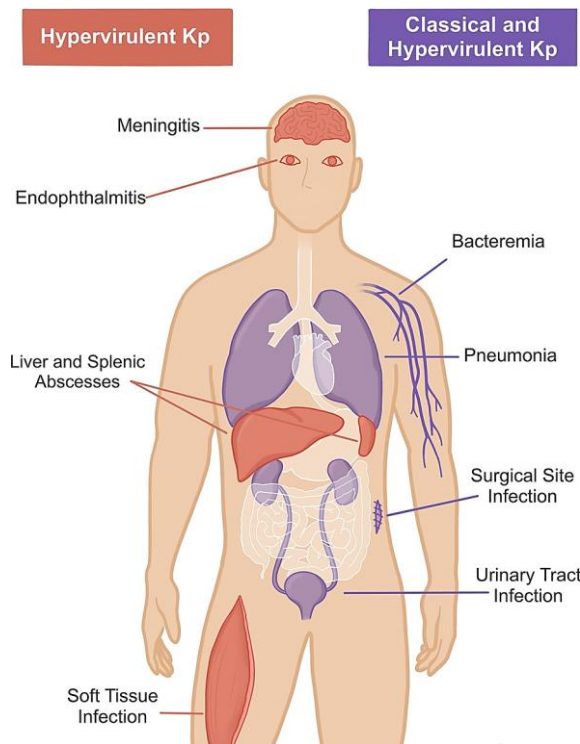


Figure 11. *K. pneumoniae* infection sites. Hypervirulent *K. pneumoniae* has been isolated, causing infection in more body sites than classical *K. pneumoniae*. Figure excerpted from (Gonzalez-Ferrer et al., 2021).

Virulence

K. pneumoniae presents defense mechanisms against the host immune system ensuring its survival. It presents four classes of virulence factors that have been deeply characterized: the capsule, lipopolysaccharides, fimbriae or pili, and siderophores (Paczosa and Meccas, 2016; Effah et al., 2020).

The capsule is an extracellular coat composed of polysaccharides (K antigen), which acts as a shield against phagocytosis, antimicrobial peptides such as defensins (present in the lungs), complement-mediated lysis, opsonization, and inflammatory response. Hypervirulent *K. pneumoniae* produces the hypercapsule, a more robust and viscous capsule than typical *K. pneumoniae* (Lan et al., 2021; Paczosa & Meccas, 2016).

The lipopolysaccharide of the outer membrane in gram-negative bacteria is composed of an O antigen, a core oligosaccharide, and lipid A. As this molecule is exposed to the extracellular space, the host immune system has evolved to detect it (primarily the lipid A) and create a potent immune response. The immune response can be so strong that it can become toxic

to the host (endotoxin). Moreover, it can protect against humoral defenses from the host (Paczosa and Meccas, 2016; Bertani and Ruiz, 2018).

Fimbriae are adhesive structures that help the bacteria to attach to biotic and abiotic surfaces, enhancing the invasion of the bacterium into the host. Fimbriae can adhere to the bladder or catheters (among others) and can start to form a biofilm. The formation of biofilms in hospitalized patients is life-threatening since the bacteria embedded in the matrix are less susceptible to antimicrobials, making difficult to remove (Paczosa and Meccas, 2016; Gonzalez-Ferrer et al., 2021).

Siderophores are molecules that scavenge iron from the host and allow a better adaptation to different tissues, improving colonization, and stopping possible inhibition of siderophores by the host's defense mechanisms. In *K. pneumoniae* there are four different types: enterobactin, aerobactin, salmochelin, and yersiniabactin.

2. OBJECTIVES

The two main objectives from this Ph.D. thesis are the following:

- To optimize the use of long-read sequencing (Nanopore) in whole-genome sequencing approaches for characterizing the bacterial genome and plasmids, including the presence of antibiotic resistance genes, mobile genetic elements, and virulence factors.
- To apply the long-read whole-genome sequencing to solve real problems from a clinical veterinarian hospital, a farm setting, and human hospitals. The specific objectives of these collaborations are:
 - To unravel the differences among pathogenic *Staphylococcus pseudintermedius* and commensal *Staphylococcus pseudintermedius*, isolated from canine skin.
 - To characterize the colistin-resistance transmission among 18 strains of *Escherichia coli* in a One-Health scenario (cattle, swine, and the farmer).
 - To describe the transmission of carbapenem-resistance among *Klebsiella pneumoniae* isolates involved in hospital outbreaks (human isolates).

3. MATERIALS AND METHODS

In this section, we describe the methodologies used in this Ph.D. thesis. This includes laboratory techniques, such as DNA extraction, library preparation, and Nanopore sequencing, as well as the associated data analysis. The bioinformatics data analysis involves the main steps to assemble a bacterial genome (or a plasmid), polish it and further characterize its antimicrobial resistance genes and virulence factors.

The associated published articles contain the complete material and methods for each study, and also those steps performed by collaborators or third parties, such as microbiological cultures, antimicrobial susceptibility tests, or Illumina sequencing.

3.1. Bacterial isolates

Staphylococcus pseudintermedius were isolated from the ear skin of a dog with otitis, from the lesional skin of dogs with pyoderma (33 dogs, 33 samples from the content of pustules or epidermal collarettes), and from the perioral and abdominal skin of healthy dogs (6 dogs, 22 isolates). Samples were obtained by rubbing a sterile swab for 15 seconds and isolated by microbiological culture in blood agar at 37°C for 24 to 48 hours. After overnight culture in brain heart infusion broth at 37°C, DNA was extracted using ZymoBIOMICS™ DNA Microprep (for otitis) or Miniprep kit (for the skin samples) (Zymo Research, Irvine, California, USA) under manufacturer's conditions. DNA quality and quantity were assessed using Nanodrop 2000 Spectrophotometer and Qubit™ dsDNA BR Assay Kit (Fisher Scientific SL, Madrid, Spain), respectively.

We performed PCR targeting *nuc* gene, which codes for a nuclease and allows species identification among the *Staphylococcus* genera; and the *mecA* gene, which codes for the penicillin-binding protein 2A conferring resistance to methicillin and other β -lactam antibiotics. PCR mixture contained 1 μ l of DNA template (\sim 1 ng), 5 μ l of 5X Phusion Buffer HF, 1.25 μ l of each primer at 10 μ M for *mecA* PCR, and 1 μ l of each primer at 10 μ M for *nuc* PCR, 2.5 μ l of dNTPs at 2mM, and 0.25 μ l Phusion Hot Start II High-Fidelity DNA polymerase (2 U/ μ l) (Thermo Scientific™, Vilnius, Lithuania). Water was added to reach the final reaction volume of 25 μ l. The genes were amplified using the primers shown in **Table 4**. For the *nuc* gene, we used an equimolar mix of the specific primers for *Staphylococcus aureus*, *Staphylococcus intermedius*, and *S. pseudintermedius*. Both genes presented the same thermal cycling profile, with the exception of the annealing temperature, 56°C for *nuc* and 59°C for *mecA*, that consisted of an initial denaturation for 30s at 98°C, followed by 40 cycles for 10s of denaturation at 98°C, 30s of annealing, 30s of extension at 72°C, and a final step of extension for 7 min at 72°C. PCR consisted of 40 cycles.

Table 4. *nuc* and *mecA* primers. Primer sets amplify the *nuc* gene to discriminate between staphylococcal species (*S. pseudintermedius*, *S. aureus*, or *S. intermedius*), and amplify the *mecA* gene to detect methicillin resistance.

Name (gene)	Sequence (5'-3')
pse-F (<i>nuc</i>)	TRG GCA GTA GGA TTC GTT AA
pse-R (<i>nuc</i>)	CTT TTG TGC TYC MTT TTG G
au-F (<i>nuc</i>)	TCG CTT GCT ATG ATT GTG G
au-R (<i>nuc</i>)	GCC AAT GTT CTA CCA TAG C
in-F (<i>nuc</i>)	CATGTC ATA TTA TTG CGA ATG A
in-R (<i>nuc</i>)	AGG ACC ATC ACC ATT GAC ATA TTG AAA CC
<i>mecA</i> -P4	TCC AGA TTA CAA CTT CAC CAG G
<i>mecA</i> -P7	CCA CTT CAT ATC TTG TAA CG

The identification of the bacterial species relies on the *nuc* amplicon's differential length: 359 bp for *S. aureus*, 430 bp for *S. intermedius*, and 926 bp for *S. pseudintermedius* (Sasaki et al., 2010). PCR amplification product was visualized running a 2% agarose gel for 45 minutes.

For Enterobacteriaceae isolates, we worked with the extracted DNA from colistin-resistant *Escherichia coli* isolated from human (n=1), swine (n=4), and cattle (n=13) feces; and eight carbapenem-resistant *Klebsiella pneumoniae* isolated from human clinical cases. *K. pneumoniae* studies included five carbapenem-resistant isolates from human clinical cases from Hospital A and three from Hospital B.

The eight *K. pneumoniae* isolates and their plasmids had been previously characterized by the hospital partners with several techniques such as MLST and PCRs for detecting the presence of genes encoding carbapenemases, extended spectrum β -lactamases (ESBLs), and 16S rRNA methyltransferases, as well as for detecting the plasmid's incompatibility group. Plasmid profiling was done by pulsed-field gel electrophoresis (PFGE) and Southern blot against specific resistance genes (*bla*_{NDM} variants, *bla*_{OXA-48}, and *bla*_{CTX-M}).

3.2. Whole-genome sequencing: read pre-processing, *de novo* assembly and polishing

Nanopore libraries were prepared by transposase fragmentation using the Rapid Barcoding Sequencing kit, following manufacturer instructions (RBK-SQK004, Oxford Nanopore Technologies, UK; ONT). The final libraries were loaded and sequenced in the MinION™ (ONT) sequencer using FLO-MIN106 flow cells v9.4 or v9.4.1.

Basecalling and demultiplexing of the fast5 files was performed with the latest ONT basecalling software as of the day of the analyses, as shown in **Table 5** for each one of the studies:

Table 5. Software used for basecalling, demultiplexing, assembly, and polishing. The number next to the software corresponds to the version used in the study.

	Base calling	Demultiplex	Assembly	Polishing
(Viñes et al., 2019)	Albacore 2.3.1	Albacore 2.3.1 + Porechop	Unicycler 0.4.6	<i>Unicycler includes a step using Illumina reads</i>
(Francino et al., 2021) (Ferrer et al., under revision)	Guppy 4.0.11	Guppy 4.0.11	Flye 2.7.1	<i>With Nanopore reads</i> Minimap2 2.17 1 x Racon 1.4.13 1 x Medaka 1.0.3
(Viñes et al., 2021)	Albacore 2.3	Albacore 2.3 + Porechop	Flye 2.6	<i>With Nanopore reads</i> Minimap2 2.17 1 x Racon 1.4.10 2 x Medaka 0.11.4 <i>With Illumina reads</i> Minimap2 2.17 1x Racon 1.4.10
Hospital A isolates (Marí- Almirall et al., 2020)	Guppy 3.0.3	qcat 1.10	Flye 2.5 Flye 2.6 Flye 2.7.1	
Hospital B isolates	Guppy 3.0.3	qcat 1.10	Flye 2.5 Flye 2.6 Flye 2.7.1	<i>With Nanopore reads</i> Minimap2 2.17 1 x Racon 1.4.10 2 x Medaka 0.11.4 <i>With Illumina reads</i> Minimap2 2.17 1x Racon 1.4.10

De novo genome assembly of *S. pseudintermedius* isolated from a dog with otitis was performed with the reads obtained from Nanopore and Illumina sequencing in a hybrid approach using Unicycler (Wick et al., 2017).

In all the other studies, the genomes were assembled using Flye (Kolmogorov et al., 2019), specifying the usage of Nanopore raw reads (--nano-raw), the genome size (--genome-size) in mega basepairs for each sample (2.6m for *S. pseudintermedius*, 5m for *E. coli*, and 5.3m for *K. pneumoniae*), and the possible presence of plasmids (--plasmids).

We had Illumina data for *E. coli* and *K. pneumoniae* samples from Hospital B (**Figure 12**). Illumina paired-end reads were merged into a unique file per isolate using a python script

A first step of polishing using only Nanopore reads was performed for each isolate. Nanopore reads were mapped to the previously generated assemblies using Minimap2. The PAF file generated by Minimap2 from each isolate was then used to perform a first round

of polishing with Racon. A second, and a third, round of polishing was done with Medaka using the “medaka_consensus” script. We had Illumina data for *E. coli* and *K. pneumoniae* samples from Hospital B (**Figure 12**). Illumina paired-end reads were merged into a unique file per isolate using a python script available at <https://github.com/isovic/racon/issues/68>. A final round of polishing was performed using Illumina reads. First, Illumina reads were mapped to the contigs polished with Nanopore reads using Minimap2 (Li, 2018), and then a round of Racon (Vaser et al., 2017) was performed with Illumina reads. The files obtained from this polishing step were the final assemblies and were used for further analyses.

For all Hospital A *K. pneumoniae* samples and HUB-3 sample (from Hospital B study), we filtered the plasmid reads by mapping fastQ reads against a curated database containing Enterobacteriaceae plasmid sequences (Orlek et al., 2017) with Minimap2 (Li, 2018). For all HA *Klebsiella pneumoniae* samples, reads that mapped to the database were used to assemble plasmids with Flye 2.5 specifying the “--plasmids” flag. No further polishing was performed for these samples. For HUB-3 sample (from HB study), reads mapped to the database were used to perform the assembly of the plasmids with Flye 2.6 (--genome-size 0.066m) as described before for *E. coli* and samples from Hospital B (hybrid sequencing).

A summary of all the data analysis steps and software versions used can be find in **Table 6**.

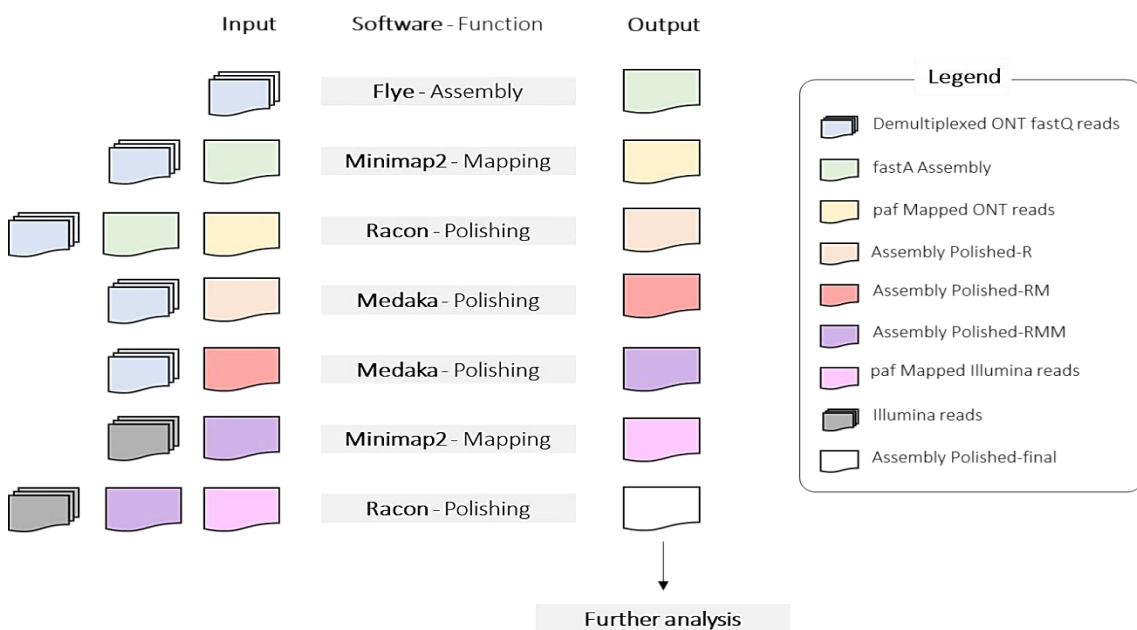


Figure 12. Workflow used for the hybrid assembly and polishing of *E. coli* and *K. pneumoniae* genomes and plasmids.

3.3. Genomic characterization

A summary of all the genome characterization analysis per study and software versions used can be found in **Table 6**.

Table 6. Software used for characterizing the genome and plasmid assemblies. In the case that the software is web-based or do not have a specific version, it is indicated with “X”. ARGs, antibiotic resistance genes; CGE DTU, Center for Genomic Epidemiology from the Technical University of Denmark; db, database; Genome compl., Genome completeness; IS, insertion sequence; MLST, Multi-Locus Sequence Type; PGAP, Prokaryotic Genome Annotation Pipeline; VF, virulence factors.

	<i>S. pseudintermedius</i>			
	Otitis	Healthy/Pyoderma	<i>E. coli</i>	<i>K. pneumoniae</i>
Assess Genome Completeness				
CheckM	v1.0.11	v1.1.11		
BUSCO			v4.0.1	v4.0.1
Genome circularization				
Circlator		v1.5.5		
Typing				
MLST CGE DTU	v2.0	v2.0	v2.0	v2.0
SeroTypeFinder CGE DTU			v2.0	
CSIPhylogeny CGE DTU			v1.4	
ClermonTyping			X	
Annotation				
Prokka	v1.13	v1.14.16	v1.14.16	v1.14.16
PGAP	X	X	X	
Abriicate	v0.8.13	v0.8.13	v0.8.13	0.8.13
+ CARD db	X	X	X	X
+ PlasmidFinder db		X	X	X
+ VFDB			X	X
+ Custom VF db		X		
SCCmecFinder		v1.2		
Phigaro		v2.2.6		
ISFinder			X	X
PHASTER			X	
OriTFinder			X	
Pangenome analysis				
Anvi'o		v6.2		
Visualization				
Bandage	v0.8.1		v0.8.1	
BRIG			v0.95	
SnapGene Viewer			v5.0.7	v5.0.7
FigTree			v1.4.3	
NCBI BLAST				X
Kablammo				X

The genome completeness and contamination was assessed using CheckM (Parks et al., 2015) for *S. pseudintermedius*, and BUSCO (Simão et al., 2015) with the Enterobacteriaceae database

(OrthoDb 10.1) (Kriventseva et al., 2019) for the *E. coli* and *K. pneumoniae* isolates. Circlator (Hunt et al., 2015) was used to identify the origin of the chromosome and set the same start position for all assemblies (fixstart --min_id 70 flags)

Gene annotation was performed with Prokka (Seemann, 2014) for all the isolates and with NCBI Prokaryotic Genome Annotation Pipeline (PGAP) (Tatusova et al., 2016) for *S. pseudintermedius* (at the time of NCBI uploading of the genomes) and *E. coli* isolates. We further characterized the genomes and plasmids by detecting the presence of specific genes –with a minimum identity and coverage of 90%– using Abricate (Seemann, 2017) with the following databases: i) PlasmidFinder (Carattoli et al., 2014) for plasmid replicons, ii) CARD (Jia et al., 2017) for antibiotic resistance genes, iii) VFDB (Chen et al., 2016) for virulence factors. For virulence factors analysis in *S. pseudintermedius*, we created a custom database that included 58 genes encoding exfoliative toxins, enterotoxins, leukocidins, pore-forming proteins, and intercellular adhesion proteins, among others (available at <http://doi.org/10.17605/OSF.IO/NS3Y4>). Insertion sequences were analyzed using ISFinder (Siguier et al., 2006); bacteriophages were analyzed through PHASTER (Arndt et al., 2016) and Phigaro (Starikova et al., 2020); and conjugative elements were analyzed using OriTFinder (Li et al., 2018b).

GC % content was calculated using <https://www.sciencebuddies.org/science-fair-projects/references/genomics-g-c-content-calculator>. MLST (Larsen et al., 2012) was assigned with MLST tool available at <https://cge.cbs.dtu.dk/services/MLST-2.0/>.

For the *S. pseudintermedius*, SCCmec type was determined with SCCmecFinder, available at <https://cge.cbs.dtu.dk/services/SCCmecFinder/>. For *E. coli*, SerotypeFinder (Joensen et al., 2015) was applied to retrieve the serotype, CSIPhylogeny (Kaas et al., 2014) to retrieve SNPs, and ClermonTyping (Beghain et al., 2018) to retrieve the phylotype.

Plasmid annotation was visualized with BLAST Ring Image Generator (BRIG) (Alikhan et al., 2011) and SnapGene Viewer (from Insightful Science; <https://www.snapgene.com/>). Phylogeny was visualized with FigTree (<http://tree.bio.ed.ac.uk/software/figtree/>). For *K. pneumoniae*, NCBI BLAST was used to perform one-vs-one alignments and obtain a dot plot for two IncN + IncR plasmids. Web-based Kablammo (Wintersinger and Wasmuth, 2015) <http://kablammowasmuthlab.org/> was used to visualize the alignment of both plasmids.

Finally, for *S. pseudintermedius* we performed a pangenome analyses and associated visualization plots using ANVIO (Eren et al., 2015). After simplifying the header lines of

the fastaA assembly, we generated an ANVI'0 contigs database using Prodigal (Hyatt et al., 2010) as a gene caller to identify open reading frames (ORFs). Genes were functionally annotated using blastp against the NCBI Clusters of Orthologous Groups (COGs) database (cog2020) (Tatusov et al., 2003). The pangenome database was created using NCBI's blastp to calculate each amino acid sequence's similarity in every genome against every other amino acid sequence across all genomes to resolve gene clusters. MCL inflation parameter that was set to 10. Both, genome storage and pangenome databases were used to display the visualization of the pangenome.

3.4. Data availability

The genome sequence of *S. pseudintermedius* from otitis was deposited in the GenBank database with accession number [CP032682.1](#) and RefSeq accession number [NZ_CP032682](#); the plasmid was deposited under GenBank accession number [MN612109](#). All raw sequence files can be found under BioProject accession number [PRJNA493792](#). The results are published in Microbiology Resource Announcements (Viñes et al., 2019)

The whole-genome assemblies from the 55 *S. pseudintermedius* isolates were deposited at NCBI under the BioProject [PRJNA685966](#), with the accession numbers [CP066702](#) to [CP066718](#), [CP066884](#), [CP066885](#), and [JAENBQ000000000](#) to [JAENDF000000000](#). The results are published in Microbiology Resource Announcements (Francino et al., 2021) and are under revision in Veterinary Dermatology (Ferrer et al., under revision).

The 18 *E. coli* genomes sequences, 48 antibiotic resistance plasmids, 13 virulence factor plasmids, Nanopore fastQ files, and Illumina fastQ files from *E. coli* were deposited in OSFHOME under the DOI [10.17605/OSF.IO/7Q2CB](#). The results are published in Antibiotics (Viñes et al, 2021).

FastQ files of *K. pneumoniae* isolates are associated with BioProject [PRJNA6346391](#) and were deposited into the NCBI Sequence Read Archive (SRA) under the following accession numbers: [SRR11828896](#) (HA-2), [SRR11828895](#) (HA-3), [SRR11828894](#) (HA-4), [SRR18228893](#) (HB-377), and [SRR11828892](#) (HB-536), respectively. The results are published in Journal of Antimicrobial Chemotherapy (Marí-Almirall et al., 2020).

Data for isolates HUB-1, HUB-2, and HUB-3 has not yet been published due to confidentiality.

4. RESULTS

The Ph.D. thesis had two main objectives:

- A technological one optimizing whole-genome sequencing for characterizing the bacterial genome, including the presence of antibiotic resistance, virulence factors, mobile genetic elements, and plasmids
- A scientific one applying whole-genome sequencing to solve real problems from animal and human health, in a One Health approach

The specific objectives were achieved by working in different studies and collaborations: we have unraveled potential differences among pathogenic and commensal *Staphylococcus pseudintermedius* isolated from canine skin; we have characterized the transmission of the *mcr-1* gene for colistin resistance among 18 strains of *Escherichia coli* in a One-Health scenario (cattle, swine, and the farmer); and we have described the transmission of carbapenem-resistance among *Klebsiella pneumoniae* isolates involved in an inter-hospital outbreak (human isolates).

4.1. Whole-genome sequencing and *de novo* assembly of a methicillin-resistant *Staphylococcus pseudintermedius* (MRSP) isolate

In this first study, and as a proof of concept of whole-genome sequencing for *de novo* assembly of bacterial genomes, we sequenced the genome of a multi-drug resistant *Staphylococcus pseudintermedius* isolate (G3C4) from canine otitis. **Figure 13** shows the methodology applied, from the sampling, to the microbiological culture and the final sequencing for *de novo* genome assembly using a hybrid approach with short (Illumina) and long reads (Nanopore).

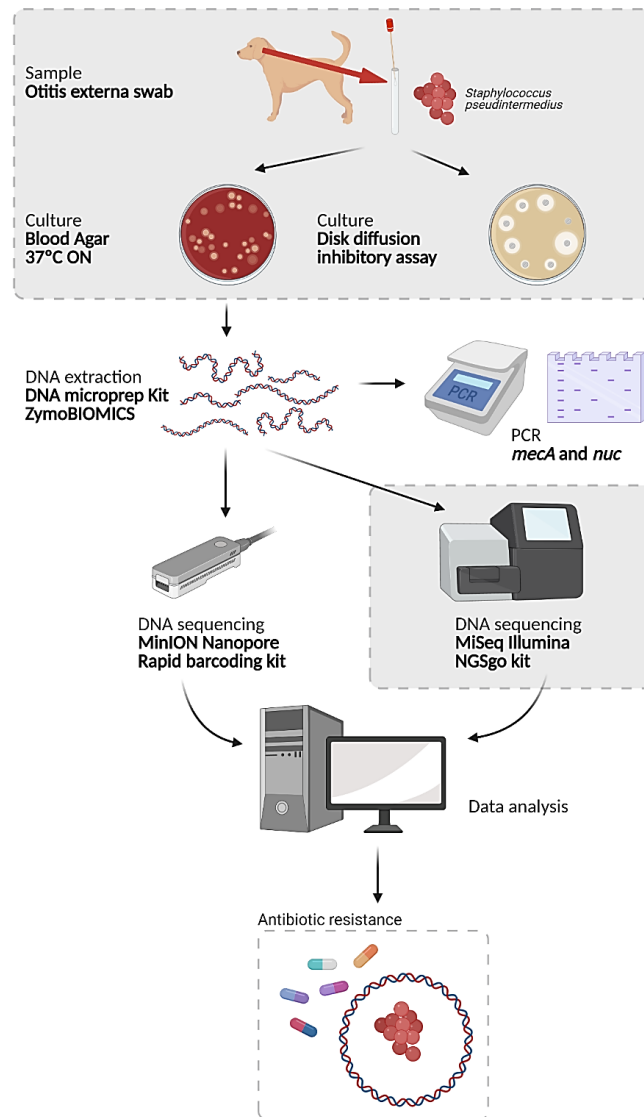


Figure 13. Whole-genome sequencing and *de novo* hybrid assembly of *S. pseudintermedius* isolated from canine otitis. Gray boxes include those techniques performed by third parties. Created in BioRender.com

After the microbiological culture and the antibiogram performed by LETI, we extracted the bacterial DNA and checked the amplification of (1) the *nuc* gene to confirm the species (expected fragment size 900 bp) and (2) the *mecA* gene responsible for the methicillin-resistance.

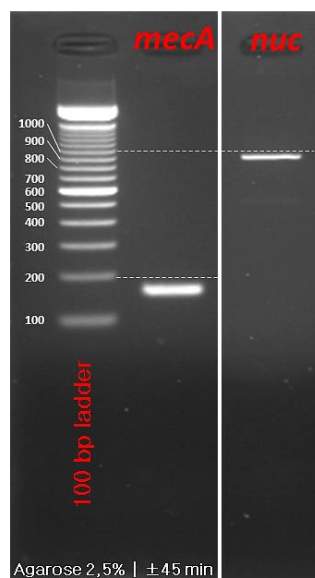


Figure 14. *mecA* and *nuc* genes PCRs results viewed using electrophoresis. Our isolate was *S. pseudintermedius* (~900 bp band in *nuc* gene electrophoresis) harboring methicillin resistance gene *mecA*.

Once confirmed that the isolate was a methicillin-resistant *S. pseudintermedius* (MRSP) (**Figure 14**), we proceeded with the whole-genome sequencing (WGS) with short-reads (Illumina) and long-reads (Nanopore) to *de novo* assemble the genome in a hybrid approach to increase the accuracy of error-prone nanopore reads. Two contigs with 60X coverage corresponded to a new *S. pseudintermedius* genome and a plasmid.

The G3C4 *S. pseudintermedius* isolate resulted in 2,717,621 bp genome size, with 37.5% G+C content. It contained 2,548 coding sequences (CDS), 59 tRNAs, and 19 rRNA copies (GenBank Accession: [CP032682.1](https://www.ncbi.nlm.nih.gov/nuccore/CP032682.1)). Moreover, it presented a completeness of 99.43%, and its MLST was ST71.

The plasmid was 4,439 bp long, with a G+C content of 30.07% (GenBank Accession: [MN612109.1](https://www.ncbi.nlm.nih.gov/nuccore/MN612109.1)). It blasted against a plasmid isolated from *Staphylococcus epidermidis*, pSE-12228-01 (NCBI accession number [NC_005008](https://www.ncbi.nlm.nih.gov/nuccore/NC_005008)) with 100% coverage and 99.9% identity.

The G3C4 *S. pseudintermedius* isolate was resistant to aminoglycosides (gentamycin and tobramycin); fluoroquinolones (ciprofloxacin, marbofloxacin, and pradofloxacin);

tetracyclines (tetracycline, doxycycline, and minocycline); macrolides (erythromycin); β -lactams (oxacillin and ceftiofur); lincosamides (clindamycin); and co-trimoxazole, as assessed by disk diffusion testing (**Table 7**).

Table 7. Summary of the antibiotic resistance determined by disk diffusion testing and its correspondence to sequencing results.

Antibiotic ^a	Susceptibility ^b	Genes or mutations associated	Location
Aminoglycosides			
GEN	R	<i>aac(6')-Ie-aph(2'')-Ia, aph(3')-IIIa, aad(6)</i>	Genome
TOB	R		
AMK	S		
Fluoroquinolones			
CIP	R	Point mutations in <i>gyrA</i>	Genome
MARBO	R		
PRADO	R		
ORBI	R		
Tetracyclines			
TET	R	<i>tet(K)</i>	Plasmid
DOX	R		
MIN	R		
Macrolide			
ERY	R	<i>erm(B)</i>	Genome
Beta-lactams			
OXA	R	<i>mecA, blaZ</i>	Genome
FOX	R		
Lincosamide			
CLI	R	<i>erm(B)</i>	Genome
Phenicol			
CHL	S		
FFC	S		
Rifamycin			
RIF	S		
Fusidane			
FD	S		
SXT	R	<i>dfpG</i>	Genome

WGS allowed to describe the genes and point mutations that conferred the aforementioned resistant phenotype. Located in the genome (**Figure 15**) were found *blaZ* and *mecA* genes conferring resistance to β -lactams; *aac(6')-Ie-aph(2'')-Ia, aph(3')-IIIa, and aad(6)* to aminoglycosides; *ermB* to erythromycin and clindamycin; and *dfpG* to trimethoprim (one of the components of co-trimoxazole). Moreover, point mutations in the topoisomerase *gyrA* gene positions 12, 214, 251, and 2032 explained the resistance to fluoroquinolones. In addition, despite not assessed phenotypically, we detected the *sat4* gene, which confers

resistance to streptothricin. Finally, the plasmid harbored the *tet(K)* gene that conferred the resistance to tetracycline.

Regarding *mecA* gene, it was located in a *SCCmec* II-III cassette, which is characteristic of *S. pseudintermedius* ST71. Moreover, five other genes (*aph(3')-IIIa*, *sat4*, *aad(6)*, *ermB*, and *dfrG*) were held in a cluster, as has previously been reported (Derbise et al., 1997).

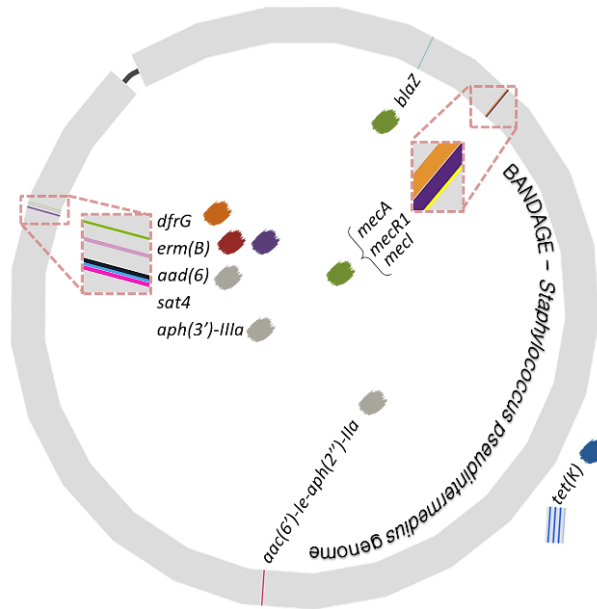


Figure 15. Representation of G3C4 *S. pseudintermedius* genome, and location of the antibiotic resistance genes retrieved by Abricate.

These results were published in Microbiology Resource Announcements “Hybrid Assembly from a Pathogenic Methicillin- and Multidrug-Resistant *Staphylococcus pseudintermedius* Strain Isolated from a Case of Canine Otitis in Spain” (Viñes et al., 2020) (**Annex 1**).

4.2. Whole-genome sequencing and *de novo* assembly of *Staphylococcus pseudintermedius* isolated from dogs with pyoderma and healthy dogs

Once optimized the hybrid genome assembly for *S. pseudintermedius* isolates, we aimed to test Nanopore-only WGS for *de novo* assembly of *S. pseudintermedius* genomes. In that case, isolates were from the lesional skin of dogs with pyoderma and from healthy dogs. The study design and methodology are shown in **Figure 16**.

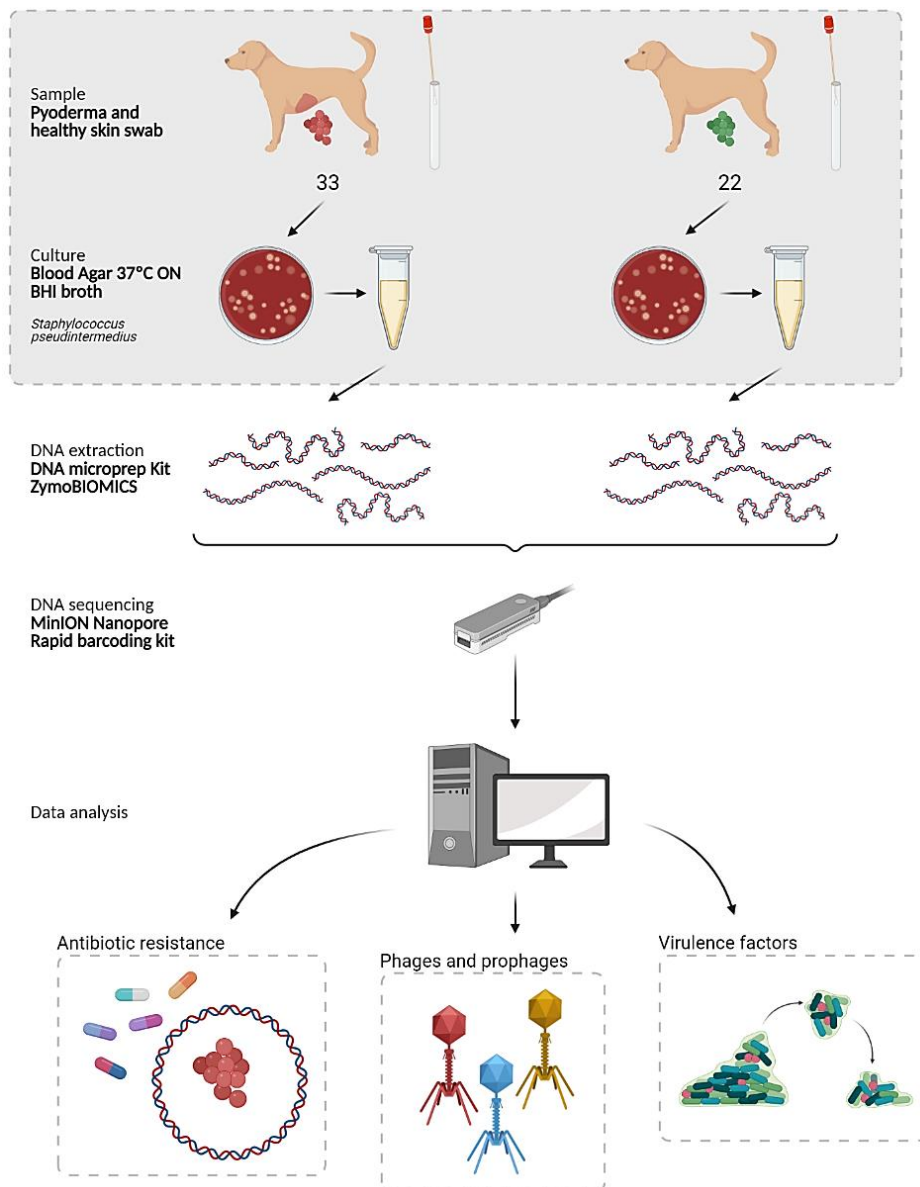


Figure 16. Whole-genome sequencing and *de novo* assembly of 55 genomes of *S. pseudintermedius* isolated from dogs with pyoderma and healthy dogs. Gray boxes include those techniques performed by third parties. Created in BioRender.com

We aimed to characterize *S. pseudintermedius* isolates in health and disease, their genomes, antimicrobial resistance genes, virulence factors genes, and prophages. We gathered 32 isolates from Spain, 19 from Italy, and four from Argentina. Samples from dogs with pyoderma (Disease, D; n= 33) were isolated from abdominal swabs of lesional skin, whereas samples from healthy dogs (Healthy, H; n= 22) were obtained from abdominal swabs and the perioral area. Perioral samples were taken to represent one of the most common isolation site for *S. pseudintermedius*.

Using Nanopore-only data, we *de novo* assembled high quality genomes, with an average of 249X coverage and completeness higher than 96% (ranging from 96.73% for H_SP082, to 99.43% for several isolates) (**Table 8 and 9**). Genomes sizes ranged from 2,512,726 bp for H_SP136, to 2,991,046 bp for D_G062, with an average size of 2,677,381 bp. Isolates from dogs with pyoderma had an average genome size larger than isolates from healthy dogs, with 2,742,915 bp versus 2,579,081 bp, respectively. Accordingly, average CDS number was higher in isolates from dogs with pyoderma (2,565) (**Table 8**) than in isolates from healthy dogs (2,362) (**Table 9**).

The complete information about the genomes has been published in Microbiology Resource Announcements in the paper “Whole-genome sequencing and *de novo* assembly of 61 *Staphylococcus pseudintermedius* isolates from healthy dogs and dogs with pyoderma” (Francino et al., 2021) (**annex 2**).

The main MLST retrieved from dogs with pyoderma was ST71 for 15/33 isolates, followed by ST258 for 4/33 isolates. A total of nine isolates from pyoderma possessed a MLST that had not been previously described (unk., unknown in **Table 8**). The remaining five pathogenic isolates were ST301, ST503, ST611, ST1631, and ST1827. In healthy dogs, 19/22 isolates had a non-previously described MLST and the remaining three isolates were ST257, ST1061, and ST1248 (**Table 9**). So, while 24/33 of the isolates from dogs with pyoderma belonged to an already described MLST, being ST71 the predominant one, only 3/22 of the *S. pseudintermedius* isolates from healthy dogs were attributed to a known MLST.

Table 8. Characteristics of the genome assemblies from the 33 *S. pseudintermedius* isolated from pyoderma. All these genomes are submitted at NCBI under the bioproject accession number [PRJNA685966](https://www.ncbi.nlm.nih.gov/bioproject/PRJNA685966). ASP, abdominal superficial pyoderma; I, Italy; S, Spain; A, Argentina; Cov, coverage; Compl, completeness; CDS, coding sequences.

Isolate	Source	Country	Genome size	Cov	GC %	MLST	Compl %	CDS
D_G040	ASP	I	2,564,892	664x	0.38	Unk.	99.43	2,369
D_G050	ASP	I	2,637,713	326x	0.38	Unk.	99.43	2,429
D_G059	ASP	I	2,573,568	223x	0.38	Unk.	99.29	2,364
D_G062	ASP	I	2,991,046	253x	0.37	ST71	99.43	2,901
D_G063	ASP	I	2,981,523	256x	0.37	ST71	99.43	2,891
D_G064	ASP	I	2,895,060	361x	0.37	ST71	99.43	2,764
D_G066	ASP	I	2,808,032	213x	0.37	ST71	99.43	2,639
D_G067	ASP	I	2,896,399	533x	0.37	ST71	99.43	2,776
D_G071	ASP	I	2,807,986	85x	0.37	ST71	99.43	2,644
D_G072	ASP	I	2,837,133	304x	0.37	ST71	99.43	2,690
D_G076	ASP	I	2,780,144	323x	0.37	ST258	99.43	2,573
D_G077	ASP	I	2,791,496	479x	0.37	ST71	99.43	2,624
D_G078	ASP	I	2,799,396	208x	0.37	ST71	99.43	2,637
D_G081	ASP	I	2,694,747	353x	0.38	ST301	99.43	2,519
D_G082	ASP	I	2,626,557	259x	0.38	ST258	99.43	2,396
D_G089	ASP	I	2,797,937	281x	0.37	ST71	99.43	2,628
D_G093	ASP	I	2,648,891	39x	0.38	ST258	99.43	2,433
D_G094	ASP	I	2,849,103	191x	0.37	ST71	99.43	2,675
D_G099	ASP	I	2,623,014	168x	0.38	Unk.	99.43	2,416
D_SP020	ASP	S	2,793,830	213x	0.37	ST71	99.15	2,637
D_SP021	ASP	S	2,795,724	197x	0.37	ST71	99.43	2,637
D_SP022	ASP	S	2,767,901	174x	0.37	Unk.	98.86	2,555
D_SP024	ASP	S	2,762,026	289x	0.38	ST611	99.43	2,595
D_SP025	ASP	S	2,805,515	295x	0.37	ST71	99.43	2,641
D_SP026	ASP	S	2,567,628	303x	0.38	ST503	99.43	2,387
D_SP027	ASP	S	2,717,194	352x	0.37	Unk.	99.43	2,537
D_SP028	ASP	S	2,575,420	238x	0.38	Unk.	98.86	2,367
D_SP029	ASP	S	2,723,805	270x	0.37	ST258	99.43	2,517
D_SP030	ASP	A	2,612,059	164x	0.38	Unk.	99.43	2,386
D_SP032	ASP	A	2,670,199	119x	0.37	ST1631	98.66	2,449
D_SP034	ASP	A	2,550,368	204x	0.38	ST1827	99.43	2,319
D_SP035	ASP	A	2,642,865	117x	0.38	Unk.	99.43	2,489
D_SP036	ASP	S	2,927,015	129x	0.37	ST71	99.43	2,755

Table 9. Characteristics of the genome assemblies from the 22 *S. pseudintermedius* isolated from healthy dogs. All these genomes are submitted at NCBI under the bioproject accession number [PRJNA685966](https://www.ncbi.nlm.nih.gov/bioproject/PRJNA685966). AH, abdominal healthy; PH, perioral healthy; S, Spain; Cov, coverage; Compl, completeness; CDS, coding sequences.

Isolate	Source	Country	Genome size	Cov	GC %	MLST	Compl %	CDS
H_SP079	PH	S	2,587,693	301x	0.38	Unk.	99.43	2,337
H_SP080	PH	S	2,587,506	199x	0.38	Unk.	99.41	2,336
H_SP081	PH	S	2,621,254	94x	0.38	Unk.	98.58	2,467
H_SP082	PH	S	2,620,663	149x	0.38	Unk.	96.73	2,466
H_SP093	AH	S	2,590,335	274x	0.38	Unk.	99.43	2,361
H_SP094	AH	S	2,570,595	550x	0.38	Unk.	99.43	2,337
H_SP095	AH	S	2,575,879	341x	0.38	Unk.	99.43	2,360
H_SP096	AH	S	2,578,330	89x	0.38	Unk.	99.43	2,359
H_SP097	AH	S	2,575,223	136x	0.38	Unk.	99.43	2,356
H_SP118	AH	S	2,512,855	313x	0.38	Unk.	99.43	2,277
H_SP125	AH	S	2,551,473	327x	0.38	ST1248	98.86	2,330
H_SP127	PH	S	2,690,618	162x	0.38	ST1061	98.86	2,507
H_SP132	PH	S	2,515,164	132x	0.38	Unk.	98.72	2,275
H_SP134	PH	S	2,514,594	146x	0.38	Unk.	98.86	2,274
H_SP135	AH	S	2,512,727	154x	0.38	Unk.	98.86	2,277
H_SP136	AH	S	2,512,726	104x	0.38	Unk.	98.86	2,274
H_SP137	AH	S	2,512,757	224x	0.38	Unk.	99.43	2,271
H_SP138	AH	S	2,512,830	227x	0.38	Unk.	98.86	2,277
H_SP140	PH	S	2,597,272	296x	0.38	Unk.	99.24	2,387
H_SP141	PH	S	2,622,529	150x	0.38	ST257	99.43	2,450
H_SP142	PH	S	2,597,098	461x	0.38	Unk.	99.43	2,393
H_SP143	PH	S	2,779,670	293x	0.38	Unk.	98.86	2,589

Analyses of antibiotic resistance genes, prophages, and virulence factors

We found that 27/33 isolates from dogs with pyoderma presented a multi-drug resistant (MDR) genotype (resistant to ≥ 3 different classes of antibiotics): all the ST71 and ST258 (15 and 4, respectively), ST301, ST611, ST1631, and five with an unknown MLST. In contrast, only 2/22 isolates from healthy dogs were MDR, both with an unknown MLST (**Table 10**). We retrieved antibiotic resistance genes (ARGs) conferring resistance to β -lactams, *mecA*, *mecI*, *mecR*, and *blaZ*; aminoglycosides, *aac(6')-Ie-aph(2'')*-Ia, *aad(6)*, *aph(3')-IIIa*; trimethoprim, *dfrG*; chloramphenicol, *cat*; macrolides and lincosamides, *ermA*, *ermB*, *lnuA*; streptothricin, *sat4*; and tetracycline, *tetK*, *tetM*.

Table 10. Antibiotic resistance genes and plasmid replicons associated to the 55 *S. pseudintermedius* (33 from disease dogs, and 22 from healthy dogs). For each isolate it is indicated if it is genotypically MDR, its MLST, the number of prophages in the genome, and the SCCmec type.

	<i>mecA</i>	<i>mecI</i>	<i>mecR1</i>	<i>blaZ</i>	<i>aac(6)-Ic-aph(2'')-Ia</i>	<i>aad(6)</i>	<i>aph(3)-IIIa</i>	<i>dhfG</i>	<i>cat</i>	<i>ermA</i>	<i>ermB</i>	<i>lnuA</i>	<i>sat4</i>	<i>tetK</i>	<i>tetM</i>	Genot. MDR	MLST	Phigaro	SCCmec type	rep21_14_rep(pKH21)	rep21_2_rep(pNVH01)	rep7_1_repC(Cassette)	rep7_7_rep(pKH7)
D_G063																	71	9	II-III				
D_G071																	71	5	II-III				
D_G078																	71	5	II-III				
D_G089																	71	5	II-III				
D_G062																	71	9	II-III				
D_G066																	71	5	II-III				
D_G094																	71	5	II-III				
D_G067																	71	8	II-III				
D_G064																	71	7	II-III				
D_G072																	71	6	II-III				
D_G077																	71	6	II-III				
D_SP020																	71	5	II-III				
D_SP021																	71	5	II-III				
D_SP025																	71	6	II-III				
D_SP036																	71	5	II-III				
D_G093																	258	2	IVg				
D_G076																	258	1	IVg				
D_SP029																	258	1	IVg				
D_G081																	301	2	IVg				
D_G082																	258	1	IVg				
D_SP026																	503	1					
D_SP024																	611	3					
D_SP032																	1631	1	no				
D_SP034																	1827	0					
D_G099																	Unk.	1					
D_G050																	Unk.	2					
D_SP022																	Unk.	3	no				
D_SP028																	Unk.	1					
D_SP035																	Unk.	2					
D_G040																	Unk.	1					
D_G059																	Unk.	1					
D_SP027																	Unk.	2					
D_SP030																	Unk.	1					
H_SP141																	257	2					
H_SP125																	1061	1					
H_SP118																	1248	0					
H_SP079																	Unk.	0					
H_SP080																	Unk.	0					
H_SP140																	Unk.	1					
H_SP142																	Unk.	1					
H_SP081																	Unk.	3					
H_SP082																	Unk.	3					
H_SP127																	Unk.	2					
H_SP093																	Unk.	2					
H_SP094																	Unk.	2					
H_SP095																	Unk.	2					
H_SP096																	Unk.	2					
H_SP097																	Unk.	2					
H_SP132																	Unk.	0					
H_SP134																	Unk.	0					
H_SP135																	Unk.	0					
H_SP136																	Unk.	0					
H_SP137																	Unk.	0					
H_SP138																	Unk.	0					
H_SP143																	Unk.	5					

Specifically, *mecA* gene –conferring resistance to methicillin– was detected in 22/33 of the isolates from dogs with pyoderma, all ST71 and ST258 (15 and 4, respectively), ST301, ST1631, and one with an unknown MLST. All the isolates that contained *mecA* were MDR. In addition, *mecI* and *mecR1* genes were present in the isolates that harbored *mecA*, with the exception of the four isolates belonging to the ST258, and the ST301 isolate. All the ST71 isolates presented the *mecA* in a SCCmec type II-III, whereas MLST ST258 and ST301 isolates presented the gene in a SCCmec type IV. It is worthy to highlight that SCCmec type III from *S. aureus* corresponds to SCCmec type II-III for *S. pseudintermedius*. The CARD database contains only SCCmec types from *Staphylococcus aureus*, and SCCmec type II-III is characteristic from *S. pseudintermedius*, which explains the lower identity for the *mecA* cassette for ST71 isolates in Table 10.

Focusing on the other antimicrobial resistance genes, *aad(6)*, *aph(3')-IIIa*, *ermB*, *sat4*, and *dfiG* genes were held in the transposon Tn5405 in ST71, ST258, and ST301 isolates. Moreover, ST71 and ST301 isolates also presented the *aac(6')-Ie-aph(2'')-Ia*, which confers resistance to aminoglycosides, presumably carried by another transposon, Tn5281.

Conversely to what has been explained above for the SSCmec cassette and the Tn5404 transposon, tetracycline resistance genes (*tetK* and *tetM*) were not uniformly spread across STs. Three ST71 (D_G062, D_G066, and D_G094) and one ST258 (D_G029) isolates harbored *tetK* gene in another contig rather than the chromosome, which was probably a plasmid because it also harbored a replicon (*rep7_1_repC*) and shows high nucleotide identity with plasmid pSP-G3C4 ([MN612109.1](#)) that was previously identified and characterized in our *S. pseudintermedius* G3C4 isolate from canine otitis (**Table 11**).

tetK plasmids coded only for three genes: the resistance gene and two proteins involved in replication. *tetM* gene was harbored in the chromosome. Finally, isolates that presented the *cat* gene –conferring resistance to chloramphenicol– were all from dogs with pyoderma (five ST71, and two unknown ST). They harbored the *cat* gene in the same contig as replicon *rep7_7_rep(pKH7)*, suggesting it is probably linked to a plasmid (**Table 11**). *cat*-harboring plasmids also coded for two other elements besides the resistance gene: a plasmid recombination enzyme and a replicative protein.

Table 11. NCBI BLAST results of the contigs that are putative plasmids. Contigs harboring *tetK* gene aligned to [MN612109.1](#); assembly did not retrieve a full-length plasmid for isolate D_G066, and misassembled two plasmids for isolates D_G093 and D_G094. Contigs harboring *cat* gene aligned to [CP016074.1](#); three plasmids presented two copies of the replicon rep7_7_rep(pKH7), which points to a misassemble.

Contigs containing *tetK* gene and rep7_1_repC replicon

Isolate	Contig size	Contig BLAST	BLAST Size (bp)	Query COV %	ID %	Accession	Comments
D_G062	4,419 bp	<i>S. pseudintermedius</i> G3C4 plasmid pSP-G3C4	4,439	100	99.94	GCF_016482085.1	
D_G066	2,613 bp	<i>S. pseudintermedius</i> G3C4 plasmid pSP-G3C4	4,439	100	100	GCF_016482585.1	Partial assembly
D_G093	8,828 bp	<i>S. pseudintermedius</i> G3C4 plasmid pSP-G3C4	4,439	100	99.98	GCF_016481905.1	2 replicons
D_G094	8,431 bp	<i>S. pseudintermedius</i> G3C4 plasmid pSP-G3C4	4,439	100	99.98	GCF_016481855.1	2 replicons

Contigs containing *cat* gene and rep7_7_rep(pKH7)

Isolate	Contig size	Contig BLAST	BLAST Size (bp)	Query COV %	ID %	Accession	Comments
D_G062	3,968 bp	<i>S. pseudintermedius</i> 081661 plasmid unnamed1	3,785	100	93.81	GCF_016482085.1	
D_G063	3,769 bp	<i>S. pseudintermedius</i> 081661 plasmid unnamed1	3,785	100	92.47	GCF_016482045.1	
D_G071	7,023 bp	<i>S. pseudintermedius</i> 081661 plasmid unnamed1	3,785	100	94.28	GCF_016482425.1	2 replicons
D_G078	4,222 bp	<i>S. pseudintermedius</i> 081661 plasmid unnamed1	3,785	100	94.33	GCF_016481935.1	
D_G089	4,075 bp	<i>S. pseudintermedius</i> 081661 plasmid unnamed1	3,785	97	94.92	GCF_016481925.1	

Another difference between *S. pseudintermedius* isolates from healthy dogs and dogs with pyoderma was the presence of phages and prophages. Isolates from healthy dogs contained an average of 1.27 phage-related sequences; however, isolates from dogs with pyoderma contained an average of 3.55 sequences. When considering only ST71 isolates, the average raises to 6.07 sequences. Specifically, all our ST71 *S. pseudintermedius* harbored the SpST71A prophage disrupting the *comG* operon, which is involved in the uptake of foreign DNA through the phenomena of bacterial transformation.

To detect VF genes, we used a custom database (available at <http://doi.org/10.17605/OSF.IO/NS3Y4>) containing 58 VF that belonged to different categories. A total number of 50 VFs were identified distributed among the 55 isolates (Table 12).

Table 12. Virulence factor genes with a variable distribution between isolates. We observed a total of 50 VF distributed in *S. pseudintermedius* isolates. This table shows those VF (n=17) that were not present in all isolates.

	MLST	<i>spsD</i>	<i>spsF</i>	<i>spsI</i>	<i>spsK</i>	<i>spsL</i>	<i>spsM</i>	<i>spsO</i>	<i>spsP</i>	<i>spsQ</i>	<i>spsR</i>	<i>exi</i>	<i>expB</i>	<i>se-int</i>	<i>seccanine</i>	<i>coa</i>	<i>htrA</i>	<i>nanB</i>
D_G062	ST71																	
D_G063	ST71																	
D_G064	ST71																	
D_G066	ST71																	
D_G067	ST71																	
D_G071	ST71																	
D_G072	ST71																	
D_G077	ST71																	
D_G078	ST71																	
D_G089	ST71																	
D_G094	ST71																	
D_SP020	ST71																	
D_SP021	ST71																	
D_SP025	ST71																	
D_SP036	ST71																	
D_G076	ST258																	
D_G082	ST258																	
D_G093	ST258																	
D_SP029	ST258																	
D_G081	ST301																	
D_SP026	ST503																	
D_SP024	ST611																	
D_SP032	ST1631																	
D_SP034	ST1827																	
D_G040	Unk.																	
D_G050	Unk.																	
D_G059	Unk.																	
D_G099	Unk.																	
D_SP022	Unk.																	
D_SP027	Unk.																	
D_SP028	Unk.																	
D_SP030	Unk.																	
D_SP035	Unk.																	
H_SP141	ST257																	
H_SP127	ST1061																	
H_SP125	ST1248																	
H_SP079	Unk.																	
H_SP080	Unk.																	
H_SP081	Unk.																	
H_SP082	Unk.																	
H_SP093	Unk.																	
H_SP094	Unk.																	
H_SP095	Unk.																	
H_SP096	Unk.																	
H_SP097	Unk.																	
H_SP118	Unk.																	
H_SP132	Unk.																	
H_SP134	Unk.																	
H_SP135	Unk.																	
H_SP136	Unk.																	
H_SP137	Unk.																	
H_SP138	Unk.																	
H_SP140	Unk.																	
H_SP142	Unk.																	
H_SP143	Unk.																	

From these 50 VFs, 33 of them were present in all 55 isolates, comprising surface proteins *spsA*, *spsB*, *spsC*, *spsE*, *spsG*, *spsH*, and *spsN*; exfoliative toxins *siet*, and *speta*; accessory gene regulators *agrA*, *agrB*, *agrC*, and *agrD*; intercellular adhesion proteins *icaA*, *icaB*, *icaC*, and *icaD*; phenol-soluble modulins *psma*, *psm β* , *psm δ* , and *psm ϵ* ; leukocidin *lukF-I*, and *lukS-I*; response regulators *saeR*, and *saeS*; ATP-dependent proteases *clpP*, *clpX*; elastin-binding protein *ebpS*; RNA polymerase σ -B factor *sigB*; β *hly*; thermonuclease *nucC*; repressor of toxins *rot*; and Staphylococcal accessory regulator *sarA*. Even though there are no differences between the VF content of isolates from dogs with pyoderma versus isolates from healthy dogs, it's noteworthy that four genes coding for surface proteins (*spsD*, *spsF*, *spsP*, and *spsQ*) involved in colonization by binding to the host's extracellular matrix were only present on isolates from the lesional skin of dogs with pyoderma.

Pangenome analysis of *Staphylococcus pseudintermedius* isolates

We performed the pangenome analyses of *S. pseudintermedius* isolates of healthy dogs and *S. pseudintermedius* isolates from the lesional skin of dogs with pyoderma. Within each pangenome we find the core genome, which comprises the genes shared by all the individuals of the group; and the accessory genome, which comprises the genes that are present in at least one (singleton), but not all the individuals of the group.

For the isolates from healthy dogs, a total number of 3,273 gene clusters were described (Figure 17). Whereas the core genome represented the 64.1% (2,098) of the gene clusters, the accessory genome represented the 35.9% (848 for the accessory, and 327 for the singletons).

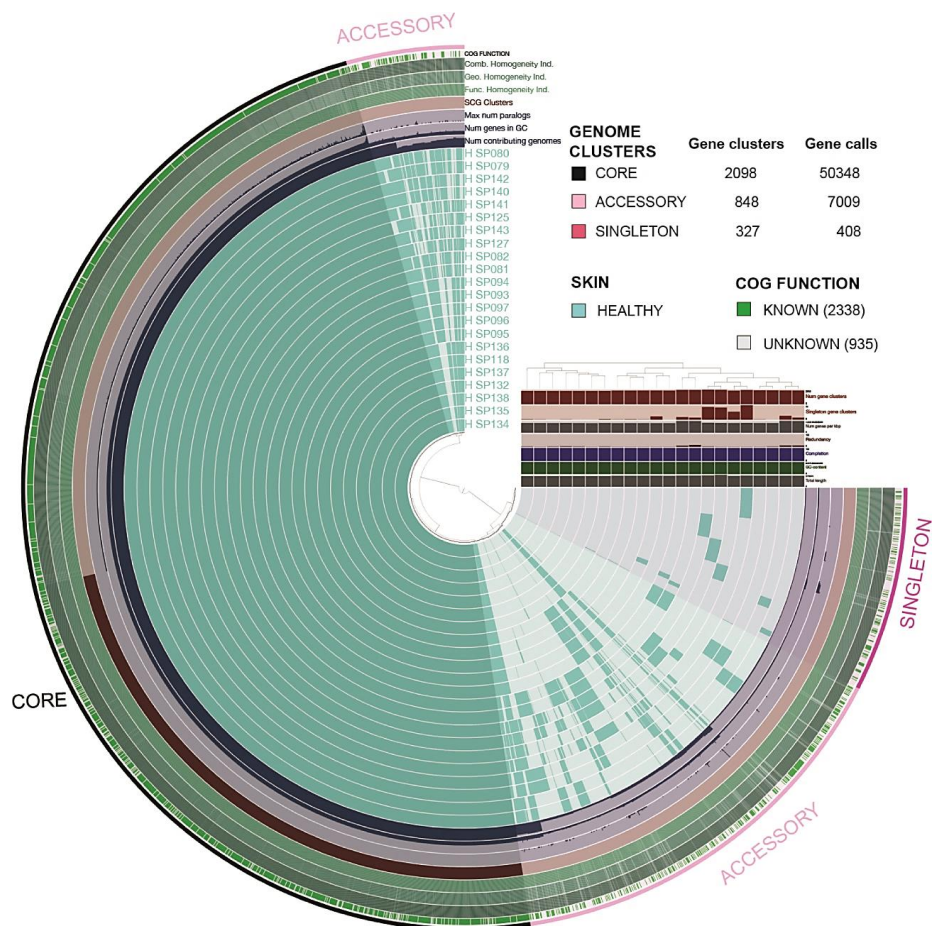


Figure 17. Pangenome visualization of the 22 isolates from healthy dogs. Core genome is present and shared by all 22 *S. pseudintermedius* genomes within the pangenome (2,098 gene clusters; 50,348 ORFs/Gene Callings). Accessory genome contains 848 gene clusters; 7,009 ORFs/Gene Callings. Singleton contains 327 unique gene clusters; 408 ORFs/Gene Callings

On the other hand, isolates from dogs with pyoderma presented 3,906 gene clusters (**Figure 18**), from which 53.5% (2,088) were core genome, and 46.5% (1,331 accessory plus 487 singleton) were accessory genome. So, isolates from dogs with pyoderma presented a larger accessory genome (46.5%) compared with isolates from healthy dogs (35.9%).

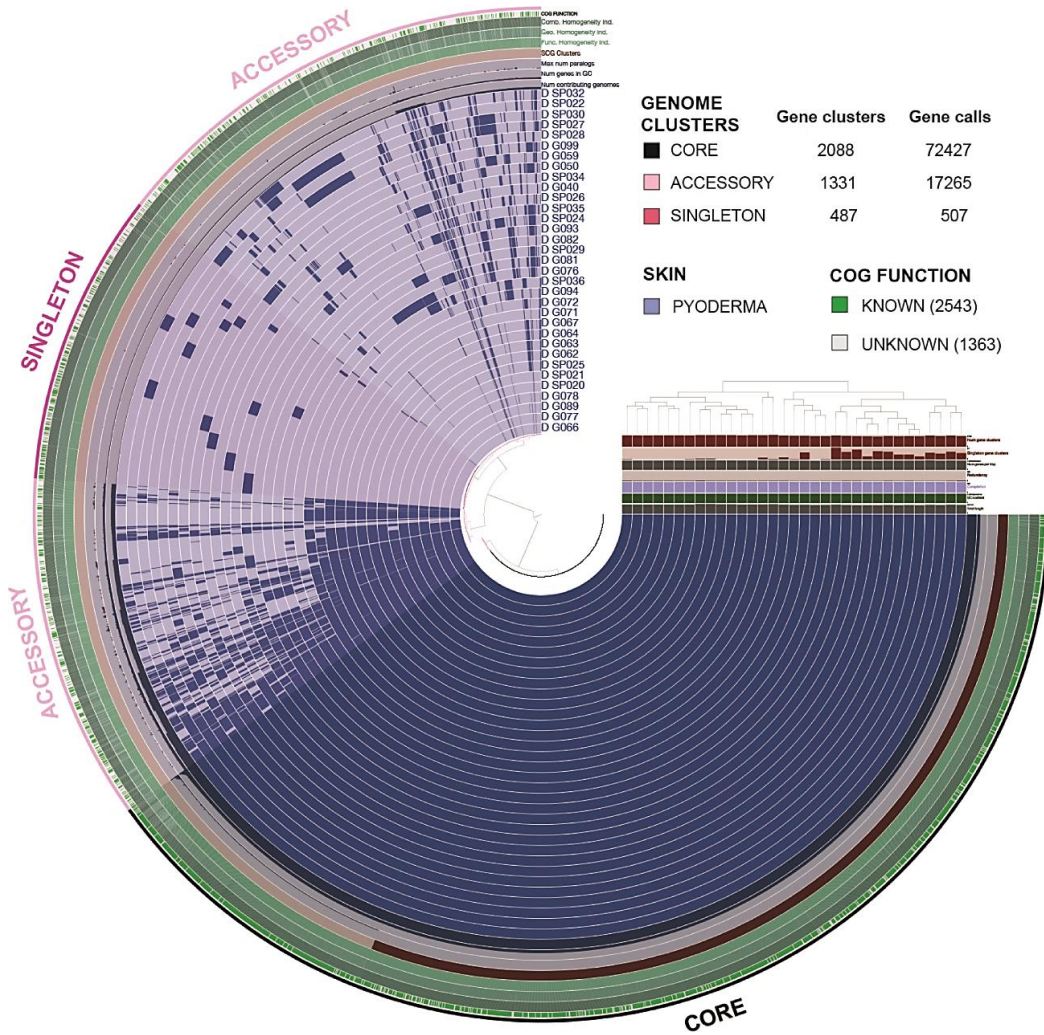


Figure 18. Pangenome visualization of the 33 isolates from dogs with pyoderma. Core genome is present and shared by all 33 *S. pseudintermedius* genomes within the pangenome (2,088 gene clusters; 72,427 ORFs/Gene Callings). Accessory genome contains 1,331 gene clusters; 17,265 ORFs/Gene Callings. Singleton contains 487 unique gene clusters; 507 ORFs/Gene Callings.

Anvi'o functional analysis identified enriched functions in isolates from dogs with pyoderma (**Table 13**) and in healthy dogs (**Table 14**). Isolates from dogs with pyoderma are enriched in mobilome category (e.g., plasmid and phage functions). Another relevant enriched function, corresponded to aminoglycoside phosphotransferase, a type of antibiotic resistance. In contrast, isolates from healthy dogs presented enhanced functions related with cell defense, with enriched CRISPR/Cas, restriction-modification systems, and recombination and repair functions.

Table 13. Enriched functions in *S. pseudintermedius* isolated from pyoderma. COG categories: E, Amino acid transport and metabolism; F, Nucleotide transport and metabolism; H, Coenzyme transport and metabolism; J, Translation, ribosomal structure, and biogenesis; L, Replication, recombination, and repair; R, General function prediction only; S, Function unknown; V, Defense mechanisms; X, mobilome: prophages, transposons.

COG FUNCTION	Adjusted q-value	Function accession	COG Category
Phage antirepressor protein YoqD, KilAC domain	4.09E-03	COG3645	X
Phage-related tail protein	6.30E-03	COG5283	X
Prophage pi2 protein 07	6.55E-03	COG4707	X
Phage-related holin (Lysis protein)	7.25E-03	COG4824	X
Phage-related protein	3.16E-02	COG4722	X
Predicted P-loop ATPase and inactivated derivatives	0.05	COG5545	X
Phage terminase large subunit	0.05	COG1783	X
Toxin component of the Txe-Axe toxin-antitoxin module, Txe/YoeB family	2.86E-04	COG4115	V
Predicted nuclease of the RNase H fold, HicB family	6.30E-03	COG1598	V
5-methylcytosine-specific restriction endonuclease McrBC, GTP-binding regulatory subunit McrB	1.09E-02	COG1401	V
DNA polymerase I - 3'-5' exonuclease and polymerase domains	1.93E-03	COG0749	L
RecB family exonuclease	6.55E-03	COG2887	L
Holliday junction resolvase RusA (prophage-encoded endonuclease)	9.49E-03	COG4570	L
Aminoglycoside phosphotransferase	4.06E-06	COG3231	J
Predicted subunit of tRNA(5-methylaminomethyl-2-thiouridylate) methyltransferase, contains the PP-loop ATPase domain	1.41E-02	COG2117	J
Acyl dehydratase	2.26E-04	COG2030	I
3-hydroxy-3-methylglutaryl CoA synthase	2.26E-04	COG3425	I
Zn-dependent peptidase ImmA, M78 family	8.79E-04	COG2856	E
Lysophospholipase L1 or related esterase	9.49E-03	COG2755	E
Uncharacterized protein, DUF927 family	2.26E-04	COG5519	S
Predicted phosphoadenosine phosphosulfate sulfurtransferase, contains C-terminal DUF3440 domain	1.41E-02	COG3969	R
Pyrimidine reductase, riboflavin biosynthesis	2.40E-05	COG1985	H
ADP-ribose pyrophosphatase YjhB, NUDIX family	1.41E-02	COG1051	F

Table 14. Enriched functions in *S. pseudintermedius* from isolates of healthy dogs. COG categories: C, Energy production and conversion; L, Replication, recombination, and repair; R, General function prediction only; S, Function unknown; V, Defense mechanisms.

COG FUNCTION	Adjusted q-value	Function accession	COG Category
CRISPR/Cas system Type II associated protein, contains McrA/HNH and RuvC-like nuclease domains	1.15E-02	COG3513	V
CRISPR/Cas system-associated protein Cas2, endoribonuclease	1.69E-02	COG3512	V
CRISPR/Cas system-associated endonuclease Cas1	1.69E-02	COG1518	V
mRNA-degrading endonuclease RelE, toxin component of the RelBE toxin-antitoxin system	2.76E-02	COG2026	V
Type I site-specific restriction endonuclease, part of a restriction-modification system	2.76E-02	COG4096	V
Predicted ATP-dependent endonuclease of the OLD family, contains P-loop ATPase and TOPRIM domains	2.13E-02	COG3593	L
Site-specific DNA-adenine methylase	2.76E-02	COG0338	L
DNA modification methylase	3.28E-02	COG0863	L
Uncharacterized membrane protein YozV, TM2 domain	3.49E-02	COG2314	S
TctA family transporter	8.79E-04	COG3333	R
Tripartite-type tricarboxylate transporter, receptor component TctC	2.76E-02	COG3181	C

In summary, *S. pseudintermedius* isolates from dogs with pyoderma presented a larger genome than isolates from healthy dogs (W = 636, P-value = 4.883e-07) most likely explained by the higher number of phages (W = 173, P-value = 0.0009233), antibiotic resistance genes (W = 68.5, P-value = 4.753e-07) and their associated sequences (for example ARGs associated to transposons) and other functional and pathogenesis related genes. In contrast, VFs do not seem to have an effect on differences in size since both categories of isolates present almost the same type and number of genes (W = 451, P-value = 0.1209) (**Figure 19**).

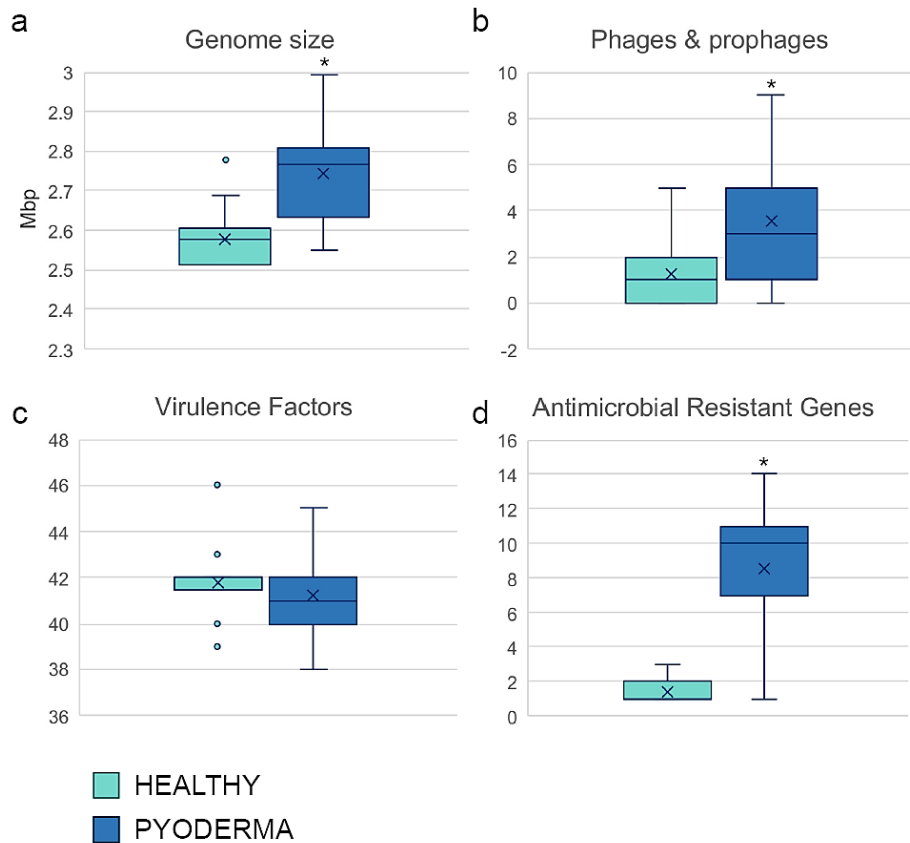


Figure 19. *S. pseudintermedius* isolated from pyoderma (darker blue) presented significant larger genomes when compared with isolates from healthy dogs (turquoise). Box plots show the distribution of the (a) genome size, (b) phage and prophage numbers, (c) virulence factor genes numbers, and (d) antimicrobial resistant gene. Asterisks denote statistical differences between healthy and pyoderma.

A paper titled “Whole genome sequencing and *de novo* assembly of *Staphylococcus pseudintermedius*: a pangenome approach to unravelling pathogenesis of canine pyoderma” including these results is under revision in Veterinary Dermatology (**annex 3**).

4.3. Transmission of similar *mcr-1* carrying plasmids among different *Escherichia coli* lineages in a mixed farm

In this study we used WGS in a hybrid approach (Nanopore and Illumina data) to analyze *E. coli* isolates resistant to colistin, a type of polymyxin categorized as a last-resort antibiotic in human health. The study aimed to characterize the transmission of the *mcr-1* gene conferring resistance to colistin in a mixed farm and specifically unravel how it was transmitted to a human isolate (**Figure 20**).

Out of 210 fecal samples from bovine, porcine and the farmer from the same facilities, 41 samples grew on McConkey agar supplemented with colistin, confirming the isolates were colistin-resistant *E. coli*. PCR confirmed the presence of *mcr-1* gene in 18 *Escherichia coli* isolates: 13 isolated from calves, four from pigs, and one from the farmer.

All the colistin-resistant isolates were also resistant to ampicillin, ciprofloxacin, streptomycin, chloramphenicol, sulphamethoxazole, and trimethoprim. Furthermore, 17/18 exhibited resistance to tetracycline, 16/18 to nalidixic acid and florfenicol, 14/18 to kanamycin, and 13/18 to gentamicin. Finally, phenotypic resistance to cephalosporines was observed: three isolates were resistant to cefotaxime, and two isolates were resistant to ceftazidime. All the isolates were MDR. These results were performed by the CRESA collaborators (**Figure 20**). For further information, see Viñes et al., 2021 (**annex 4**).

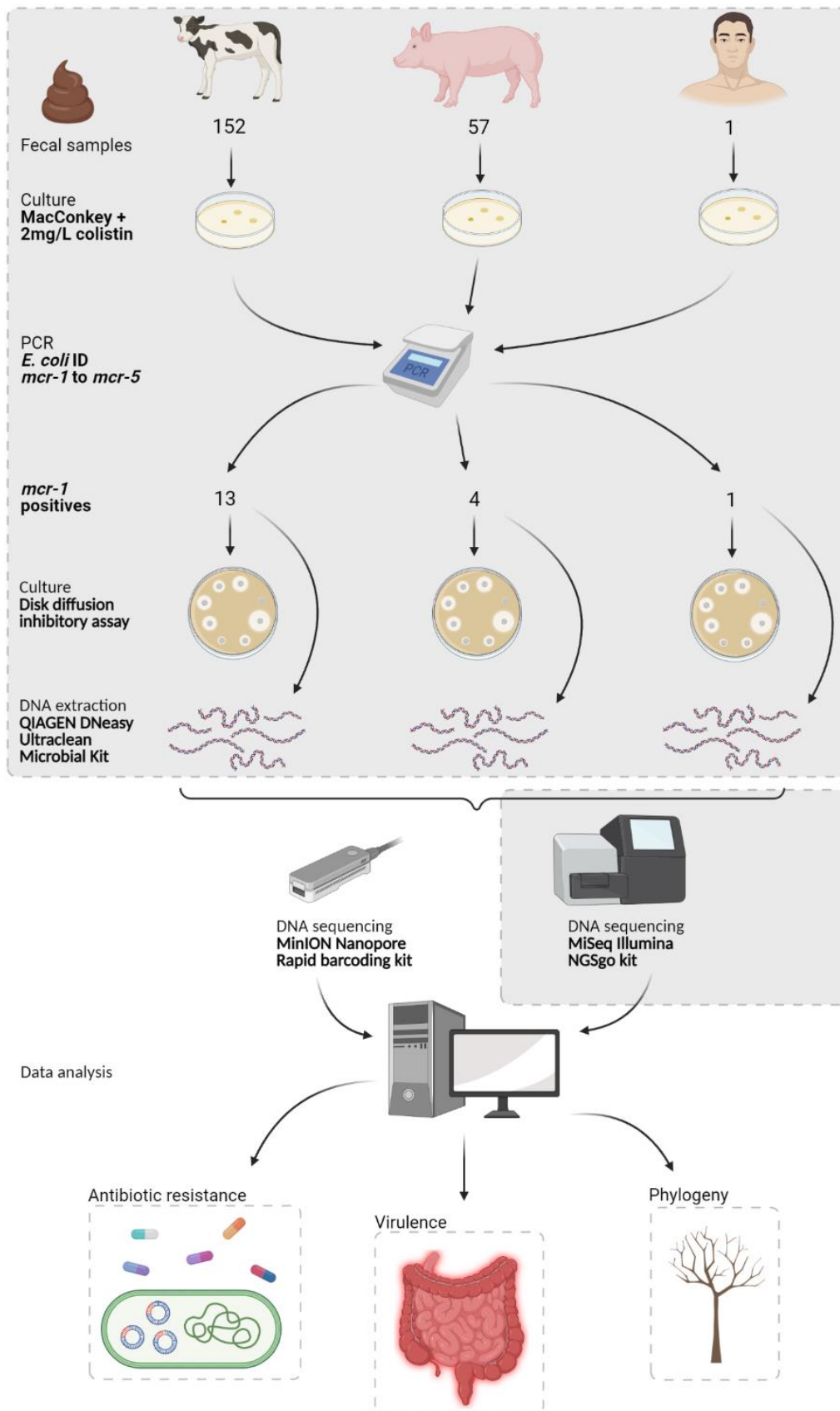


Figure 20. Methodology applied to characterize the colistin-resistant *E. coli* isolated from bovine, porcine, and human fecal samples from a mixed farm. Gray boxes include those techniques performed by third parties. Created in BioRender.com

Hybrid assemblies of the chromosomes and plasmids harboring antibiotic resistance genes

The 18 *mcr-1* PCR positive isolates were sequenced using both long- and short-read technologies (Nanopore and Illumina). The hybrid assembly retrieved *E. coli* chromosomes ranging from 4,613,927 bp (Farmer) to 5,586,543 (calf 15B_22), with an average size of 5,009,072 bp (**Table 15**). Fourteen out of the 18 chromosomes were single-contig. Completeness values ranged from 91.9% (pig P2_16), to 99.8% (calves 15A_11 and 14_4), with an average of 98.5%, except for the pig isolate P2_2 (76.1%).

The phylogenetic analysis clustered isolates to phylotype A and B1, with 10/18 isolates to phylotype A (seven calves, two pigs, and the farmer), and 8/18 to phylotype B1 (six calves, and two pigs) (**Figure 21**). The genome size and CDS number were similar to their respective NCBI genome references ([NC_000913.3](#) for phylotype A and [NC_018658.1](#) for phylotype B1).

The most represented MLSTs were ST6395 (phylotype A; three isolates from calves), ST224 (phylotype B; three isolates from calves), and ST10 (phylotype A; two isolates from swine). ST6395 isolates shared the same serotype (O4:H26), as well as the ST10 isolates (O98:H12).

We retrieved 48 plasmids bearing antibiotic resistance genes including those encoding for *mcr-1* (**Table 16**): 36 plasmids from the bovine isolates (ranging from one to five per isolate), seven from porcine (from one to two per isolate), and five from the farmer's isolate. Nineteen different replicon combinations were identified, e.g., IncHI2 / IncHI2A or IncFIB / IncFIC(FII). The most prevalent replicon was IncX4 (n=14), harboring the *mcr-1* gene and present in 10 isolates from calves, 3 from pigs, and the farmer's one. Other common replicons were IncFIB (n=9), IncHI2 / IncHI2A combination (n=7), IncFIC (=6), and replicon combination IncFIB / IncFIC (n=6).

Table 15. Chromosomal genome assembly and location and genomic context of *mcr-1* gene. Phylotype, serotype and MLST were determined with ClermonTyping, and with SerotypeFinder and MLST from CGE-DTU. CDS, rRNA and tRNA were annotated with PROKKA. BUSCO completeness assessed with a total of 440 genes. Data from NCBI references for phylotype B1 and A correspond to NC_018658.1 and NC_000913.3 respectively. *mcr-1* gene was found in 17 out of the 18 colistin-resistant *E. coli* isolates either in a plasmid (14 in IncX4, one in IncI2, and one in IncHI2 replicons), or the chromosome. Isolate 15B_22 contained two plasmids with *mcr-1* gene (IncX4 and IncHI2). *Abbreviations:* Ctgs, contigs; C, BUSCO completeness; loc., location; Pl., plasmid.

Host	Isolate	Size (bp)	Ctgs/genome	GC%	Phylotype	Serotype	MLST	CDS	rRNA	tRNA	C (%)	<i>mcr-1</i>	<i>mcr-1</i> loc.	Pl. GC%	Pl. size (bp)	<i>mcr-1</i> genomic context
Human	Farmer	4,613,927	1	50.9	A	O18/ac:H20	ST398	4,438	22	86	98.5	yes	IncX4	41.9	33,270	<i>mcr-1-pap2</i>
Swine	P2_16	4,975,525	1	50.7	B1	H51	ST5229	5,070	21	90	91.9	yes	Chr.	-	-	<i>mcr-1-pap2</i>
	P2_27	5,148,438	1	50.9	A	O98:H12	ST10	5,210	22	100	97.5	yes	IncX4	42.5	35,326	<i>mcr-1-pap2-ΔISAp1</i>
	P2_2	5,187,306	1	50.9	A	O98:H12	ST10	6,421	22	99	76.1	yes	IncX4	42.5	35,296	<i>mcr-1-pap2-ΔISAp1</i>
	P1_10	5,494,625	4	50.6	B1	O51:H49	ST20	5,496	22	93	98.9	yes	IncX4	44.1	45,441	<i>mcr-1-pap2</i>
Bovine	15B_27	4,659,272	1	50.8	A	O4:H26	ST6395	4,400	22	88	97.8	yes	IncX4	42.2	34,706	<i>mcr-1-pap2-ΔISAp1</i>
	15B_17	4,676,547	1	50.8	A	O4:H26	ST6395	4,450	22	87	98.2	yes	IncX4	42.2	34,758	<i>mcr-1-pap2-ΔISAp1</i>
	15B_4	4,704,000	1	50.8	A	O4:H26	ST6395	4,482	22	88	99.6	yes	IncX4	41.8	33,577	<i>mcr-1-pap2-ΔISAp1</i>
	15A_16	4,788,248	1	50.7	A	O5:H10	ST43	4,498	22	90	99.1	yes	IncX4	41.8	33,242	<i>mcr-1-pap2</i>
	15A_1	4,874,933	1	50.8	B1	O123:H16	ST1431	4,584	22	88	99.4	yes	IncI2	42.5	61,766	ISAp1- <i>mcr-1-pap2</i>
	14_4	4,880,223	1	50.7	B1	O117:H38	ST2539	4,611	22	89	99.8	yes	IncX4	41.8	33,262	<i>mcr-1-pap2</i>
	14_24	4,936,618	1	50.9	B1	O109:H51	ST224	4,697	22	91	99.4	yes	IncX4	41.8	33,557	<i>mcr-1-pap2-ΔISAp1</i>
	14_20	4,942,904	1	51	B1	O109:H23	ST224	4,704	21	89	98.2	yes	IncX4	41.8	33,283	<i>mcr-1-pap2</i>
	15A_11	5,031,610	1	50.8	A	H9	ST4981	4,771	22	89	99.8	no	-	-	-	-
	V7_18	5,141,039	1	50.8	B1	O102:H23	ST224	4,933	22	88	99.1	yes	IncX4	41.9	33,268	<i>mcr-1-pap2</i>
	V7_16	5,166,701	9	50.9	A	O49:H10	ST206	5,198	22	93	98.5	yes	IncX4	42.2	34,618	<i>mcr-1-pap2-ΔISAp1</i>
	15B_13	5,354,833	2	50.7	B1	O81:H31	ST101	5,249	22	94	99.4	yes	Chr.	-	-	ISAp1- <i>mcr-1-pap2</i> -ISAp1
	15B_22	5,586,543	32	50.9	A	O3	ST1638	5,576	22	97	99.3	yes	IncX4 IncHI2/IncHI2A	41.9 45.4	33,268 234,156	<i>mcr-1-pap2</i> ISAp1- <i>mcr-1-pap2</i>
References	NC_018658.1	5,273,097		50.7	B1	O104:H4	ST678	5,202	22	92						
	NC_000913.3	4,641,652		50.8	A	O16:H48	ST10	4,301	22	88						

Figure 21. Chromosome phylogeny based on SNPs. Two *E. coli* references were included, belonging to different phylotypes: NC_018658.1 for phylotype B1; NC_000913.3 for phylotype A.

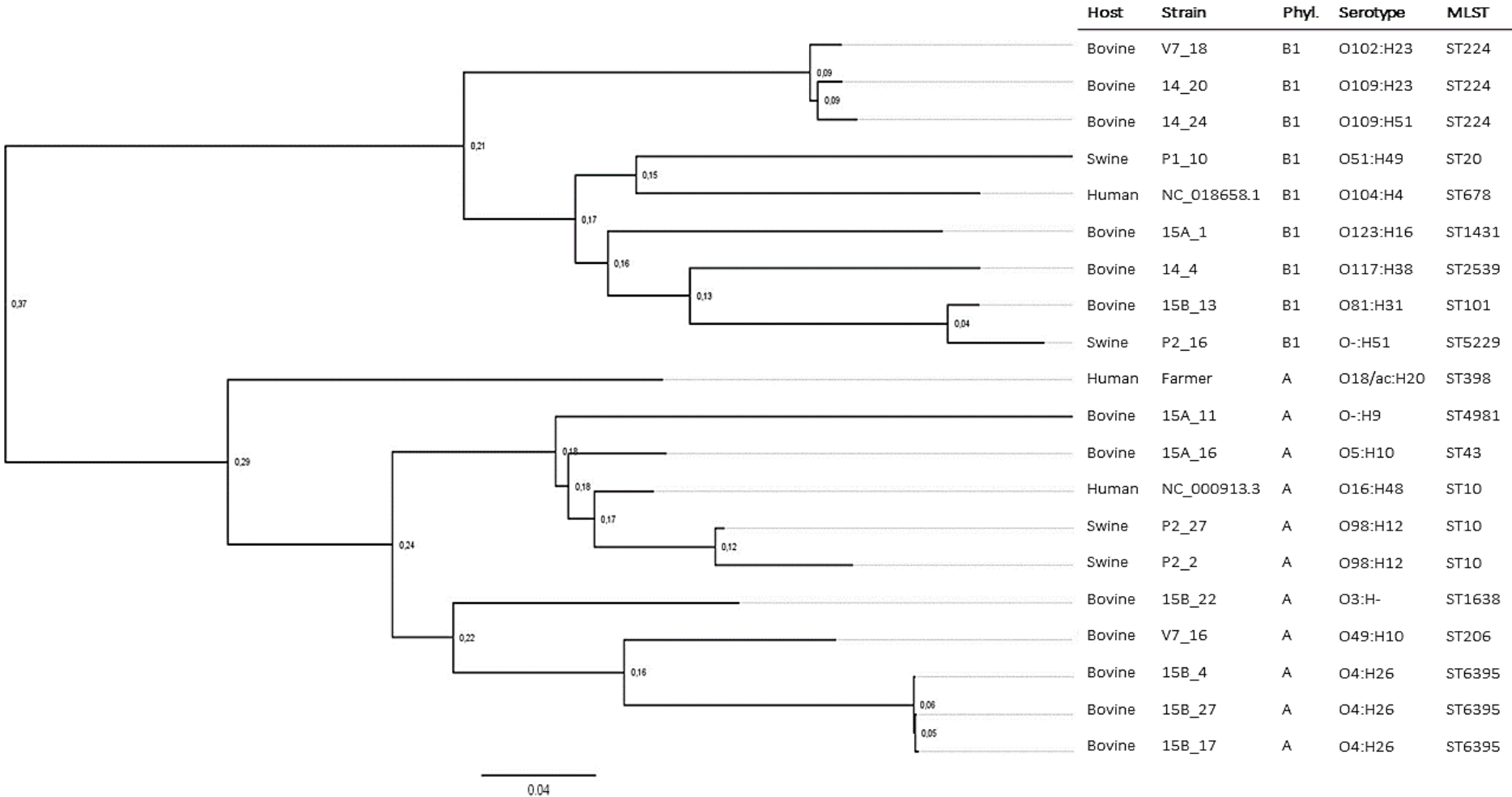


Table 16. Plasmids bearing ARGs retrieved from the 18 isolates. Aminoglycoside ARGs: *aac(3)-IIa*, *aac(3)-IIc*, *aac(3)-IV*, *aph(3')-Ia*, *aph(3'')-Ib*, *aph(4)-Ia*, *aph(6)-Ib*, *aph(6)-Id*, *aadA*, *aadA2*, *aadA17*; β -lactam ARGs: *bla_{TEM-1}*, *bla_{TEM-150}*, *bla_{TEM-156}*; trimethoprim ARGs: *dhfrA12*; phenicols ARGs: *cmlA6*, *floR*, *catI*; sulphonamide ARGs: *sul1*, *sul2*, *sul3*; colistin ARGs: *mcr-1*; (fluoro)quinolones ARGs: *qacH*, *qnrS1*, *qnrB5*; tetracycline ARGs: *tetA*, *tetD*, *tetM*; macrolide ARGs: *mphB*, *mphE*; lincosamide ARGs: *linG*, *lnuG*; other ARGs: *vgaC*, *msrE*. bp, base pairs; ARGs, antibiotic resistance genes.

Replicon(s)	Origin	Isolate	Plasmid	Size (bp)	ARGs
ColR _{NAI}	Bovine	15A_11	2	35,393	2 × <i>bla_{TEM-1}</i>
IncY	Porcine	P1_10	1	117,186	<i>aadA</i> , <i>aph(3'')-Ib</i> , <i>aph(6)-Id</i> , <i>bla_{TEM-1}</i> , <i>sul3</i> , <i>qacH</i>
IncX1	Bovine	14_20	1	103,984	<i>aadA2</i> , <i>bla_{TEM-1}</i> , <i>dhfrA12</i> , Δ <i>cmlA6</i> , <i>tetA</i>
IncX1	Human	Farmer	2	56,283	2 × <i>aadA2</i> , <i>bla_{TEM-1}</i> , <i>sul3</i> , <i>linG</i>
IncX4	Bovine	14_20	3	33,283	<i>mcr-1</i>
IncX4	Bovine	14_24	3	33,557	<i>mcr-1</i>
IncX4	Bovine	14_4	3	33,262	<i>mcr-1</i>
IncX4	Bovine	15A_16	2	33,242	<i>mcr-1</i>
IncX4	Bovine	15B_17	5	34,758	<i>mcr-1</i>
IncX4	Bovine	15B_22	2	33,268	<i>mcr-1</i>
IncX4	Bovine	15B_27	5	34,706	<i>mcr-1</i>
IncX4	Bovine	15B_4	5	33,577	<i>mcr-1</i>
IncX4	Bovine	V7_16	2	34,618	<i>mcr-1</i>
IncX4	Bovine	V7_18	1	33,268	<i>mcr-1</i>
IncX4	Porcine	P1_10	2	45,441	<i>mcr-1</i> , <i>tetM</i>
IncX4	Porcine	P2_2	2	35,296	<i>mcr-1</i>
IncX4	Porcine	P2_27	2	35,326	<i>mcr-1</i>
IncX4	Human	Farmer	5	33,270	<i>mcr-1</i>
IncI1	Bovine	14_24	1	100,042	<i>aac(3)-IV</i> , <i>aph(4)-Ia</i> , <i>aph(6)-Id</i> , <i>aph(3'')-Ib</i> , <i>floR</i> , <i>vgaC</i>
IncI1	Human	Farmer	4	102,225	<i>bla_{TEM-150}</i> or <i>bla_{TEM-156}</i>
IncI2	Bovine	15A_1	2	61,766	<i>mcr-1</i>
IncN	Bovine	15B_17	3	42,342	<i>bla_{TEM-150}</i> or <i>bla_{TEM-156}</i>
IncN	Bovine	15B_27	3	42,360	<i>bla_{TEM-150}</i> or <i>bla_{TEM-156}</i>
IncN	Bovine	15B_4	3	42,357	<i>bla_{TEM-156}</i>
p0111	Bovine	15B_17	4	98,813	<i>bla_{TEM-156}</i>
p0111	Bovine	15B_27	4	97,594	<i>bla_{TEM-150}</i> or <i>bla_{TEM-156}</i>
p0111	Bovine	15B_4	4	97,593	<i>bla_{TEM-150}</i> or <i>bla_{TEM-156}</i>
IncFII	Human	Farmer	3	71,076	<i>bla_{TEM-156}</i>
IncQ1	Bovine	14_20	2	105,996	<i>aph(3'')-Ib</i> , <i>aph(6)-Id</i> , <i>bla_{TEM-1}</i> , <i>floR</i> , IncI1 2 × <i>sul2</i> , <i>tetA</i>
IncQ1	Bovine	14_4	2	109,871	<i>aph(3'')-Ib</i> , <i>aph(6)-Id</i> , <i>bla_{TEM-1}</i> , <i>floR</i> , 2 × <i>sul2</i> , <i>sul3</i> , <i>tetA</i> IncI1
IncFIB	Porcine	P2_2	1	100,333	<i>aac(3)-IIa</i> , <i>aadA</i> , <i>aadA17</i> , <i>aadA2</i> , <i>aph(3')-Ia</i> , <i>bla_{TEM-1}</i> , <i>dhfrA12</i> , <i>cmlA6</i> , <i>floR</i> , <i>sul2</i> , <i>sul3</i> , <i>qacH</i> , <i>tetM</i> , <i>tetA</i> , <i>linG</i>
IncFIB	Porcine	P2_27	1	99,339	<i>aac(3)-IIa</i> , <i>aadA</i> , <i>aadA17</i> , <i>aadA2</i> , <i>aph(3')-Ia</i> , <i>bla_{TEM-1}</i> , <i>dhfrA12</i> , <i>cmlA6</i> , <i>floR</i> , <i>sul2</i> , <i>sul3</i> , <i>qacH</i> , <i>tetM</i> , <i>tetA</i> , <i>linG</i>
IncFIB	Bovine	15A_1	1	132,204	<i>aac(3)-IIa</i> , <i>aadA</i> , <i>aadA17</i> , <i>aadA2</i> , <i>aph(3')-Ia</i> , <i>bla_{TEM-1}</i> , IncFIC(FII) <i>dhfrA12</i> , <i>cmlA6</i> , Δ <i>floR</i> , <i>sul2</i> , <i>sul3</i> , <i>qacH</i> , <i>tetM</i> , <i>tetA</i> , <i>linG</i>

Table 16. Plasmids bearing ARGs retrieved from the 18 isolates. Continuation.

Replicon(s)	Origin	Isolate	Plasmid	Size (bp)	ARGs
IncFIB IncFIC(FII)	Bovine	15B_17	1	128,901	<i>aac(3)-Iia, aadA, aadA2, aph(3')-Ia, bla_{TEM-1}, dfrA12, cmlA6, floR, sul2, sul3, qacH, tetM, tetA</i>
IncFIB IncFIC(FII)	Bovine	15B_27	1	128,918	<i>aac(3)-Iia, aadA, aadA2, aph(3')-Ia, bla_{TEM-1}, dfrA12, cmlA6, floR, sul2, sul3, qacH, tetM, tetA</i>
IncFIB IncFIC(FII)	Bovine	15B_4	1	128,921	<i>aac(3)-Iia, aadA, aadA2, aph(3')-Ia, bla_{TEM-1}, dfrA12, cmlA6, floR, sul2, sul3, qacH, tetM, tetA</i>
IncFIB IncFIC(FII)	Porcine	P2_16	1	98,420	<i>aac(3)-Iia, aadA, aadA17, aadA2, aph(3')-Ia, bla_{TEM-1}, dfrA12, cmlA6, floR, sul2, sul3, qacH, tetM, tetA, linG</i>
IncHI2 IncHI2A	Bovine	15B_22	1	234,156	<i>aadA2, aph(3'')-Ib, aph(6)-Id, dfrA12, floR, mcr-1, tetM</i>
IncHI2 IncHI2A	Human	Farmer	1	242,389	<i>2 × aadA2, aph(3')-Ia, 2 × aph(3'')-Ib, 2 × aph(6)-Ib, dfrA12, floR, lnuG</i>
IncFIA(HI1) IncHI1A IncHI1B(R27)	Bovine	14_4	1	256,281	<i>aadA, aadA2, bla_{TEM-1}, dfrA12, cmlA6, floR, sul2, sul3, qacH, qnrS1, tetM</i>
IncFIA(HI1) IncHI1A IncHI1B(R27)	Bovine	15A_16	1	241,094	<i>aac(3)-Iic, 2 × aadA, aadA2, aph(3')-Ia, aph(3'')-Ib, aph(6)-Id, bla_{TEM-1}, cmlA6, sul3, qacH, qnrB, tetA, mphE, lnuG, msrE</i>
IncN IncHI2 IncHI2A	Bovine	15B_27	2	332,562	<i>aph(3')-Ia, aph(3'')-Ib, aph(6)-Id, sul1</i>
IncN IncHI2 IncHI2A	Bovine	15B_4	2	334,706	<i>aph(3')-Ia, aph(3'')-Ib, aph(6)-Id, sul1</i>
IncN IncHI2 IncHI2A	Bovine	15B_17	2	332,555	<i>aph(3')-Ia, aph(3'')-Ib, aph(6)-Id, sul1</i>
IncQ1 IncHI2 IncHI2A	Bovine	15B_13	1	185,122	<i>aac(3)-Iic, aadA, aph(3'')-Ib, aph(6)-Id, 2 × bla_{TEM-150}, sul1, sul2, tetA, mphB</i>
IncFIA(HI1) IncFIB(K) IncX1	Bovine	14_24	2	80,947	<i>aadA, aadA2, bla_{TEM-1}, dfrA12, cmlA6, sul3, qacH, tetM, tetA</i>
IncFIB IncFIC(FII) IncQ1	Bovine	15A_11	1	188,534	<i>aadA5, aph(3')-Ia, aph(3'')-Ib, aph(6)-Id, 2 × bla_{TEM-1}, sul2, tetA, tetD</i>
IncN IncQ1 IncHI2 IncHI2A	Bovine	V7_16	1	269,799	<i>aac(3)-Iic, 2 × aadA, aadA2, aph(3')-Ia, 3 × aph(3'')-Ib, 3 × aph(6)-Id, bla_{TEM-150} or bla_{TEM-156}, catI, cmlA6, floR, 2 × sul1, sul2, sul3, qacH, tetA</i>

Analyses of antibiotic resistance genes

A total number of 85 ARGs were identified using Abricate with CARD database, which belonged to different families: β -lactams, aminoglycosides, fluoroquinolones, lincosamides, macrolides, polymyxins (colistin), phenicols, sulphonamides, tetracyclines, and trimethoprim among others. All isolates were classified as MDR genotypically, confirming previous antibiotic susceptibility testing results.

Seventeen out of the 18 *E. coli* isolates from the mixed farm carried the *mcr-1* gene (**Table 15**), which confers colistin resistance. The *mcr-1* gene was located in the chromosome in two isolates (15B_13 and P2_16) and carried by plasmids for 15 of the isolates: 14 belonging to the incompatibility group IncX4, one to IncI2, and one to IncHI2 / IncH2A. Isolate 15B_22 contained two copies of the *mcr-1* gene in two different plasmids, IncX4 and IncHI2 / IncH2A. The eighteenth isolate, 15A_11, lost its *mcr-1* gene presumably due to subculturing steps. All the plasmids held the type 4 secretion system (T4SS), the necessary machinery to perform conjugation.

Four different genetic contexts for *mcr-1* gene were described among the *E. coli* isolates (**Figure 22 and Table 15**). All contexts presented the gene *pap2* (Mg^{2+} -independent phosphatidic acid phosphatase) in tandem with *mcr-1*. Another element was the insertion sequence ISAp11, which codes for its own transposase. This MGE is the responsible of the context diversity for *mcr-1* gene among our isolates. Only one isolate with *mcr-1* located in the genome presented the construct with two copies of the transposable element flanking *mcr-1-pap2* genes (**Figure 22-1**). This structure (ISAp11-*mcr-1-pap2*-ISAp11) is known as Tn6330 (Li et al., 2017a), a transposon. On the other hand, plasmids belonging to the incompatibility groups IncI2 and IncHI2 / IncH2A presented the same genetic context, in which only one complete copy of the insertion sequence was present upstream *mcr-1-pap2* (**Figure 22-2**). Seven plasmids from the IncX4 incompatibility group lacked ISAp11 upstream; but presented an inverted 355 bp fragment of this MGE downstream, plus a complete inverted copy of the insertion sequence IS26 downstream the *mcr-1* complex (**Figure 22-3**). Finally, seven isolates with *mcr-1* located either in IncX4 plasmids or the genome completely lack ISAp11 (**Figure 22-4**).

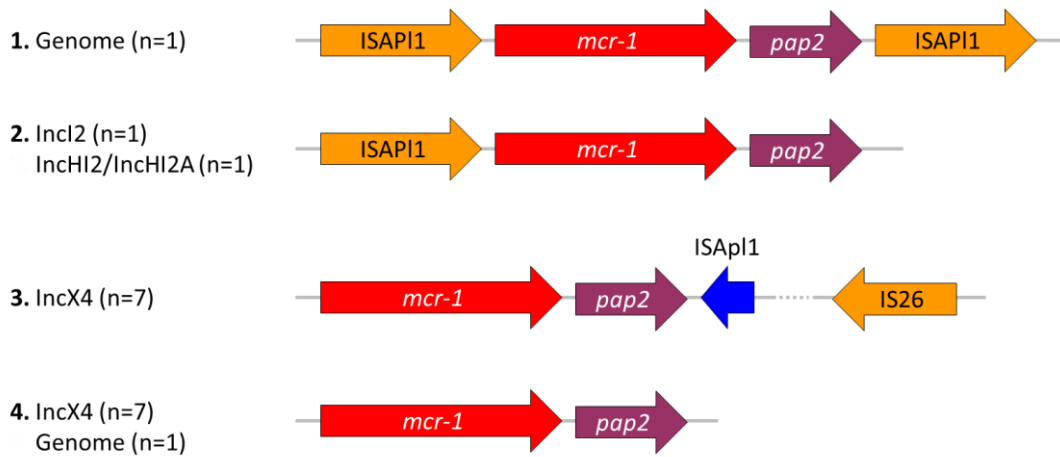


Figure 22. Schematic visualization of the genetic context surrounding *mcr-1* gene. *mcr-1* was present in the genome of two isolates, and in 16 plasmids belonging to IncX4 (14), IncI2 (1), and IncHI2/IncHI2A (1) incompatibility groups. An incomplete copy of the insertion sequence ISAp1 (355 bp versus 1070 bp from the complete IS) was found in seven IncX4 plasmids, followed downstream by a complete copy of the insertion sequence IS26. In red, antibiotic resistance genes; in orange, full-length MGEs; in blue, partial, or truncated MGEs; in purple, other genes.

Only one of our isolates (15B_13) presented *mcr-1* embedded in a full Tn6330, inserted in the chromosome, which could transpose to other locations. The two plasmids harboring a copy of the ISAp1 element upstream *mcr-1* gene (IncHI2/IncHI2A and IncI2) did not harbor any remnant of the same insertion sequence downstream, so no transposition could succeed. The same happens for the constructs presenting an incomplete copy of ISAp1 downstream. This fragment of 355 bp did not code for the necessary sequence for the circular intermediate formation.

Regarding the localization of the ARGs, 51 of them were located exclusively in the chromosome, 19 in plasmids (**Table 16**), and 15 either in the chromosome or in plasmids (**Figure 23**). The bovine isolates (n= 13) harbored the 85/85 ARGs, and 18/85 were exclusive of cattle. Porcine Isolates (n= 4) harbored 64/85, and the human isolate contained 53 of the described ARGs.

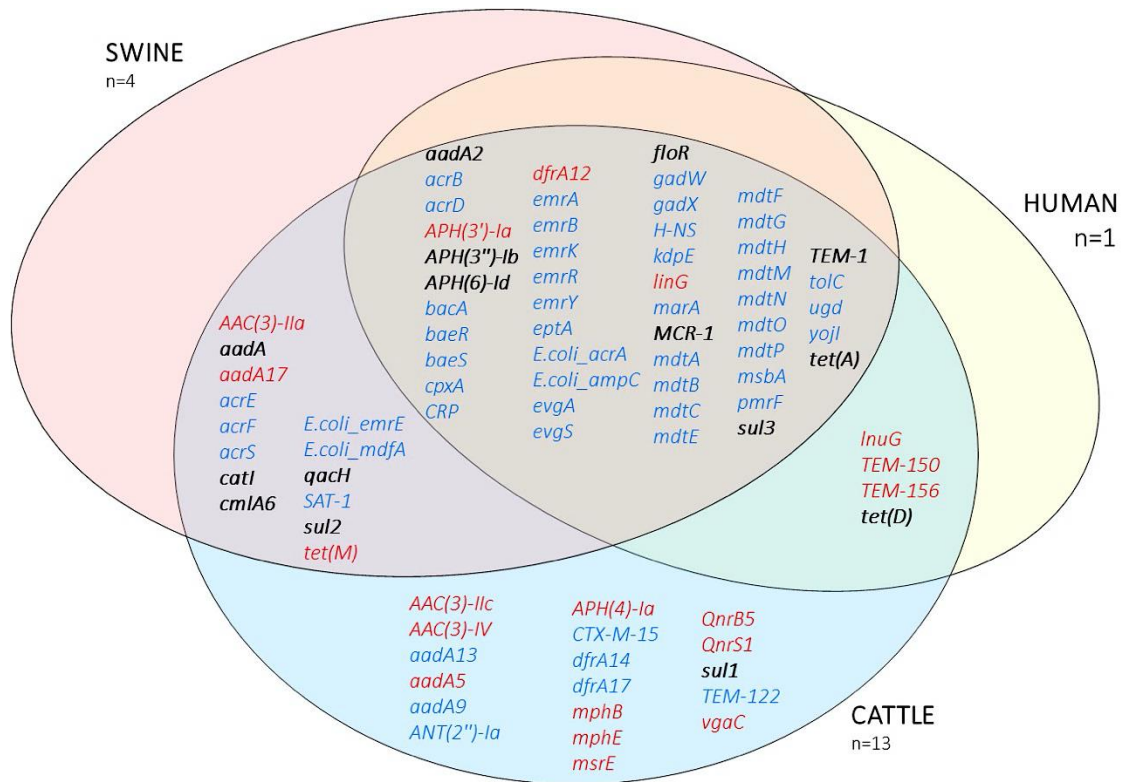


Figure 23. Venn diagram of the Antibiotic Resistance Genes described in the 18 colistin-resistant *E. coli* isolated from a mixed farm. Blue, chromosomal location; red, plasmid location; black, located either in the chromosome or plasmid.

The bovine isolate 15A_11 –the one lacking the *mcr-1* gene– carried the *bla*_{CTX-M-15} gene in the chromosome. This gene confers resistance to cephalosporines, a widely used antibiotic in hospital settings against Enterobacteriaceae. Upstream *bla*_{CTX-M-15} we identified a complete IS3 element and a Δ ISEcp1 element, while downstream there was a Δ Tn2 (**Figure 24**).

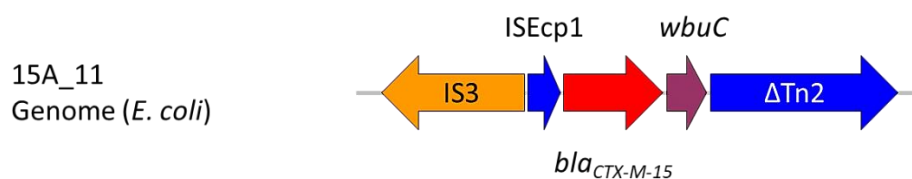


Figure 24. *bla*_{CTX-M-15} genetic context in bovine 15A_11 isolate. In red, antibiotic resistance gene; in orange, full-length MGEs; in blue, partial, or truncated MGEs; in purple, other genes.

IncX4 plasmids presented the same backbone with minor modifications (**Figure 25**). While 13 out of the 14 IncX4 plasmids were approximately 33-35 kbp and presented a GC content around 42%, the IncX4 plasmid from the porcine isolate P1_10 was larger (45,441 bp), and

with higher GC content (44.1%). The latest harbored the *tetM* gene conferring resistance to tetracycline. Two IS26 elements were flanking this extra-region of approximately 12,000 bp (**Figure 26**). All IncX4 plasmids carried the type IV secretion system (T4SS), allowing the plasmid to be self-transmissible, and HicAB toxin-antitoxin system for plasmid maintenance and stability. The IncX4 plasmid from the farmer shared highest identity (99.97%) and coverage (99%) with their counterparts from calves (**Table 17**).

IncI2 plasmid presented a size of 61,766 bp and contained the conjugative mechanism T4SS and the replication machinery. It contained the RelE/ParE, Hok, and HicAB toxin-antitoxin systems. IncHI2 / IncHI2A plasmid sized 234,156 bp and also presented the conjugative and replication machinery. It contained the HipA toxin-antitoxin system. Moreover, IncHI2 plasmid not only coded for resistance to colistin, but also coded other resistances: to aminoglycosides (*aadA2*, *aph(3'')-Ib*, and *aph(6)-Id*), to trimethoprim (*dfrA12*), to florfenicol (*floR*), and tetracycline (*tetM*).

Table 17. Comparison of coverage (COV) and identity (ID) of the *mcr-1*-IncX4 plasmid from the farmer versus the bovine and porcine isolates.

	COV (%)	ID (%)
P1_10	74	99.99
P2_2	94	99.87
P2_27	94	100
V7_16	95	99.97
15B_17	95	99.99
15B_27	95	100
15B_4	98	99.97
14_24	98	99.99
14_4	99	99.96
V7_18	99	99.96
15A_16	99	99.97
14_20	99	99.97
15B_22	99	99.97

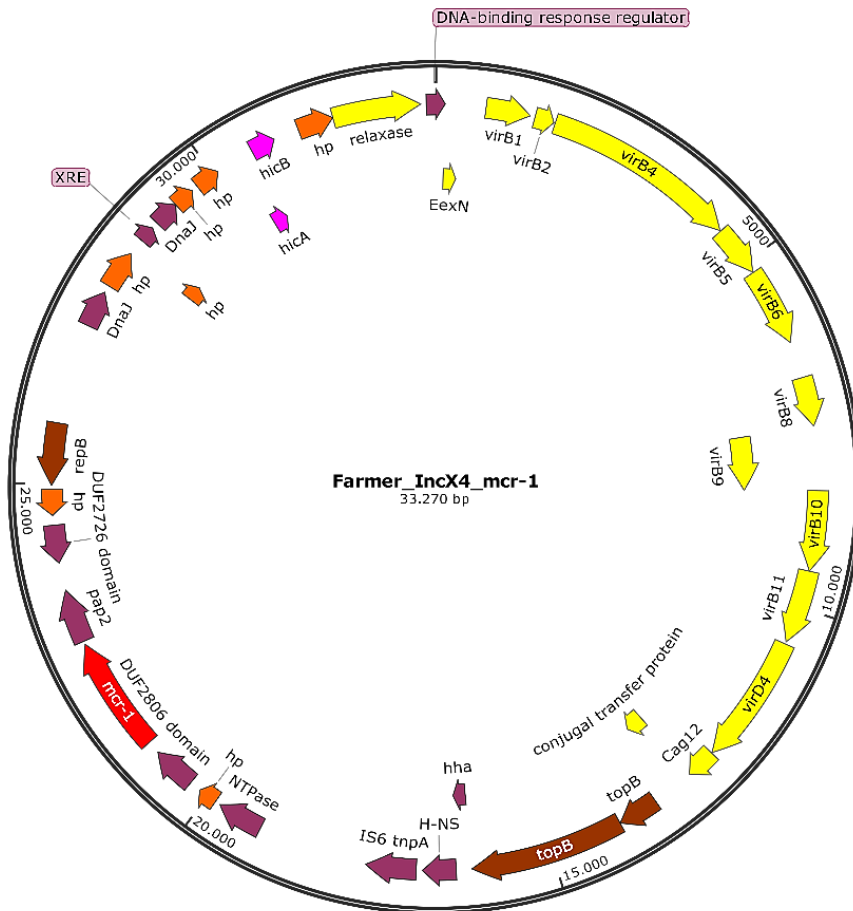


Figure 25. Annotation of the IncX4 plasmid from the Farmer. In yellow the T4SS; in red the *mcr-1* gene; in pink the toxin-antitoxin system; in orange hypothetical proteins; in brown the replication machinery; in purple other elements.

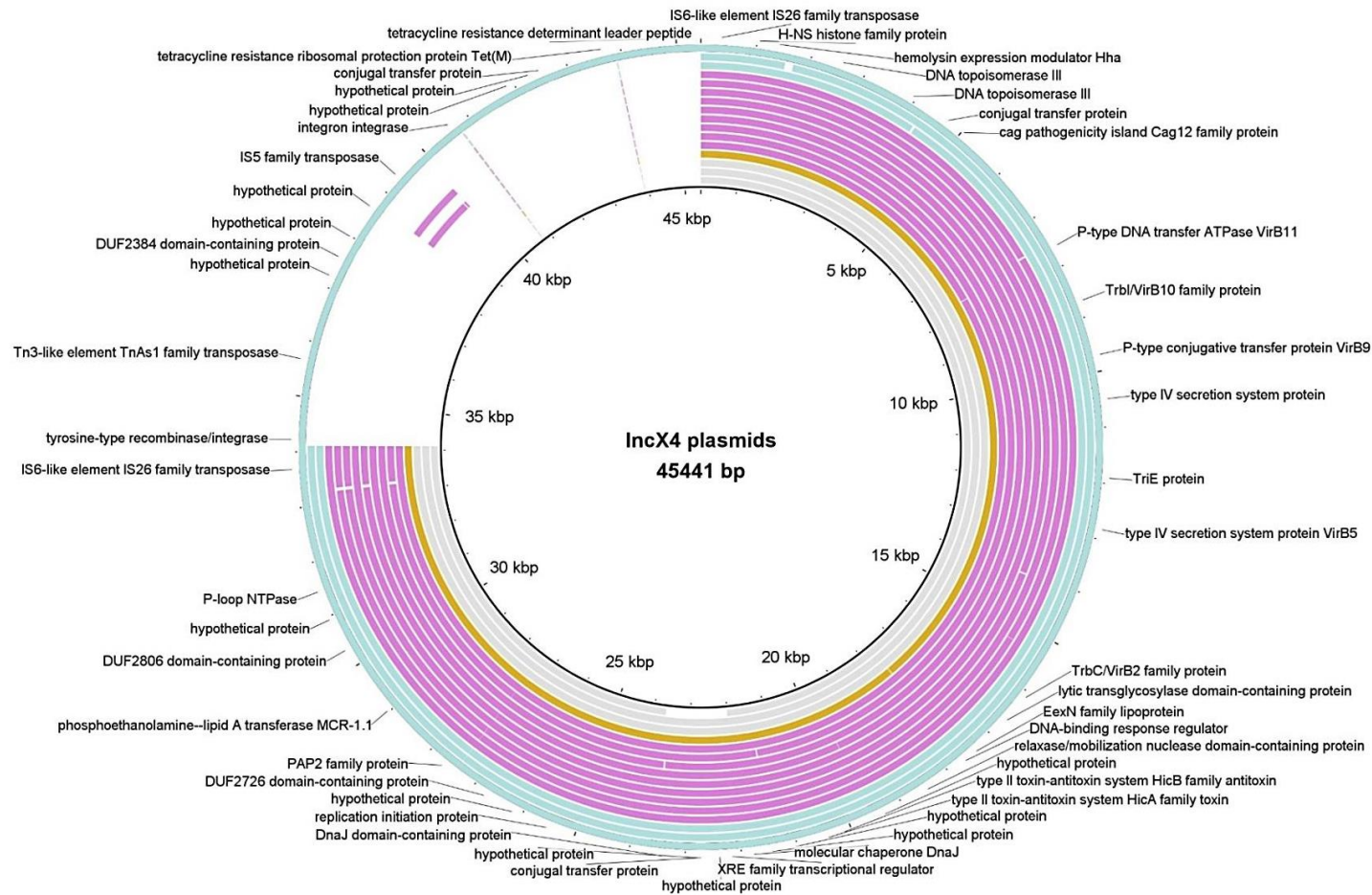


Figure 26. BLAST Ring Image Generator (BRIG) visualization of the 14 IncX4 plasmids from this study and three IncX4 plasmids from NCBI: pEC11b, pMCR1-NJ-IncX4 and pP744T-MCR1. Rings from outside to inside: P1_10, P2_2, P2_27 (blue); V7_18, V7_16, 15B_4, 15B_27, 15B_22, 15B_17, 15A_16, 14_4, 14_24, 14_20 (pink); farmer (orange); pP744T-MCR1, pMCR1-NJ-IncX4, pEC11b (grey). IncX4 plasmid from P1_10 is shown as the reference (longest sequence), with an extra-region of approximately 12,000 bp that is flanked by two IS26 elements and harbours the *tetM* gene conferring resistance to tetracycline. Isolates 15B_27 and 15_17 presented IS5 transposase, as P1_10 (pink fragments near 40 kb location for P1_10).

Analyses of virulence factor genes

A total of 33 virulence factor genes were detected in the 18 *E. coli* isolates from the mixed farm. While 9/33 genes were found exclusively in plasmids, 18/33 were located in the chromosome. The remaining 6/33 virulence factor genes were found in either the chromosome or plasmids. In general, *E. coli* from bovine isolates (n= 13) contained the highest amount of virulence factor genes (27/33), followed by swine (18/33) (n=4), and the isolate from the farmer (5/33) (n= 1) (**Figure 27**). Twelve genes were exclusively described in cattle (*cdtB*, *ehxA*, *espI*, *espP*, *f17A*, *f17G*, *mchB*, *mchC*, *mchF*, *sta1*, *tccP* and *stx2*), and six exclusively in swine (*aaiC*, *cif*, *espB*, *espJ*, *katP*, and *nleA*). Only two virulence factor genes were shared among bovine, porcine and the farmer (*gad*, *iss*).

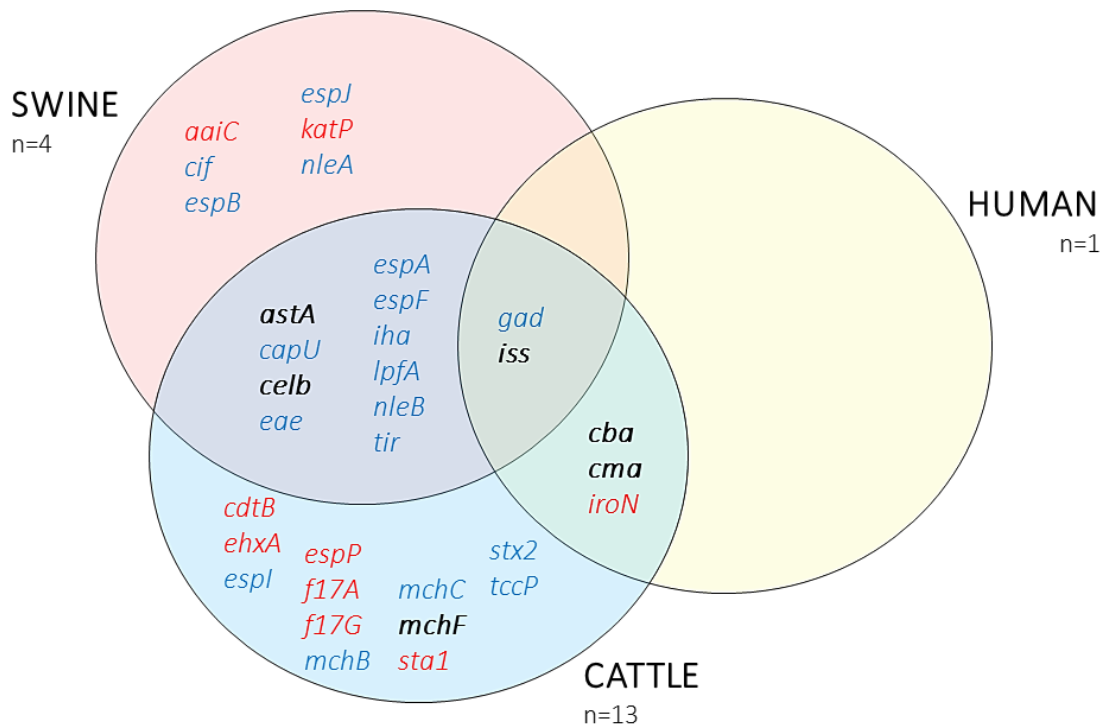


Figure 27. Venn diagram representing the virulence factor genes described in the 18 colistin-resistant *E. coli* isolated from a mixed farm by VirulenceFinder. Blue, chromosomal location; red, plasmid location; black, located either in the chromosome or plasmid.

A total of 13 plasmids of mainly two replicon families, IncF (11) and Col (2), presented virulence factor genes. While Col plasmids presented only endonuclease colicin E2 (encoded by *celb* gene), IncF plasmids encoded for the rest of the virulence factors (*ehxA*, *espP*, *astA*, *sta1*, *cba*, *cma*, *katP*, *aaiC*, *iss*, *iroN*, *f17A*, *f17G*, *cdtB*, *mchF*). Among IncF plasmids, there were

two subfamilies, IncFII (n=4) and IncFIB (n=7, one of which also presents IncFIC(FII) and IncQ1 replicons) (Table 18).

Table 18. IncF-family plasmids harboring virulence factor (VF) genes and antibiotic resistance genes (ARGs).

Abbreviations: T4SS, type 4 secretion system. Yes (?), some of the components of the T4SS were missing.

Strain	Replicon(s)	Size (bp)	VF	T4SS
V7_16	IncFII	69,161	<i>ehxA, espP, astA, sta1</i>	No
Farmer	IncFII	71,076	<i>cba, cma</i>	Yes
P2_2	IncFII	153,810	<i>katP, aaiC</i>	Yes (?)
P2_27	IncFII	153,823	<i>katP, aaiC</i>	Yes (?)
Farmer	IncFIB	80,264	<i>iss, iroN, cma</i>	No
15A_16	IncFIB	94,593	<i>f17A, f17C, f17D, f17G, cdtA, cdtB, cdtC</i>	No
14_24	IncFIB	117,948	<i>f17A, f17C, f17D, f17G</i>	Yes
14_20	IncFIB	138,808	<i>f17A, f17C, f17D, f17G, cdtA, cdtB, cdtC</i>	Yes
V7_18	IncFIB	139,182	<i>f17C, f17D, f17G, cdtA, cdtB, cdtC</i>	Yes
15B_22	IncFIB	141,709	<i>f17C, f17D, f17G, cdtA, cdtB, cdtC</i>	Yes
15A_11	IncFIB/IncFIC(FII)/IncQ1*	188,534	<i>iss, iroN, mcbF</i>	Yes

*Plasmid IncFIB/IncFIC(FII)/IncQ1 from 15A_11 isolate, a part from harboring VF, also harbored ARGs: *aadA5, aph(3')-Ia, aph(3'')-Ib, aph(6)-Id, blaTEM-1, sul2, tetA, tetD*

Four of the isolates (14_20, 15A_16, 15B_22, and V7_18) presented IncFIB plasmids, one of them non-conjugative (15A_16), which encoded for two elements that participate in pathogenicity: a F17 fimbriae and the cytolethal distending toxin (CDT). P1_10 isolate encoded for several locus of enterocyte effacement (LEE)-related virulence factor genes (*eeA, tir, cij, espA, espB, espF* and *espJ*) and some non-LEE genes (*nleA, nleB*). V7_16 isolate harbored some of the genes (*eeA, tir, espA, espF, nleB*). Moreover, P1_10 also encoded for translocation-pore protein EspD, which was not detected by VirulenceFinder, but found by aligning the P1_10 contigs against the reference *E. coli* strain NCCP 14540 chromosome (accession number [CP042982.1](https://ncbi.nlm.nih.gov/nuccp/CP042982.1)).

P2_2 and P2_27 are two swine isolates that share a 154 kbp IncFII plasmid that carries two virulence factor genes: *aaiC* and *katP*. *aaiC* encodes for a protein involved in type VI secretion system. Finally, calf's 15B_13 isolate (phylotype B1, serotype O81:H31, ST101) contained different virulence factor genes: *iba, lpfA, gad, iss, astA, cba, cellB, mcbB, mcbC, mcbF* and *stx2* (*stx2A* and *stx2B* subunits). The farmer's isolate harbored five virulence factor genes (*gad, iss, cba, cma, and iroN*), two of them (*cba* and *cma*) located in a plasmid with the necessary machinery to perform conjugation.

The results have been published in a paper titled “Transmission of similar *mcr-1* carrying plasmids among different *Escherichia coli* lineages isolated from livestock and the farmer” in Antibiotics (Viñes et al., 2021) (**annex 4**).

4.4. Dissemination of carbapenem-resistant *Klebsiella pneumoniae* in healthcare institutions

The last part of this thesis focuses on the study of Enterobacteriaceae resistance to carbapenems, a type of β -lactams frequently used in hospitals. We aimed to assemble the plasmids harboring specific β -lactamase genes, such as *bla*_{NDM-1}, *bla*_{NDM-7}, *bla*_{OXA-48}, and *bla*_{CTX}.

M-15.

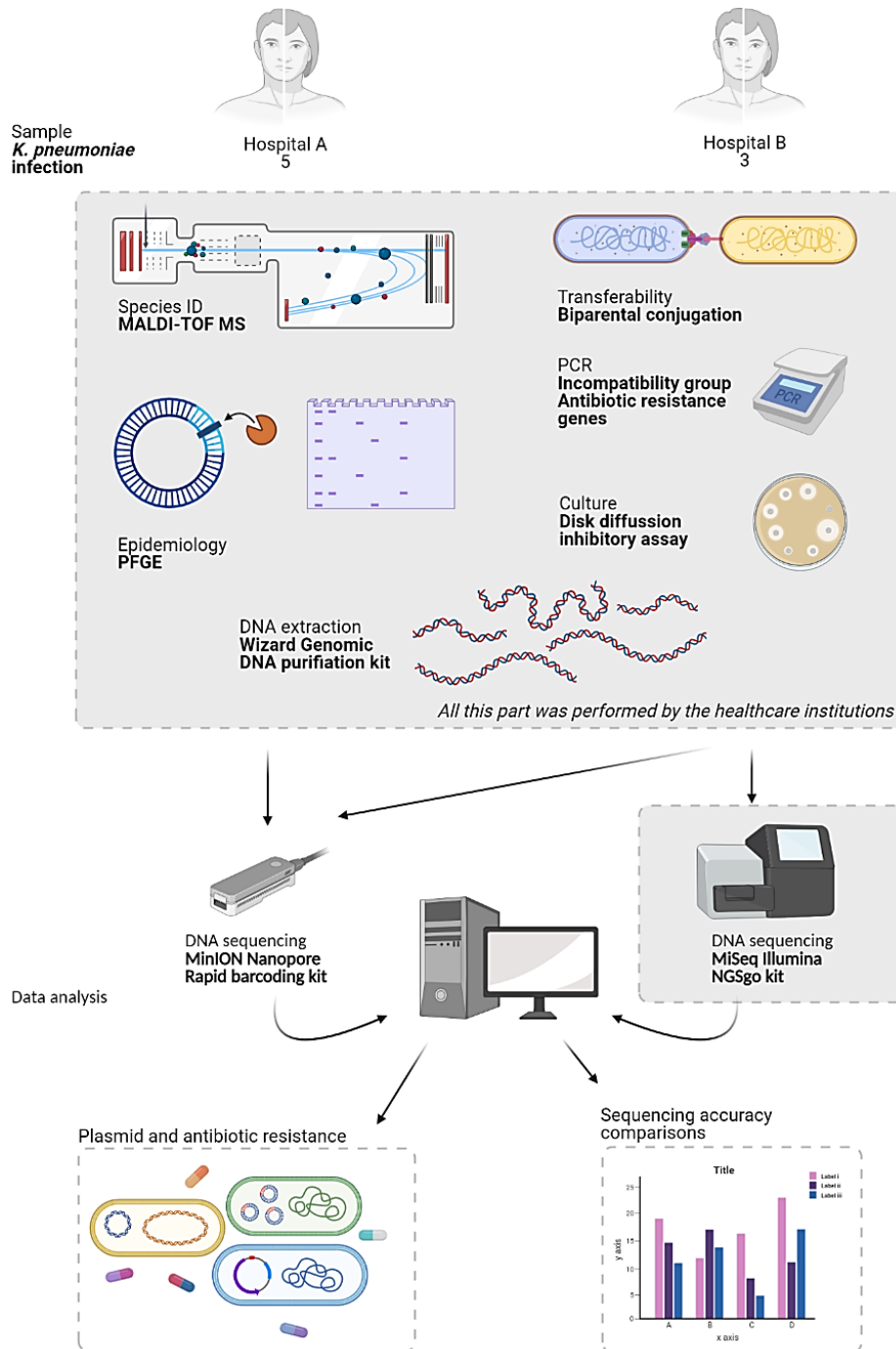


Figure 28. Methodology approach to characterize the *K. pneumoniae* isolated from human clinical cases. Gray boxes include those techniques performed by third parties. Created in BioRender.com

We received five *K. pneumoniae* isolates from Hospital A (HA-2, HA-3, HA-4, HB-377, and HB-536) and three from Hospital B (HUB-1, HUB-2, and HUB-3). The isolates had been previously characterized through MALDI-TOF MS, antibiotic resistance, and plasmid interference (gray box in **Figure 28**). Previous characterization results performed by the collaborators showed that all the *K. pneumoniae* isolates were ST147 except from HB-536 from Hospital A (ST307) (**Table 19**).

Table 19. *K. pneumoniae* isolates main characteristics: MLST, antibiotic resistance genes, plasmids' incompatibility groups, and plasmids' size. MLST, multi locus sequence type; ARGs, antibiotic resistance genes; pl., plasmid; Inc, incompatibility group (replicons).

Isolate	MLST	ARGs	Size pl.1	ARGs pl.1	Inc pl.1	Size pl.2	ARGs pl.2	Inc pl.2	Inc pl.3
HA-2	147	<i>bla</i> _{NDM-1} , <i>bla</i> _{CTX-M-15}	-	<i>bla</i> _{NDM-1} , <i>bla</i> _{CTX-M-15}	IncR	-	-	-	
HA-3	147	<i>bla</i> _{NDM-1} , <i>bla</i> _{CTX-M-15}	-	<i>bla</i> _{NDM-1} , <i>bla</i> _{CTX-M-15}	IncR	-	-	-	
HA-4	147	<i>bla</i> _{NDM-1} , <i>bla</i> _{CTX-M-15} , <i>bla</i> _{OXA-48} , <i>rmtF</i>	90/310 kb	<i>bla</i> _{NDM-1} , <i>bla</i> _{CTX-M-15}	IncR	60 kb	<i>bla</i> _{OXA-48}	IncL	
HB-377	147	<i>bla</i> _{NDM-1} , <i>bla</i> _{CTX-M-15} , <i>rmtF</i>	90/310 kb	<i>bla</i> _{NDM-1} , <i>bla</i> _{CTX-M-15}	IncR	-	-	-	
HB-536	307	<i>bla</i> _{NDM-7} , <i>bla</i> _{CTX-M-15} , <i>bla</i> _{TEM}	50/250 kb	<i>bla</i> _{NDM-7}	IncX3	-	-	-	
HUB-1	147	<i>bla</i> _{NDM-1} , <i>bla</i> _{CTX-M-15}	-	-	IncR	-	-	-	IncFII
HUB-2	147	<i>bla</i> _{NDM-1} , <i>bla</i> _{CTX-M-15} , <i>bla</i> _{OXA-48}	-	-	IncR	-	-	IncL/M	IncFII
HUB-3	147	<i>bla</i> _{CTX-M-15} , <i>bla</i> _{OXA-48}	-	-	IncR	-	-	IncL/M	IncFII

The isolates presented some of the genes conferring resistance to carbapenems (*bla*_{NDM-1}, *bla*_{NDM-7}, and *bla*_{OXA-48}), and extended-spectrum β-lactamases (ESBLs) (*bla*_{CTX-M-15} and *bla*_{TEM}).

In relation to *bla*_{NDM} gene, ST147 isolates carried *bla*_{NDM-1} and ST307, *bla*_{NDM-7}. Four isolates from Hospital A (HA-2, HA-3, HA-4, and HB-377) carried a plasmid of the IncR incompatibility group with the *bla*_{NDM-1} and *bla*_{CTX-M-15} genes. For HA-4, an IncL plasmid carrying *bla*_{OXA-48} was also described. For ST307 (isolate HB-536), a IncX3 plasmid carrying *bla*_{NDM-7} gene was described.

Our main goal was to sequence and assemble plasmids harboring genes encoding for carbapenemases and ESBLs. More specifically, in the study from Hospital A we used a Nanopore-only WGS approach to assemble and close the plasmids from five *K. pneumoniae*

isolates (Marí-Almirall et al., 2020). In the study from Hospital B, we used hybrid WGS to assemble and characterize the chromosomes and plasmids of three *K. pneumoniae* isolates. We identified three incompatibility group plasmids harboring these β -lactamases, confirming the previous results: IncN + IncR carrying *bla*_{NDM-1} and *bla*_{CTX-M-15}; IncL/M carrying *bla*_{OXA-48}; and finally, IncX3 carrying *bla*_{NDM-7} and *bla*_{CTX-M-15} (**Table 20**).

Table 20. Whole-genome sequencing and assembly of plasmids harboring genes encoding for carbapenemases and ESBLs (genes in bold). Hospital A isolates were sequenced only with Nanopore long reads, whereas Hospital B isolates were sequenced using hybrid sequencing (Nanopore long reads and Illumina short reads). Inc, incompatibility group (replicon/s); bp, base pairs; ARGs, antibiotic resistance genes; Cov, Nanopore reads coverage.

NANOPORE-ONLY SEQUENCING RESULTS (Hospital A)				
Isolate	Inc	Size (bp)	GC %	ARGs
HA-2	IncN + IncR	67,726	52.9	<i>dfrA12</i> , <i>dfrA14</i> , <i>bla</i>_{CTX-M-15} , <i>vgaC</i> , <i>mphA</i> , <i>Mrx</i> , <i>sul1</i> , <i>QnrB17</i> , <i>bleomycin</i> resistance, <i>bla</i>_{NDM-1}
HA-3	IncN + IncR	74,564	53.3	<i>aph(3')-Ia</i> , <i>dfrA12</i> , <i>dfrA14</i> , <i>bla</i>_{CTX-M-15} , <i>vgaC</i> , <i>mphA</i> , <i>Mrx</i> , <i>sul1</i> , <i>QnrB17</i> , <i>bleomycin</i> resistance, <i>bla</i>_{NDM-1}
HA-4	IncL/M	63,818	51.4	<i>bla</i>_{OXA-48}
	IncN + IncR	74,374	53.1	<i>aph(3')-Ia</i> , <i>dfrA12</i> , <i>dfrA14</i> , <i>bla</i>_{CTX-M-15} , <i>vgaC</i> , <i>mphA</i> , <i>Mrx</i> , <i>QnrB17</i> , <i>bleomycin</i> resistance, <i>bla</i>_{NDM-1}
HB-377	IncN + IncR	67,344	53.3	<i>dfrA12</i> , <i>dfrA14</i> , <i>bla</i>_{CTX-M-15} , <i>vgaC</i> , <i>mphA</i> , <i>Mrx</i> , <i>QnrB17</i> , <i>bleomycin</i> resistance, <i>bla</i>_{NDM-1}
HB-536	IncX3	50,593	46.9	<i>bleomycin</i> resistance, <i>bla</i>_{NDM-7} , <i>bla</i>_{CTX-M-15}
HYBRID SEQUENCING RESULTS (Hospital B)				
Isolate	Inc	Size (bp)	GC %	ARGs
HUB-1	IncN + IncR	74,592	53.2	<i>aph(3')-Ia</i> , <i>dfrA12</i> , <i>dfrA14</i> , <i>bla</i>_{CTX-M-15} , <i>vgaC</i> , <i>mphA</i> , <i>Mrx</i> , <i>sul1</i> , <i>QnrB17</i> , <i>bleomycin</i> resistance, <i>bla</i>_{NDM-1}
	IncL/M	63,865	51.2	<i>bla</i>_{OXA-48}
HUB-2	IncN + IncR	74,611	53.2	<i>aph(3')-Ia</i> , <i>dfrA12</i> , <i>dfrA14</i> , <i>bla</i>_{CTX-M-15} , <i>vgaC</i> , <i>mphA</i> , <i>Mrx</i> , <i>sul1</i> , <i>QnrB17</i> , <i>bleomycin</i> resistance, <i>bla</i>_{NDM-1}
	IncL/M	63,849	51.2	<i>bla</i>_{OXA-48}
HUB-3	IncN + IncR	66,004	52.6	<i>aph(3')-Ia</i> , <i>dfrA12</i> , <i>dfrA14</i> , <i>bla</i>_{CTX-M-15} , <i>vgaC</i> , <i>mphA</i> , <i>Mrx</i> , <i>sul1</i> , <i>QnrB17</i>

Plasmids belonging to IncN + IncR were heterogeneous and presented different sizes: 74,500 bp (HA-3, HA,4, HUB-1, and HUB-2) (example in **Figure 29**), 67,500 bp (HA-2 and HB-377) and 66,004 bp (HUB-3). The main difference between 74,500 bp and 67,500 bp plasmid sizes is that the first presented a *aph(3')-Ia* gene (819 bp) (resistance to aminoglycosides) surrounded by two copies of the insertion sequence IS26 (809 bp), followed by an inserted transposon Tn5403 (3,674 bp). These four genetic elements (two copies of IS26 surrounding *aph(3')-Ia*, and the transposon), measure 6,111 bp. The 66,004 bp plasmid (HUB-3) also presented the *aph(3')-Ia* resistance gene flanked by two copies of IS26, but it lacked a region of approximately 7,200 bp (**Figure 30**). This genetic region is flanked by two IS3000 insertion sequences and includes seven genes and a truncated ISAb125 insertion sequence. These genes are *bla*_{NDM-1}; *ble*, conferring resistance to bleomycin; *trpF*,

which encodes for a N-(5'-phosphoribosyl)anthranilate isomerase involved in the synthesis of L-tryptophan; *dsbC*, which encodes for a thiol:disulfide interchange protein that rescue oxidatively damaged secreted proteins correcting non-native disulfide bonds; *cutA*, which encodes for a divalent-cation tolerance protein; and *groS* and *groL* that encode for 60 kDa and 10 kDa chaperonines respectively. ISAbal25 element appears upstream *bla_{NDM-1}* gene variants in all the plasmids carrying this antibiotic resistance gene.

IncN + IncR plasmids presented other genes conferring resistance to other antibiotics rather than β -lactams and aminoglycosides: *dfrA12* and *dfrA14* conferring resistance to trimethoprim; *vgcA*, to streptogramin A, and other antibiotics such as lincosamides; *mphA* and *Mrx* to macrolides; *sul1* to sulfonamides; and *QnrB17* to quinolones.

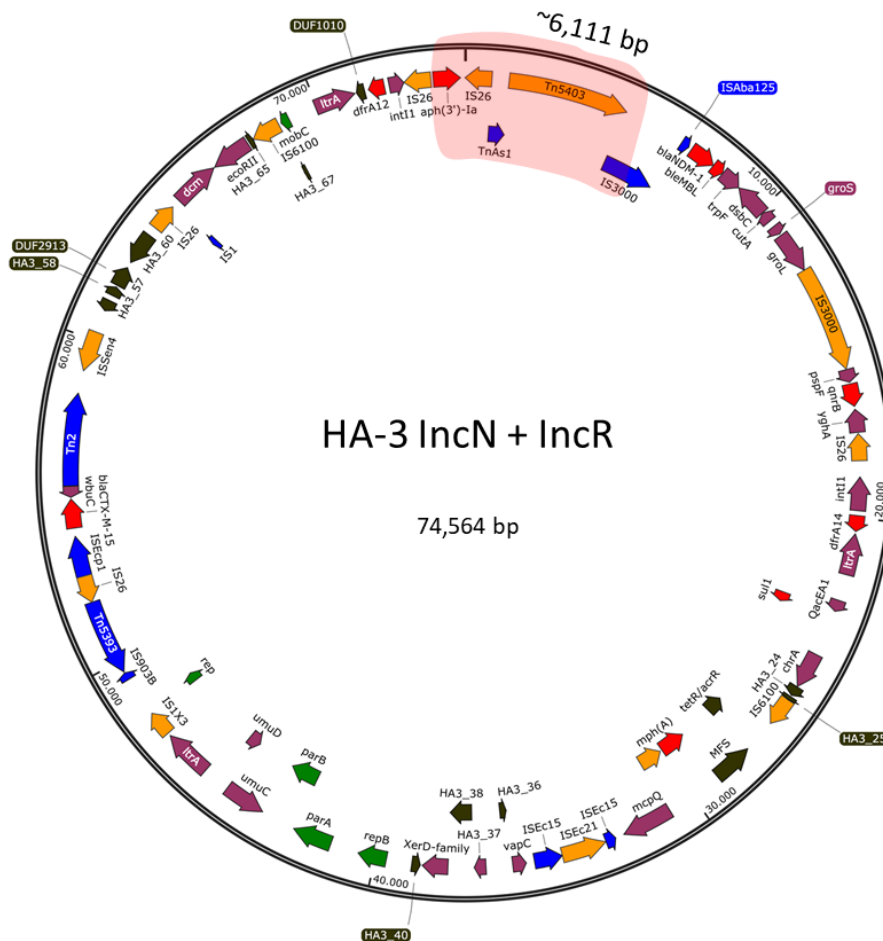


Figure 29. Schematic visualization of the plasmid harboring *bla_{NDM-1}* gene in HA-3 isolate. The red faded region shows the insertion carrying *aph(3)-Ia* resistance gene, which measures approximately 6,111 bp. In red, antibiotic resistance genes; in blue and orange, truncated or full-length mobile genetic elements respectively; in green, genes involved in plasmid mobilization and maintenance; in dark green, hypothetical genes; and finally, in purple other genes. Figure excerpted and modified from (Marí-Almirall et al., 2020).

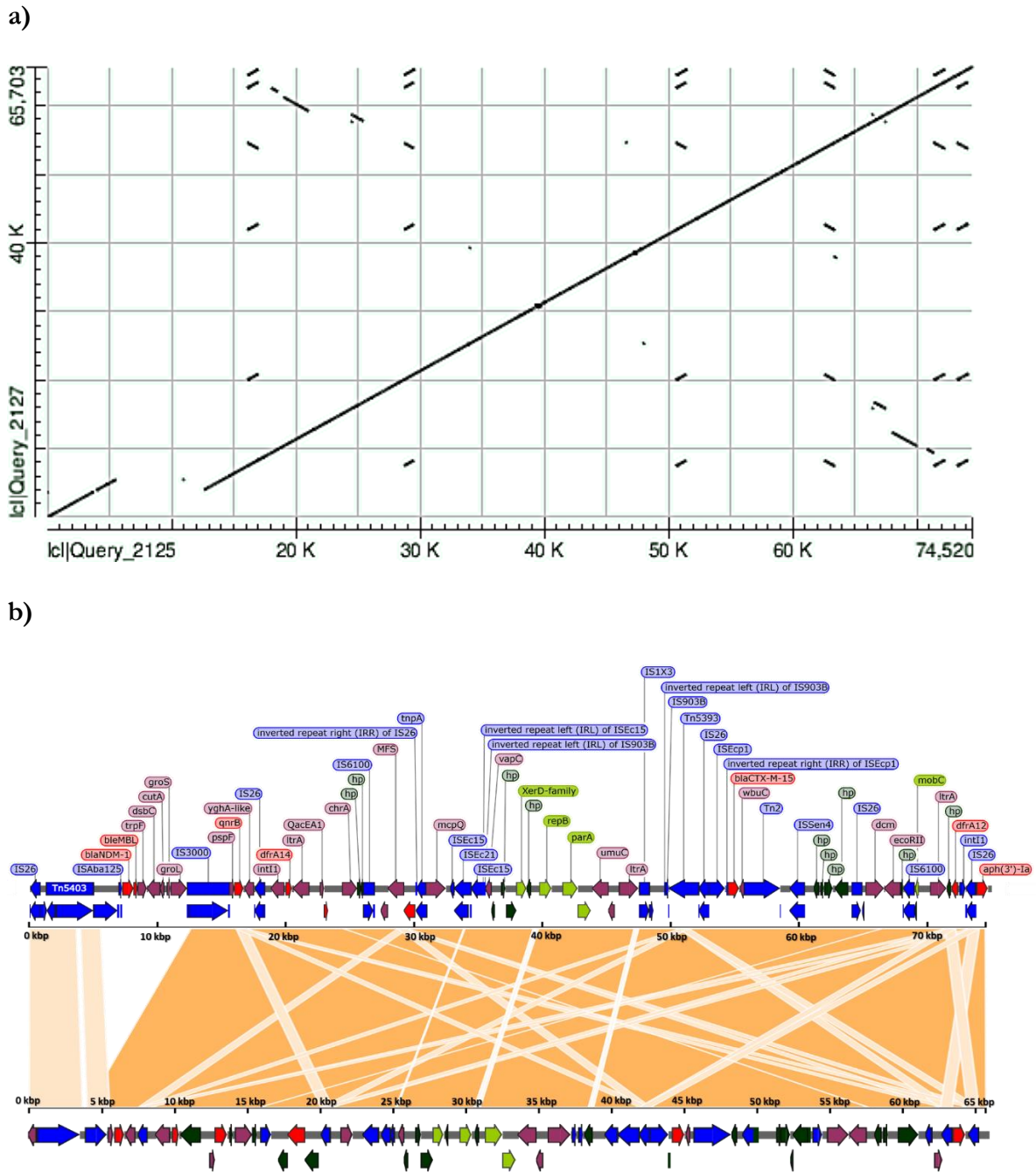


Figure 30. Comparison of plasmids IncN + IncR from isolates HUB-3 and HA-3. a) Dot Plot generated with NCBI BLAST of the HUB-3 IncN + IncR plasmid (ordinate axis) versus the HA-3 IncN + IncR plasmid (abscissa axis). We can see a gap that represents the missing part in HUB-3 plasmid, which carries the *bla_{NDM-1}* gene; the rest of the plasmid is the same. The little dots and lines represent repetitive regions along the plasmid, which are mainly mobile genetic elements; b) visual alignment of HUB-3 (top) and HA-3 (bottom) IncN + IncR plasmids generated with NCBI BLAST and Kahlammo. As seen in panel a), there is a region in HA-3 plasmid of approximately 7,200 bp absent in HUB-3 plasmid. This region is flanked by two IS3000 copies, and harbors different genes, such as *bla_{NDM-1}*. In red, antibiotic resistance genes; in blue, mobile genetic elements; in green, genes involved in plasmid mobilization and maintenance; in dark green; hypothetical genes; and finally, in purple other genes.

The size of the conjugative plasmid IncL/M was approximately 64 Kbp (**Figure 31**). This plasmid harbored the carbapenem-resistance gene *bla_{OXA-48}* and did not contain any co-resistance. This gene was located in a Tn1999.2 transposon inserted in the *tir* gene (Giani et al., 2012), flanked by two copies of the insertion sequence IS1999 (**Figure 32**).

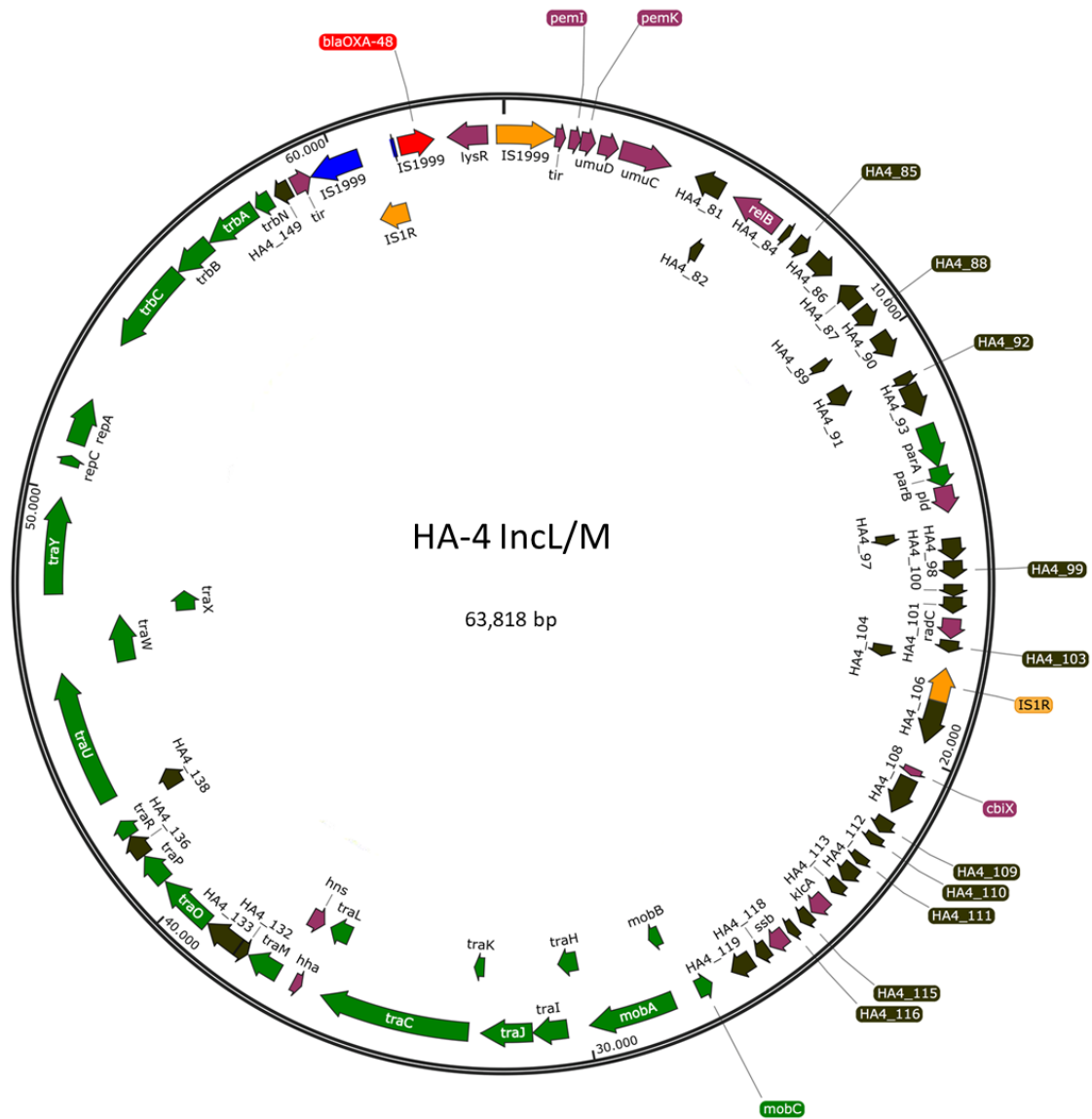


Figure 31. Schematic visualization of the plasmid harboring *bla_{OXA-48}* gene in HA-4 isolate. In red, antibiotic resistance genes; in blue and orange, truncated or full-length mobile genetic elements respectively; in green, genes involved in plasmid mobilization and maintenance; in dark green; hypothetical genes; and finally, in purple other genes. Figure excerpted and modified from (Marí-Almirall et al., 2020).

Finally, IncX3 plasmid (only found in HB-536) was 50,593 bp and harbored *bla*_{NDM-7}, and *bla*_{CTX-M-15}, as well as *ble* gene for bleomycin resistance, a glycopeptide antibiotic. In fact, this gene appears to be in tandem with *bla*_{NDM} genes in all plasmids that present a *bla*_{NDM} gene variant.

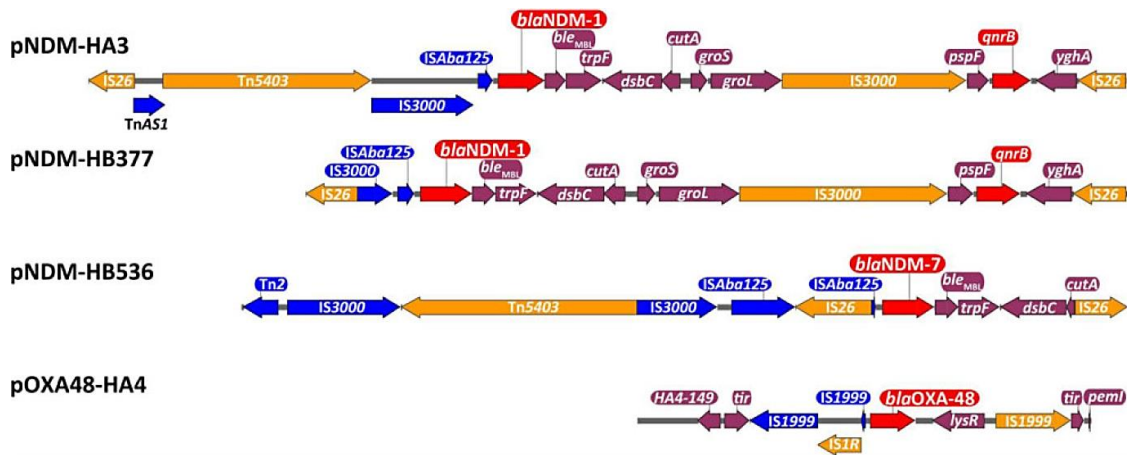


Figure 32. Visualization of genetic context of *bla*_{NDM-1}, *bla*_{NDM-7}, and *bla*_{OXA-48}. In red, antibiotic resistance genes; in orange, full-length MGEs; in blue, partial or truncated MGEs; in violet, other genes. Figure excerpted from (Marí-Almirall et al., 2020).

Despite *bla*_{NDM-1}, *bla*_{NDM-7} and *bla*_{OXA-48} were located in different plasmids, they shared a similar genetic environment (**Figure 32**): downstream the *bla*_{NDM} gene there was the bleomycin resistant gene *ble*, followed by phosphoribosyl anthranilate isomerase *trpF*, thiol:disulfide interchange *dsbC*, and dihydroorotate dehydrogenase *cutA*. In the case of *bla*_{NDM-1}, after this last gene there were two genes encoding chaperonin subunits (*groS* and *groL*). Upstream right before *bla*_{NDM} genes there were different truncated copies of different lengths of the ISAbal25 insertion sequence; moreover, all constructs presented complete insertion sequences IS26 flanking the construct. IS26 code for its own transposase. More differences relied on other MGEs presence. These contexts agreed with the previously described (Gottig et al., 2013; Pérez-Vázquez et al., 2019).

Hybrid assembly of *Klebsiella pneumoniae* isolates from Hospital B

For the three samples from Hospital B (HUB-1 to HUB-3), we also assembled and polished the *K. pneumoniae* chromosome. Nanopore coverage was 144X for HUB-1, 366X for HUB-2, and 83X for HUB-3. After polishing with Illumina data, the sizes retrieved were 5,255,272 bp for HUB-1; 5,289,995 bp for HUB-2; and 5,321,111 bp for HUB-3 (**Table 21**). All isolates were ST147, which confirmed prior PCR results (**Table 19**). The average GC% content was 57.43 % (57.4% for HUB-1 and HUB-3, and 57.5% for HUB-2).

Table 21. Genome characteristics and other plasmids bearing antibiotic resistances genes rather than β -lactamases in the three isolates from Hospital B. They share the same virulence factor genes and antibiotic resistance gene patterns. Inc, plasmid incompatibility group; VF, virulence factor; ARGs, antibiotic resistance genes; Cov, Nanopore coverage.

HYBRID SEQUENCING RESULTS (<i>Hospital B</i>)				
	Inc	Size (bp)	VF	ARGs
HUB-1	Genome	5,255,272	<i>fyuA, ybtE, ybtT, ybtU, irp1, irp2, ybtA, ybtP, ybtQ, ybtX, ybtS</i>	<i>vgaC, bla_{SHV-11}, OmpK37, bla_{CTX-M-15}, acrA, fosA6, oqxB, oqxA</i>
HUB-2	Genome	5,289,995	<i>fyuA, ybtE, ybtT, ybtU, irp1, irp2, ybtA, ybtP, ybtQ, ybtX, ybtS</i>	<i>vgaC, bla_{SHV-11}, OmpK37, bla_{CTX-M-15}, acrA, fosA6, oqxB, oqxA</i>
HUB-3	Genome	5,321,111	<i>fyuA, ybtE, ybtT, ybtU, irp1, irp2, ybtA, ybtP, ybtQ, ybtX, ybtS</i>	<i>vgaC, bla_{SHV-11}, OmpK37, bla_{CTX-M-15}, acrA, fosA6, oqxB, oqxA</i>
HUB-1	IncFII	121,011	-	<i>aac(6')-Ib-cr, arr-1, rmtF</i>
HUB-2	IncFII	121,022	-	<i>aac(6')-Ib-cr, arr-1, rmtF</i>
HUB-3	IncFII	119,094	-	<i>aac(6')-Ib-cr, arr-1, rmtF</i>
HUB-1	IncN + IncR	74,592	-	<i>aph(3')-Ia, dfrA12, dfrA14, bla_{CTX-M-15}, vgaC, mphA, Mrx, sul1, QnrB17, bleomycin resistance, bla_{NDM-1}</i>
HUB-2	IncL/M	63,865	-	<i>bla_{OXA-48}</i>
	IncN + IncR	74,611	-	<i>aph(3')-Ia, dfrA12, dfrA14, bla_{CTX-M-15}, vgaC, mphA, Mrx, sul1, QnrB17, bleomycin resistance, bla_{NDM-1}</i>
HUB-3	IncL/M	63,849	-	<i>bla_{OXA-48}</i>
	IncN + IncR	66,004	-	<i>aph(3')-Ia, dfrA12, dfrA14, bla_{CTX-M-15}, vgaC, mphA, Mrx, sul1, QnrB17</i>

The three *K. pneumoniae* from hospital B presented the *bla_{CTX-M-15}* gene located in the chromosome. This gene confers resistance to cephalosporines, a highly used antibiotic as a treatment for bacterial infections, so resistance to these antibiotics pose a challenge in infection treatment. *bla_{CTX-M-15}* gene presented upstream a complete copy of the insertion sequence ISEcp1, while downstream there was *wbuC* gene and a truncated copy of the transposon Tn2 (**Figure 33**).

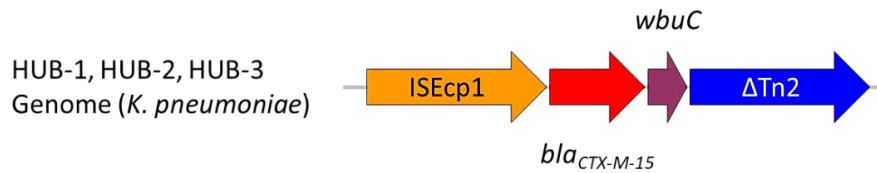


Figure 33. *bla*_{CTX-M-15} was present in the genome of three carbapenem-resistant *K. pneumoniae*, HUB-1, HUB-2, and HUB-3. In red, antibiotic resistance genes; in orange, full-length MGEs; in blue, partial, or truncated MGEs; in violet, other genes.

The three isolates harboured the same virulence factor genes and antibiotic resistance gene patterns in the chromosome. All the virulent factor genes are related to yersiniabactin siderophore (*fyuA*, *irp*, and *ybt* genes), which regulates the iron-uptake. These bacterial chromosomes presented genotypic resistance to streptogramin A (*vgaC*), β -lactams (*bla*_{CTX-M-15}, *bla*_{SHV-11}, *OmpK37*), fosfomycin (*fosA6*), fluoroquinolones (*oqxA*, *oqxB*) and others (*acrA*).

At the technical level, we further used this hybrid assembly approach to assess the improvement of the genome quality parameters through the polishing steps: first, after assembly with Flye; then after one step of Racon and two steps of Medaka using Nanopore reads; and finally, after one step of Racon using Illumina reads. Through each one of the polishing steps, we observed a sequential decrease on the number of CDS, as well as an increase on the completeness values (**Table 22**). All the genomes go from having approximately 8,000 CDS to approximately 5,000 CDS after Nanopore and Illumina polishing. Nanopore polishing only decreases CDS number by 1,000 approximately. On the other hand, completeness goes from an average of 46.9% to an average of 97.6% after final polishing, with an average of 57.5% with Nanopore-only polishing.

Table 22. Genome CDS number retrieved by Prokka, and genome completeness from Hospital B isolates by means of BUSCO. In this case, the completeness was assessed with the Enterobacteriaceae database, which includes 440 orthologs. Completeness column is the sum of Single and Duplicated columns. In parenthesis is the %. Nano., nanopore; Illum., illumina.

		CDS	Completeness	Single	Duplicated	Fragmented	Missing
HUB-1	Assembly	7,877	209 (47.5)	209 (47.5)	0 (0)	136 (30.9)	95 (21.6)
	Nano. Polish	7,047	261 (59.3)	261 (59.3)	0 (0)	108 (24.5)	71 (16.2)
	Nano + Illum. Polish	4,871	430 (97.8)	428 (97.3)	2 (0.5)	4 (0.9)	6 (1.3)
HUB-2	Assembly	7,927	197 (44.8)	197 (44.8)	0 (0)	153 (34.8)	90 (20.4)
	Nano. Polish	6,932	257 (58.5)	255 (58)	2 (0.5)	119 (27)	64 (14.5)
	Nano + Illum. Polish	4,897	431 (98)	429 (97.5)	2 (0.5)	3 (0.7)	6 (1.3)
HUB-3	Assembly	8,039	213 (48.4)	213 (48.4)	0 (0)	137 (31.1)	90 (20.5)
	Nano. Polish	7,187	244 (55.4)	243 (55.2)	1 (0.2)	130 (24.5)	66 (15.1)
	Nano + Illum. Polish	4,943	427 (97.1)	425 (96.6)	2 (0.5)	7 (1.6)	6 (1.3)

The results from Hospital A isolates have been published in the Journal of Antimicrobial Chemotherapy under the title “Dissemination of NDM-producing *Klebsiella pneumoniae* and *Escherichia coli* high-risk clones in Catalan healthcare institutions” (Marí-Almirall et al., 2020) (**annex 5**).

5. DISCUSSION

5.1. Harnessing long-read whole-genome sequencing to characterize One-Health pathogens

The increase in the spread of multidrug-resistant (MDR) bacteria due to the abusive and unregulated use of antibiotics puts the whole world on alert due to the difficulty in treating the associated infections. The infections produced by MDR pathogens are hard to treat even with last-resort antibiotics like colistin or carbapenems, which can ultimately lead to severe clinical complications, longer hospital stays, or even death (Kaye and Pogue, 2015). In addition, approximately 60% of the pathogens that cause infections in humans are of zoonotic origin –those transmitted from animals to humans– and can present a MDR pattern, so being animals a large reservoir of potential human pathogens (Bueno-Marí, 2015). Thus, One-Health studies and surveillance are crucial to characterize this kind of pathogens and understand the associated infections. Throughout this PhD project, we have applied whole-genome sequencing using long-read sequencing (Nanopore) in different One-Health scenarios to characterize three MDR pathogens: *Staphylococcus pseudintermedius* on dog skin, *Escherichia coli* on fecal samples from a mixed farm and *Klebsiella pneumoniae* on clinical isolates from a hospital outbreak.

The classical methods to characterize these pathogens in a clinical infection or an outbreak –such as those in hospitals or those caused by foodborne pathogens– are microbial culture, typically followed by typing methods such as 16S rRNA sequencing or multilocus sequence type (MLST). On one hand, microbial cultures have been the gold standard for bacterial isolation and characterization for decades. For a more in-depth characterization, microbial culture needs to be complemented by multiple phenotypic techniques (e.g., antibiograms for antibiotic susceptibility or APIs –analytical profile index– to classify microorganisms according to biochemistry test), which increase the time and resources for the identification and characterization of the microorganism (Figdor and Gulabivala, 2008).

Typing methods such as 16S rRNA sequencing or MLST focus on a tiny part of the complete genome. It has been thoroughly validated that, when appropriately performed, the analysis of full-length 16S rRNA gene (approximately 1,500 bp) serve as a potent tool to perform an accurate taxonomic classification of bacterial isolates (Woese et al., 1985; Winker and Woese, 1991), but this analysis only provides low taxonomic resolution (up to genus). For example, 16S rRNA sequencing cannot discriminate among *E. coli* and *Shigella* due to low divergence between them (>99% of 16S rRNA gene sequence identity in most cases) (Jenkins et al.,

2012; Devanga Ragupathi et al., 2018). A similar case happens with the members of the *Staphylococcus intermedius* Group (SIG), in which 16S rRNA sequencing fails to discriminate among species because 16S rRNA similarities are >99% (Devriese et al., 2005; Sasaki et al., 2007b; Devriese et al., 2009; Magleby et al., 2019; Perreten et al., 2020).

For the microorganisms in our studies, MLST takes into account seven housekeeping genes specific for each bacterium. The sum of the sizes of these seven genes is approximately 2,944 bp for *S. pseudintermedius*, 3,423 bp for *E. coli*, and 3,012 bp for *K. pneumoniae* (Larsen et al., 2012). Considering an average genome size of 3.09 Mbp for Firmicutes (phylum in which *S. pseudintermedius* is included) and 4.23 Mbp for Gammaproteobacteria (phylum in which *E. coli* and *K. pneumoniae* are included) (Větrovský and Baldrian, 2013), MLST typing would only be considering 0.09% of *S. pseudintermedius*'s genome, 0.08% of *E. coli*'s genome, and 0.07% of *K. pneumoniae*'s genome. On the other hand, genomic recombination plays a pivotal role in the evolution of bacteria; however, MLST analysis does not consider if a recombination event has occurred, which can affect in the analysis of phylogenetic relations (Chaudhuri and Henderson, 2012).

Sequencing the whole bacterial genome (WGS) in few hours is an approach that complements perfectly the gold standard for bacterial isolation, the microbial culture, providing a significantly higher resolution (Gardy and Loman, 2018).

The first studies that considered WGS were performed using short-read sequencing. The short-read WGS main pitfall is the raw read lengths. Reads of 100 bp, 250 bp, or 500 bp do not span repetitive sequences (such as those representing MGEs), duplications, inversions, or other structural variations, which hampers the complete assembly the chromosomes and plasmids.

In May 2011-June 2011, an outbreak caused by a Shiga-toxin-producing *E. coli* O104:H4 from contaminated bean sprouts was described in Germany, with more than 3,000 people infected and more than 40 deaths. Different research groups studied the outbreak applying short-read sequencing (Brzuszkiewicz et al., 2011; Mellmann et al., 2011; Rohde et al., 2011). Short-read WGS allowed determining the species and serotype of the microorganism causing the outbreak, *E. coli* O104:H4. Moreover, it also allowed detecting antibiotic-resistance genes categorized as plasmid-borne (such as *bla*_{CTX-M-15} gene) and other elements like the gene encoding for Shiga-toxin (*stx2* gene). However, the genome assemblies for *E. coli* (including the chromosome and putative plasmids) were recovered in several contigs (of the order of hundreds per isolate). They had to map their contigs to references for unravelling if the

sequence was chromosomal or plasmidic, as well as perform additional assays to detect the presence of plasmids, such as electrophoresis. So, with short-read WGS, they could not retrieve the entire length of the chromosome or plasmids in a single contig. In contrast in our *E. coli* study, using long-read WGS we were able to assemble *de novo* –without the need of using a pre-existent reference– 14/18 full chromosomes and 60 plasmids in single-contigs. We succeeded in giving context to the genes conferring resistance to antibiotics, locating them to the chromosome or the plasmid. Other authors have already used nanopore WGS to sequence the genome of *E. coli*, retrieving the chromosome and plasmids in one contig each (Schneider et al., 2020; Matrasingh et al., 2021).

Between May 2012 and September 2013, there was an outbreak of ST15 CTX-M-15-producing *K. pneumoniae* in the north of Netherlands (Zhou et al., 2016). They performed WGS of 18 samples from clinical and environmental origin using short-read (Illumina MiSeq) and they successfully described the presence of ST15 *K. pneumoniae* causing the outbreak in healthcare settings. However, they did not assemble closed plasmids, they only described some “plasmid-borne resistance genes” (such as *bla_{CTX-M-15}*) by comparing to previous data. Another study characterized the emergence of a plasmid-borne *bla_{KPC-3}* carbapenem-resistant *K. pneumoniae* causing infections by sequencing 10 isolates using Illumina (Shields et al., 2017). The assembly of the plasmids was partial and incomplete, and they also referred to “plasmid-borne genes”. To further characterize plasmids, they complemented the work experimentally by performing laboratory transfer of the plasmids from the isolates to *E. coli* and assessed it with microbial culture with ceftazidime-avibactam –a combination of a cephalosporine and a β -lactamase inhibitor–. In contrast, in our *K. pneumoniae* study using only long-read WGS we were able to confirm the previous results regarding carbapenem-resistance plasmids obtained through MALDI-TOF MS, PFGE, biparental conjugation, disk diffusion susceptibility test, and PCR for plasmid’s incompatibility groups and ARGs. We assembled the plasmids from Hospital A and Hospital B isolates harboring *bla_{NDM-1}*, *bla_{NDM-7}*, *bla_{CTX-M-15}*, and *bla_{OXA-48}* in circular single-contigs, rather than only describing contigs containing “plasmid-borne genes”. We also described the location and genetic context of the antibiotic resistance genes, including repetitive sequences like MGEs. The full characterization of the plasmids allowed to confirm the transmission of *K. pneumoniae* carbapenem-resistance plasmids among different healthcare centers included in the study of Hospital A.

5.2. Long-read whole-genome sequencing to unravel antimicrobial resistance and its transmission patterns

With long-read WGS, we have been able to locate the antimicrobial resistance genes in their genetic (e.g. presence of MGE) and genomic context (chromosomal or plasmid), and further understand their transmission.

In the *E. coli* study, we evaluated the transmission of colistin resistance plasmids within a mixed farm applying long-read WGS. The 15 isolates bearing *mcr-1* in mobile genetic elements were associated with IncX4, IncI2, and IncHI2\IncHI2A plasmids, with IncX4 being the most prevalent in agreement with previous studies (Li et al., 2017b; Sun et al., 2017; Zurfluh et al., 2017; Bai et al., 2018; Li et al., 2018a; Wang et al., 2018; Wu et al., 2018). All IncX4 plasmids shared the same backbone, and differences were due to inserted sequences. Different families of ARGs located in the same plasmid facilitated the persistence and selection of resistance to antibiotics not used in the farm. As previously described (Sun et al., 2017; Bai et al., 2018; Li et al., 2018a; Shen et al., 2018; Wu et al., 2018), herein, *mcr-1* was also integrated into the genome in two isolates of different animal origins. In one of them, the ISApI1 element was flanking *mcr-1* upstream and downstream, a structure that probably facilitated the movement of the whole element by transposition. The other isolate had lost the ISApI1 element, establishing the *mcr-1* as a heritable trait overcoming any possible fitness cost of plasmid maintenance (Dunn et al., 2019). Furthermore, this isolate had become permanently resistant even when the selective pressure was removed (Bai et al., 2018; San Millan, 2018).

Although phylogenetic analysis clustered the *E. coli* isolates in phylotype A and B1, there were different MLST lineages harboring the colistin resistance genes in highly similar IncX4 plasmids. The farmer's isolate (ST398) did not match the MLST type of any of the livestock isolates. Conversely, the IncX4 plasmid from the farmer's isolate was highly similar (identity ranging from 99.96% to 100%) to those obtained from calves (14-4, 14-20, 15A-16, 15B-22, and V7_18), sharing length, GC content, and genomic context (*mcr-1-pap2*). These results suggest the transmission of antimicrobial resistance carrying plasmid between different *E. coli* lineages from the calves to the farmer (**Figure 34**). Several studies have demonstrated the spread of ARGs from food-producing animals to veterinarians and personnel in direct contact with animals (Tomley and Shirley, 2009; McDaniel et al., 2014; Saliu et al., 2017), highlighting the importance of implementing hygiene measures to reduce this transmission.

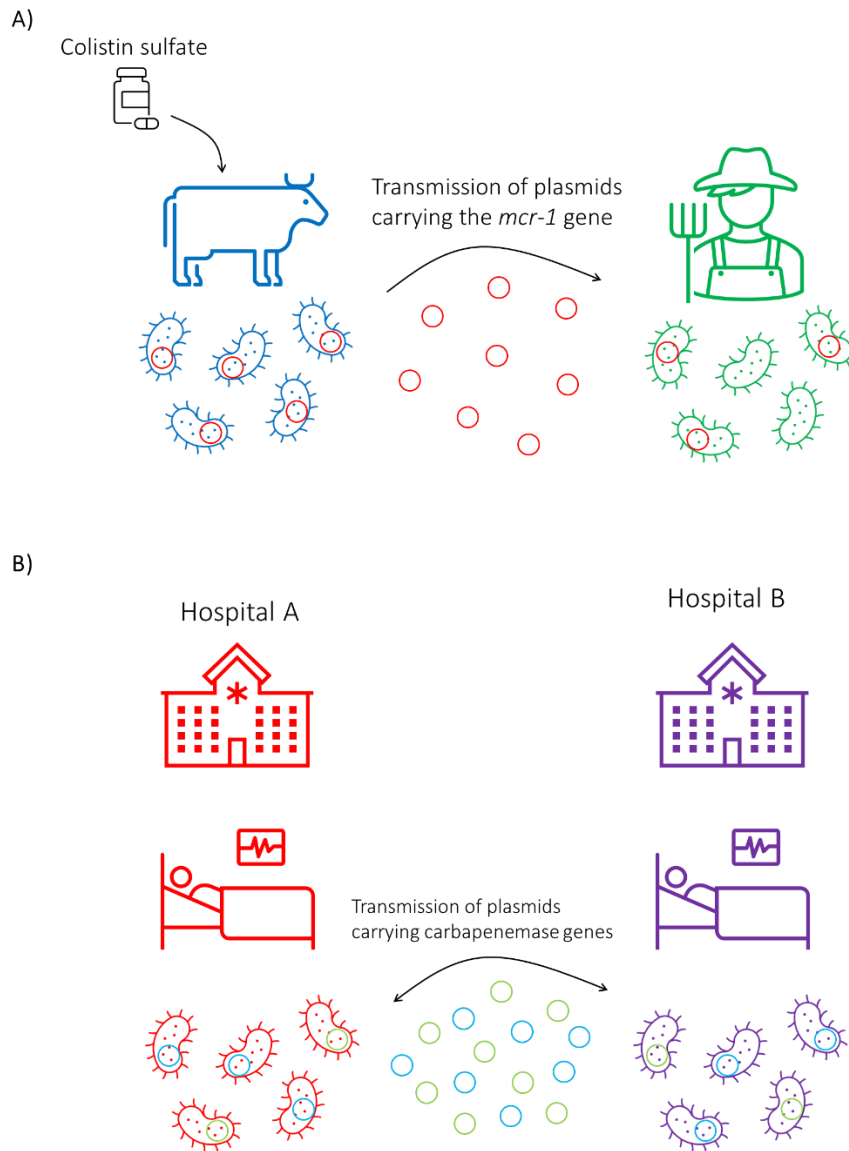


Figure 34. Clonal transmission of plasmids within a mixed farm and between hospitals. A) The *E. coli* isolated from the Farmer (green) was not phylogenetically related to the *E. coli* isolated from swine or bovine (blue) fecal samples. However, the *mcr-1* gene conferring resistance to colistin was described in the Farmer's isolate in an IncX4 plasmid, as well as for some isolates from bovine and swine origin. Through WGS, we described that the plasmid held by the human isolate was potentially transmitted from bovine *E. coli*. B) The plasmids bearing carbapenem resistance (in blue and green) described in Hospital A (red) were also described in Hospital B (violet). The flux of patients allowed for the clonal expansion of these plasmids.

All the isolates from this study exhibited a MDR profile. In addition, ARGs, as well as virulence factors, were described both in the chromosome and plasmids. *E. coli* isolates of cattle origin showed the highest number and diversity of plasmids encoding for both ARGs and virulence genes, including *stx2*. Shiga toxin *E. coli* (STEC) serotype O81:H31 bearing *stx2* are considered important foodborne zoonotic pathogens (Hussein and Bollinger, 2005;

Padola and Etcheverri-a, 2014; Thomas et al., 2016; Fan et al., 2019). To our knowledge, this is the first description of a *mcr-1* positive STEC of cattle origin and highlights the importance of food producing animals as reservoirs of ARG and virulence determinants.

The isolate that lost *mcr-1* gene (15A_11, phylotype A, ST4981) was resistant to cephalosporins (cefotaxime and ceftazidime) with *bla*_{CTX-M-15} inserted in the chromosome. Interestingly, upstream of the gene, there was an IS3 element, and downstream there was a truncated Tn2, indicating a possible recombination event, as has been previously described (Komoda et al., 1991; Yasui and Kurosawa, 1993). The acquisition of *bla*_{CTX-M-15} in livestock is concerning, since it is widely disseminated (Cantón and Coque, 2006; Bevan et al., 2017; Chong et al., 2018), especially in healthcare facilities (Boyd et al., 2004; Mehrad et al., 2015; Bevan et al., 2017; Yasir et al., 2020), and can compromise the treatment of Gram-negative infections.

In the *K. pneumoniae* study, we characterized the spread of carbapenem-resistant isolates between different healthcare institutions. With long-read WGS, we have assembled IncN + IncR and IncL/M plasmids from both hospitals in circular contigs. HA-3 and HA-4 from Hospital A, and HUB-1 and HUB-2 from Hospital B presented the same IncN + IncR plasmid (identities >99%). WGS corroborated previous results through conventional approaches showing that ST147 *K. pneumoniae* isolates harbored both the *bla*_{NDM-1} and *bla*_{CTX-M-15} genes in a single plasmid belonging to the IncR incompatibility group. We also described the same IncL/M plasmid harboring *bla*_{OXA-48} carbapenemase gene in isolates from both hospitals (Hospital A: HA-4; Hospital B: HUB-2 and HUB-3).

Another concerning issue relates to the presence of yersiniabactin in the *K. pneumoniae* isolates from Hospital B. Yersiniabactin is a siderophore present in 90% of the hypervirulent *K. pneumoniae* isolated from clinical cases related with severe lung infections such as community-acquired pneumonia (Paczosa and Mecsas, 2016; Kramer et al., 2020). An outbreak of yersiniabactin-producing *K. pneumoniae* has recently been reported related to fulminant necrotizing enterocolitis and sepsis in a neonatal intensive care unit (Wisgrill et al., 2019). In our case, yersiniabactin-coding locus is in the chromosome. Yersiniabactin-coding locus was firstly described in a high-pathogenicity island of *Yersinia* (Paczosa and Mecsas, 2016) carried in an integrative conjugative element, ICE*Kp*, which is a highly self-transmissible mobile genetic element within the bacterial population (Lam et al., 2018). Thus, these isolates have the potential to transfer the locus coding for yersiniabactin to other bacteria while causing infection.

5.3. *Staphylococcus pseudintermedius* in dogs with pyoderma and healthy dogs

Methicillin-resistant *S. pseudintermedius* (MRSP) is a confirmed zoonotic pathogen from dogs (Van Hoovels et al., 2006). In human, *S. aureus* is one of the main commensal bacteria in the skin and opportunistic pathogen (Williams, 1967). Thus, as described before for coagulase-negative staphylococci to *S. aureus* (Jamale, 2011; Xu et al., 2018b), MRSP isolates have the potential to transmit the resistance to other Staphylococci associated with human infections (e.g., *S. aureus*), leading to the need for MRSP surveillance with a One-Health approach. In fact, as of May of 2021, while *S. aureus*—a deeply studied pathogen—present 12,585 available genomes at the Genome Assembly and Annotation report in NCBI (<https://www.ncbi.nlm.nih.gov/genome/>), *S. pseudintermedius* present only 376 genomes, from which our group has submitted 62/376: the one isolated from otitis, 22 from healthy canine skin, 33 from the lesioned skin of dogs with pyoderma, and six isolated from the healthy skin of dogs affected with pyoderma (these last six isolates were not included in the results of this thesis, for more information see (Francino et al., 2021)).

In our studies applying long-read WGS for *S. pseudintermedius* sequencing, we decided to take a clinical approach to analyze *S. pseudintermedius* isolates from the lesional skin of dogs with pyoderma and compare them with isolates from the skin of healthy dogs (perioral and abdominal).

With only one approach, we have described the MLST of the isolates, the genetic bases of antibiotic resistances, and the presence of virulence factor genes. Antibiotic resistance of the otitis isolate was previously tested through disk diffusion susceptibility test, and our hybrid sequencing results corroborated the genetic bases for all the resistances described, either caused by acquired genes (in the chromosome or a plasmid) or caused by point mutations (fluoroquinolone resistance due to mutations in the *gyrA* gene).

The most represented MLST among the 56 *S. pseudintermedius* studied within this thesis was ST71 (16/56), which coincides with the most represented MLST in Europe. ST258 has been reported as an emerging lineage in France, gaining growth over ST71 clones (Bergot et al., 2018). In our study, ST71 harbored the greatest variety of ARGs among pathogenic isolates, followed by ST258 and ST301 (from clonal complex 258), in agreement with previous results (Bergot et al., 2018).

S. pseudintermedius presented a wide range of antibiotic resistance genes against both first-line antibiotics (cephalosporines, amoxicillin, lincosamides, tetracyclines and sulfonamides) and

third-line antibiotics (chloramphenicol and aminoglycosides). In fact, we have described resistance to all these antibiotics in our isolates, which is concerning regarding infection treatment. Alternatively, topical treatment using antiseptics such as shampoos with chlorhexidine, benzoyl peroxide, and ethyl lactate improved antibacterial treatment by accelerating the resolution of clinical signs (Beco et al., 2013; Bajwa, 2016).

The average genome size for *S. pseudintermedius* isolates was approximately 2.68 Mbp, which was similar to the size reported by other authors (Shah et al., 2018; Little et al., 2019; Cao et al., 2020; Eichhorn et al., 2020; Vitali et al., 2021). However, if we take a closer look at our results, *S. pseudintermedius* isolated from healthy dogs presented a smaller average genome size (2.58 Mbp) than isolates retrieved from the lesional skin of dogs with pyoderma (2.74 Mbp). A significantly higher number of ARGs and phages explains the differences in the genome size.

Pangenome analysis of healthy versus pyoderma isolates concluded that *S. pseudintermedius* presents an open genome –a pangenome that increases in size when a new genome is added (Rouli et al., 2015)–. These results were in concordance with the results obtained by Brooks and collaborators, in which they analyzed 371 genomes, and found that *S. pseudintermedius* had an open pangenome, similar to other *Staphylococcus* species. The specimens isolated from the lesional skin of dogs with pyoderma exhibited a higher accessory genome (46.5%) than the healthy ones (35.9%). A higher accessory genome portion indicates more particular functions, such as antibiotic resistance or the presence of MGEs (such as plasmids, transposons, prophages) (Brooks et al., 2020).

At the functional level, *S. pseudintermedius* isolated from healthy dogs presented enrichment in the CRISPR-Cas system, components of toxin-antitoxin systems, and endonucleases and methylases from restriction-modification systems, as well as lower number of phage sequences inserted in the genome compared to isolates from pyoderma. Therefore, *S. pseudintermedius* isolated from healthy dogs presented enriched functions that participate in the defense of the bacterial cell against exogenous nucleic acids, such as those from phages or plasmids. This could explain why healthy isolates did not present phage and plasmid enriched functions like the pathogenic strains and the difference in phage presence with respect to pyoderma isolates.

While the average number of phages in isolates from healthy dogs was 1.27, isolates from pyoderma presented an average number of 3.55. More specifically, pyoderma isolates ST71 presented an average of 6.07 phage sequences. This agrees with previous results, that state

that ST71 is one of the clones carrying higher numbers of intact prophages (Brooks et al., 2020). They described the SpST71A as a lineage-specific prophage for ST71 inserted in the *comG* operon –responsible for pilus formation to transform exogen DNA–, truncating it (Brooks et al., 2020). SpST71A prophage truncating *comG* operon may affect the capacity of ST71 clones to transform DNA, which could lead to its clonal expansion rather than transfer genetic elements horizontally (Brooks et al., 2020). All our ST71 *S. pseudintermedius* harbored the SpST71A prophage disrupting the *comG* operon. Moreover, since no conjugative plasmids were found among our *S. pseudintermedius*, transduction could be the leading mechanism for horizontal gene transfer among isolates from infections. In fact, previous studies have described the role of transduction in the transmission of antibiotic resistance genes among staphylococci (Novick and Morse, 1967), even in the transmission of MGEs including *SCCmec* in *S. aureus*, indicating that prophages play a role in the origin and evolution of methicillin resistance (Mašláňová et al., 2013). Further studies and analysis are needed to decipher the role of prophages in the virulence and adaptation of *S. pseudintermedius*.

5.4. Future steps

In this thesis we have applied long-read WGS to assess the transmission of antimicrobial resistance both in animal and human health. However, one of the main pitfalls of WGS is that it relies on a previous culture step. Future steps should consider a metagenomics approach (clinical metagenomics) sequencing all the genetic material from the clinical sample on low-cost and portable sequencers for the rapid, real-time identification of pathogens and antimicrobial resistance genes. Clinical metagenomics could help in overcoming the incubation time and associated delay in the results, especially for fastidious microorganisms (e.g., tuberculosis may take up to two/four weeks to grow on plate, and two/four weeks more to perform antibiotic susceptibility (Ghodbane et al., 2015)), and to personalize antimicrobial stewardship, tackling infection and antimicrobial resistance globally.

6. CONCLUSIONS

1. Long-read whole genome sequencing and *de novo* assembly retrieved complete chromosomes and plasmids as single contigs, locating the antibiotic resistance genes in plasmids or chromosomes, and spanning mobile genetic elements, thus overcoming the pitfalls associated with short-read.
2. Long-read whole genome sequencing and *de novo* assembly unraveled the transmission of similar plasmids harboring antibiotic resistance genes in different One-Health scenarios: colistin-resistant *Escherichia coli* from livestock to human and carbapenem-resistant *Klebsiella pneumoniae* in an inter-hospital outbreak.
3. Different *Escherichia coli* lineages harbored highly similar IncX4 plasmids carrying the *mcr-1* gene. Specifically, the farmer's isolate presented an IncX4 plasmid most likely transmitted by horizontal gene transfer from cattle, even though the farmer's isolate was phylogenetically unrelated to the livestock's ones.
4. Methicillin resistance was only detected in isolates from dogs with pyoderma, being *Staphylococcus pseudintermedius* ST71 and ST258 the most frequent sequence types. In contrast, most of the sequence types in healthy isolates have not been described yet.
5. The genome size of *Staphylococcus pseudintermedius* was significantly larger in pyoderma than in healthy dogs' isolates. *Staphylococcus pseudintermedius* were enriched in antibiotic resistances and mobilome functions in pyoderma isolates. In contrast, isolates from healthy skin presented enriched functions related to self-defense against exogenous DNA.
6. The multi-drug resistant and virulence profiles of *Staphylococcus pseudintermedius* from dogs and *Escherichia coli* from livestock highlight the role of domestic animals as a reservoir of pathogens with highly zoonotic potential.

7. REFERENCES

- Aguayo-Reyes A, Quezada-Aguiluz M, Mella S, Riedel G, Opazo-Capurro A, Bello-Toledo H, Domínguez M, González-Rocha G** (2018) Bases moleculares de la resistencia a meticilina en *Staphylococcus aureus*. *Rev Chil Infectol* **35**: 7–14
- Alibayov B, Baba-Moussa L, Sina H, Zdeňková K, Demnerová K** (2014) *Staphylococcus aureus* mobile genetic elements. *Mol Biol Rep* **41**: 5005–5018
- Alikhan NF, Petty NK, Ben Zakour NL, Beatson SA** (2011) BLAST Ring Image Generator (BRIG): Simple prokaryote genome comparisons. *BMC Genomics* **12**: 402
- Arahal DR** (2014) Whole-genome analyses: Average nucleotide identity. *Methods Microbiol*. Academic Press Inc., pp 103–122
- Arndt D, Grant JR, Marcu A, Sajed T, Pon A, Liang Y, Wishart DS** (2016) PHASTER: a better, faster version of the PHAST phage search tool. *Nucleic Acids Res*. doi: 10.1093/nar/gkw387
- Bai F, Li X, Niu B, Zhang Z, Malakar PK, Liu H, Pan Y, Zhao Y** (2018) A *mcr-1*-Carrying Conjugative IncX4 Plasmid in Colistin-Resistant *Escherichia coli* ST278 Strain Isolated From Dairy Cow Feces in Shanghai, China. *Front Microbiol* **9**: 1–9
- Bajwa J** (2016) Canine superficial pyoderma and therapeutic considerations. *Can Vet J* **57**: 204–6
- Balachandran M, Bemis DA, Kania SA** (2018) Expression and function of protein A in *Staphylococcus pseudintermedius*. *Virulence* **9**: 390–401
- Bannoehr J, Franco A, Iurescia M, Battisti A, Fitzgerald JR** (2009) Molecular Diagnostic Identification of *Staphylococcus pseudintermedius*. *J Clin Microbiol* **47**: 469–471
- Bannoehr J, Guardabassi L** (2012) *Staphylococcus pseudintermedius* in the dog: taxonomy, diagnostics, ecology, epidemiology and pathogenicity. *Vet Dermatol* **23**: 253-e52
- Bannoehr J, Ben Zakour NL, Reglinski M, Inglis NF, Prabhakaran S, Fossum E, Smith DG, Wilson GJ, Cartwright RA, Haas J, et al** (2011) Genomic and Surface Proteomic Analysis of the Canine Pathogen *Staphylococcus pseudintermedius* Reveals Proteins That Mediate Adherence to the Extracellular Matrix. *Infect Immun* **79**:

- Bassett E, Keith M, Armelagos G, Martin D, Villanueva A** (1980) Tetracycline-labeled human bone from ancient Sudanese Nubia (A.D. 350). *Science* (80-) **209**: 1532–1534
- Beco L, Guaguère E, Lorente Méndez C, Noli C, Nuttall T, Vroom M** (2013) Suggested guidelines for using systemic antimicrobials in bacterial skin infections (2): Antimicrobial choice, treatment regimens and compliance. *Vet Rec* **172**: 156–160
- Beghain J, Bridier-Nahmias A, Le Nagard H, Denamur E, Clermont O** (2018) ClermonTyping: an easy-to-use and accurate in silico method for Escherichia genus strain phylotyping. *Microb Genomics*. doi: 10.1099/mgen.0.000192
- Bennett PM** (1999) Integrons and gene cassettes: a genetic construction kit for bacteria. *J Antimicrob Chemother* **43**: 1–4
- Bergot M, Martins-Simoes P, Kilian H, Châtre P, Worthing KA, Norris JM, Madec JY, Laurent F, Haenni M** (2018) Evolution of the population structure of staphylococcus pseudintermedius in France. *Front Microbiol*. doi: 10.3389/fmicb.2018.03055
- Bertani B, Ruiz N** (2018) Function and Biogenesis of Lipopolysaccharides. *EcoSal Plus*. doi: 10.1128/ecosalplus.ESP-0001-2018
- Bevan ER, Jones AM, Hawkey PM** (2017) Global epidemiology of CTX-M β -lactamases: temporal and geographical shifts in genotype. *J Antimicrob Chemother* **72**: 2145–2155
- Bonnet M, Lagier JC, Raoult D, Khelaifia S** (2020) Bacterial culture through selective and non-selective conditions: the evolution of culture media in clinical microbiology. *New Microbes New Infect* **34**: 100622
- Boyd DA, Tyler S, Christianson S, McGeer A, Muller MP, Willey BM, Bryce E, Gardam M, Nordmann P, Mulvey MR, et al** (2004) Complete Nucleotide Sequence of a 92-Kilobase Plasmid Harboring the CTX-M-15 Extended-Spectrum Beta-Lactamase Involved in an Outbreak in Long-Term-Care Facilities in Toronto, Canada. *Antimicrob Agents Chemother* **48**: 3758–3764
- Brooks MR, Padilla-Vélez L, Khan TA, Qureshi AA, Pieper JB, Maddox CW, Alam MT** (2020) Prophage-Mediated Disruption of Genetic Competence in

Staphylococcus pseudintermedius . mSystems. doi: 10.1128/msystems.00684-19

Brunder W, Schmidt H, Karch H (1996) KatP, a novel catalase-peroxidase encoded by the large plasmid of enterohaemorrhagic *Escherichia coli* O157:H7. *Microbiology* **142**: 3305–3315

Brzuszkiewicz E, Thürmer A, Schuldes J, Leimbach A, Liesegang H, Meyer F-D, Boelter J, Petersen H, Gottschalk G, Daniel R (2011) Genome sequence analyses of two isolates from the recent *Escherichia coli* outbreak in Germany reveal the emergence of a new pathotype: Entero-Aggregative-Haemorrhagic *Escherichia coli* (EAHEC). *Arch Microbiol* **193**: 883–891

Bueno-Marí R (2015) Editorial: Emerging Zoonoses: Eco-Epidemiology, Involved Mechanisms, and Public Health Implications. *Front Public Heal*. doi: 10.3389/fpubh.2015.00157

Bugarel M, Martin A, Fach P, Beutin L (2011) Virulence gene profiling of enterohemorrhagic (EHEC) and enteropathogenic (EPEC) *Escherichia coli* strains: A basis for molecular risk assessment of typical and atypical EPEC strains. *BMC Microbiol* **11**: 142

C Reygaert W (2018) An overview of the antimicrobial resistance mechanisms of bacteria. *AIMS Microbiol* **4**: 482–501

Cáceres ME, Etcheverría AI, Fernández D, Rodríguez EM, Padola NL (2017) Variation in the distribution of putative virulence and colonization factors in shiga toxin-producing *Escherichia coli* Isolated from different categories of cattle. *Front Cell Infect Microbiol*. doi: 10.3389/fcimb.2017.00147

Cantón R, Coque TM (2006) The CTX-M β -lactamase pandemic. *Curr Opin Microbiol* **9**: 466–475

Cao W, Hicks K, White A, Hathcock T, Kennis R, Boothe D, Zhang D, Wang X (2020) Draft Genome Assemblies of Two *Staphylococcus pseudintermedius* Strains Isolated from Canine Skin Biopsy Specimens . *Microbiol Resour Announc*. doi: 10.1128/mra.00369-20

Carattoli A, Zankari E, García-Fernández A, Voldby Larsen M, Lund O, Villa L, Møller Aarestrup F, Hasman H (2014) In Silico Detection and Typing of Plasmids using PlasmidFinder and Plasmid Multilocus Sequence Typing. *Antimicrob Agents*

Chemother **58**: 3895–3903

- Castro VS, Carvalho RCT, Conte-Junior CA, Figueiredo EES** (2017) Shiga-toxin Producing *Escherichia coli*: Pathogenicity, Supershedding, Diagnostic Methods, Occurrence, and Foodborne Outbreaks. *Compr Rev Food Sci Food Saf* **16**: 1269–1280
- Catry B, Cavaleri M, Baptiste K, Grave K, Grein K, Holm A, Jukes H, Liebana E, Navas AL, Mackay D, et al** (2015) Use of colistin-containing products within the European Union and European Economic Area (EU/EEA): development of resistance in animals and possible impact on human and animal health. *Int J Antimicrob Agents* **46**: 297–306
- CDC** (2018) One Health Basics. Centers Dis. Control Prev. , Natl. Cent. Emerg. Zoonotic Infect. Dis., <https://www.cdc.gov/onehealth/basics/index.html>
- CDC** (2020) Antibiotic / Antimicrobial Resistance (AR/AMR). <https://www.cdc.gov/drugresistance/about/how-resistance-happens.html>
- Cepeda-Molero M, Berger CN, Walsham ADS, Ellis SJ, Wemyss-Holden S, Schüller S, Frankel G, Fernández LÁ** (2017) Attaching and effacing (A/E) lesion formation by enteropathogenic *E. coli* on human intestinal mucosa is dependent on non-LEE effectors. *PLOS Pathog* **13**: e1006706
- Cepeda-Molero M, Schüller S, Frankel G, Ángel Fernández L** (2020) Systematic Deletion of Type III Secretion System Effectors in Enteropathogenic *E. coli* Unveils the Role of Non-LEE Effectors in A/E Lesion Formation. *E coli Infect.* doi: 10.5772/intechopen.91677
- Chakravorty S, Helb D, Burday M, Connell N** (2007) A detailed analysis of 16S ribosomal RNA gene segments for the diagnosis of pathogenic bacteria. *J Microbiol Methods* **69**: 330–339
- Chaudhuri RR, Henderson IR** (2012) The evolution of the *Escherichia coli* phylogeny. *Infect Genet Evol* **12**: 214–226
- Chen L, Zheng D, Liu B, Yang J, Jin Q** (2016) VFDB 2016: hierarchical and refined dataset for big data analysis—10 years on. *Nucleic Acids Res* **44**: D694–D697
- Cheung GYC, Joo HS, Chatterjee SS, Otto M** (2014) Phenol-soluble modulins - critical

determinants of staphylococcal virulence. *FEMS Microbiol Rev* **38**: 698–719

Chong Y, Shimoda S, Shimono N (2018) Current epidemiology, genetic evolution and clinical impact of extended-spectrum β -lactamase-producing *Escherichia coli* and *Klebsiella pneumoniae*. *Infect Genet Evol* **61**: 185–188

Chopra I, Roberts M (2001) Tetracycline Antibiotics: Mode of Action, Applications, Molecular Biology, and Epidemiology of Bacterial Resistance. *Microbiol Mol Biol Rev* **65**: 232–260

Chun J, Oren A, Ventosa A, Christensen H, Arahal DR, da Costa MS, Rooney AP, Yi H, Xu XW, De Meyer S, et al (2018) Proposed minimal standards for the use of genome data for the taxonomy of prokaryotes. *Int J Syst Evol Microbiol* **68**: 461–466

Codjoe F, Donkor E (2017) Carbapenem Resistance: A Review. *Med Sci* **6**: 1

Cunningham AA, Daszak P, Wood JLN (2017) One Health, emerging infectious diseases and wildlife: two decades of progress? *Philos Trans R Soc B Biol Sci* **372**: 20160167

Damborg P, Moodley A, Aalbæk B, Ventrella G, dos Santos TP, Guardabassi L (2016) High genotypic diversity among methicillin-resistant *Staphylococcus pseudintermedius* isolated from canine infections in Denmark. *BMC Vet Res*. doi: 10.1186/s12917-016-0756-y

Daszak P (2000) Emerging Infectious Diseases of Wildlife-- Threats to Biodiversity and Human Health. *Science* (80-) **287**: 443–449

Denamur E, Clermont O, Bonacorsi S, Gordon D (2021) The population genetics of pathogenic *Escherichia coli*. *Nat Rev Microbiol* **19**: 37–54

Derbise A, Aubert S, El Solh N (1997) Mapping the regions carrying the three contiguous antibiotic resistance genes *aadE*, *sat4*, and *aphA-3* in the genomes of staphylococci. *Antimicrob Agents Chemother* **41**: 1024–1032

Descloux S, Rossano A, Perreten V (2008) Characterization of new staphylococcal cassette chromosome *mec* (SCC*mec*) and topoisomerase genes in fluoroquinolone- and methicillin-resistant *Staphylococcus pseudintermedius*. *J Clin Microbiol* **46**: 1818–1823

Devanga Ragupathi NK, Muthuirulandi Sethuvel DP, Inbanathan FY,

- Veeraraghavan B** (2018) Accurate differentiation of *Escherichia coli* and *Shigella* serogroups: challenges and strategies. *New Microbes New Infect* **21**: 58–62
- Devriese LA, Hermans K, Baele M, Haesebrouck F** (2009) *Staphylococcus pseudintermedius* versus *Staphylococcus intermedius*. *Vet Microbiol* **133**: 206–207
- Devriese LA, Vancanneyt M, Baele M, Vanechoutte M, De Graef E, Snauwaert C, Cleenwerck I, Dawyndt P, Swings J, Decostere A, et al** (2005) *Staphylococcus pseudintermedius* sp. nov., a coagulase-positive species from animals. *Int J Syst Evol Microbiol* **55**: 1569–1573
- Dmitrenko OA, Balbutskaya AA, Skvortsov VN** (2016) Ecological features, pathogenic properties, and role of *Staphylococcus intermedius* group representatives in animal and human infectious pathology. *Mol Genet Microbiol Virol* **31**: 117–124
- Downer R, Roche F, Park PW, Mecham RP, Foster TJ** (2002) The Elastin-binding Protein of *Staphylococcus aureus* (EbpS) Is Expressed at the Cell Surface as an Integral Membrane Protein and Not as a Cell Wall-associated Protein. *J Biol Chem* **277**: 243–250
- Dubreuil JD, Isaacson RE, Schifferli DM** (2016) Animal Enterotoxigenic *Escherichia coli*. *EcoSal Plus*. doi: 10.1128/ecosalplus.ESP-0006-2016
- van Duijkeren E, Kamphuis M, van der Mije IC, Laarhoven LM, Duim B, Wagenaar JA, Houwers DJ** (2011) Transmission of methicillin-resistant *Staphylococcus pseudintermedius* between infected dogs and cats and contact pets, humans and the environment in households and veterinary clinics. *Vet Microbiol* **150**: 338–343
- Dunn SJ, Connor C, McNally A** (2019) The evolution and transmission of multi-drug resistant *Escherichia coli* and *Klebsiella pneumoniae*: the complexity of clones and plasmids. *Curr Opin Microbiol* **51**: 51–56
- Effah CY, Sun T, Liu S, Wu Y** (2020) *Klebsiella pneumoniae*: an increasing threat to public health. *Ann Clin Microbiol Antimicrob* **19**: 1
- Eichhorn I, Lübke-Becker A, Lapschies A-M, Jacob M, Bäumer W, Fulde M** (2020) Draft Genome Sequence of *Staphylococcus pseudintermedius* Strain 13-13613, Isolated from a Case of Canine Pyoderma. *Microbiol Resour Announc*. doi: 10.1128/mra.00027-20

- Elbediwi, Li, Paudyal, Pan, Li, Xie, Rajkovic, Feng, Fang, Rankin, et al** (2019) Global Burden of Colistin-Resistant Bacteria: Mobilized Colistin Resistance Genes Study (1980–2018). *Microorganisms* **7**: 461
- Elwell C, Chao K, Patel K, Dreyfus L** (2001) Escherichia coli CdtB Mediates Cytolethal Distending Toxin Cell Cycle Arrest. *Infect Immun* **69**: 3418–3422
- Eren AM, Esen OC, Quince C, Vineis JH, Morrison HG, Sogin ML, Delmont TO** (2015) Anvi'o: An advanced analysis and visualization platform for 'omics data. *PeerJ*. doi: 10.7717/peerj.1319
- Etcheverría AI, Padola NL** (2013) Shiga toxin-producing Escherichia coli: Factors involved in virulence and cattle colonization. *Virulence* **4**: 366–372
- Evans BR, Leighton FA** (2014) A history of One Health. *Rev Sci Tech OIE* **33**: 413–420
- Faïs T, Delmas J, Serres A, Bonnet R, Dalmasso G** (2016) Impact of CDT toxin on human diseases. *Toxins (Basel)*. doi: 10.3390/toxins8070220
- Fan R, Shao K, Yang X, Bai X, Fu S, Sun H, Xu Y, Wang H, Li Q, Hu B, et al** (2019) High prevalence of non-O157 Shiga toxin-producing Escherichia coli in beef cattle detected by combining four selective agars. *BMC Microbiol* **19**: 213
- Ference EH, Danielian A, Kim HW, Yoo F, Kuan EC, Suh JD** (2019) Zoonotic Staphylococcus pseudintermedius sinonasal infections: risk factors and resistance patterns. *Int Forum Allergy Rhinol* **9**: 22329
- Figdor D, Gulabivala K** (2008) Survival against the odds: microbiology of root canals associated with post-treatment disease. *Endod Top* **18**: 62–77
- Filice GA, Nyman JA, Lexau C, Lees CH, Bockstedt LA, Como-Sabetti K, Lesher LJ, Lynfield R** (2010) Excess Costs and Utilization Associated with Methicillin Resistance for Patients with Staphylococcus aureus Infection. *Infect Control Hosp Epidemiol* **31**: 365–373
- Fleming A** (1929) On the antibacterial action of cultures of a Penicillium, with special reference to their use in the isolation of B. influenzae. Wiley-Blackwell
- Fouts DE** (2006) Phage_Finder: Automated identification and classification of prophage regions in complete bacterial genome sequences. *Nucleic Acids Res* **34**: 5839–5851

- Francino O, Pérez D, Viñes J, Fonticoba R, Madroñero S, Meroni G, Martino P, Martínez S, Cusco A, Fàbregas N, et al** (2021) Whole-Genome Sequencing and *De Novo* Assembly of 61 *Staphylococcus pseudintermedius* Isolates from Healthy Dogs and Dogs with Pyoderma. *Microbiol Resour Announc*. doi: 10.1128/MRA.00152-21
- Frost LS, Leplae R, Summers AO, Toussaint A** (2005) Mobile genetic elements: the agents of open source evolution. *Nat Rev Microbiol* **3**: 722–732
- Gardy JL, Loman NJ** (2018) Towards a genomics-informed, real-time, global pathogen surveillance system. *Nat Rev Genet* **19**: 9–20
- Gargi A, Reno M, Blanke SR** (2012) Bacterial toxin modulation of the eukaryotic cell cycle: are all cytolethal distending toxins created equally? *Front Cell Infect Microbiol* **2**: 124
- Ghodbane R, Raoult D, Drancourt M** (2015) Dramatic reduction of culture time of *Mycobacterium tuberculosis*. *Sci Rep* **4**: 4236
- Giani T, Conte V, Di Pilato V, Aschbacher R, Weber C, Larcher C, Rossolini GM** (2012) *Escherichia coli* from Italy Producing OXA-48 Carbapenemase Encoded by a Novel Tn 1999 Transposon Derivative. *Antimicrob Agents Chemother* **56**: 2211–2213
- Gibb R, Redding DW, Chin KQ, Donnelly CA, Blackburn TM, Newbold T, Jones KE** (2020) Zoonotic host diversity increases in human-dominated ecosystems. *Nature* **584**: 398–402
- Gill AAS, Singh S, Thapliyal N, Karpoormath R** (2019) Nanomaterial-based optical and electrochemical techniques for detection of methicillin-resistant *Staphylococcus aureus*: a review. *Microchim Acta* **186**: 114
- Gleckman R, Blagg N, Joubert DW** (1981) Trimethoprim: Mechanisms of Action, Antimicrobial Activity, Bacterial Resistance, Pharmacokinetics, Adverse Reactions, and Therapeutic Indications. *Pharmacother J Hum Pharmacol Drug Ther* **1**: 14–19
- Golicz AA, Bayer PE, Bhalla PL, Batley J, Edwards D** (2020) Pangenomics Comes of Age: From Bacteria to Plant and Animal Applications. *Trends Genet* **36**: 132–145
- Gonzalez-Ferrer S, Peñaloza HF, Budnick JA, Bain WG, Nordstrom HR, Lee JS, Van Tyne D** (2021) Finding Order in the Chaos: Outstanding Questions in *Klebsiella*

pneumoniae Pathogenesis. *Infect Immun.* doi: 10.1128/IAI.00693-20

- González-Martín M, Corbera JA, Suárez-Bonnet A, Tejedor-Junco MT** (2020) Virulence factors in coagulase-positive staphylococci of veterinary interest other than *Staphylococcus aureus*. *Vet Q* **40**: 118–131
- Goodwin S, McPherson JD, Richard McCombie W** (2016) Coming of age: ten years of next-generation sequencing technologies. *Nat Publ Gr.* doi: 10.1038/nrg.2016.49
- Gortel K, Campbell KL, Kakoma I, Whittam T, Schaeffer DJ, Weisiger RM** (1999) Methicillin resistance among staphylococci isolated from dogs. *Am J Vet Res* **60**: 1526–30
- Gottig S, Hamprecht AG, Christ S, Kempf VAJ, Wichelhaus TA** (2013) Detection of NDM-7 in Germany, a new variant of the New Delhi metallo- β -lactamase with increased carbapenemase activity. *J Antimicrob Chemother* **68**: 1737–1740
- Greig DR, Jenkins C, Gharbia S, Dallman TJ** (2019) Comparison of single nucleotide variants identified by Illumina and Oxford Nanopore technologies in the context of a potential outbreak of Shiga Toxin Producing *Escherichia coli*. bioRxiv 570192
- Grönthal T, Moodley A, Nykäsenoja S, Junnila J, Guardabassi L, Thomson K, Rantala M** (2014) Large outbreak caused by Methicillin resistant staphylococcus pseudintermedius ST71 in a Finnish veterinary teaching hospital - From outbreak control to outbreak prevention. *PLoS One.* doi: 10.1371/journal.pone.0110084
- Hajek V** (1976) *Staphylococcus intermedius*, a new species isolated from animals. *Int J Syst Bacteriol* **26**: 401–408
- Hanssen A-M, Ericson Sollid JU** (2006) SCCmec in staphylococci: genes on the move. *FEMS Immunol Med Microbiol* **46**: 8–20
- Heather JM, Chain B** (2016) The sequence of sequencers: The history of sequencing DNA. *Genomics* **107**: 1–8
- van Hoek AHAM, Mevius D, Guerra B, Mullany P, Roberts AP, Aarts HJM** (2011) Acquired Antibiotic Resistance Genes: An Overview. *Front Microbiol.* doi: 10.3389/fmicb.2011.00203
- Van Hoovels L, Vankeerberghen A, Boel A, Van Vaerenbergh K, De Beenhouwer H** (2006) First Case of *Staphylococcus pseudintermedius* Infection in a Human. *J Clin*

Microbiol **44**: 4609–4612

Horstmann C, Mueller RS, Straubinger RK, Werckenthin C (2012) Detection of methicillin-resistant *Staphylococcus pseudintermedius* with commercially available selective media. *Lett Appl Microbiol* **54**: 26–31

Hritcu OM, Schmidt VM, Salem SE, Maciuca IE, Moraru RF, Lipovan I, Mareş M, Solcan G, Timofte D (2020) Geographical Variations in Virulence Factors and Antimicrobial Resistance Amongst *Staphylococci* Isolated From Dogs From the United Kingdom and Romania. *Front Vet Sci* **7**: 414

Hu Y, Xie Y, Tang J, Shi X (2012) Comparative Expression Analysis of Two Thermostable Nuclease Genes in *Staphylococcus aureus*. *Foodborne Pathog Dis* **9**: 265–271

Hummert JR, Van Gerven DP (1982) Tetracycline-Labeled Human Bone From A Medieval Population In Nubia's Batn El Hajar (550-1450 A.D.). *Hum Biol* **54**: 355–363

Hunt M, Silva N De, Otto TD, Parkhill J, Keane JA, Harris SR (2015) Circlator: Automated circularization of genome assemblies using long sequencing reads. *Genome Biol*. doi: 10.1186/s13059-015-0849-0

Hussein HS, Bollinger LM (2005) Prevalence of Shiga toxin-producing *Escherichia coli* in beef cattle. *J Food Prot* **68**: 2224–2241

Hyatt D, Chen G-L, LoCascio PF, Land ML, Larimer FW, Hauser LJ (2010) Prodigal: prokaryotic gene recognition and translation initiation site identification. *BMC Bioinformatics* **11**: 119

Ishihara K, Koizumi A, Saito M, Muramatsu Y, Tamura Y (2016) Detection of methicillin-resistant *Staphylococcus pseudintermedius* ST169 and novel ST354 SCCmec II-III isolates related to the worldwide ST71 clone. *Epidemiol Infect* **144**: 434–442

Iverson SA, Brazil AM, Ferguson JM, Nelson K, Lautenbach E, Rankin SC, Morris DO, Davis MF (2015) Anatomical patterns of colonization of pets with staphylococcal species in homes of people with methicillin-resistant *Staphylococcus aureus* (MRSA) skin or soft tissue infection (SSTI). *Vet Microbiol* **176**: 202–208

- Jain C, Rodriguez-R LM, Phillippy AM, Konstantinidis KT, Aluru S** (2018) High throughput ANI analysis of 90K prokaryotic genomes reveals clear species boundaries. *Nat Commun* **9**: 1–8
- Jamale T** (2011) Acute Kidney Injury Due to Arsenic Contained in Alternative Medicines in the Setting of Adult Nephrotic Syndrome. *J Clin Toxicol*. doi: 10.4172/2161-0494.1000101
- Janda JM, Abbott SL** (2007) 16S rRNA gene sequencing for bacterial identification in the diagnostic laboratory: Pluses, perils, and pitfalls. *J Clin Microbiol* **45**: 2761–2764
- Jenkins C, Ling CL, Ciesielczuk HL, Lockwood J, Hopkins S, McHugh TD, Gillespie SH, Kibbler CC** (2012) Detection and identification of bacteria in clinical samples by 16S rRNA gene sequencing: comparison of two different approaches in clinical practice. *J Med Microbiol* **61**: 483–488
- Jenul C, Horswill AR** (2019) Regulation of *Staphylococcus aureus* Virulence. *Microbiol Spectr*. doi: 10.1128/microbiolspec.GPP3-0031-2018
- Jia B, Raphenya AR, Alcock B, Waglechner N, Guo P, Tsang KK, Lago BA, Dave BM, Pereira S, Sharma AN, et al** (2017) CARD 2017: expansion and model-centric curation of the comprehensive antibiotic resistance database. *Nucleic Acids Res* **45**: D566–D573
- Joensen KG, Tetzschner AMM, Iguchi A, Aarestrup FM, Scheutz F** (2015) Rapid and Easy In Silico Serotyping of *Escherichia coli* Isolates by Use of Whole-Genome Sequencing Data. *J Clin Microbiol* **53**: 2410–2426
- Joffré E, von Mentzer A, Svennerholm AM, Sjöling Å** (2016) Identification of new heat-stable (STa) enterotoxin allele variants produced by human enterotoxigenic *Escherichia coli* (ETEC). *Int J Med Microbiol* **306**: 586–594
- Johura F-T, Tasnim J, Barman I, Biswas SR, Jubyda FT, Sultana M, George CM, Camilli A, Seed KD, Ahmed N, et al** (2020) Colistin-resistant *Escherichia coli* carrying *mcr-1* in food, water, hand rinse, and healthy human gut in Bangladesh. *Gut Pathog* **12**: 5
- Kaas RS, Leekitcharoenphon P, Aarestrup FM, Lund O** (2014) Solving the Problem of Comparing Whole Bacterial Genomes across Different Sequencing Platforms. *PLoS One* **9**: e104984

- Karesh WB, Dobson A, Lloyd-Smith JO, Lubroth J, Dixon MA, Bennett M, Aldrich S, Harrington T, Formenty P, Loh EH, et al** (2012) Ecology of zoonoses: natural and unnatural histories. *Lancet* **380**: 1936–1945
- Kaye KS, Pogue JM** (2015) Infections Caused by Resistant Gram-Negative Bacteria: Epidemiology and Management. *Pharmacother J Hum Pharmacol Drug Ther* **35**: 949–962
- Kjellman EE, Slettemeås JS, Small H, Sunde M** (2015) Methicillin-resistant *Staphylococcus pseudintermedius* (MRSP) from healthy dogs in Norway - occurrence, genotypes and comparison to clinical MRSP. *Microbiologyopen* **4**: 857–866
- Kmiecik W, Szewczyk EM** (2018) Are zoonotic *Staphylococcus pseudintermedius* strains a growing threat for humans? *Folia Microbiol (Praha)* **63**: 743–747
- Kochan TJ, Ozer EA, Pincus NB, Fitzpatrick MA, Hauser AR** (2020) Complete Genome Sequence of *Klebsiella pneumoniae* Strain TK421, a Conjugative Hypervirulent Isolate. *Microbiol Resour Announc*. doi: 10.1128/MRA.01408-19
- Kolmogorov M, Yuan J, Lin Y, Pevzner PA** (2019) Assembly of long, error-prone reads using repeat graphs. *Nat Biotechnol* **37**: 540–546
- Komoda Y, Enomoto M, Tominaga A** (1991) Large Inversion in *Escherichia coli* K-12 1485IN Between Inversely Oriented IS3 Elements Near *lac* and *cdd*. *Genetics* **129**: 639–645
- Kramer J, Özkaya Ö, Kümmerli R** (2020) Bacterial siderophores in community and host interactions. *Nat Rev Microbiol* **18**: 152–163
- Krause KM, Serio AW, Kane TR, Connolly LE** (2016) Aminoglycosides: An Overview. *Cold Spring Harb Perspect Med* **6**: a027029
- Krawczyk B, Kur J** (2018) Molecular Identification and Genotyping of *Staphylococci*: Genus, Species, Strains, Clones, Lineages, and Interspecies Exchanges. *Pet-to-Man Travel. Staphylococci A World Prog*. Elsevier Inc., pp 199–223
- Kriventseva E V, Kuznetsov D, Tegenfeldt F, Manni M, Dias R, Simão FA, Zdobnov EM** (2019) OrthoDB v10: sampling the diversity of animal, plant, fungal, protist, bacterial and viral genomes for evolutionary and functional annotations of orthologs. *Nucleic Acids Res* **47**: D807–D811

- Lainhart W, Yarbrough ML, Burnham C-AD** (2018) The Brief Case: *Staphylococcus intermedius* Group—Look What the Dog Dragged In. *J Clin Microbiol*. doi: 10.1128/JCM.00839-17
- Lakhundi S, Zhang K** (2018) Methicillin-Resistant *Staphylococcus aureus*: Molecular Characterization, Evolution, and Epidemiology. *Clin Microbiol Rev*. doi: 10.1128/CMR.00020-18
- Lam MMC, Wick RR, Wyres KL, Gorrie CL, Judd LM, Jenney AWJ, Brisse S, Holt KE** (2018) Genetic diversity, mobilisation and spread of the yersiniabactin-encoding mobile element ICEKp in *klebsiella pneumoniae* populations. *Microb Genomics*. doi: 10.1099/mgen.0.000196
- Lan P, Jiang Y, Zhou J, Yu Y** (2021) A global perspective on the convergence of hypervirulence and carbapenem resistance in *Klebsiella pneumoniae*. *J Glob Antimicrob Resist* **25**: 26–34
- Larsen M V., Cosentino S, Rasmussen S, Friis C, Hasman H, Marvig RL, Jelsbak L, Sicheritz-Ponten T, Ussery DW, Aarestrup FM, et al** (2012) Multilocus Sequence Typing of Total-Genome-Sequenced Bacteria. *J Clin Microbiol* **50**: 1355–1361
- Latronico F, Moodley A, Nielsen S, Guardabassi L** (2014) Enhanced adherence of methicillin-resistant *Staphylococcus pseudintermedius* sequence type 71 to canine and human corneocytes. *Vet Res* **45**: 70
- Laver T, Harrison J, O'Neill PA, Moore K, Farbos A, Paszkiewicz K, Studholme DJ** (2015) Assessing the performance of the Oxford Nanopore Technologies MinION. *Biomol Detect Quantif* **3**: 1–8
- Lee J, Murray A, Bendall R, Gaze W, Zhang L, Vos M** (2015) Improved Detection of *Staphylococcus intermedius* Group in a Routine Diagnostic Laboratory. *J Clin Microbiol* **53**: 961–963
- Li B, Ke B, Zhao X, Guo Y, Wang W, Wang X, Zhu H** (2018a) Antimicrobial resistance profile of *mcr-1* positive clinical isolates of *Escherichia coli* in China from 2013 to 2016. *Front Microbiol* **9**: 1–10
- Li H** (2018) Minimap2: pairwise alignment for nucleotide sequences. *Bioinformatics* **34**: 3094–3100

- Li R, Xie M, Lv J, Wai-Chi Chan E, Chen S** (2017a) Complete genetic analysis of plasmids carrying *mcr-1* and other resistance genes in an *Escherichia coli* isolate of animal origin. *J Antimicrob Chemother* **72**: 696–699
- Li R, Xie M, Zhang J, Yang Z, Liu L, Liu X, Zheng Z, Chan EWC, Chen S** (2017b) Genetic characterization of *mcr-1*-bearing plasmids to depict molecular mechanisms underlying dissemination of the colistin resistance determinant. *J Antimicrob Chemother* **72**: 393–401
- Li X, Xie Y, Liu M, Tai C, Sun J, Deng Z, Ou H-Y** (2018b) oriTfinder: a web-based tool for the identification of origin of transfers in DNA sequences of bacterial mobile genetic elements. *Nucleic Acids Res* **46**: 229–234
- Little S V., Bryan LK, Hillhouse AE, Konganti K, Lawhon SD** (2019) Whole-Genome Sequences of *Staphylococcus pseudintermedius* Isolates from Canine and Human Bacteremia Infections. *Microbiol Resour Announc* **8**: 735–754
- Loeffler A, Lloyd DH** (2018) What has changed in canine pyoderma? A narrative review. *Vet J* **235**: 73–82
- Loho T, Dharmayanti A** (2015) Colistin: an Antibiotic and Its Role in Multiresistant Gram-negative Infections. *Acta Med Indones-Indones J Intern Med* **47**: 157–168
- Lopez-Castejon G, Brough D** (2011) Understanding the mechanism of IL-1 β secretion. *Cytokine Growth Factor Rev* **22**: 189–195
- Lozano C, Rezusta A, Ferrer I, Pérez-Laguna V, Zarazaga M, Ruiz-Ripa L, Revillo MJ, Torres C** (2017) *Staphylococcus pseudintermedius* Human Infection Cases in Spain: Dog-to-Human Transmission. *Vector-Borne Zoonotic Dis* **17**: 268–270
- Maali Y, Badiou C, Martins-Simões P, Hodille E, Bes M, Vandenesch F, Lina G, Diot A, Laurent F, Trouillet-Assant S** (2018) Understanding the Virulence of *Staphylococcus pseudintermedius*: A Major Role of Pore-Forming Toxins. *Front Cell Infect Microbiol* **8**: 221
- MacConkey A** (1905) Lactose-Fermenting Bacteria in Faeces. *J Hyg (Lond)* **5**: 333–379
- Magleby R, Bemis DA, Kim D, Carroll KC, Castanheira M, Kania SA, Jenkins SG, Westblade LF** (2019) First reported human isolation of *Staphylococcus delphini*. *Diagn Microbiol Infect Dis* **94**: 274–276

- Malone CL, Boles BR, Horswill AR** (2007) Biosynthesis of *Staphylococcus aureus* autoinducing peptides by using the *Synechocystis* DnaB mini-intein. *Appl Environ Microbiol* **73**: 6036–6044
- Mardis ER** (2017) DNA sequencing technologies: 2006–2016. *Nat Protoc* **12**: 213–218
- Marí-Almirall M, Cosgaya C, Pitart C, Viñes J, Muñoz L, Campo I, Cuscó A, Rodríguez-Serna L, Santana G, Del Río A, et al** (2020) Dissemination of NDM-producing *Klebsiella pneumoniae* and *Escherichia coli* high-risk clones in Catalan healthcare institutions. *J Antimicrob Chemother* 1–10
- Mašlaňová I, Doškař J, Varga M, Kuntová L, Mužik J, Malúšková D, Růžičková V, Pantůček R** (2013) Bacteriophages of *Staphylococcus aureus* efficiently package various bacterial genes and mobile genetic elements including SCC mec with different frequencies. *Environ Microbiol Rep* **5**: 66–73
- Mattasingh D, Hinz A, Phillips L, Carroll AC, Wong A** (2021) Hybrid Nanopore-Illumina Assemblies for Five Extraintestinal Pathogenic *Escherichia coli* Isolates. *Microbiol Resour Announc*. doi: 10.1128/MRA.01027-20
- McCarthy AJ, Harrison EM, Stanczak-Mrozek K, Leggett B, Waller A, Holmes MA, Lloyd DH, Lindsay JA, Loeffler A** (2014) Genomic insights into the rapid emergence and evolution of MDR in *Staphylococcus pseudintermedius*. *J Antimicrob Chemother* **70**: 997–1007
- McDaniel CJ, Cardwell DM, Moeller RB, Jr., Gray GC** (2014) Humans and Cattle: A Review of Bovine Zoonoses. *Vector Borne Zoonotic Dis* **14**: 1
- Mehrad B, Clark NM, Zhanel GG, Lynch JP** (2015) Antimicrobial resistance in hospital-acquired gram-negative bacterial infections. *Chest* **147**: 1413–1421
- Mellmann A, Harmsen D, Cummings CA, Zentz EB, Leopold SR, Rico A, Prior K, Szczepanowski R, Ji Y, Zhang W, et al** (2011) Prospective Genomic Characterization of the German Enterohemorrhagic *Escherichia coli* O104:H4 Outbreak by Rapid Next Generation Sequencing Technology. *PLoS One* **6**: e22751
- Menandro ML, Dotto G, Mondin A, Martini M, Ceglie L, Pasotto D** (2019) Prevalence and characterization of methicillin-resistant *Staphylococcus pseudintermedius* from symptomatic companion animals in Northern Italy: Clonal diversity and novel sequence types. *Comp Immunol Microbiol Infect Dis*. doi:

10.1016/j.cimid.2019.101331

- Meroni G, Filipe JFS, Drago L, Martino PA** (2019) Investigation on antibiotic-resistance, biofilm formation and virulence factors in multi drug resistant and non multi drug resistant *Staphylococcus pseudintermedius*. *Microorganisms*. doi: 10.3390/microorganisms7120702
- Minakshi P, Ranjan K, Brar B, Ambawat S, Shafiq M, Alisha A** (2014) New Approaches for Diagnosis of Viral Diseases in Animals. *2*: 55–63
- Miragaia M** (2018) Factors contributing to the evolution of Meca-mediated β -lactam resistance in staphylococci: Update and new insights from whole genome sequencing (WGS). *Front Microbiol* **9**: 2723
- Mirzarazi M, Rezatofghi SE, Pourmahdi M, Mohajeri MR** (2015) Occurrence of genes encoding enterotoxins in uropathogenic *Escherichia coli* isolates. *Brazilian J Microbiol* **46**: 155–159
- Monte DF, Mem A, Fernandes MR, Cerdeira L, Esposito F, Galvão JA, Franco BDGM, Lincopan N, Landgraf M** (2017) Chicken Meat as a Reservoir of Colistin-Resistant *Escherichia coli* Strains Carrying *mcr-1* Genes in South America. *Antimicrob Agents Chemother*. doi: 10.1128/AAC.02718-16
- Moreno-Cinos C, Goossens K, Salado IG, Van Der Veken P, De Winter H, Augustyns K** (2019) ClpP Protease, a Promising Antimicrobial Target. *Int J Mol Sci*. doi: 10.3390/ijms20092232
- Mulani MS, Kamble EE, Kumkar SN, Tawre MS, Pardesi KR** (2019) Emerging Strategies to Combat ESKAPE Pathogens in the Era of Antimicrobial Resistance: A Review. *Front Microbiol*. doi: 10.3389/fmicb.2019.00539
- Murray AK, Lee J, Bendall R, Zhang L, Sunde M, Slette-meås JS, Gaze W, Page AJ, Vos M** (2018) *Staphylococcus cornubiensis* sp. nov., a member of the *staphylococcus intermedius* group (SIG). *Int J Syst Evol Microbiol* **68**: 3404–3408
- NanoporeTech** (2021) Bonito. GitHub, <https://github.com/nanoporetech/bonito>
- Noll LW, Worley JN, Yang X, Shridhar PB, Ludwig JB, Shi X, Bai J, Caragea D, Meng J, Nagaraja TG** (2018) Comparative genomics reveals differences in mobile virulence genes of *Escherichia coli* O103 pathotypes of bovine fecal origin. *PLoS*

One. doi: 10.1371/journal.pone.0191362

Novick RP, Morse SI (1967) In vivo transmission of drug resistance factors between strains of *Staphylococcus aureus*. *J Exp Med* **125**: 45–59

O’Neil J (2016) Tackling drug-resistant infections globally: final report and recommendations.

De Oliveira DMP, Forde BM, Kidd TJ, Harris PNA, Schembri MA, Beatson SA, Paterson DL, Walker MJ (2020) Antimicrobial resistance in ESKAPE pathogens. *Clin Microbiol Rev.* doi: 10.1128/CMR.00181-19

Ono HK, Suzuki Y, Kubota H, Asano K, Takai S, Nakane A, Hu D-L (2021) Complete Genome Sequence of *Staphylococcus aureus* Strain 834, Isolated from a Septic Patient in Japan. *Microbiol Resour Announc.* doi: 10.1128/MRA.01477-20

Orlek A, Phan H, Sheppard AE, Doumith M, Ellington M, Peto T, Crook D, Walker AS, Woodford N, Anjum MF, et al (2017) A curated dataset of complete Enterobacteriaceae plasmids compiled from the NCBI nucleotide database. *Data Br* **12**: 423–426

Oxford Nanopore Technologies (2014) How It Works.
<https://nanoporetech.com/how-it-works>

Oxford Nanopore Technologies (2021) Guppy v5.0.7 release note. nanoporetech,
<https://community.nanoporetech.com/posts/guppy-v5-0-7-release-note>

Oxford Nanopore Technologies (2020) Guppy.
https://community.nanoporetech.com/protocols/Guppy-protocol/v/gpb_2003_v1_rev1_14dec2018/windows-guppy

Oxford Nanopore Technologies (2018) Medaka. GitHub,
<https://github.com/nanoporetech/medaka>

Paczosa MK, Mecsas J (2016) *Klebsiella pneumoniae*: Going on the Offense with a Strong Defense. *Microbiol Mol Biol Rev* **80**: 629–661

Padola NL, Etcheverri-a AI (2014) Shiga toxin-producing *Escherichia coli* in human, cattle, and foods. Strategies for detection and control. *Front Cell Infect Microbiol* **4**: 89

Pandey M, Khan A, Das SC, Sarkar B, Kahali S, Chakraborty S, Chattopadhyay S,

- Yamasaki S, Takeda Y, Balakrish Nair G, et al** (2003) Association of Cytolethal Distending Toxin Locus *cdtB* with Enteropathogenic *Escherichia coli* Isolated from Patients with Acute Diarrhea in Calcutta, India. *J Clin Microbiol* **41**: 5277–5281
- Pankey GA, Sabath LD** (2004) Clinical Relevance of Bacteriostatic versus Bactericidal Mechanisms of Action in the Treatment of Gram-Positive Bacterial Infections. *Clin Infect Dis* **38**: 864–870
- Paraboschi EM, Menegatti M, Rimoldi V, Borhany M, Abdelwahab M, Gemmati D, Peyvandi F, Duga S, Asselta R** (2019) Profiling the mutational landscape of coagulation factor V deficiency. *Haematologica* **105**: haematol.2019.232587
- Parks DH, Imelfort M, Skennerton CT, Hugenholtz P, Tyson GW** (2015) CheckM: assessing the quality of microbial genomes recovered from isolates, single cells, and metagenomes. *Genome Res* **25**: 1043–1055
- Partridge SR, Kwong SM, Firth N, Jensen SO** (2018) Mobile genetic elements associated with antimicrobial resistance. *Clin Microbiol Rev.* doi: 10.1128/CMR.00088-17
- Patel K, Bunachita S, Agarwal AA, Bhamidipati A, Patel UK** (2021) A Comprehensive Overview of Antibiotic Selection and the Factors Affecting It. *Cureus.* doi: 10.7759/cureus.13925
- Peacock SJ, Paterson GK** (2015) Mechanisms of methicillin resistance in *Staphylococcus aureus*. *Annu Rev Biochem* **84**: 577–601
- Pérez-Vázquez M, Sola Campoy PJ, Ortega A, Bautista V, Monzón S, Ruiz-Carrascoso G, Mingorance J, González-Barberá EM, Gimeno C, Aracil B, et al** (2019) Emergence of NDM-producing *Klebsiella pneumoniae* and *Escherichia coli* in Spain: phylogeny, resistome, virulence and plasmids encoding blaNDM-like genes as determined by WGS. *J Antimicrob Chemother.* doi: 10.1093/jac/dkz366
- Perreten V, Kadlec K, Schwarz S, Gronlund Andersson U, Finn M, Greko C, Moodley A, Kania SA, Frank LA, Bemis DA, et al** (2010) Clonal spread of methicillin-resistant *Staphylococcus pseudintermedius* in Europe and North America: an international multicentre study. *J Antimicrob Chemother* **65**: 1145–1154
- Perreten V, Kania S, Bemis D** (2020) *Staphylococcus ursi* sp. nov., a new member of the ‘*Staphylococcus intermedius* group’ isolated from healthy black bears. *Int J Syst Evol*

- Phumthanakorn N, Chanchaithong P, Prapasarakul N** (2017) Development of a set of multiplex PCRs for detection of genes encoding cell wall-associated proteins in *Staphylococcus pseudintermedius* isolates from dogs, humans and the environment. *J Microbiol Methods* **142**: 90–95
- Pightling AW, Pettengill JB, Luo Y, Baugher JD, Rand H, Strain E** (2018) Interpreting Whole-Genome Sequence Analyses of Foodborne Bacteria for Regulatory Applications and Outbreak Investigations. *Front Microbiol*. doi: 10.3389/fmicb.2018.01482
- Poirel L, Madec J-Y, Lupo A, Schink A-K, Kieffer N, Nordmann P, Schwarz S** (2018) Antimicrobial Resistance in *Escherichia coli*. *Antimicrob. Resist. Bact. from Livest. Companion Anim.* American Society of Microbiology, pp 289–316
- Quainoo S, Coolen JPM, van Hijum SAFT, Huynen MA, Melchers WJG, van Schaik W, Wertheim HFL** (2017) Whole-Genome Sequencing of Bacterial Pathogens: the Future of Nosocomial Outbreak Analysis. *Clin Microbiol Rev* **30**: 1015–1063
- Rennings L van, Münchhausen C von, Otilie H, Hartmann M, Merle R, Honscha W, Käsbohrer A, Kreienbrock L** (2015) Cross-Sectional Study on Antibiotic Usage in Pigs in Germany. *PLoS One* **10**: e0119114
- Riegel P, Jesel-Morel L, Laventie B, Boisset S, Vandenesch F, Prévost G** (2011) Coagulase-positive *Staphylococcus pseudintermedius* from animals causing human endocarditis. *Int J Med Microbiol* **301**: 237–239
- Rigoulay C, Entenza JM, Halpern D, Widmer E, Moreillon P, Poquet I, Gruss A** (2005) Comparative analysis of the roles of HtrA-like surface proteases in two virulent *Staphylococcus aureus* strains. *Infect Immun* **73**: 563–72
- Rodríguez-Beltrán J, DelaFuente J, León-Sampedro R, MacLean RC, San Millán Á** (2021) Beyond horizontal gene transfer: the role of plasmids in bacterial evolution. *Nat Rev Microbiol*. doi: 10.1038/s41579-020-00497-1
- Rohde H, Qin J, Cui Y, Li D, Loman NJ, Hentschke M, Chen W, Pu F, Peng Y, Li J, et al** (2011) Open-Source Genomic Analysis of Shiga-Toxin-Producing *E. coli* O104:H4. *N Engl J Med* **365**: 718–724

- Rosselló-Móra R, Urdiain M, López-López A** (2011) DNA-DNA Hybridization. *Methods Microbiol. Academic Press*, pp 325–347
- Rouli L, Merhej V, Fournier P-E, Raoult D** (2015) The bacterial pangenome as a new tool for analysing pathogenic bacteria. *New Microbes New Infect* **7**: 72–85
- Saha RP, Lou Z, Meng L, Harshey RM** (2013) Transposable Prophage Mu Is Organized as a Stable Chromosomal Domain of *E. coli*. *PLoS Genet* **9**: 1003902
- Saliu E-M, Vahjen W, Zentek J** (2017) Types and prevalence of extended-spectrum beta-lactamase producing Enterobacteriaceae in poultry. *Anim Heal Res Rev* **18**: 46–57
- San Millan A** (2018) Evolution of Plasmid-Mediated Antibiotic Resistance in the Clinical Context. *Trends Microbiol* **26**: 978–985
- Sanger F, Nicklen S, Coulson a R** (1977) DNA sequencing with chain-terminating inhibitors. *Proc Natl Acad Sci U S A* **74**: 5463–7
- Sanseverino I, Navarro-Cuenca A, Loos R, Marinov D, Lettieri T** (2018) State of the art on the contribution of water to antimicrobial resistance. doi: 10.2760/82376
- Santajit S, Indrawattana N** (2016) Mechanisms of Antimicrobial Resistance in ESKAPE Pathogens. *Biomed Res Int*. doi: 10.1155/2016/2475067
- Dos Santos TP, Damborg P, Moodley A, Guardabassi L** (2016) Systematic review on global epidemiology of methicillin-resistant staphylococcus pseudintermedius: Inference of population structure from multilocus sequence typing data. *Front Microbiol* **7**: 1599
- Sasaki T, Kikuchi K, Tanaka Y, Takahashi N, Kamata S, Hiramatsu K** (2007a) Reclassification of phenotypically identified *Staphylococcus intermedius* strains. *J Clin Microbiol* **45**: 2770–2778
- Sasaki T, Kikuchi K, Tanaka Y, Takahashi N, Kamata S, Hiramatsu K** (2007b) Methicillin-resistant *Staphylococcus pseudintermedius* in a veterinary teaching hospital. *J Clin Microbiol* **45**: 1118–1125
- Sasaki T, Tsubakishita S, Tanaka Y, Sakusabe A, Ohtsuka M, Hirota S, Kawakami T, Fukata T, Hiramatsu K** (2010) Multiplex-PCR method for species identification of coagulase-positive staphylococci. *J Clin Microbiol* **48**: 765–769

- Schneider D, Zühlke D, Petscheleit T, Poehlein A, Riedel K, Daniel R** (2020) Complete Genome Sequence of *Escherichia coli* GW-AmxH19, Isolated from Hospital Wastewater in Greifswald, Germany. *Microbiol Resour Announc.* doi: 10.1128/MRA.00279-20
- Schubert S, Kostrzewa M** (2017) MALDI-TOF MS in the Microbiology Laboratory: Current Trends. *Curr Issues Mol Biol* 17–20
- Schürch AC, Arredondo-Alonso S, Willems RJL, Goering RV** (2018) Whole genome sequencing options for bacterial strain typing and epidemiologic analysis based on single nucleotide polymorphism versus gene-by-gene-based approaches. *Clin Microbiol Infect* **24**: 350–354
- Scuron MD, Boesze-Battaglia K, Dlakic M, Shenker BJ** (2016) The cytolethal distending toxin contributes to microbial virulence and disease pathogenesis by acting as a tri-perditious toxin. *Front Cell Infect Microbiol.* doi: 10.3389/fcimb.2016.00168
- Seemann T** (2014) Prokka: rapid prokaryotic genome annotation. *Bioinformatics* **30**: 2068–2069
- Seemann T** (2017) Abricate. GitHub, <https://github.com/tseemann/abricate>
- Shah DH, Jones LP, Paul N, Davis MA** (2018) Draft genome sequences of 12 clinical and environmental methicillin-resistant *Staphylococcus pseudintermedius* strains isolated from a veterinary teaching hospital in Washington State. *Genome Announc.* doi: 10.1128/genomeA.00290-18
- Sharma VK, Akavaram S, Schaut RG, Bayles DO** (2019) Comparative genomics reveals structural and functional features specific to the genome of a foodborne *Escherichia coli* O157:H7. *BMC Genomics* **20**: 196
- Shen Y, Wu Z, Wang Y, Zhang R, Zhou HW, Wang S, Lei L, Li M, Cai J, Tyrrell J, et al** (2018) Heterogeneous and flexible transmission of *mcr-1* in hospital-associated *Escherichia coli*. *MBio.* doi: 10.1128/mBio.00943-18
- Shields RK, Chen L, Cheng S, Chavda KD, Press EG, Snyder A, Pandey R, Doi Y, Kreiswirth BN, Nguyen MH, et al** (2017) Emergence of Ceftazidime-Avibactam Resistance Due to Plasmid-Borne *bla*KPC-3 Mutations during Treatment of Carbapenem-Resistant *Klebsiella pneumoniae* Infections. *Antimicrob Agents Chemother.* doi: 10.1128/AAC.02097-16

- Shridhar PB, Patel IR, Gangiredla J, Noll LW, Shi X, Bai J, Elkins CA, Strockbine NA, Nagaraja TG** (2018) Genetic analysis of virulence potential of *Escherichia coli* O104 serotypes isolated from cattle feces using whole genome sequencing. *Front Microbiol.* doi: 10.3389/fmicb.2018.00341
- Siguier P, Perochon J, Lestrade L, Mahillon J, Chandler M** (2006) ISfinder: the reference centre for bacterial insertion sequences. *Nucleic Acids Res* **34**: D32-6
- Sikora A, Zahra F** (2021) Nosocomial Infections.
- Simão FA, Waterhouse RM, Ioannidis P, Kriventseva E V., Zdobnov EM** (2015) BUSCO: assessing genome assembly and annotation completeness with single-copy orthologs. *Bioinformatics* **31**: 3210–3212
- Singhal N, Kumar M, Kanaujia PK, Viridi JS** (2015) MALDI-TOF mass spectrometry: an emerging technology for microbial identification and diagnosis. *Front Microbiol.* doi: 10.3389/fmicb.2015.00791
- Solyman SM, Black CC, Duim B, Perreten V, van Duijkeren E, Wagenaar JA, Eberlein LC, Sadeghi LN, Videla R, Bemis DA, et al** (2013) Multilocus Sequence Typing for Characterization of *Staphylococcus pseudintermedius*. *J Clin Microbiol* **51**: 306–310
- Somayaji R, Priyantha MAR, Rubin JE, Church D** (2016) Human infections due to *Staphylococcus pseudintermedius*, an emerging zoonosis of canine origin: report of 24 cases. *Diagn Microbiol Infect Dis* **85**: 471–476
- Starikova E V., Tikhonova PO, Prianichnikov NA, Rands CM, Zdobnov EM, Ilina EN, Govorun VM** (2020) Phigaro: high-throughput prophage sequence annotation. *Bioinformatics* **36**: 3882–3884
- Sun J, Fang LX, Wu Z, Deng H, Yang RS, Li XP, Li SM, Liao XP, Feng Y, Liu YH** (2017) Genetic Analysis of the IncX4 Plasmids: Implications for a Unique Pattern in the *mcr-1* Acquisition. *Sci Rep* **7**: 424
- Tatusov RL, Fedorova ND, Jackson JD, Jacobs AR, Kiryutin B, Koonin E V, Krylov DM, Mazumder R, Mekhedov SL, Nikolskaya AN, et al** (2003) The COG database: an updated version includes eukaryotes. *BMC Bioinformatics* **4**: 41
- Tatusova T, DiCuccio M, Badretdin A, Chetvernin V, Nawrocki EP, Zaslavsky L,**

- Lomsadze A, Pruitt KD, Borodovsky M, Ostell J** (2016) NCBI prokaryotic genome annotation pipeline. *Nucleic Acids Res* **44**: 6614–6624
- Thomas NA, Navarro-Garcia F, Jorge Blanco M, Robins-Browne RM, Holt KE, Ingle DJ, Hocking DM, Yang J, Tauschek M** (2016) Are *Escherichia coli* Pathotypes Still Relevant in the Era of Whole-Genome Sequencing? *Front Cell Infect Microbiol* | www.frontiersin.org **1**: 141
- Tomley FM, Shirley MW** (2009) Livestock infectious diseases and zoonoses. *Philos Trans R Soc Lond B Biol Sci* **364**: 2637–42
- UC** (2021) Lab 12: Isolation and Identification of Enterobacteriaceae and Pseudomonas, Part 1. *Biol. Libr.*, https://bio.libretexts.org/Learning_Objects/Laboratory_Experiments/Microbiology_Labs/Microbiology_Labs_II/Lab_12%3A_Isolation_and_Identification_of_Enterobacteriaceae_and_Pseudomonas%2C_Part_1
- Uelze L, Grützke J, Borowiak M, Hammerl JA, Juraschek K, Deneke C, Tausch SH, Malorny B** (2020) Typing methods based on whole genome sequencing data. *One Heal Outlook* **2**: 3
- Varaldo PE, Kilpper-Balz R, Biavasco F, Satta G, Schleifer KH** (1988) *Staphylococcus delphini* sp. nov., a coagulase-positive species isolated from dolphins. *Int J Syst Bacteriol* **38**: 436–439
- Vaser R, Sovic I, Nagarajan N, Sikic M** (2017) Fast and accurate de novo genome assembly from long uncorrected reads. *Genome Res* **27**: gr.214270.116
- Větrovský T, Baldrian P** (2013) The Variability of the 16S rRNA Gene in Bacterial Genomes and Its Consequences for Bacterial Community Analyses. *PLoS One* **8**: e57923
- Viñes J, Cuscó A, Francino O** (2019) Hybrid assembly from a pathogenic Methicillin and Multi-Drug Resistant *Staphylococcus pseudintermedius* isolated from a canine otitis, Spain. *Microbiol. Resour. Announc.*
- Viñes J, Cuscó A, Napp S, Alvarez J, Saez-Llorente JL, Rosàs-Rodoreda M, Francino O, Migura-Garcia L** (2021) Transmission of Similar Mcr-1 Carrying Plasmids among Different *Escherichia coli* Lineages Isolated from Livestock and the Farmer. *Antibiotics* **10**: 313

- Vitali LA, Daniela B, Massimo B, Dezemona P** (2021) Draft genome of an extremely-drug resistant st551 *Staphylococcus pseudintermedius* from an Italian dog with otitis externa. *J Glob Antimicrob Resist*. doi: 10.1016/j.jgar.2021.02.025
- Wang R, Van Dorp L, Shaw LP, Bradley P, Wang Q, Wang X, Jin L, Zhang Q, Liu Y, Rieux A, et al** (2018) The global distribution and spread of the mobilized colistin resistance gene *mcr-1*. *Nat Commun* **9**: 1–9
- Wegener A, Broens EM, Zomer A, Spaninks M, Wagenaar JA, Duim B** (2018) Comparative genomics of phenotypic antimicrobial resistances in methicillin-resistant *Staphylococcus pseudintermedius* of canine origin. *Vet Microbiol* **225**: 125–131
- Wehrli W** (1983) Rifampin: Mechanisms of Action and Resistance. *Clin Infect Dis* **5**: S407–S411
- Wick RR, Judd LM, Gorrie CL, Holt KE** (2017) Unicycler: Resolving bacterial genome assemblies from short and long sequencing reads. *PLOS Comput Biol* **13**: e1005595
- Williams RE** (1967) *Staphylococcus aureus* as commensal and pathogen. *Pathol Microbiol (Basel)* **30**: 932–45
- Winker S, Woese CR** (1991) A Definition of the Domains Archaea, Bacteria and Eucarya in Terms of Small Subunit Ribosomal RNA Characteristics. *Syst Appl Microbiol* **14**: 305–310
- Wintersinger JA, Wasmuth JD** (2015) Kablammo: an interactive, web-based BLAST results visualizer. *Bioinformatics* **31**: 1305–1306
- Wisgrill L, Lepuschitz S, Blaschitz M, Rittenschober-Böhm J, Diab-El Schahawi M, Schubert S, Indra A, Berger A** (2019) Outbreak of yersiniabactin-producing *klebsiella pneumoniae* in a neonatal intensive care unit. *Pediatr Infect Dis J* **38**: 638–642
- Woese CR, Stackebrandt E, Macke TJ, Fox GE** (1985) A Phylogenetic Definition of the Major Eubacterial Taxa. *Syst Appl Microbiol* **6**: 143–151
- World Health Organization** (2019) WHO Technical Report Series 1021 - The Selection and Use of Essential Medicines.
- Wu R, Yi LX, Yu LF, Wang J, Liu Y, Chen X, Lv L, Yang J, Liu JH** (2018) Fitness advantage of *mcr-1*-bearing IncI2 and IncX4 plasmids in vitro. *Front Microbiol*. doi:

- Xu Y, Wei W, Lei S, Lin J, Srinivas S, Feng Y** (2018a) An evolutionarily conserved mechanism for intrinsic and transferable polymyxin resistance. *MBio* **9**: 1–18
- Xu Z, Shah HN, Misra R, Chen J, Zhang W, Liu Y, Cutler RR, Mkrtchyan H V.** (2018b) The prevalence, antibiotic resistance and *mecA* characterization of coagulase negative staphylococci recovered from non-healthcare settings in London, UK. *Antimicrob Resist Infect Control* **7**: 73
- Yarza P, Yilmaz P, Pruesse E, Glöckner FO, Ludwig W, Schleifer KH, Whitman WB, Euzéby J, Amann R, Rosselló-Móra R** (2014) Uniting the classification of cultured and uncultured bacteria and archaea using 16S rRNA gene sequences. *Nat Rev Microbiol* **12**: 635–645
- Yasir M, Farman M, Shah MW, Jiman-Fatani AA, Othman NA, Almasaudi SB, Alawi M, Shakil S, Al-Abdullah N, Ismaeel NA, et al** (2020) Genomic and antimicrobial resistance genes diversity in multidrug-resistant CTX-M-positive isolates of *Escherichia coli* at a health care facility in Jeddah. *J Infect Public Health* **13**: 94–100
- Yasui H, Kurosawa Y** (1993) Measurement of recombination frequencies between two homologous DNA segments embedded in a YAC vector. *Gene* **129**: 135–139
- Yelin I, Kishony R** (2018) Antibiotic Resistance. *Cell* **172**: 1136-1136.e1
- Yin R, Kwoh CK, Zheng J** (2018) Whole genome sequencing analysis. *Encycl. Bioinforma. Comput. Biol. ABC Bioinforma.* Elsevier, pp 176–183
- Zakošek Pipan M, Švara T, Zdovc I, Papić B, Avberšek J, Kušar D, Mrkun J** (2019) *Staphylococcus pseudintermedius* septicemia in puppies after elective cesarean section: confirmed transmission via dam's milk. *BMC Vet Res* **15**: 41
- Zhanel GG, Ennis K, Vercaigne L, Walkty A, Gin AS, Embil J, Smith H, Hoban DJ** (2002) A critical review of the fluoroquinolones: focus on respiratory infections. *Drugs* **62**: 13–59
- Zhou K, Lokate M, Deurenberg RH, Tepper M, Arends JP, Raangs EGC, Lo-Ten-Foe J, Grundmann H, Rossen JWA, Friedrich AW** (2016) Use of whole-genome sequencing to trace, control and characterize the regional expansion of extended-spectrum β -lactamase producing ST15 *Klebsiella pneumoniae*. *Sci Rep* **6**: 20840

Zurfluh K, Nüesch-Inderbinnen M, Klumpp J, Poirel L, Nordmann P, Stephan R

(2017) Key features of *mcr-1*-bearing plasmids from *Escherichia coli* isolated from humans and food. *Antimicrob Resist Infect Control* **6**: 1–6

8. ACKNOWLEDGMENTS

M'agradaria començar aquest últim apartat d'agraïments donant les gràcies a dues de les persones que més m'han ajudat i aportat durant aquests darrers anys, les que considero la meva mare i germana científiques: les meves directores de tesi Olga i Anna C. Em sento molt agraït per totes les experiències que he pogut viure, tots els congressos als que hem assistit junts, tot l'aprenentatge i creixement personal que he realitzat al vostre costat. Moltes gràcies també al meu tutor, l'Armand, per confiar en mi com a candidat a doctor a Vetgenomics SL. És una empresa petiteta però amb un gran esperit molt maco. També agrair al pol sud de Vetgenomics SL per tot el suport: a la Laura, la Lorena, la Marta H., l'Àlicia, la Erika, la Justa. Formeu un equip genial noies! Espero poder treballar amb vosaltres més endavant.

Ara bé, la família científica que he anat construint no es queda aquí ja que podríem dir que ara tinc molts germans i germanes, tiets i tietes, cosins i cosines. Moltes gràcies a totes les persones que m'han acompanyat durant aquesta experiència, o que almenys han estat present durant un període de temps. A la Sara D. per compartir tots els moments que hem compartit i els que hem de compartir (he d'anar a Itàlia a alguna de les teves cases, *I promise*), i totes les *gocciolate* que m'he menjat per culpa teva; a la Melani per entendre'm perfectament i donar-me suport ja que hem viscut el doctorat al mateix temps (molt d'ànims, et queda molt poc!); a la Carlotta per ser tan *hard-working* però alhora una persona de confiança i divertida; a en Dani P. per tot el suport i les xarrades de *mamarracheo* que hem tingut i tenim, que fan més amens els dies al despatx; a la Norma que, tot i que fa molt poc que et conec, veig que ets una persona 10, súper treballadora i divertida. A les altres persones que han passat, o que no he coincidit tant en el temps, també els agraeixo el fet d'haver-me aportat la seva amistat: Morena, Francesca, Savino, Samir, Josep, Jordi, Marta V., Yulixaxis, etc. Em sap greu si em deixo algú, però de tot cor us agraeixo haver fet aquesta experiència el que ha estat.

Lògicament no me n'oblido dels sèniors, que realment han hagut d'aguantar MOLT les meves bromes (tot i que sé que realment les gaudeixen encara que no m'ho vulguin dir). A la Natalia J*z*b*1 per ser una de les persones amb més bon rotllo que he conegut (i més despreocupades... on tens les claus?); a l'Anna M. per, tot i anar tant atrafegada per la feina, deixar-se animar i els moments de dinar junts ja que ningú més venia; a en Quim C. i la Marta F. per ser qui realment em van introduir a la facultat de veterinària farà ja uns anys, i per tots els esmorzars i dinars i tot el que hem viscut (Quim, quan s'ha de fer la barbacoa?); a la Montse S. per tota la feina que fa i sempre dur una aura vital feliç súper contagiosa; a l'Àngels D. també per ser una de les tècnics més eficients i una persona molt atenta.

Agrair també a tots els col·laboradors/es que han comptat amb nosaltres per a realitzar els estudis que formen aquesta tesi o que ens han proporcionat mostres, LETIPharma, l'Hospital Clínic, Lluís i Lourdes entre d'altres. Vull fer especial menció a Lourdes per ser una de les persones més esbojarrades que he conegut dins l'àmbit científic, m'encanta que hi hagi gent tant diferent (en el bon sentit) dins la ciència, dones molt bon *feeling* i ets súper divertida. També agrair a l'Àngels C. i al Leo tota l'ajuda, consells, i amistat que m'han ofert durant aquests anys i que sé que perdurarà pels anys.

Vull agrair també a la meva família, a me mare, Montse; a me àvia, Emilia; a mon germà, Iñaki; i a la meva cunyada, Iris. Sé que no tenim molt en comú, però també sé que us sentiu molt orgulloses/os per tot el que estic aconseguint, i també sé que, pel que necessiti, hi sereu. Això també em porta a agrair a algú que ja no hi és i que, realment, em sap molt de greu i em posa molt trist que no hi sigui per veure com assolixo aquesta fita: el meu pare, Joaquim. Te'n vas anar que, malauradament, encara no m'havia graduat com a microbiòleg. Tot i així sé que eres una de les persones a la que li feia més il·lusió que anés a la universitat i que assolís tots aquests èxit. M'agradaria haver-los compartit amb tu, però em reconforta saber que, siguis on siguis, estàs orgullós del teu fill petit.

M'agradaria donar les gràcies a totes les amistats que també m'han acompanyat en aquest camí i m'han donat suport quan m'ha fet falta. Sobretot a la Sara A. i a la Maria R. per ser de les persones més atentes. Us estimo molt i us agraeixo de tot cor la vostra ajuda. També agrair totes les experiències que he viscut, tals com viatges, festes, i altres, amb els micritos (Anna S., Alba, Irene, Carlos, Marc, Martí, Pancha, Aina, Edgar, Ferran, Laura G., Neus., Pau, etc). Sense vosaltres, realment, no hagués estat el mateix ja que heu estat de les primeres amistats reals que he fet i us estaré sempre agraïts. També volia agrair a en Dani G. tot el que m'ha aportat i m'ha ajudat. Ens coneixem des de fa relativament poc, però has estat una de les persones que ha hagut d'aguantar més aquesta última etapa i, tot i així, ha seguit al pie del cañón, apostant per la relació que estem muntant. Moltes gràcies de tot cor per haver-hi estat i haver-me animat tant com ho has fet en els pitjors dies.

I finalment l'agraïment més important que crec que havia de fer. A qui més ens ha animat a tots... GRÀCIES LUPO PER SER UN SUPORT TANT IMPORTANT PER TOT HOM ENCARA QUE LA TEVA "CO LE GA" t'hagi educat taaaaant bé (entiéndase la ironia).

Moltes gràcies a tothom per aportar tant a aquesta experiència i fer-la el que ha estat.

9. ANNEXES

This section includes the papers mentioned in this thesis:

1. “Hybrid Assembly from a Pathogenic Methicillin- and Multidrug-Resistant *Staphylococcus pseudintermedius* Strain Isolated from a Case of Canine Otitis in Spain”
2. “Whole-Genome Sequencing and *De Novo* Assembly of 61 *Staphylococcus pseudintermedius* Isolates from Healthy Dogs and Dogs with Pyoderma”
3. “Whole genome sequencing and de novo assembly of *Staphylococcus pseudintermedius*: a pangenome approach to unravelling pathogenesis of canine pyoderma” (Under revision)
4. “Transmission of Similar Mcr-1 Carrying Plasmids among Different *Escherichia coli* Lineages Isolated from Livestock and the Farmer”
5. “Dissemination of NDM-producing *Klebsiella pneumoniae* and *Escherichia coli* high-risk clones in Catalan healthcare institutions”

Annex 1

“Hybrid Assembly from a Pathogenic Methicillin- and Multidrug-Resistant *Staphylococcus pseudintermedius* Strain Isolated from a Case of Canine Otitis in Spain”



Hybrid Assembly from a Pathogenic Methicillin- and Multidrug-Resistant *Staphylococcus pseudintermedius* Strain Isolated from a Case of Canine Otitis in Spain

 Joaquim Viñes,^{a,b}  Anna Cuscó,^b  Olga Francino^a

^aServei Veterinari de Genètica Molecular (SVGm), Universitat Autònoma de Barcelona, Bellaterra, Cerdanyola del Vallès, Barcelona, Spain

^bVetgenomics SL, Bellaterra, Cerdanyola del Vallès, Barcelona, Spain

ABSTRACT Here we report the genome assembly, using a hybrid approach with Illumina and Nanopore sequencing, of a pathogenic *Staphylococcus pseudintermedius* strain isolated from a case of canine otitis. Genome assembly confirmed the antimicrobial resistance profile (disk diffusion testing) with specific genes and mutations.

Staphylococcus pseudintermedius is a coagulase-positive *Staphylococcus* species within the *Staphylococcus intermedius* group (1), which is formed by *S. intermedius*, *S. pseudintermedius*, *S. delphini*, and *S. cornubiensis* (2). This bacterium is a commensal in pets' microbiota, typically related to dogs and primarily associated with skin, fur, and mucocutaneous sites. However, it has opportunistic behavior, causing several types of infections related mostly to the skin, such as wound infections, pyoderma, and otitis, among others. *S. pseudintermedius* colonizes 90% of dogs, and methicillin-resistant *S. pseudintermedius* (MRSP) demonstrates high prevalence worldwide, e.g., 70% in Japan, 50% in China, and 30% in Europe. The report of zoonotic infections due to MRSP highlights its One Health threat. Sequence type 71 (ST71) is the most prevalent in Europe (3–8).

Swab extension of the sample and further Diff-Quick staining revealed the presence of a few cocci in the left ear of a 6-year-old Yorkshire terrier with otitis externa. The *S. pseudintermedius* G3C4 strain was isolated by overnight culture at 37°C on blood agar. Different antibiotics were tested in a disk diffusion inhibitory assay, with the sensitivity range criteria shown at Table 1 for aminoglycosides, fluoroquinolones, tetracyclines, macrolides, beta-lactams, lincosamides, phenicols, rifamycins, fusidic acid, and cotrimoxazole.

DNA from *S. pseudintermedius* G3C4 was extracted using a DNA microprep kit (ZymoBIOMICS), following the manufacturer's instructions, and DNA quality was assessed by measurements with a Qubit fluorimeter (Invitrogen). The library for Nanopore sequencing was prepared by transposase fragmentation using a rapid barcoding kit (product number RBK-SQK004; Oxford Nanopore Technologies), according to the manufacturer's instructions. The final library was loaded and sequenced in a MinION FLO-MIN106 flow cell v9.4.

An Illumina (San Diego, CA, USA) library was prepared by enzymatic fragmentation and double indexing using an NGSgo kit (GenDx, Utrecht, Netherlands), according to the manufacturer's instructions. The indexed libraries were pooled, denatured, and diluted to a final concentration of 4 nM. The pooled library was sequenced on the MiSeq system (Illumina) with a 300-cycle MiSeq reagent kit v2.

The fast5 files generated by Nanopore sequencing were base called and demultiplexed (sorted by barcode) using Albacore v2.3.1, yielding fastq files. A second round of demultiplexing was performed with Porechop (9) (by default), in which barcodes that agreed with Albacore were kept and the others were removed. Porechop was also used

Citation Viñes J, Cuscó A, Francino O. 2020. Hybrid assembly from a pathogenic methicillin- and multidrug-resistant *Staphylococcus pseudintermedius* strain isolated from a case of canine otitis in Spain. *Microbiol Resour Announc* 9:e01121-19. <https://doi.org/10.1128/MRA.01121-19>.

Editor Irene L. G. Newton, Indiana University, Bloomington

Copyright © 2020 Viñes et al. This is an open-access article distributed under the terms of the [Creative Commons Attribution 4.0 International license](https://creativecommons.org/licenses/by/4.0/).

Address correspondence to Joaquim Viñes, joaquim.vines@vetgenomics.com, or Olga Francino, olga.francino@uab.cat.

Received 4 October 2019

Accepted 22 November 2019

Published 2 January 2020

TABLE 1 Summary of the antibiotic resistance determined by disk diffusion testing and sequencing

Antibiotic ^a	Disk diffusion testing results			Sequencing results		
	Zone of inhibition (mm)	Sensitivity range (μg/ml)	Susceptibility ^b	Gene(s) associated	Mutation associated	Location
Aminoglycosides						
GEN	12	<12 to >15	R	<i>aac(6′)-Ie-aph(2′′)-Ia</i> , <i>aph(3′)-IIIa</i> , <i>aad(6)</i>		Genome
TOB	17	<17 to >19	R			
AMK	25	<14 to >17	S			
Fluoroquinolones						
CIP	9	<20 to >22	R		Point mutations in <i>gyrA</i> (positions 12, 251, 2023, and 2140)	Genome
MARBO	0	<14 to >20	R			
PRADO	15	<19 to >24	R			
ORBI	0	<17 to >23	R			
Tetracyclines						
TET	10	<18 to >23	R	<i>tet(K)</i>		Plasmid
DOX	14	<20 to >25	R			
MIN	18	<19 to >24	R			
Macrolide						
ERY	0	<13 to >23	R	<i>ermB</i>		Genome
Beta-lactams						
OXA	0	<16 to >18	R	<i>mecA</i> , <i>blaZ</i>		Genome
FOX	30	<34 to >36	R			
Lincosamide						
CLI	0	<14 to >21	R	<i>ermB</i>		Genome
Phenicol						
CHL	34	<12 to >18	S			
FFC	30	<12 to >18	S			
Rifamycin						
RIF	44	<16 to >20	S			
Fusidane						
FD	40	<23 to >25	S			
SXT	0	<10 to >16	R	<i>dfrG</i>		Genome

^a GEN, gentamicin; TOB, tobramycin; AMK, amikacin; CIP, ciprofloxacin; MARBO, marbofloxacin; PRADO, pradofloxacin; ORBI, orbifloxacin; TET, tetracycline; DOX, doxycycline; MIN, minocycline; ERY, erythromycin; OXA, oxacillin; FOX, ceftiofur; CLI, clindamycin; CHL, chloramphenicol; FFC, florfenicol; RIF, rifampin; FD, fusidic acid; SXT, co-trimoxazole.

^b R, resistant; S, sensitive.

to trim barcodes and other adapters from the sequences. A total of 93,340 Nanopore reads were retrieved and used for further steps; the median read length was 2,774 bp, the N_{50} read length was 4,382 bp, and the median Phred read quality was 14.2. A total of 2,338,855 Illumina reads were generated by the sequencer, with a median Phred read quality of 37.8. *De novo* genome assembly was performed with data retrieved from Nanopore and Illumina sequencing in a hybrid approach, using Unicycler v0.4.6 (10) (parameters were as follows: R1, Illumina file; R2, Illumina file; I, Nanopore reads). Further analyses included assessment of genome completeness with CheckM v1.0.11 (11) (by default), multilocus sequence typing (MLST) using CGE DTU tools (12), and annotation with Prokka v1.13 (13) (by default); the NCBI Prokaryotic Genome Annotation Pipeline v4.6 was used to determine the number of coding sequences, rRNAs, and tRNAs. We used ABRicate (14) with the CARD and NCBI databases to retrieve antibiotic resistance genes.

Unicycler assembly retrieved 7 contigs. Two of the contigs corresponded to the complete genome and a plasmid, with 60× coverage and lengths of 2.72 Mb and 4.4 kb, respectively. The 5 other contigs had coverage between 1.71× and 1.83×.

The assembled genome of this *S. pseudintermedius* isolate (63× coverage) has a size of 2,717,621 bp, with a G+C content of 37.50% and 2,548 coding sequences, 59 tRNAs,

and 19 rRNA copies. CheckM determined completeness of 99.43%. MLST (12) showed that the strain belongs to the most prevalent ST in Europe, ST71, achieving 100% coverage and identity for all of the genes tested (*ack*, *cpn60*, *fdh*, *pta*, *purA*, *sar*, and *tuf*).

A plasmid of 4,439 bp, pSP-G3C4, was also obtained. It has a G+C content of 30.07% and 64× coverage. In a BLAST search, we obtained a match with *Staphylococcus epidermidis* ATCC 12228 plasmid pSE-12228-01 (NCBI accession number [NC_005008](#)).

Table 1 shows the results of disk diffusion susceptibility tests with aminoglycosides, fluoroquinolones, tetracyclines, macrolides, beta-lactams, clindamycin, and co-trimoxazole. Genome analyses with ABRicate revealed the presence of several genes that confer resistance to most of the aforementioned antibiotics, including *blaZ* and *mecA* for beta-lactam resistance, *aac(6′)-Ie-aph(2′)-Ia*, *aph(3′)-IIIa*, and *aad(6)* for aminoglycoside resistance, *ermB* for erythromycin and clindamycin resistance, and *dfpG* for trimethoprim resistance. We also found *sat4*, which confers resistance to streptothricin. Point mutations at positions 12, 251, 2032, and 2140 in the *gyrA* gene (encoding a topoisomerase) explain quinolone resistance (15). The *tet(K)* gene, conferring resistance to tetracycline, was found in the plasmid.

A SCC*mec* II-III cassette characteristic of *S. pseudintermedius* (15) harbors the methicillin resistance gene *mecA*. Furthermore, *aad(6)*, *sat4*, and *aph(3′)-IIIa* genes are located contiguously in the genome, which is an antibiotic resistance gene cluster already described for this species (16). It seems that a fourth gene could be involved in the cluster, namely, *ermB*, which is located near the triad of genes mentioned previously. Boerlin et al. (17) already reported that there could be a link between macrolide and aminoglycoside resistance in *Staphylococcus* strains of canine origin.

We confirm that a long- and short-read hybrid approach is an excellent option for sequencing and assembling *de novo* genomes for in-depth assembly and characterization.

Data availability. The genome sequence of *S. pseudintermedius* G3C4 has been deposited in the GenBank database with accession number [CP032682](#) and RefSeq accession number [NZ_CP032682](#); the plasmid has been deposited under GenBank accession number [MN612109](#). All raw sequence files can be found under BioProject accession number [PRJNA493792](#).

ACKNOWLEDGMENTS

The *S. pseudintermedius* isolate was kindly donated by LETIPharma.

This study was supported by a grant awarded by the Generalitat de Catalunya (Industrial Doctorate Program, grant 2017DI037) and by Vetgenomics.

REFERENCES

- Fitzgerald JR. 2009. The *Staphylococcus intermedius* group of bacterial pathogens: species re-classification, pathogenesis and the emergence of methicillin resistance. *Vet Dermatol* 20:490–495. <https://doi.org/10.1111/j.1365-3164.2009.00828.x>.
- Murray AK, Lee J, Bendall R, Zhang L, Sunde M, Slettemeås JS, Gaze W, Page AJ, Vos M. 2018. *Staphylococcus cornubiensis* sp. nov., a member of the *Staphylococcus intermedius* group (SIG). *Int J Syst Evol Microbiol* 68:3404–3408. <https://doi.org/10.1099/ijsem.0.002992>.
- Iverson SA, Brazil AM, Ferguson JM, Nelson K, Lautenbach E, Rankin SC, Morris DO, Davis MF. 2015. Anatomical patterns of colonization of pets with staphylococcal species in homes of people with methicillin-resistant *Staphylococcus aureus* (MRSA) skin or soft tissue infection (SSTI). *Vet Microbiol* 176:202–208. <https://doi.org/10.1016/j.vetmic.2015.01.003>.
- Somayaji R, Priyantha MAR, Rubin JE, Church D. 2016. Human infections due to *Staphylococcus pseudintermedius*, an emerging zoonosis of canine origin: report of 24 cases. *Diagn Microbiol Infect Dis* 85:471–476. <https://doi.org/10.1016/j.diagmicrobio.2016.05.008>.
- Bannoehr J, Guardabassi L. 2012. *Staphylococcus pseudintermedius* in the dog: taxonomy, diagnostics, ecology, epidemiology and pathogenicity. *Vet Dermatol* 23:253–266.e51. <https://doi.org/10.1111/j.1365-3164.2012.01046.x>.
- Grönthal T, Moodley A, Nykäsenoja S, Junnila J, Guardabassi L, Thomson K, Rantala M. 2014. Large outbreak caused by methicillin resistant *Staphylococcus pseudintermedius* ST71 in a Finnish veterinary teaching hospital: from outbreak control to outbreak prevention. *PLoS One* 9:e110084. <https://doi.org/10.1371/journal.pone.0110084>.
- Dmitrenko OA, Balbutskaya AA, Skvortsov VN. 2016. Ecological features, pathogenic properties, and role of *Staphylococcus intermedius* group representatives in animal and human infectious pathology. *Mol Genet Microbiol Virol* 31:117–124. <https://doi.org/10.3103/S0891416816030034>.
- Loeffler A, Lloyd DH. 2018. What has changed in canine pyoderma? A narrative review. *Vet J* 235:73–82. <https://doi.org/10.1016/j.tvjl.2018.04.002>.
- Wick R. 2017. Porechop. <https://github.com/rwick/Porechop>.
- Wick RR, Judd LM, Gorrie CL, Holt KE. 2017. Unicycler: resolving bacterial genome assemblies from short and long sequencing reads. *PLoS Comput Biol* 13:e1005595. <https://doi.org/10.1371/journal.pcbi.1005595>.
- Parks DH, Imelfort M, Skennerton CT, Hugenholtz P, Tyson GW. 2015. CheckM: assessing the quality of microbial genomes recovered from isolates, single cells, and metagenomes. *Genome Res* 25:1043–1055. <https://doi.org/10.1101/gr.186072.114>.
- Larsen MV, Cosentino S, Rasmussen S, Friis C, Hasman H, Marvig RL, Jelsbak L, Sicheritz-Pontén T, Ussery DW, Aarestrup FM, Lund O. 2012. Multilocus sequence typing of total-genome-sequenced bacteria. *J Clin Microbiol* 50:1355–1361. <https://doi.org/10.1128/JCM.06094-11>.
- Seemann T. 2014. Prokka: rapid prokaryotic genome annotation. *Bioinformatics* 30:2068–2069. <https://doi.org/10.1093/bioinformatics/btu153>.

14. Seemann T. 2017. ABRicate. <https://github.com/tseemann/abricate>.
15. Descloux S, Rossano A, Perreten V. 2008. Characterization of new staphylococcal cassette chromosome *mec* (SCC*mec*) and topoisomerase genes in fluoroquinolone- and methicillin-resistant *Staphylococcus pseudintermedius*. *J Clin Microbiol* 46:1818–1823. <https://doi.org/10.1128/JCM.02255-07>.
16. Derbise A, Aubert S, El Solh N. 1997. Mapping the regions carrying the three contiguous antibiotic resistance genes *aadE*, *sat4*, and *aphA-3* in the genomes of staphylococci. *Antimicrob Agents Chemother* 41:1024–1032. <https://doi.org/10.1128/AAC.41.5.1024>.
17. Boerlin P, Burnens AP, Frey J, Kuhnert P, Nicolet J. 2001. Molecular epidemiology and genetic linkage of macrolide and aminoglycoside resistance in *Staphylococcus intermedius* of canine origin. *Vet Microbiol* 79:155–169. [https://doi.org/10.1016/S0378-1135\(00\)00347-3](https://doi.org/10.1016/S0378-1135(00)00347-3).

Annex 2

“Whole-Genome Sequencing and *De Novo* Assembly of 61 *Staphylococcus pseudintermedius* Isolates from Healthy Dogs and Dogs with Pyoderma”

1 **Whole genome sequencing and *de novo* assembly of**
2 ***Staphylococcus pseudintermedius*: a pangenome approach to**
3 **unravelling pathogenesis of canine pyoderma**

4
5 L. FERRER*, R. GARCÍA-FONTICOPA*, D. PÉREZ †, J. VIÑES[±], N. FÀBREGAS[±],
6 S. MADROÑERO[†], G. MERONI[§], P MARTINO[§], MARTÍNEZ, S[‡], A. CUSCO[±], L.
7 MIGURA[¶] and O. FRANCINO[†]

8 * Departament de Medicina i Cirurgia Animals, Universitat Autònoma de Barcelona,
9 Spain.

10 † Servei Veterinari de Genètica Molecular, Universitat Autònoma de Barcelona, Spain.

11 [±] Vetgenomics, PRUAB, Bellaterra, Barcelona, Spain.

12 [§]Department of Biomedical, Surgical and Dental Sciences – One Health Unit, Via
13 Pascal 36, 20133 Milano, Italy.

14 [‡]Hospital Escuela de Pequeños Animales (HEPA), Facultad de Ciencias Veterinarias
15 de la Universidad Nacional del Centro de la Provincia de Buenos Aires, Tandil, Buenos
16 Aires, Argentina.

17 [¶] Centre de Recerca en Sanitat Animal, IRTA, Bellaterra, Barcelona, Spain.

18
19 Correspondence: Lluís Ferrer, Department de Medicina i Cirurgia Animals, Universitat
20 Autònoma de Barcelona, 08193, Bellaterra, Barcelona, Spain.

21 E-mail: lluis.ferrer@uab.cat

22
23 Funding: Research Grant RTI2018-101991-B-100 from the Ministerio de Ciencia e
24 Innovación, Spain; Industrial Doctorate Program Grant 2017DI037 AGAUR,
25 Generalitat de Catalunya, Spain.

26 The authors do not declare any conflict of interest.

27 This study was presented as a Supporting Original Study at the 9th World Congress of
28 Veterinary Dermatology, Sidney, 20-24 October 2020.

29

30 Abstract

31 **Background** –*Staphylococcus pseudintermedius* is the main etiologic agent of
32 canine pyoderma. The mechanisms leading a commensal bacterium to transform
33 itself into a pathogen have so far remained elusive to research. Whole genome
34 sequencing is the most comprehensive way of obtaining relevant genomic
35 information about microorganisms.

36 **Hypothesis/Objectives** – The comparative analysis of the complete genome of *S.*
37 *pseudintermedius* strains isolated from healthy dogs and dogs with pyoderma could
38 help to understand the pathogenesis of pyoderma.

39 **Methods and materials** – Twenty-two strains of *S. pseudintermedius* isolated from
40 the skin of five healthy dogs and 33 strains isolated from lesional skin of 33 dogs
41 with pyoderma were analyzed. DNA was extracted and sequenced using Oxford
42 Nanopore MinION, a new technology that delivers longer reads in a hand-held
43 device. The pangenome was analyzed and visualized with Anvi'o 6.1.

44 **Results** –The average genome size of *S. pseudintermedius* was 2,62MB, with 45%
45 being core genome. The genomes of the pathogenic strains were, on average, larger
46 than those of the strains from healthy dogs (2,743MB vs. 2,579MB; (*P*-value =
47 4.883e-07), due to a greater presence of phages and prophages (3.55 vs. 1.35; *P*-
48 value = 0.0009233) and antimicrobial resistance genes (*P*-value = 4.753e-0). In
49 contrast, the total number of virulence factors did not change between samples from
50 healthy dogs and dogs with pyoderma.

51 **Conclusions and clinical importance** – The analysis of the pangenome of *S.*
52 *pseudintermedius* is a very promising tool to understand the pathogenesis of canine
53 pyoderma and the transformation of a commensal bacterium into a pathogen.

54

55 Introduction

56 *Staphylococcus pseudintermedius* (*S. pseudintermedius*) is a component of the dog
57 skin microbiota^{21, 25} and the main causative agent of pyoderma in this species.^{1, 18} A
58 study in dogs with pyoderma concluded that *S. pseudintermedius* isolated from skin
59 lesions (pustules) were identical, using pulse-field gel electrophoresis (PFGE), to the
60 *S. pseudintermedius* isolated from non-lesional sites of the same dog.²³ This finding
61 indicated that the *S. pseudintermedius* causing skin infections very likely originated
62 from commensal *S. pseudintermedius* populations in the canine skin. Thus, the
63 current paradigm indicates that infection usually arises when the skin and mucosal
64 barriers are altered by predisposing factors such as atopic dermatitis, medical and
65 surgical procedures, and/or immunosuppressive disorders.¹ *Staphylococcus*
66 *pseudintermedius* is considered, therefore, an opportunistic pathogen. Nevertheless,
67 the mechanisms by which a commensal microorganism is transformed into a
68 pathogen are poorly understood.

69 The reduction and rational use of antibiotics in veterinary medicine is one of the main
70 strategies to reduce bacterial resistance and one that is advocated by health
71 organizations. One of the main indications for using antibiotics in small animal
72 medicine is the bacterial skin infection or pyoderma caused by *S. pseudintermedius*.
73 Understanding the pathogenic mechanisms of pyoderma could help prevent the
74 development of pyoderma and help develop new therapies, which could reduce the

75 use of antibiotics. Nevertheless, to date, it has been challenging to find a research
76 strategy to learn more about how pathogenic *S. pseudintermedius* populations
77 originate and what the difference, if any, is between commensal and pathogenic *S.*
78 *pseudintermedius* populations.

79 The recent development of next-generation sequencing (NGS) techniques that allow
80 relatively easy and economical mass sequencing of genomes has opened up a new
81 pathway for studying infectious diseases. In particular, the sequencing of the
82 complete genome of microorganisms allows a very precise genotypic
83 characterisation, identifying, for example, factors of virulence or antimicrobial
84 resistance and allowing the comparison of different strains and isolates. The release
85 of Oxford Nanopore Technologies's (ONT) MinION in 2014 generated much
86 excitement in the genomics community by offering portability (it measures 3 cm x 10
87 cm approximately), speed, and the capability of producing reads of virtually any
88 length.¹² The fact that it can work with longer reads facilitates the assembly of
89 genomes and the characterization, location, and genomic context of virulence and
90 resistance genes.³¹ So even though it has a higher error rate than the Illumina
91 system, it has quickly become very useful for rapid clinical responses and
92 sequencing in the field.^{9, 19}

93 Our research strategy was to perform a whole-genome analysis of *S.*
94 *pseudintermedius* using nanopore sequencing on MinION Mk1B from ONT. We
95 planned to compare the genome of *S. pseudintermedius* isolated from the skin of
96 healthy dogs with the genome of *S. pseudintermedius* isolated from skin lesions of
97 dogs with pyoderma. We aimed to understand the complete genome of *S.*
98 *pseudintermedius* better and detect differences that could explain the change from a
99 commensal microorganism to a pathogen.

100

101 **Materials and methods**

102 **Bacterial cultures**

103 The present study was carried out on 22 cultures of *S. pseudintermedius* isolated
104 from the skin of 6 healthy dogs and 33 cultures isolated from 33 dogs diagnosed with
105 pyoderma. In the case of the healthy dogs, the samples were obtained by rubbing a
106 sterile swab on the perioral or abdominal skin for 15 seconds. In the dogs with
107 pyoderma, samples were obtained, whenever possible, from the content of the
108 pustules. In three cases where no obvious pustules were present, the samples were
109 obtained from epidermal collarettes, as described in the literature.¹⁰ The samples
110 were cultured in blood agar at 37°C and incubated for 24 or 48 hours, depending on
111 the visual growth on the plate. Colonies with characteristic morphology of *S.*
112 *pseudintermedius* were sub-cultured and stored in brain heart infusion (BHI) broth
113 with 20% glycerol at -80°C for further studies. Before the DNA extraction procedure,
114 cultures were plated in blood agar and seeded in 3mL of BHI broth at 37°C for 24
115 hours.

116 **DNA extraction and sequencing**

117 *S. pseudintermedius* DNA from the BHI broth cultures was extracted with a Zymo
118 BIOMICS™ DNA Miniprep Kit (Zymo Research, Irvine, CA, USA). DNA quality and
119 quantity were determined using Nanodrop 2000 Spectrophotometer and Qubit™

120 dsDNA BR Assay Kit (Fisher Scientific SL, Madrid, Spain). The sequencing libraries
121 were prepared by transposase fragmentation using the Rapid Barcoding Sequencing
122 kit (SQK-RBK004; Oxford Nanopore Technologies), and 12 barcoded samples were
123 loaded in a MinION FLO-MIN106 v9.4.1 flow cell (Oxford Nanopore Technologies,
124 Oxford Science Park, OX4 4DQ, UK) and sequenced in a MinION Mk1B. The fast5
125 files were basecalled with Guppy 4.0.11 (Oxford Nanopore Technologies) with high
126 accuracy basecalling mode, demultiplexed, and with adapters trimmed. Reads with a
127 quality score lower than 7 were discarded.

128

129 **Assembling and visualization of the genomes**

130 Nanoplot 1.27 (<https://github.com/wdecoster/NanoPlot>) was used to obtain the run
131 summary statistics.⁵ Sequences corresponding to *S. pseudintermedius* after
132 taxonomy assignment using What's in my pot (WIMP) workflow from EPI2ME
133 platform¹⁴ were *de novo* assembled using Flye 2.7.1.¹⁵ Minimap 2.17 was used to
134 align the assembled sequences to the raw data files.¹⁷ The resulting contigs were
135 then first polished with the graph-based correction method used by Racon 1.4.13
136 (<https://github.com/lbcb-sci/racon>), followed by the neural-network based correction
137 method used by Medaka 1.0.3 (<https://nanoporetech.github.io/medaka/>).

138 Genome completeness was assessed with CheckM 1.1.1.²⁰ Circlator 1.5.5 was
139 used to identify the origin and the reverse complementary sequences.¹¹ Genomes
140 were annotated with NCBI Prokaryotic Genome Annotation Pipeline (PGAP)²⁹ (after
141 uploading to NCBI (Bioproject PRJNA685966), as well as the total number of coding
142 sequences, rRNA, and tRNA.

143 Anvi'o 6.2⁷ (<https://merenlab.org/2016/11/08/pangenomics-v2/>) allows comparison
144 of shared genes. It was used to determine the core genome and accessory genome
145 of *S. pseudintermedius* isolates.

146 **Multi-locus sequence type, antibiotic-resistance genes, virulence factors, and 147 bacteriophages**

148 Multi-locus sequence types (MLST) were assigned with MLST 2.0. software and
149 database 2.0.0.¹⁶ Antibiotic resistance genes were identified with Abricate 0.8.13²⁶
150 (<https://github.com/tseemann/abricate>) with the CARD database.¹³ Plasmids
151 (replicons) were identified with PlasmidFinder 2.1.⁴ A custom database was also
152 created to analyse the virulence factors (SPVFDB), containing 58 genes encoding
153 for virulence factors that include exfoliative toxins, enterotoxins, leukocidins, pore-
154 forming proteins, and intercellular adhesion proteins. Subsequently, the results were
155 filtered by genes with identity and coverage $\geq 90\%$. Phigaro 2.2.6²⁷ and Virsorter
156 1.0.6²⁴ were used to identify phage and bacteriophage sequences within the
157 genomes.

158

159 **Data availability**

160 The whole-genome assemblies were deposited at DDBJ/ENA/GenBank under
161 BIOPROJECT PRJNA685966 and with the accession numbers CP066702 to
162 CP066718, and CP066884, CP066885, and JAENBQ000000000 to
163 JAENDF000000000. The version described in this paper is version 1.

164

165 Results

166 DNA extraction and purification from BHI broth cultures developed as expected.
167 Sequencing libraries were prepared with 12 isolates per library with the Rapid
168 Barcoding kit (12-plex barcode libraries) and sequenced in the Nanopore MinION
169 Mk1B for 24 hours. The mean size of the reads was 2,600 bp. After quality
170 assessment of the reads, all genomes were assembled, achieving completeness
171 >96.7% and considered high-quality (completeness >90%, contamination <5%) for
172 further analyses. Mean sequencing coverage was 249.18x. Table 1 shows the
173 identification of the different isolates of *S. pseudintermedius* according to the MLST
174 and country of origin of the sample. In the case of isolates from dogs with pyoderma,
175 ST71 and ST257 were predominant. However, in isolates from healthy dogs, these
176 two STs were absent, and a long list of previously unreported STs was identified (19
177 out of 22), even with 100% coverage and identity values for the alleles of the seven
178 genes analysed in the MLST.

179 Considering all 55 samples together, the average genome size of *S.*
180 *pseudintermedius* was 2.62 MB. Comparing the genomes of the isolated from dogs
181 with pyoderma (N=33) with those from healthy dogs (N=22), several differences
182 were detected. The genomes of the pathogenic strains were, on average, larger than
183 those of the strains from healthy dogs (2,743 MB vs. 2,579 MB; (*P*-value = 4.883e-
184 07; Figure 1a). The larger genome size in *S. pseudintermedius* isolated from lesional
185 skin resulted from a greater presence of phages and prophages (3.55 vs. 1.35; *P*-
186 value = 0.0009233; Figure 1b) and antimicrobial resistance genes (*P*-value = 4.753e-
187 07; Figure 1d). In contrast, the total number of virulence factors did not change
188 between samples from healthy dogs and dogs with pyoderma (Figure 1b).

189 Global pangenome analyses of the 55 *S. pseudintermedius* genomes revealed 48%
190 of core genome and 52% of accessory genome (Figure 2). The accessory genome
191 of *S. pseudintermedius* is larger in pyoderma isolates (47% vs. 36%; Figure 3).

192 Considering that multi-drug resistance (MDR) is defined when the microorganism is
193 resistant to at least three families of antibiotics, we observed an MDR gene profile in
194 81.82% (27/33) of the *S. pseudintermedius* isolates from lesional skin vs. 9.09%
195 (2/22) of the isolates from healthy dogs. Among the 27 MDR strains isolated from
196 dogs with pyoderma, 22 held the *mecA* gene, and we characterized them
197 genotypically as methicillin-resistant *S. pseudintermedius* (MRSP).

198 Furthermore, *mecI* and *mecR1* genes, two genes involved in *mecA* gene expression,
199 were present in all ST71 isolates, the ST1631 isolate, and one unknown ST. On the
200 other hand, the five isolates that belonged to clonal complex 258 (4 ST258 and 1
201 ST301) possessed only the *mecA* gene. The samples from healthy dogs did not
202 harbor *mecA* gene.

203 Fifty virulence genes were identified, including accessory gene regulators (*agr*
204 A,B,C, D), adhesins and biofilm formation genes (*sps* A-H, ICA A-D, *ebps*), toxins
205 (*expA*, *expB*, *siet*, *speta*), and invasins (*Luk F*, *S*; *Hlb*, *Coa*). Thirty-two (58.18%) of
206 the virulence factors were present in all 55 isolates. Four virulence factor genes, all
207 encoding for surface proteins (*spsD*, *spsF*, *spsP*, and *spsQ*), were detected only in
208 isolates from lesional skin. The remaining genes for virulence factors were present
209 only in some isolates but without being specific for isolates from healthy dogs or
210 dogs with pyoderma.

211 Discussion

212 In the present study, we were able to sequence and assemble the complete genome
213 of multiple isolates of *S. pseudintermedius* using Nanopore technology. The method
214 is notably faster, simpler, and less expensive than other sequencing systems, such
215 as the traditional Illumina system. In addition, the use of Anvi'o allowed for easy
216 comparison of the genomes between isolates from lesional skin of dogs with
217 pyoderma and isolates from healthy dogs.

218 With this approach, the complete genome of 55 *S. pseudintermedius* isolates was
219 analysable. *S. pseudintermedius* isolates from our study have an average genome
220 size of 2.6 MB. This size is similar to that reported by other authors^{3, 6, 30} and the
221 NCBI *S. pseudintermedius* reference genome (NC_014925.1). This is an example of
222 an open genome, with a core genome of 48% and an accessory genome of 52%.

223 *S. pseudintermedius* isolates from pyoderma cases had a significantly larger
224 genome than isolates from healthy skin. This was at least partly due to the increased
225 presence of prophages and antimicrobial resistance genes. The presence of a larger
226 number of resistance genes seems logical in samples from animals with pyoderma
227 that had possibly been treated with antibiotics. It is more difficult to uncover the
228 meaning of the increased presence of prophages, and further analysis of the
229 genome will be needed to interpret this.

230 Interestingly, hardly any differences were found in the presence of virulence factor
231 genes. Only a few genes encoding surface proteins (sps BF) were found, exclusively
232 or much more frequently in samples from pyoderma cases. The surface proteins of
233 *S. pseudintermedius* express binding activity to components of the host's
234 extracellular matrix (ECM), including fibronectin, fibrinogen, and cytokeratin10, and
235 they are considered to be virulence factors associated with bacterial survival,
236 immune evasion, and biofilm formation.^{8,28} Our results support previous data
237 indicating that these proteins may play a role in *Staphylococcus* colonization and/or
238 infection.^{2, 22, 29} Interestingly, however, most virulence factors are present in strains
239 isolated from healthy dogs, indicating that commensal populations of *Staphylococcus*
240 already have full pathogenic potential. In any case, it is worth noting that this
241 genomic approach only investigates the presence of certain genetic elements in the
242 bacterial genome, but not their expression or functionality. In the case of both
243 antimicrobial resistance and virulence factors, it is necessary to complement genetic
244 studies with functionality tests.

245 An unexpected result was the difference in the MLSTs identified in animals with
246 pyoderma and in healthy animals. In the strains from dogs with pyoderma, the STs
247 identified were those most frequently described in Europe (ST71, ST259). However,
248 none of these STs were detected in samples from healthy dogs, which seems to go
249 against the paradigm constructed from the study by Pinchberk and colleagues.²³
250 However, our results should be interpreted with caution because the number of
251 samples is small, especially in healthy dogs. Extensive research and sequencing of
252 *S. pseudintermedius* from healthy dogs are needed to clarify whether there are
253 typically pathogenic STs and others that are associated only with commensal
254 behaviour.

255 In summary, our approach has allowed the sequencing and assembling of the
256 complete genome of 55 *S. pseudintermedius* strains isolated from healthy dogs and

257 dogs with pyoderma, and their analysis and comparison. Our hope is that this new
258 approach will lead to better a understanding of the pathogenesis of canine pyodermas.

259

260 **References**

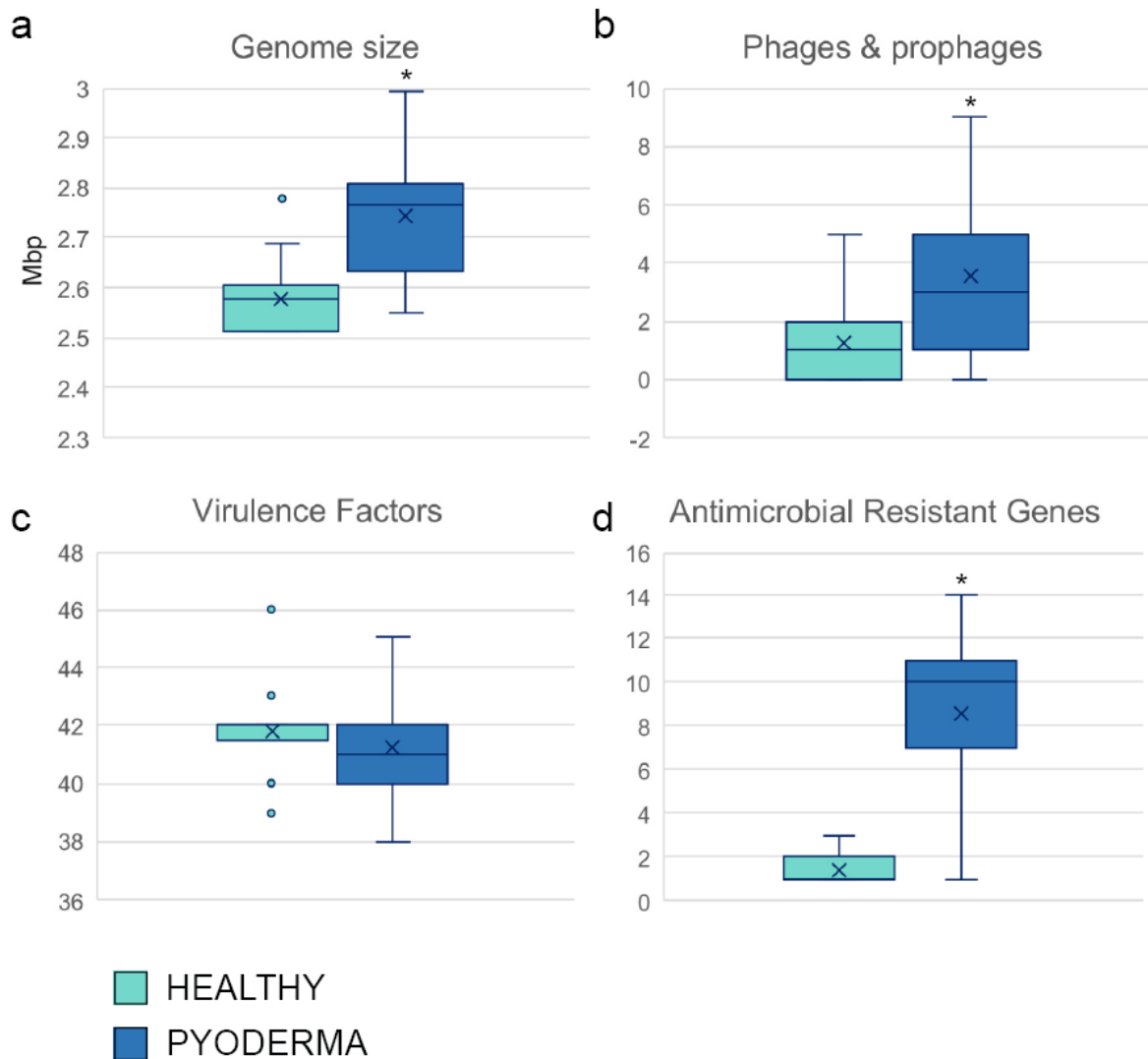
261

- 262 1. Bannoehr J, Guardabassi L. *Staphylococcus pseudintermedius* in the dog:
263 taxonomy, diagnostics, ecology, epidemiology and pathogenicity. *Vet*
264 *Dermatol* 2012; 23:253-66, e51-2.
- 265 2. Bannoehr J, Zakour NLB, Reglinski M et al. Genomic and surface proteomic
266 analysis of the canine pathogen *Staphylococcus pseudintermedius* reveals
267 proteins that mediate adherence to the extracellular matrix. *Infect Immun*
268 2011; 79:3074–3086.
- 269 3. Cao W, Hicks K, White A et al. Draft Genome assemblies of
270 two *Staphylococcus pseudintermedius* strains isolated from canine skin
271 biopsy specimens. *Microbiol Resour Announc* 2020; 9: e00369-20.
- 272 4. Carattoli A, Zankari E, García-Fernández A et al. *In silico* detection and typing
273 of plasmids using plasmidfinder and plasmid multilocus sequence typing.
274 *Antimicrob Agents Chemother* 2014; 58:3895–3903.
- 275 5. De Coster W, D’Hert S, Schultz DT et al. NanoPack: visualizing and
276 processing long-read sequencing data, *Bioinformatics* 2018; 34:2666–2669.
- 277 6. Eichhorn I, Lübke-Becker A, Lapschies AM et al. Draft genome sequence of
278 *Staphylococcus pseudintermedius* strain 13-13613, isolated from a case of
279 canine pyoderma. *Microbiol Resour Announc* 2020; 9:e00027-20.
- 280 7. Eren AM, Esen OC, Quince C, et al. Anvi’o: An advanced analysis and
281 visualization platform for ’omics data. *PeerJ* 2015; 3:e1319.
- 282 8. Foster TJ. 2009. Colonization and infection of the human host by
283 staphylococci: adhesion, survival and immune evasion. *Vet. Dermatol* 2009;
284 20:456–470.
- 285 9. Gardy J, Loman N. Towards a genomics-informed, real-time, global pathogen
286 surveillance system. *Nat Rev Genet* 2018;19: 9–20.
- 287 10. Hillier A, Lloyd DH, Weese S et al. Guidelines for the diagnosis and
288 antimicrobial therapy of canine superficial bacterial folliculitis (Antimicrobial
289 Guidelines Working Group of the International Society for Companion Animal
290 Infectious Diseases). *Vet Dermatol* 2014; 25:163-e43.
- 291 11. Hunt M, Silva N De, Otto TD et al. Circlator: Automated circularization of
292 genome assemblies using long sequencing reads. *Genome Biol* 2015;
293 16:294.
- 294 12. Jain M, Olsen HE, Paten B et al. The Oxford Nanopore MinION: delivery of
295 nanopore sequencing to the genomics community. *Genome Biology* 2016; 17:
296 239.
- 297 13. Jia B, Raphenya AR, Alcock B et al. CARD 2017: Expansion and model-
298 centric curation of the comprehensive antibiotic resistance database. *Nucleic*
299 *Acids Res* 2017, 45:D566-D573.
- 300 14. Juul S, Izquierdo F, Hurst A et al. What's in my pot? Real-time species
301 identification on the MinION™. *BioRxiv* 2015; 0307422.

- 302 15. Kolmogorov M, Yuan J, Lin Y et al. Assembly of long, error-prone reads using
303 repeat graphs. *Nat Biotechnol* 2019; 37:540-549.
- 304 16. Larsen MV, Cosentino S, Rasmussen S, et al. Multilocus sequence typing of
305 total-genome-sequenced bacteria. *J Clin Microbiol* 2012; 50:1355-1361.
- 306 17. Li H. Minimap2: Pairwise alignment for nucleotide sequences. *Bioinformatics*
307 2018; 34: 3094-3100.
- 308 18. Loeffler A, Lloyd DH. What has changed in canine pyoderma? A narrative
309 review. *Vet J* 2018; 235:73-82.
- 310 19. Lu H, Giordano F, Ning Z. Oxford Nanopore MinION Sequencing and
311 Genome Assembly. *Genomics, Proteomics & Bioinformatics* 2016; 14:265–
312 279.
- 313 20. Parks DH, Imelfort M, Skennerton CT et al. CheckM: Assessing the quality of
314 microbial genomes recovered from isolates, single cells, and metagenomes.
315 *Genome Res* 2015; 25:1043-1055.
- 316 21. Paul NC, Bärghman SC, Moodley A et al. *Staphylococcus pseudintermedius*
317 colonization patterns and strain diversity in healthy dogs: A cross-sectional
318 and longitudinal study. *Vet Microbiol* 2012; 160:420–427.
- 319 22. Phumthanakorn N, Chanchaithong P, Prapasarakul N. Development of a set
320 of multiplex PCRs for detection of genes encoding cell wall-associated
321 proteins in *Staphylococcus pseudintermedius* isolates from dogs, humans and
322 the environment. *J Microbiol Methods* 2017; 142:90–95.
- 323 23. Pinchbeck LR, Cole LK, Hillier A et al. Genotypic relatedness of
324 staphylococcal strains isolated from pustules and carriage sites in dogs with
325 superficial bacterial folliculitis. *Am J Vet Res* 2006; 67:1337–1346.
- 326 24. Roux S, Enault F, Hurwitz BL et al. VirSorter: Mining viral signal from
327 microbial genomic data. *PeerJ* 2015; 3:e985.
- 328 25. Rubin JE, Chirino-Trejo M. Prevalence, sites of colonization, an antimicrobial
329 resistance among *Staphylococcus pseudintermedius* isolated from healthy
330 dogs in Saskatoon, Canada. *J Vet Diagn Invest* 2011; 23:351–354.
- 331 26. Seemann T. Abricate. GitHub 2017.
- 332 27. Starikova E V, Tikhonova PO, Prianichnikov NA et al. Phigaro: high-
333 throughput prophage sequence annotation. *Bioinformatics* 2020; 36:3882-
334 3884.
- 335 28. Sung, J.M, Lloyd, DH, Lindsay JA. *Staphylococcus aureus* host specificity:
336 comparative genomics of human versus animal isolates by multi-strain
337 microarray. *Microbiology* 2008; 154:1949–1959.
- 338 29. Tatusova T, DiCuccio M, Badretdin A et al. NCBI prokaryotic genome
339 annotation pipeline. *Nucleic Acids Res.* 2016; 44:6614-6624.
- 340 30. Tse H, Tsoi HW, Leung SP et al. Complete genome sequence of the
341 veterinary pathogen *staphylococcus pseudintermedius* strain HKU10-03,
342 isolated in a case of canine pyoderma. *J Bacteriology* 2011; 193:1783-1784.
- 343 31. Viñes J, Cuscó A, Francino O. Hybrid assembly from a pathogenic methicillin-
344 and multidrug-resistant *Staphylococcus pseudintermedius* strain Isolated from
345 a case of canine otitis in Spain. *Microbiol Resour Announc* 2020; 9:e01121-
346 19.

347 **Figure legends**

348



349

350

351

352

353

354

355

356

357

358

359

360

361

362

363

364

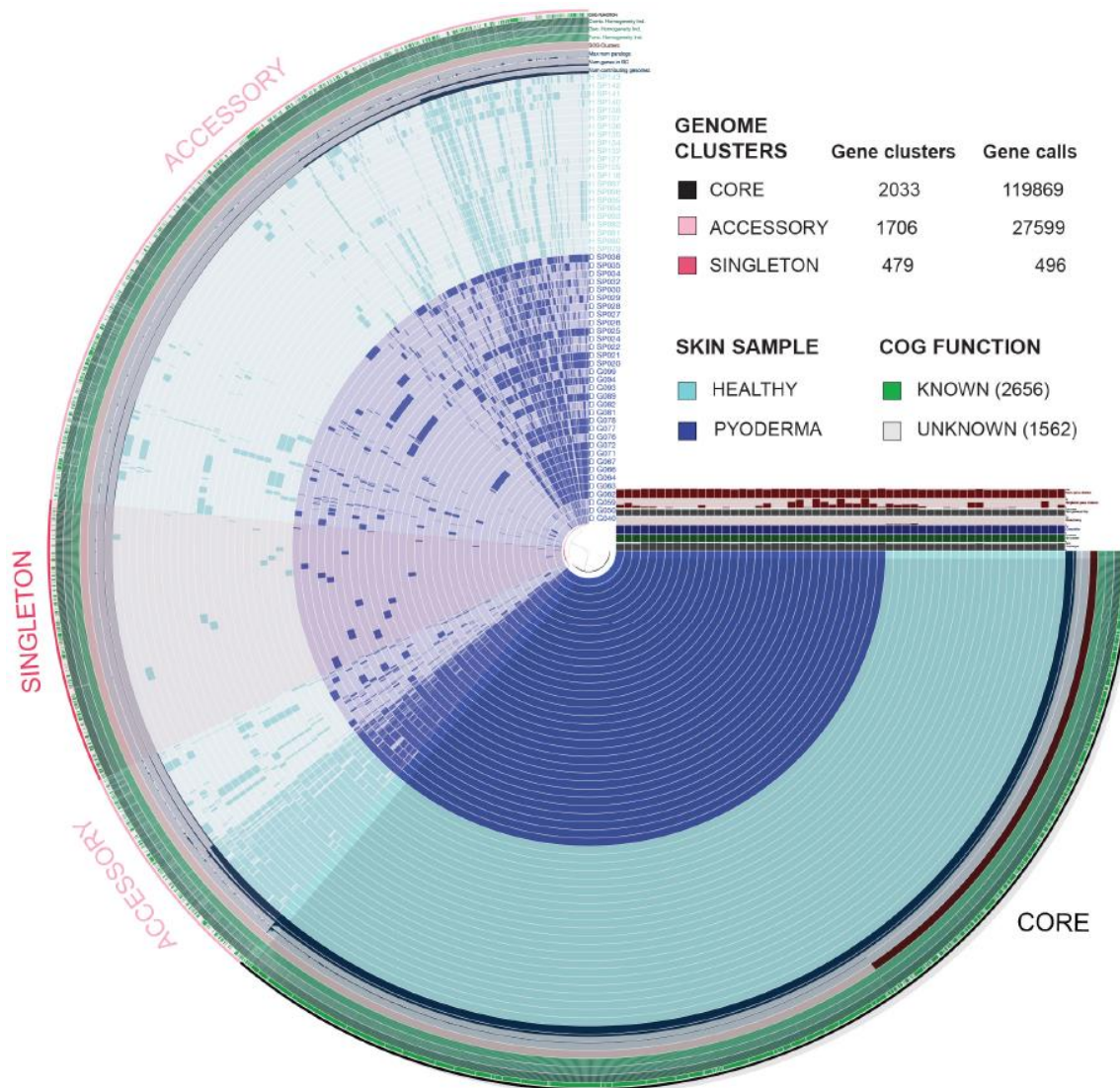
365

366

367

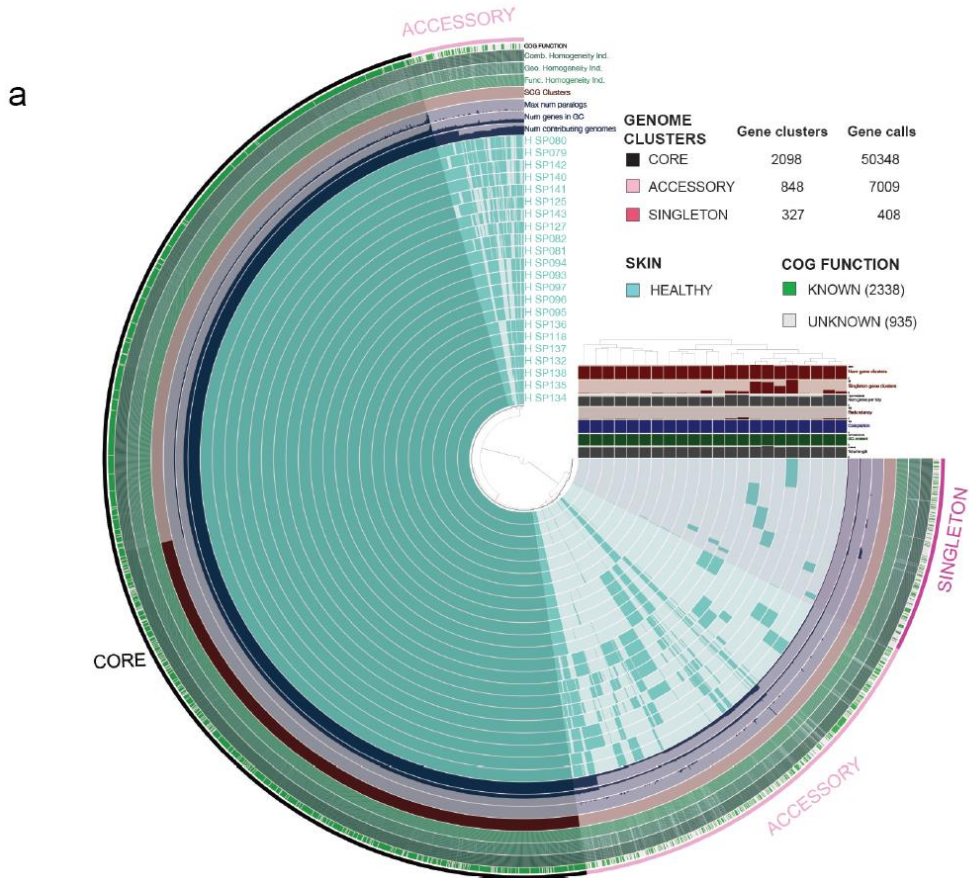
Figure 1. Genome of pathogenic *S. pseudintermedius* was larger and contained more phages, prophages, and antimicrobial resistant genes than genome of *S. pseudintermedius* strains from healthy dogs.

Box plots show the distribution of the (a) genome size (b) phage and prophage numbers (c) virulence factor numbers and (d) antimicrobial resistant gene numbers of *S. pseudintermedius* isolated from healthy dogs depicted in turquoise (healthy) and isolated from dogs with pyoderma depicted in blue (pyoderma). Asterisks denote statistical differences between healthy and pyoderma. Shapiro-Wilk normality tests revealed that samples were not normally distributed with the exception of two datasets: genome size (pyoderma) and virulence factors (pyoderma). Wilcoxon rank sum exact test revealed significant differences between genome sizes ($W = 636$, P -value = $4.883e-07$), phage and prophage numbers ($W = 173$, P -value = 0.0009233), and antimicrobial resistant genes ($W = 68.5$, P -value = $4.753e-07$). The number of virulence factor numbers was not different ($W = 451$, P -value = 0.1209).

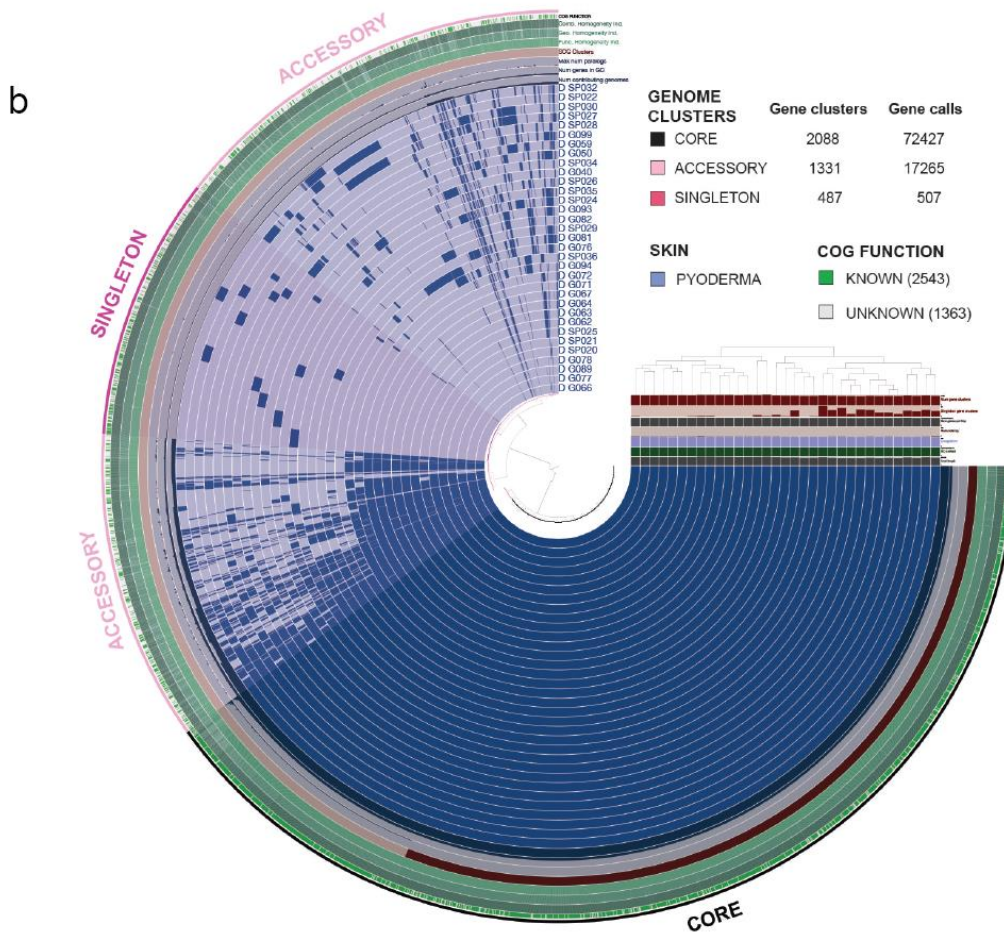


368
 369
 370
 371
 372
 373
 374
 375
 376
 377
 378
 379
 380
 381
 382
 383
 384
 385
 386
 387
 388

Figure 2. Pangenome visualization of all *S. pseudintermedius* strains
 Core genome is by definition the part of the pangenome that is present and shared by all the 55 *S. pseudintermedius* genomes within the pangenome (2033 gene clusters; 119869 ORFs/Gene Callings). Accessory genome is present and shared by at least 54 genomes within the pangenome (1706 gene clusters; 27599 ORFs/Gene Callings). Singleton contains unique genomes within the pangenome (479 gene clusters; 496 ORFs/Gene Callings). Visualization of pangenome analyses carried out with ANVI'O. Central dendrogram clustering of samples is ordered by gene cluster presence/absence. Item order: Presence absence (D: Euclidean; L: Ward).



389



390

391 **Figure 3. Pangenome visualization of healthy vs pyoderma *S.***
 392 ***pseudintermedius***

393 (a) Split pangenome analyses show 22 genomes of *S. pseudintermedius* isolated
 394 from healthy dogs. Core genome is present and shared by all 22 *S.*
 395 *pseudintermedius* genomes within the pangenome (2098 gene clusters; 50348
 396 ORFs/Gene Callings). Accessory genome contains 848 gene clusters; 7009
 397 ORFs/Gene Callings. Singleton contains 327 unique gene clusters; 408 ORFs/Gene
 398 Callings. (b) Split pangenome analyses show 33 genomes of *S. pseudintermedius*
 399 isolated from dogs with pyoderma. Core genome is present and shared by all 33 *S.*
 400 *pseudintermedius* genomes within the pangenome (2088 gene clusters; 72427
 401 ORFs/Gene Callings). Accessory genome contains 1331 gene clusters; 17265
 402 ORFs/Gene Callings. Singleton contains 487 unique gene clusters; 507 ORFs/Gene
 403 Callings. (a, b) Visualization of pangenome analyses carried out with ANVI'O.
 404 Central dendrogram clustering of samples is ordered by gene cluster
 405 presence/absence. Items order: Presence absence (D: Euclidean; L: Ward).
 406
 407
 408

409 **Table 1.** Multi-Locus Sequence Types (MLST) of the different *S. pseudintermedius*
 410 isolates. In brackets, country of origin of the sample.





	From healthy dogs	From dogs with pyoderma	Total
ST 257	1 (Spain)		1
ST 1061	1 (Spain)		1
ST 1248	1 (Spain)		1
Unknown ST	19 (Spain)	9 (Spain: 3, Italy: 4; Argentina: 2)	28
ST 71		15 (Spain: 6; Italy: 9)	15
ST258		4 (Italy: 3; Spain: 1)	4
ST301		1 (Italy)	1
ST503		1	1
ST611		1	1
ST1631		1	1
ST1827		1	1
Total	22	33	55

Annex 3

“Whole genome sequencing and de novo assembly of *Staphylococcus pseudintermedius*: a pangenome approach to unravelling pathogenesis of canine pyoderma” (Under revision)



Whole-Genome Sequencing and *De Novo* Assembly of 61 *Staphylococcus pseudintermedius* Isolates from Healthy Dogs and Dogs with Pyoderma

 O. Francino,^a  D. Pérez,^a  J. Viñes,^{a,c} R. Fonticoba,^b S. Madroñero,^a G. Meroni,^d P. Martino,^d S. Martínez,^e  A. Cusco,^c
 N. Fàbregas,^c  L. Migura-García,^f L. Ferrer^{b,g}

^aSVGM, Molecular Genetics Veterinary Service, Universitat Autònoma de Barcelona, Bellaterra, Barcelona, Spain

^bDepartment of Animal Medicine and Surgery, Universitat Autònoma de Barcelona, Bellaterra, Barcelona, Spain

^cVetgenomics, Edifici EUREKA, PRUAB, Bellaterra, Barcelona, Spain

^dDepartment of Biomedical, Surgical and Dental Sciences—One Health Unit, Milan, Italy

^eHospital Escuela de Pequeños Animales (HEPA), Facultad de Ciencias Veterinarias de la Universidad Nacional del Centro de la Provincia de Buenos Aires, Tandil, Buenos Aires, Argentina

^fIRTA, Centre de Recerca en Sanitat Animal (CRESA, IRTA-UAB), Bellaterra, Barcelona, Spain

^gAnimal Medicine and Surgery, Universitat Autònoma de Barcelona, Bellaterra, Barcelona, Spain

ABSTRACT We have *de novo* assembled and polished 61 *Staphylococcus pseudintermedius* genome sequences with Nanopore-only long reads. Completeness was 99.25%. The average genome size was 2.70 Mbp, comprising 2,506 coding sequences, 19 complete rRNAs, 56 to 59 tRNAs, and 4 noncoding RNAs (ncRNAs), as well as CRISPR arrays.

Staphylococcus pseudintermedius is a common microorganism of canine skin (1, 2) and the leading cause of pyoderma in dogs (3, 4). In this study, we aimed to retrieve *S. pseudintermedius* high-quality genome sequences from healthy dogs and dogs with pyoderma using a *de novo* assembly and polishing strategy with Nanopore-only long reads.

Samples were obtained by rubbing a sterile swab on the skin of healthy dogs ($n = 22$; H) and the nonlesional skin of a dog with pyoderma ($n = 6$; DH) or from the pustules of dogs with pyoderma ($n = 33$; D). After culture in blood agar at 37°C for 24 hours, colonies were seeded in 3 ml of brain heart infusion (BHI) broth at 37°C for 16 hours. DNA was extracted with a ZymoBIOMICS DNA miniprep kit (Zymo Research, Irvine, CA, USA). DNA quality and quantity were determined using a Nanodrop 2000 spectrophotometer and Qubit double-stranded DNA (dsDNA) broad-range (BR) assay kit (Fisher Scientific SL, Madrid, Spain). The sequencing libraries were prepared with the rapid barcoding sequencing kit (SQK-RBK004; Oxford Nanopore Technologies, UK). Twelve barcoded samples were loaded into a MinION FLO-MIN106 v9.4.1 flow cell (Oxford Nanopore Technologies Ltd.) and sequenced into a MinION Mk1B instrument. The fast5 files were basecalled and demultiplexed and adapters trimmed with Guppy 4.0.11 (Oxford Nanopore Technologies) (--config dna_r9.4.1_450bp-s_hac.cfg) (--config configuration.cfg --barcode_kits SQK-RBK004 --trim_barcode; min_score threshold default 60). Reads with a quality score lower than 7 were discarded. Run summary statistics were obtained with Nanoplot 1.27 (5) (--N50 --fastq).

Samples assigned to *S. pseudintermedius* by WIMP (6) were *de novo* assembled using Flye 2.7.1 (7) (--nano-raw --genome-size 2.6m --plasmids --trestle). After minimap 2.17 alignment (8), the resulting contigs were polished with Racon 1.4.13 (<https://github.com/lcb-science/racon>) and Medaka 1.0.3 (<https://nanoporetech.github.io/medaka/>) (medaka_consensus; -m r941_min_high_g360). Genome completeness was assessed with CheckM 1.1.1 (lineage_wf) (9). Circlator 1.5.5 was used to identify the origin (10) (fixstart --min_id 70). Genomes were annotated with NCBI Prokaryotic Genome Annotation Pipeline (PGAP) (11).

Citation Francino O, Pérez D, Viñes J, Fonticoba R, Madroñero S, Meroni G, Martino P, Martínez S, Cusco A, Fàbregas N, Migura-García L, Ferrer L. 2021. Whole-genome sequencing and *de novo* assembly of 61 *Staphylococcus pseudintermedius* isolates from healthy dogs and dogs with pyoderma. *Microbiol Resour Announc* 10:e00152-21. <https://doi.org/10.1128/MRA.00152-21>.

Editor Irene L. G. Newton, Indiana University, Bloomington

Copyright © 2021 Francino et al. This is an open-access article distributed under the terms of the [Creative Commons Attribution 4.0 International license](https://creativecommons.org/licenses/by/4.0/).

Address correspondence to O. Francino, olga.francino@uab.cat.

Received 9 February 2021

Accepted 22 March 2021

Published 22 April 2021

TABLE 1 Characteristics and accession numbers for high-quality genome assemblies from 61 *Staphylococcus pseudintermedius* isolates^a

Isolate ID ^b	MLST ^c	Source ^d	Yr of isolation	Country of isolation	Assembly ID (accession version no.)	Assembly level ^e	Genome accession no.	Genome assembly	No. of contigs	N ₅₀ (bp)	Genome size (all contigs) (bp)	No. of CDS (total)	COV ^f (x)	Comp ^f (%)	Cont ^f (%)
DG040	Unknown	Cf, A, SP	2017	Italy	GCF_016482145.1	Contig	JAENDF000000000	Circular	3	2,527,299	2,564,892	2,369	664	99.43	0.00
DG050	Unknown	Cf, A, SP	2016	Italy	GCF_016482445.1	Contig	JAENDE000000000	Circular	4	2,594,061	2,637,713	2,429	326	99.43	0.57
DG059	Unknown	Cf, A, SP	2017	Italy	GCF_016481825.1	Contig	JAENDD000000000	Circular	2	2,568,059	2,573,568	2,364	223	99.29	0.00
DG062	ST71	Cf, A, SP	2016	Italy	GCF_016482085.1	Contig	JAENDC000000000	Linear	10	2,096,046	2,991,046	2,901	253	99.43	2.84
DG063	ST71	Cf, A, SP	2016	Italy	GCF_016482045.1	Contig	JAENDB000000000	Linear	10	2,099,753	2,981,523	2,891	256	99.43	0.57
DG064	ST71	Cf, A, SP	2017	Italy	GCF_016455205.1	Contig	CP066718	Circular	1	2,895,060	2,895,060	2,764	361	99.43	0.57
DG066	ST71	Cf, A, SP	2017	Italy	GCF_016482585.1	Contig	JAENDA000000000	Circular	3	2,804,246	2,808,032	2,639	213	99.43	0.57
DG067	ST71	Cf, A, SP	2017	Italy	GCF_016482535.1	Contig	JAENCZ000000000	Linear	3	2,890,387	2,896,399	2,776	533	99.43	0.57
DG071	ST71	Cf, A, SP	2012	Italy	GCF_016482425.1	Contig	JAENCY000000000	Linear	3	2,800,617	2,807,986	2,644	85	99.43	0.57
DG072	ST71	Cf, A, SP	2012	Italy	GCF_016455165.1	Contig	CP066717	Circular	1	2,837,133	2,837,133	2,690	304	99.43	0.57
DG076	ST258	Cf, A, SP	2012	Italy	GCF_016482525.1	Contig	JAENCX000000000	Circular	5	2,732,273	2,780,144	2,573	323	99.43	0.85
DG077	ST71	Cf, A, SP	2016	Italy	GCF_016481985.1	Contig	JAENCW000000000	Circular	4	2,789,419	2,791,496	2,624	479	99.43	0.57
DG078	ST71	Cf, A, SP	2012	Italy	GCF_016481935.1	Contig	JAENCV000000000	Circular	3	2,792,180	2,799,396	2,637	208	99.43	0.57
DG081	ST301	Cf, A, SP	2012	Italy	GCF_016482005.1	Contig	JAENCU000000000	Circular	3	2,676,449	2,694,747	2,519	353	99.43	0.00
DG082	ST258	Cf, A, SP	2017	Italy	GCF_016481945.1	Contig	JAENCT000000000	Circular	2	2,623,528	2,626,557	2,396	259	99.43	0.00
DG089	ST71	Cf, A, SP	2012	Italy	GCF_016481925.1	Contig	JAENCS000000000	Circular	2	2,793,862	2,797,937	2,628	281	99.43	0.57
DG093	ST258	Cf, A, SP	2017	Italy	GCF_016481905.1	Contig	JAENCR000000000	Circular	2	2,640,063	2,648,891	2,433	39	99.43	0.00
DG094	ST71	Cf, A, SP	2017	Italy	GCF_016481855.1	Contig	JAENCQ000000000	Circular	2	2,840,672	2,849,103	2,675	191	99.43	0.57
DG099	Unknown	Cf, A, SP	2017	Italy	GCF_016455185.1	Chrom	CP066716	Linear	1	2,623,014	2,623,014	2,416	168	99.43	0.57
DSP020	ST71	Cf, A, SP	2013	Spain	GCF_016455145.1	Contig	CP066715	Circular	1	2,793,830	2,793,830	2,637	213	99.15	0.57
DSP021	ST71	Cf, A, SP	2013	Spain	GCF_016455225.1	Contig	CP066714	Circular	1	2,795,724	2,795,724	2,637	197	99.43	0.57
DSP022	Unknown	Cf, A, SP	2014	Spain	GCF_016481865.1	Contig	JAENCP000000000	Circular	3	2,718,542	2,767,901	2,555	174	98.86	0.28
DSP024	ST611	Cf, A, SP	2014	Spain	GCF_016482205.1	Contig	JAENCO000000000	Circular	2	2,758,929	2,762,026	2,595	289	99.43	0.57
DSP025	ST71	Cf, A, SP	2014	Spain	GCF_016482155.1	Contig	JAENCN000000000	Circular	6	2,801,923	2,805,515	2,641	295	99.43	0.57
DSP026	ST503	Cf, A, SP	2014	Spain	GCF_016455085.1	Contig	CP066713	Circular	1	2,567,628	2,567,628	2,387	303	99.43	0.00
DSP027	Unknown	Cf, A, SP	2014	Spain	GCA_016455285.1	Contig	CP066712	Circular	1	2,717,194	2,717,194	2,537	352	99.43	0.28
DSP028	Unknown	Cf, A, SP	2019	Spain	GCF_016482125.1	Contig	JAENCM000000000	Circular	2	2,569,147	2,575,420	2,367	238	98.86	0.00
DSP029	ST258	Cf, A, SP	2019	Spain	GCF_016481265.1	Contig	JAENBQ000000000	Linear	8	2,413,604	2,723,805	2,517	270	99.43	0.00
DSP030	Unknown	Cf, A, SP	2018	Argentina	GCF_016455265.1	Contig	CP066711	Circular	1	2,612,059	2,612,059	2,386	164	99.43	0.00
DSP032	ST1631	Cf, A, SP	2019	Argentina	GCA_016482035.1	Contig	JAENCL000000000	Linear	3	1,369,210	2,670,199	2,449	119	98.66	0.57
DSP034	ST1827	Cf, A, SP	2018	Argentina	GCF_016455025.1	Contig	CP066710	Linear	1	2,550,368	2,550,368	2,319	204	99.43	0.00
DSP035	Unknown	Cf, A, SP	2019	Argentina	GCF_016481845.1	Contig	JAENCK000000000	Linear	2	2,640,488	2,642,865	2,489	117	99.43	0.00
DSP036	ST71	Cf, A, SP	2019	Spain	GCF_016482105.1	Contig	JAENCJ000000000	Circular	7	2,849,760	2,927,015	2,755	129	99.43	0.57
DHSP041	ST71	Cf, A, H	2019	Spain	GCF_016482265.1	Contig	JAENBW000000000	Linear	3	2,849,717	2,909,751	2,748	123	99.41	0.57
DHSP042	ST71	Cf, A, H	2019	Spain	GCF_016482345.1	Contig	JAENBV000000000	Linear	6	2,822,064	2,930,017	2,768	72	99.43	0.57
DHSP043	ST71	Cf, A, H	2019	Spain	GCF_016482305.1	Contig	JAENBU000000000	Linear	12	1,649,358	2,931,289	2,776	66	99.43	0.57
DHSP044	ST71	Cf, A, H	2019	Spain	GCF_016482205.1	Contig	JAENBT000000000	Circular	4	2,849,602	2,907,542	2,748	132	99.43	0.57
DHSP045	ST71	Cf, A, H	2019	Spain	GCF_016482025.1	Contig	JAENBS000000000	Circular	5	2,849,736	2,915,461	2,742	127	99.41	0.57
DHSP046	ST496	Cf, P, H	2019	Spain	GCF_016481295.1	Contig	JAENBR000000000	Circular	2	2,695,721	2,710,903	2,475	100	99.43	0.00
HSP079	Unknown	Cf, P, H	2019	Spain	GCF_010659889.1	Contig	CP066885	Circular	1	2,585,691	2,587,693	2,337	301	99.43	0.00
HSP080	Unknown	Cf, P, H	2019	Spain	GCF_016598915.1	Contig	CP066884	Circular	1	2,585,570	2,587,506	2,336	199	99.41	0.00
HSP081	Unknown	Cf, P, H	2019	Spain	GCA_016482135.1	Contig	JAENCI000000000	Circular	4	2,617,897	2,621,254	2,467	94	98.58	1.14

(Continued on next page)

TABLE 1 (Continued)

Isolate ID ^b	MLST ^c	Source ^d	Yr of isolation	Country of isolation	Assembly ID (accession version no.)	Assembly level ^e	Genome accession no.	Genome assembly	No. of contigs	N ₅₀ (contigs) (bp)	Genome size (all contigs) (bp)	No. of CDS (total)	COV ^f (x)	Comp ^g (%)	Cont ^h (%)
HSP082	Unknown	Cf, P, H	2019	Spain	GCA_016481725.1	Contig	JAENCH0000000000	Circular	2	2,617,857	2,620,663	2,466	149	96.73	1.14
HSP093	Unknown	Cf, A, H	2019	Spain	GCF_016481735.1	Contig	JAENCG0000000000	Circular	3	2,571,836	2,590,335	2,361	274	99.43	0.57
HSP094	Unknown	Cf, A, H	2019	Spain	GCF_016481805.1	Contig	JAENCF0000000000	Circular	2	2,567,494	2,570,595	2,337	550	99.43	0.57
HSP095	Unknown	Cf, A, H	2019	Spain	GCF_016482325.1	Contig	JAENCF0000000000	Circular	2	2,570,328	2,575,879	2,360	341	99.43	0.57
HSP096	Unknown	Cf, A, H	2019	Spain	GCF_016482245.1	Contig	JAENCD0000000000	Circular	3	2,570,206	2,578,330	2,359	89	99.43	0.57
HSP097	Unknown	Cf, A, H	2019	Spain	GCF_016481665.1	Contig	JAENCC0000000000	Circular	3	2,570,223	2,575,223	2,356	136	99.43	0.57
HSP118	Unknown	Cf, A, H	2019	Spain	GCF_016455005.1	Compl	CP066709	Circular	1	2,512,855	2,512,855	2,277	313	99.43	0.00
HSP125	ST1248	Cf, A, H	2019	Spain	GCF_016455245.1	Compl	CP066708	Circular	1	2,551,473	2,551,473	2,330	327	98.86	0.00
HSP127	ST1061	Cf, P, H	2019	Spain	GCF_016481685.1	Contig	JAENCB0000000000	Circular	2	2,660,509	2,690,618	2,507	162	98.86	1.14
HSP132	Unknown	Cf, P, H	2019	Spain	GCA_016455125.1	Chrom	CP066707	Linear	1	2,515,164	2,515,164	2,275	132	98.72	0.00
HSP134	Unknown	Cf, P, H	2019	Spain	GCA_016455105.1	Compl	CP066706	Circular	1	2,514,594	2,514,594	2,274	146	98.86	0.00
HSP135	Unknown	Cf, A, H	2019	Spain	GCF_016455065.1	Compl	CP066705	Circular	1	2,512,727	2,512,727	2,277	154	98.86	0.00
HSP136	Unknown	Cf, A, H	2019	Spain	GCA_016455045.1	Chrom	CP066704	Linear	1	2,512,726	2,512,726	2,274	104	98.86	0.00
HSP137	Unknown	Cf, A, H	2019	Spain	GCF_016454985.1	Compl	CP066703	Circular	1	2,512,757	2,512,757	2,271	224	99.43	0.00
HSP138	Unknown	Cf, A, H	2019	Spain	GCF_016454965.1	Compl	CP066702	Circular	1	2,512,830	2,512,830	2,277	227	98.86	0.00
HSP140	Unknown	Cf, P, H	2019	Spain	GCF_016482365.1	Contig	JAENCA0000000000	Circular	2	2,594,004	2,597,272	2,387	296	99.24	0.00
HSP141	ST257	Cf, P, H	2019	Spain	GCF_016482355.1	Contig	JAENBZ0000000000	Circular	4	2,615,633	2,622,529	2,450	150	99.43	0.57
HSP142	Unknown	Cf, P, H	2019	Spain	GCF_016482405.1	Contig	JAENBY0000000000	Circular	2	2,594,059	2,597,098	2,393	461	99.43	0.00
HSP143	Unknown	Cf, P, H	2019	Spain	GCF_016482235.1	Contig	JAENBX0000000000	Linear	6	2,537,079	2,779,670	2,589	293	98.86	0.57

^aObtained from the lesional skin of 33 dogs with pyoderma (33 D), the nonlesional skin of a dog with pyoderma (6 DH), and 6 healthy dogs (22 H).

^bID, identifier.

^cMLST, multilocus sequence type; ST, sequence type.

^dCf, *Canis lupus familiaris*; A, abdominal skin swab; P, perioral skin swab; SP, superficial pyoderma; H, healthy.

^eCompl, complete genome; Chrom, chromosome.

^fCOV, coverage; Comp, completeness; Cont, contamination.

Multilocus sequence types (MLSTs) were assigned with software MLST 2.0. and database 2.0.0 (<https://cge.cbs.dtu.dk/services/MLST-2.0/>) (12).

Nanopore sequencing allowed successful *de novo* assembly and polishing of 61 *S. pseudintermedius* isolates (Table 1). The average read N_{50} value was 4,223.38 bp for 2,848,339.50 reads per flow cell (237,361.63 per barcoded sample). The mean genome coverage was $235\times$ ($39\times$ to $664\times$), with an average contig N_{50} value of 2.6 Mbp (1.6 Mbp to 2.9 Mbp). The average genome completeness was 99.25% (98.6% to 99.4%, except for HSP082), which is close to previous results with hybrid assemblies (13). The number of contigs per isolate ranged from 1 to 12 (median, 2). The main contig was circular for 47 isolates. The average genome size of *S. pseudintermedius* was 2.70 Mbp (2.51 to 2.99 Mb), comprising 2,506 coding sequences (CDS; 2,271 to 2,901), 19 complete rRNAs (6 to 7 5S, 6 16S, and 6 23S rRNA genes), 56 to 59 tRNAs, and 4 noncoding RNAs (ncRNAs), as well as CRISPR arrays (0.5; range from 0 to 2). Pangenome analyses of isolates from healthy and diseased individuals will help unravel the differences, if any, that exist between commensal and pathogenic *S. pseudintermedius* populations.

Data availability. The standardized strain descriptions and accession numbers are presented in Table 1; the genome sequence assemblies and genomic data are publicly available in DDBJ/ENA/GenBank under BioProject no. [PRJNA685966](https://www.ncbi.nlm.nih.gov/bioproject/PRJNA685966) with the accession numbers [CP066702](https://www.ncbi.nlm.nih.gov/nuclink/CP066702) to [CP066718](https://www.ncbi.nlm.nih.gov/nuclink/CP066718), [CP066884](https://www.ncbi.nlm.nih.gov/nuclink/CP066884), [CP066885](https://www.ncbi.nlm.nih.gov/nuclink/CP066885), and [JAENBQ000000000](https://www.ncbi.nlm.nih.gov/nuclink/JAENBQ000000000) to [JAENDF000000000](https://www.ncbi.nlm.nih.gov/nuclink/JAENDF000000000). The versions described in this paper are the first versions. The raw data are available from the Sequence Read Archive (SRA) under the same BioProject no., [PRJNA685966](https://www.ncbi.nlm.nih.gov/bioproject/PRJNA685966).

ACKNOWLEDGMENTS

Funding sources were as follows: Research Project RTI2018-101991-B-100 ("From whole genome sequencing to clinical metagenomics: investigations on the pathogenesis of *Staphylococcus pseudintermedius* pyoderma in the dog"); Spanish Ministry of Science, Innovation and Universities; Industrial Doctorate Program grant 2017DI037 AGAUR; and Generalitat de Catalunya, Spain. The Spanish Ministry of Science and Innovation granted a Torres Quevedo Project to Vegenomics, S.L. with reference PTQ2018-009961 that is cofinanced by the European Social Fund.

L.F. has received unrelated honoraria for lecturing from Zoetis, Bayer, LETI, and Affinity Petcare. O.F. and A.C. have received unrelated honoraria for lecturing from Oxford Nanopore Technologies.

REFERENCES

- Paul NC, Bärman SC, Moodley A, Nielsen SS, Guardabassi L. 2012. *Staphylococcus pseudintermedius* colonization patterns and strain diversity in healthy dogs: a cross-sectional and longitudinal study. *Vet Microbiol* 160:420–427. <https://doi.org/10.1016/j.vetmic.2012.06.012>.
- Rubin JE, Chirino-Trejo M. 2011. Prevalence, sites of colonization, antimicrobial resistance among *Staphylococcus pseudintermedius* isolated from healthy dogs in Saskatoon, Canada. *J Vet Diagn Invest* 23:351–354. <https://doi.org/10.1177/104063871102300227>.
- Bannoehr J, Guardabassi L. 2012. *Staphylococcus pseudintermedius* in the dog: taxonomy, diagnostics, ecology, epidemiology and pathogenicity. *Vet Dermatol* 23:253–266, e51–2. <https://doi.org/10.1111/j.1365-3164.2012.01046.x>.
- Loeffler A, Lloyd DH. 2018. What has changed in canine pyoderma? A narrative review. *Vet J* 235:73–82. <https://doi.org/10.1016/j.tvjl.2018.04.002>.
- De Coster W, D'Hert S, Schultz DT, Cruts M, Van Broeckhoven C. 2018. NanoPack: visualizing and processing long-read sequencing data. *Bioinformatics* 34:2666–2669. <https://doi.org/10.1093/bioinformatics/bty149>.
- Juul S, Izquierdo F, Hurst A, Dai X, Wright A, Kulesha E, Pettett R, Turner DJ. 2015. What's in my pot? Real-time species identification on the MinION. *bioRxiv* <https://doi.org/10.1101/030742>.
- Kolmogorov M, Yuan J, Lin Y, Pevzner PA. 2019. Assembly of long, error-prone reads using repeat graphs. *Nat Biotechnol* 37:540–549. <https://doi.org/10.1038/s41587-019-0072-8>.
- Li H. 2018. minimap2: pairwise alignment for nucleotide sequences. *Bioinformatics* 34:3094–3100. <https://doi.org/10.1093/bioinformatics/bty191>.
- Parks DH, Imelfort M, Skennerton CT, Hugenholz P, Tyson GW. 2015. CheckM: assessing the quality of microbial genomes recovered from isolates, single cells, and metagenomes. *Genome Res* 25:1043–1055. <https://doi.org/10.1101/gr.186072.114>.
- Hunt M, De Silva N, Otto TD, Parkhill J, Keane J, Harris SR. 2015. Circlator: automated circularization of genome assemblies using long sequencing reads. *Genome Biol* 16:294. <https://doi.org/10.1186/s13059-015-0849-0>.
- Tatusova T, DiCuccio M, Badretdin A, Chetverin V, Nawrocki EP, Zaslavsky L, Lomsadze A, Pruitt KD, Borodovsky M, Ostell J. 2016. NCBI Prokaryotic Genome Annotation Pipeline. *Nucleic Acids Res* 44:6614–6624. <https://doi.org/10.1093/nar/gkw569>.
- Larsen MV, Cosentino S, Rasmussen S, Friis C, Hasman H, Marvig RL, Jelsbak L, Sicheritz-Pontén T, Ussery DW, Aarestrup FM, Lund O. 2012. Multilocus sequence typing of total-genome-sequenced bacteria. *J Clin Microbiol* 50:1355–1361. <https://doi.org/10.1128/JCM.06094-11>.
- Viñes J, Cuscó A, Francino O. 2020. Hybrid assembly from a pathogenic methicillin- and multidrug-resistant *Staphylococcus pseudintermedius* strain isolated from a case of canine otitis in Spain. *Microbiol Resour Announc* 9:e01121-19. <https://doi.org/10.1128/MRA.01121-19>.

Annex 4

“Transmission of Similar Mcr-1 Carrying Plasmids among Different *Escherichia coli* Lineages Isolated from Livestock and the Farmer”



Article

Transmission of Similar Mcr-1 Carrying Plasmids among Different *Escherichia coli* Lineages Isolated from Livestock and the Farmer

Joaquim Viñes ^{1,2}, Anna Cuscó ², Sebastian Napp ^{3,4}, Julio Alvarez ^{5,6}, Jose Luis Saez-Llorente ⁷, Montserrat Rosàs-Rodoreda ⁸, Olga Francino ¹ and Lourdes Migura-Garcia ^{3,4,*}

- ¹ Servei Veterinari de Genètica Molecular (SVGM), Universitat Autònoma de Barcelona, 08193 Barcelona, Spain; joaquim.vines@vetgenomics.com (J.V.); olga.francino@uab.cat (O.F.)
- ² Vetgenomics, Edifici EUREKA, Parc de Recerca de la UAB, Campus UAB, 08193 Barcelona, Spain; anna.cusco@vetgenomics.com
- ³ IRTA, Centre de Recerca en Sanitat Animal (CRESA, IRTA-UAB), Campus UAB, Universitat Autònoma de Barcelona, 08193 Barcelona, Spain; sebastian.napp@irta.cat
- ⁴ OIE Collaborating Centre for the Research and Control of Emerging and Re-emerging Swine Diseases in Europe (IRTA-CReSA), 08193 Barcelona, Spain
- ⁵ Centro de Vigilancia Sanitaria Veterinaria (VISAVET), Universidad Complutense, 28040 Madrid, Spain; jalvarez@ucm.es
- ⁶ Departamento de Sanidad Animal, Facultad de Veterinaria, Universidad Complutense, 28040 Madrid, Spain
- ⁷ Area de Programas Sanitarios y Zoonosis, S.G. de Sanidad e Higiene Animal y Trazabilidad, Ministerio de Agricultura, Pesca y Alimentación, 28014 Madrid, Spain; jsaezll@mapama.es
- ⁸ Departament d'Agricultura, Ramaderia, Pesca i Alimentació, Servei d'Alimentació Animal i Seguretat de la Producció Ramadera, 08007 Barcelona, Spain; montse.rosas@gencat.cat
- * Correspondence: Lourdes.migura@irta.cat; Tel.: +34-93-467-4040 (ext. 1769)



Citation: Viñes, J.; Cuscó, A.; Napp, S.; Alvarez, J.; Saez-Llorente, J.L.; Rosàs-Rodoreda, M.; Francino, O.; Migura-Garcia, L. Transmission of Similar Mcr-1 Carrying Plasmids among Different *Escherichia coli* Lineages Isolated from Livestock and the Farmer. *Antibiotics* **2021**, *10*, 313. <https://doi.org/10.3390/antibiotics10030313>

Academic Editor: Kazuki Harada

Received: 16 February 2021

Accepted: 16 March 2021

Published: 17 March 2021

Publisher's Note: MDPI stays neutral with regard to jurisdictional claims in published maps and institutional affiliations.



Copyright: © 2021 by the authors. Licensee MDPI, Basel, Switzerland. This article is an open access article distributed under the terms and conditions of the Creative Commons Attribution (CC BY) license (<https://creativecommons.org/licenses/by/4.0/>).

Abstract: Colistin use has mostly been stopped in human medicine, due to its toxicity. However, nowadays, it still is used as a last-resort antibiotic to treat hospital infections caused by multi-drug resistant Enterobacteriaceae. On the contrary, colistin has been used in veterinary medicine until recently. In this study, 210 fecal samples from pigs ($n = 57$), calves ($n = 152$), and the farmer ($n = 1$) were collected from a farm where *E. coli* harboring *mcr-1–mcr-3* was previously detected. Samples were plated, and *mcr*-genes presence was confirmed by multiplex-PCR. Hybrid sequencing which determined the presence and location of *mcr-1*, other antibiotic resistance genes, and virulence factors. Eighteen colistin resistant isolates (13 from calves, four from pigs, and one from the farmer) contained *mcr-1* associated with plasmids (IncX4, IncI2, and IncHI2), except for two that yielded *mcr-1* in the chromosome. Similar plasmids were distributed in different *E. coli* lineages. Transmission of *mcr-1* to the farmer most likely occurred by horizontal gene transfer from *E. coli* of calf origin, since plasmids were highly similar (99% coverage, 99.97% identity). Moreover, 33 virulence factors, including *stx2* for Shiga toxin *E. coli* (STEC) were detected, highlighting the role of livestock as a reservoir of pathotypes with zoonotic potential.

Keywords: *Escherichia coli*; colistin; *mcr*; plasmids; MinION nanopore; hybrid sequencing; livestock

1. Introduction

The vast majority of antimicrobials used in veterinary medicine are also used in human medicine. The consumption of antimicrobial agents has increased the selection of resistant bacteria in both human and veterinary medicine. Additionally, the presence of resistance genes in mobile genetic elements has probably played a major role in the inter- and intra-species transmission of antimicrobial resistance.

Use of colistin in human medicine has been abandoned, due to its toxicity when applied systemically. Nevertheless, nowadays, the emergence of multidrug-resistant (MDR) Gram-negative bacteria in hospital settings has left no other choice but to use colistin

as the last-line treatment option despite its toxicity. Contrarily, in veterinary medicine, colistin sulfate has been used orally for many decades to treat infections caused by *Enterobacterales* [1]. In particular, colistin tablets are available for calves in many countries for the prevention and treatment of neonatal colibacillosis [2]. Additionally, studies performed in different EU countries have reported the prophylactic and metaphylactic use of colistin for the prevention and treatment of enteric diarrheas in pigs [3–6]. In this scenario, Spain was the country with the highest sales of colistin for food-producing animals in the EU in 2014 [7]. Fortunately, colistin consumption has been drastically reduced in the last years after the implementation of a specific program “Reduce Colistin”, targeting pig production with the voluntary agreement of producers [8].

Until 2015, resistance to colistin was only associated with chromosomal mutations. More recently, different plasmid-mediated mechanisms conferring resistance to colistin have been identified [9–13], with the most prevalent one, *mcr-1*, being distributed worldwide [14]. The emergence of colistin resistance in mobile genetic elements has raised the concern of the scientific community, since the transmission of resistance from farm to fork could further complicate the treatment of severe infections in human hospitals.

Back in 2017, the co-occurrence of *mcr-1* and *mcr-3* was described for the first time in Spain in an *Escherichia coli* of calf origin [15]. This isolate was obtained from a fecal sample at a slaughterhouse in the frame of the Spanish National Monitoring Program for antimicrobial resistance carried out in 2015. The farm of origin of the calf was identified, and a visit was carried out in September 2017 to sample the premises and to determine if this *E. coli* genotype was endemic in the farm. In this context, whole genome sequencing combining Nanopore and Illumina technologies was applied to study the dynamics of the transmission of colistin resistance within the livestock and the farmer, the characterization of plasmids, the location and genomic context of resistance genes, and the detection of virulence factors.

2. Results and Discussion

Visible growth on MacConkey agar supplemented with colistin was observed for 18/210 fecal samples. The multiplex PCR confirmed the presence of *mcr-1* in the 18 *E. coli* isolates (13 from calves, four from pigs and one from the farmer). No additional *mcr*-gene variants were detected.

2.1. Antimicrobial Susceptibility Testing

MIC values for colistin varied, with one isolate exhibiting a MIC of 2 mg/L, 15 isolates equal to 4 mg/L, and two showing a MIC \geq 8 mg/L (Table S1). Furthermore, all the colistin-resistant isolates were also resistant to ampicillin, ciprofloxacin, streptomycin, chloramphenicol, sulfamethoxazole, and trimethoprim. Additionally, 17 isolates exhibited resistance to tetracycline, 16 to nalidixic acid and florfenicol, 14 to kanamycin, and 13 to gentamicin. Finally, phenotypic resistance to cefotaxime was observed in three isolates, whereas resistance to ceftazidime was detected in two (Table S1). All the isolates were MDR.

The 18 *mcr-1* positive isolates were sequenced. Chromosome size ranged from 4,613,927 bp (Farmer) to 5,586,543 (calve 15B_22), with an average size of 5,009,072 bp (Table S2). Completeness ranged from 91.9% (P2_16) to 99.8% (15A_11 and 14_4), with an average of 98.5%, except for the isolate P2_2 (76.1%). The genome size and CDS number were similar when compared with the values obtained for phylotype A reference (NC_000913.3) and for phylotype B1 reference (NC_018658.1).

Ten isolates belonged to phylotype A (seven from cattle, two from swine, and one from the farmer), and eight to phylotype B1 (six from cattle and two from swine). Phylogenetic analysis based on Single Nucleotide Polymorphisms (SNPs) clustered isolates from phylotype A and B1 separately (Figure 1). The most represented multi-locus sequence type (MLST) was ST6395 (three isolates from calves) and ST224 (three isolates from calves), followed by ST10 (two swine isolates). The ST6395 isolates shared the same serotype (O4:H26), as well as the ST10 isolates (O96:H1) (Table S2).

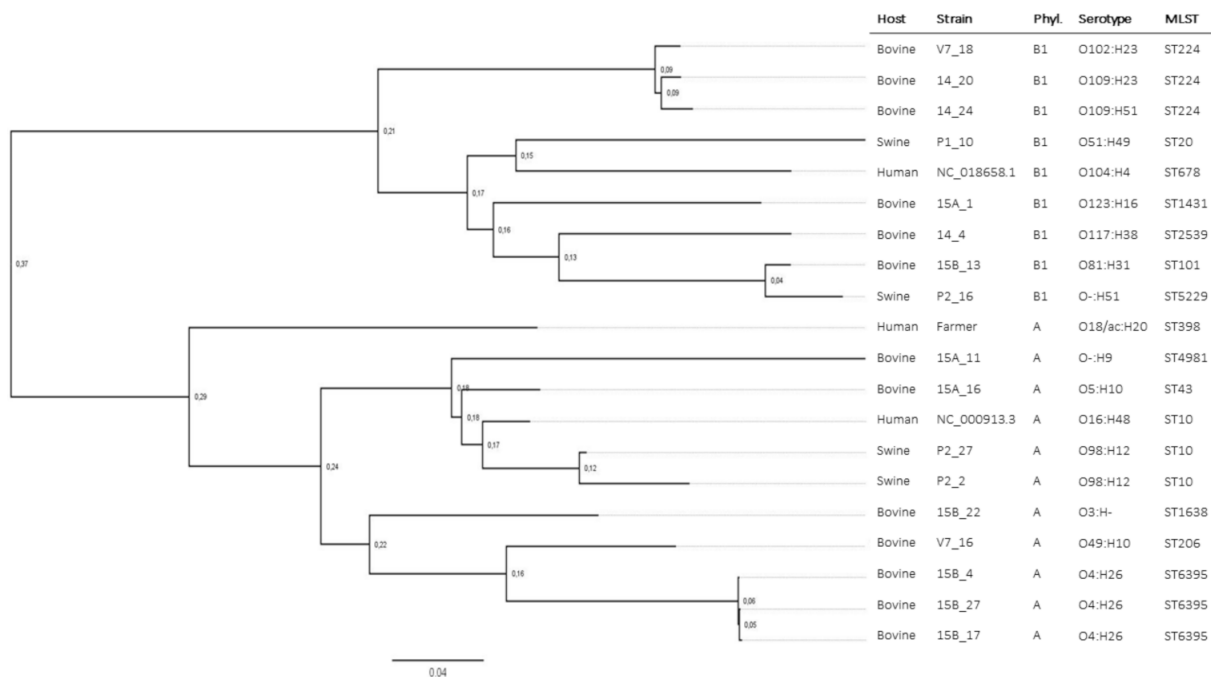


Figure 1. Chromosome phylogeny based on Single Nucleotide Polymorphisms (SNPs) retrieved with CSIPhylogeny and visualized with FigTree. Isolates are clustered according to phylotype and serotype. Two *E. coli* references were included that belonged to different phylotypes: NC_018658.1 for phylotype B1, and NC_000913.3 for phylotype A.

A total of 48 plasmids bearing antimicrobial resistance genes (ARGs) (including those encoding for *mcr-1*) were retrieved after sequencing and assembling: 36 plasmids from the bovine isolates (ranging from one to five per isolate), seven from porcine (from one to two per isolate), and five from the farmer's isolate (Table S3). Several replicons were identified in these plasmids, some of them in the same mobile genetic element, and 19 different replicon combinations (Figure 2). The most prevalent replicon was IncX4 ($n = 14$), which harbored the *mcr-1* gene and was present in isolates from the three hosts considered. Other common replicons were IncFIB ($n = 9$), IncHI2 / IncHI2A combination ($n = 7$), IncFIC ($n = 6$), and replicon combination IncFIB / IncFIC ($n = 6$).

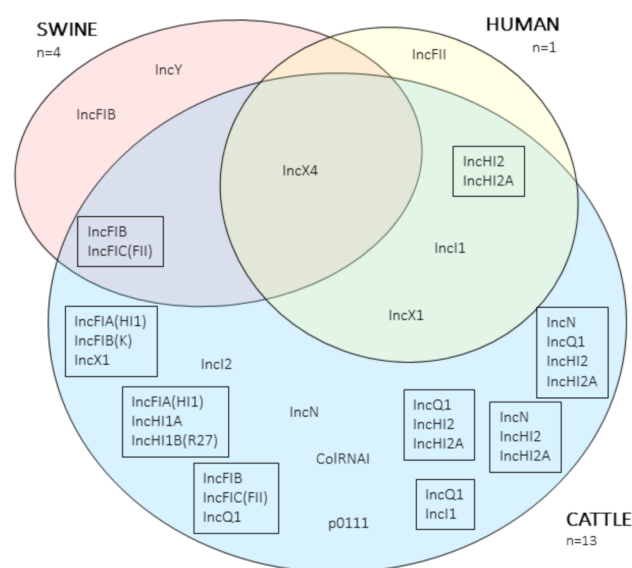


Figure 2. Venn diagram representing the replicons of the antimicrobial resistance gene (ARGs) plasmids. Replicons inside a box indicate a combination of replicons within the same plasmid.

2.2. Antibiotic Resistance Genes

A total number of 85 ARGs were identified using Abricate with CARD (Table S3), encoding resistance to different antibiotic classes; cephalosporins, beta-lactams, aminoglycosides, fluoroquinolones, lincosamides, macrolides, peptides, phenicols, sulfonamides, tetracyclines, and trimethoprim among others. All the isolates were classified as MDR genotypically. Furthermore, all 85 ARG were encountered in isolates of cattle origin, while 63 of them were found in pigs and 53 in the human isolate (Figure 3).

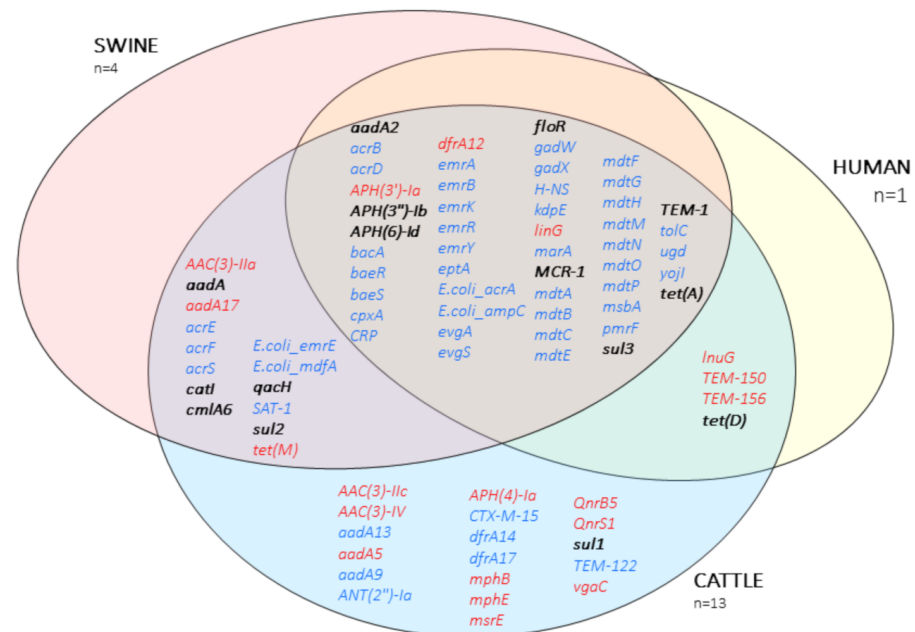


Figure 3. Venn diagram of the antibiotic resistance genes described in this study. Text in blue, chromosomal location; text in red, plasmid location; bold, located either in the chromosome or plasmid.

Regarding the localization of the ARGs, 51 were located exclusively in the chromosome, 19 in plasmids, and 15 either in the chromosome or in plasmids (Figure 3).

After the in-silico analysis, *mcr-1* gene was not found in one isolate of calf origin (15A_11), even though it had tested positive by PCR. This isolate contained the *bla*_{CTX-M-15} gene located in the chromosome. Upstream CTX-M-15 was a complete IS3 element and Δ *tnpA* from the ISEcp1 element, while downstream, there was Δ *tnpA* from the Tn2 element.

2.3. Genetic Context of *mcr-1*

Of the 17 isolates in which the *mcr-1* gene was identified by WGS, 15 carried the *mcr*-genes in plasmids (14 IncX4, one IncHI2, and one IncI2). Isolate 15B_22 contained two copies of the gene in two different plasmids, IncX4 and IncHI2 / IncHI2A. The remaining two isolates harboured the gene inserted in the chromosome (15B_13 and P2_16).

Four different environments for the *mcr-1* gene were found within these isolates (Table 1). All of these constructs have been previously described in other studies [16]. The main IncX4-plasmid backbone was present in all IncX4 plasmids (Figure 4 and Figure S1 and Figure S2). The IncX4 plasmid from the farmer shared the highest identity and coverage with their counterparts from calves (99.97% and 99%, respectively, Table 2). While 13 of the 14 IncX4 plasmids were approximately 33–35 kbp and had a GC content around 42%, the IncX4 plasmid from isolate P1_10 was larger (45,441 bp), and with higher GC content (44.1%). The latest harbored the *tetM* gene conferring resistance to tetracycline. Two IS26 elements were flanking this extra-region of approximately 12,000 bp. All IncX4 plasmids carried the type IV secretion system (T4SS), allowing the plasmid to be self-transmissible, and the HicAB toxin-antitoxin system for plasmid maintenance and stability.

Table 1. Location and genomic context of *mcr-1* gene. *mcr-1* gene was found in 17 out of the 18 colistin resistant *E. coli* isolates either in a plasmid (14 in IncX4, one in IncI2, and one in IncHI2 replicons), or the chromosome. Isolate 15B_22 contained two plasmids with *mcr-1* gene (IncX4 and IncHI2). No correlation between phylotypes and specific genomic context were described. Phyl., phylotype; loc., location; Pl., plasmid; Chr., chromosome.

Host	Isolate	Phyl.	MLST	<i>mcr-1</i>	<i>mcr-1</i> loc.	Pl. GC%	Pl. Size (bp)	<i>mcr-1</i> Genomic Context
Human	Farmer	A	ST398	yes	IncX4	41.9	33,270	<i>mcr-1-pap2</i>
Swine	P2_16	B1	ST5229	Yes	Chr.	-	-	<i>mcr-1-pap2</i>
	P1_10	B1	ST20	yes	IncX4	44.1	45,441	<i>mcr-1-pap2</i>
	P2_2	A	ST10	yes	IncX4	42.5	35,296	<i>mcr-1-pap2-ΔISAp11</i>
Bovine	P2_27	A	ST10	yes	IncX4	42.5	35,326	<i>mcr-1-pap2-ΔISAp11</i>
	15B_27	A	ST6395	yes	IncX4	42.2	34,706	<i>mcr-1-pap2-ΔISAp11</i>
	15B_17	A	ST6395	yes	IncX4	42.2	34,758	<i>mcr-1-pap2-ΔISAp11</i>
	15B_4	A	ST6395	yes	IncX4	41.8	33,577	<i>mcr-1-pap2-ΔISAp11</i>
	14_24	B1	ST224	yes	IncX4	41.8	33,557	<i>mcr-1-pap2-ΔISAp11</i>
	V7_16	A	ST206	yes	IncX4	42.2	34,618	<i>mcr-1-pap2-ΔISAp11</i>
	15A_16	A	ST43	yes	IncX4	41.8	33,242	<i>mcr-1-pap2</i>
	14_20	B1	ST224	yes	IncX4	41.8	33,283	<i>mcr-1-pap2</i>
	14_4	B1	ST2539	yes	IncX4	41.8	33,262	<i>mcr-1-pap2</i>
	V7_18	B1	ST224	yes	IncX4	41.9	33,268	<i>mcr-1-pap2</i>
	15B_22	A	ST1638	yes	IncX4	41.9	33,268	<i>mcr-1-pap2</i>
	15B_22	A	ST1638	yes	IncHI2	45.4	234,156	ISAp11- <i>mcr-1-pap2</i>
	15A_1	A	ST1431	yes	IncI2	42.5	61,766	ISAp11- <i>mcr-1-pap2</i>
15B_13	B1	ST101	Yes	Chr.	-	-	ISAp11- <i>mcr-1-pap2</i> -ISAp11	
15A_11	B1	ST4981	no	-	-	-	-	

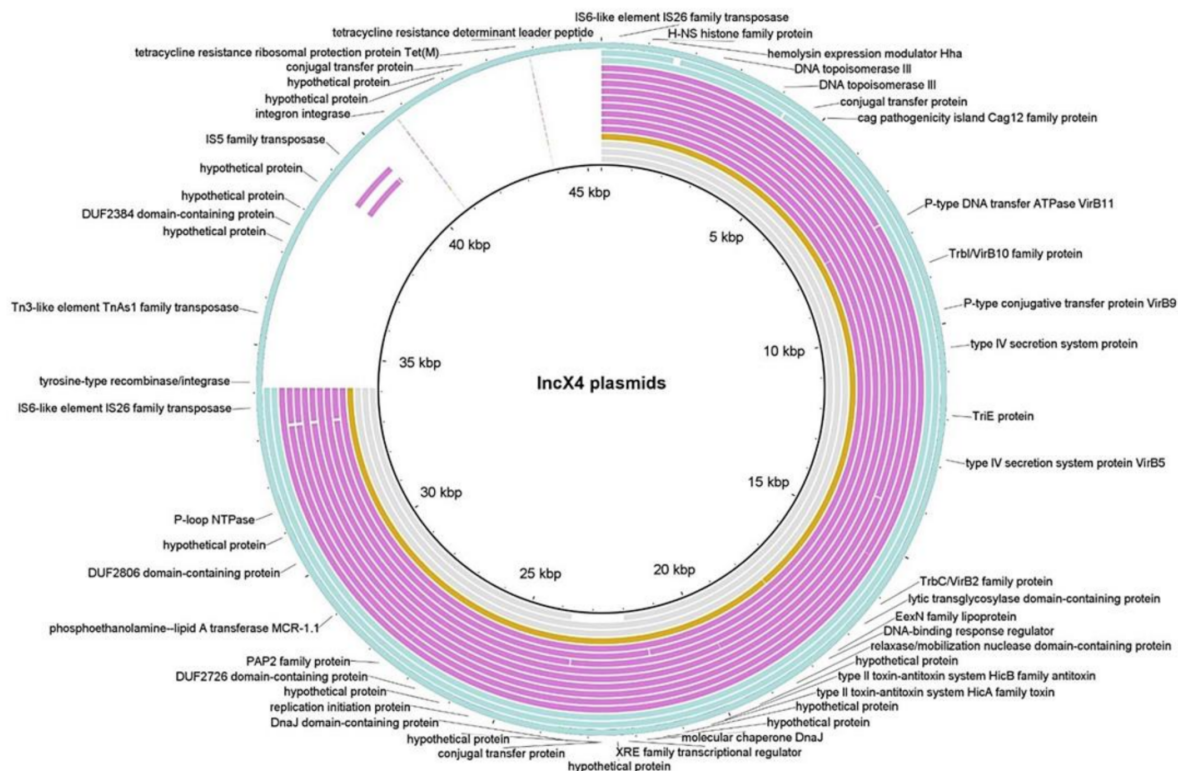


Figure 4. BLAST Ring Image Generator (BRIG) visualization of the 14 IncX4 plasmids from this study and three IncX4 plasmids from NCBI: pEC11b, pMCR1-NJ-IncX4, and pP744T-MCR1. Rings from outside to inside: P1_10, P2_2, P2_27 (blue); V7_18, V7_16, 15B_4, 15B_27, 15B_22, 15B_17, 15A_16, 14_4, 14_24, 14_20 (pink); farmer (orange); pP744T-MCR1, pMCR1-NJ-IncX4, pEC11b (grey). IncX4 plasmid from P1_10 is shown as the reference (longest sequence), with an extra-region of approximately 12,000 bp that is flanked by two IS26 elements and harbors the *tetM* gene conferring resistance to tetracycline. Isolates 15B_27 and 15_17 presented IS5 transposase, as P1_10 (pink fragments near 40 kb location for P1_10).

Table 2. Coverage and identity comparison of the farmer's *mcr-1*-IncX4 plasmid versus livestock IncX4 plasmids.

Isolate ID	Coverage (%)	Identity (%)
P1_10	74	99.99
P2_2	94	99.87
P2_27	94	100
V7_16	95	99.97
15B_17	95	99.99
15B_27	95	100
15B_4	98	99.97
14_24	98	99.99
14_4	99	99.96
V7_18	99	99.96
15A_16	99	99.97
14_20	99	99.97
15B_22	99	99.97

IncI2 and IncHI2 plasmids presented a size of 61,766 bp and 234,156 bp, respectively (File S1 and File S2, respectively). Both plasmids contained the conjugative mechanism T4SS and the replication machinery. While IncHI2 yielded HipA toxin-antitoxin system, IncI2 plasmid harbored RelE/ParE, Hok, and HicAB toxin-antitoxin systems. Finally, the IncHI2 plasmid contained *mcr-1* together with six other AMR genes; *aadA2*, *aph(3')-Ib*, *aph(6)-Id*, *dfrA12*, *floR*, and *tetM*.

2.4. Virulence Factors

A total of 33 virulence factors were detected (Table S3). While nine genes were found exclusively in plasmids, 18 were located in the chromosome. The remaining six virulence genes were found in both locations, chromosome and plasmids. In general, *E. coli* from cattle origin contained the highest amount of virulence genes (27) (Figure 5), followed by swine (18) and the isolate from the farmer (5).

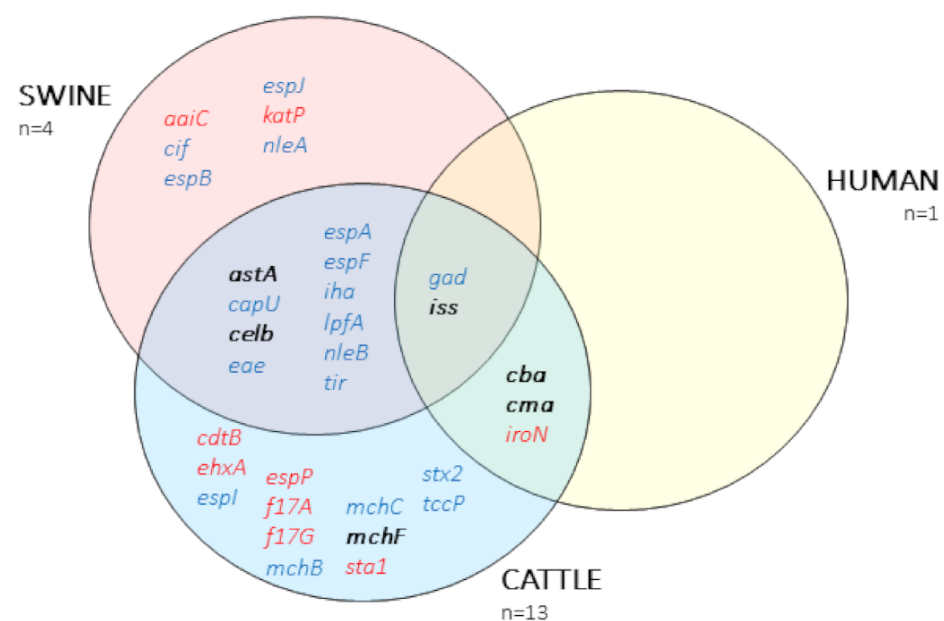


Figure 5. Venn diagram representing the virulence factors described by VirulenceFinder. Text in blue, chromosomal location; text in red, plasmid location; bold, located either in the chromosome or plasmid.

A total of 13 plasmids of mainly two replicon families, IncF ($n = 11$) and Col ($n = 2$) harbored these virulence genes (IncF-plasmids information in Table S4).

Some of these virulence factors conferred different pathotypes, such as adherence factors *eae* (intimin), *tir* (translocated intimin receptor), *f17A* (major F17 fimbriae subunit), *f17G* (adherence F17 fimbriae subunit); enzymes *katP* (plasmid-encoded catalase peroxidase), *ehxA* (enterohemolysin), *espP* (plasmid-encoded extracellular serine protease); secretion-related genes *espA* (type III secreted effector, needle sheath), *espB* (type III secreted effector, translocation pore), *nleA* (non-LEE encoded effector A), *nleB* (non-LEE encoded effector B); toxins *astA* (enteroaggregative heat-stable toxin, EAST-1), *sta1* (heat-stable enterotoxin ST-1a), *cdtB* (cytotolethal distending toxin subunit B), and *stx2* (Shiga toxin).

Isolate 15B_13 of calf origin (phylogroup B1, serotype O81:H31, ST101) harbored the *mcr-1* gene in the chromosome and contained *stx2* (*stx2A* and *stx2B* subunits) encoding for Shiga toxin. A complete phage D108 was found spanning a region of 86.6 Kbp that harbored the *stx2* gene. Additionally, this isolate also contained several virulence factors; *iha*, *lpfA*, *gad*, *iss*, *astA*, *cba*, *celb*, *mchB*, *mchC*, and *mchF*.

3. Discussion

The aim of this study was to conduct a cross-sectional thorough sampling of a farm where co-occurrence of *mcr-1-mcr-3 E. coli* was previously detected, and evaluate the transmission of colistin resistance plasmids within the farm applying WGS. Our approach using long-reads to assemble, and short reads to polish (hybrid assembly), allowed to close chromosomes and circular plasmids harboring *mcr-1* genes, and to study their location and genomic context among different *E. coli* lineages.

mcr-1 positive *E. coli* were detected in all host species present in the facilities, including one human (the farmer). According to the farm book, pigs and calves sampled in 2017 were orally treated with colistin. Going back through the farm book, batches of both pigs and calves reared between 2015 and 2017 were consistently prescribed colistin in the same phases of their production cycle. This management practice in terms of medication regime suggests a routine use of colistin in consecutive batches, facilitating the persistence of colistin resistance mechanisms. Additionally, phenotypic and genotypic resistance to other families of antimicrobials widely used in the farm were also detected, such as β -lactams, tetracycline, aminoglycosides, and sulfonamides.

In agreement with previous studies [14,17–22], the 15 isolates bearing *mcr-1* in mobile genetic elements were associated with IncX4, IncI2, and IncHI2 plasmids, with IncX4 being the most prevalent. All IncX4 plasmids shared the same backbone, and differences were due to inserted sequences. In the case of isolate P1_10, this insertion expanded 12 kbp and comprised the *tetM* gene. Additionally, isolate 15B_22, presented two plasmids encoding for *mcr-1* [18–20] with IncHI2 plasmid carrying also resistance genes for tetracycline (*tetM*), trimethoprim (*dfrA12*), aminoglycosides (*aph(3'')-Ib*, *aph(6)-Id*) and florfenicol (*floR*), as well as colistin (*mcr-1*). Different families of ARGs located in the same plasmid facilitated the persistence and selection of resistance to antibiotics not used in the farm. Even if colistin was withdrawn (as it happened after our visit to the farm), the use of doxycycline could co-select indirectly for the *mcr-1* gene.

As previously described [17,19,21–23], herein, *mcr-1* was also integrated into the genome in two isolates of different animal origins. In one of them, the *ISAp11* element was flanking *mcr-1* upstream and downstream, a structure that probably facilitated the movement of the whole element by transposition. The other isolate had lost the *ISAp11* element, establishing the *mcr-1* as a heritable trait overcoming any possible fitness cost of plasmid maintenance [24]. Furthermore, this isolate had become permanently resistant even when the selective pressure was removed [17,25].

Although phylogenetic analysis clustered the *E. coli* isolates in phylogroup A and B1, there were different MLST lineages harboring the colistin resistance genes in highly similar plasmids (identity ranging from 99.96% to 100%). The farmer's isolate (ST398) did not match the MLST type of any of the livestock isolates. Interestingly, ST398 was the only

ST shared between livestock and bloodstream infections in a study carried out across the United Kingdom, underlying the zoonotic potential of some *E. coli* lineages [26]. Conversely, the IncX4 plasmid from the farmer's isolate was highly similar to those obtained from calves (14-4, 14-20, 15A-16, 15B-22, and V7_18), sharing length, GC content, and genomic context (*mcr-1-pap2*). These results suggest the transmission of resistance through mobile genetic elements between different *E. coli* lineages from livestock to the farmer. Several studies have demonstrated the spread of ARGs from food-producing animals to veterinarians and personnel in direct contact with animals [27–29], highlighting the importance of implementing hygiene measures to reduce this transmission. Even though our approach was focused on detecting the presence or absence of *mcr-1-mcr-3* genes by picking a unique colony per sample, further studies including within-host diversity of *mcr-1 E. coli* isolates should be performed to introduce the variability of the *E. coli* population within a sample.

All the isolates from this study exhibited a MDR profile. In addition, ARGs, as well as virulence factors, were described both in the chromosome and plasmids. *E. coli* isolates of cattle origin showed the highest number and diversity of plasmids encoding for both ARGs and virulence genes, including *stx2*. Shiga toxin *E. coli* (STEC) serotype O81:H31 bearing *stx2* have also been described previously [30] and are considered important foodborne zoonotic pathogens [30–33]. To our knowledge, this is the first description of a *mcr-1* positive STEC of cattle origin and highlights the importance of food producing animals as reservoirs of ARG and virulence determinants.

On the contrary, isolate 15A_11 resulted negative for the *mcr-1* gene after in silico analysis, even though previous PCR tested positive for this gene. Presumably, the isolate lost the *mcr-1* plasmid during sub-culturing steps, resulting in a false-negative result. Besides, 15A_11 isolate (phylogroup A, ST4981) was resistant to cephalosporins (cefotaxime and ceftazidime) with *bla_{CTX-M-15}* inserted in the chromosome. Interestingly, upstream of the gene, there was an IS3 element, and downstream there was a truncated Tn2, indicating a possible recombination event, as has been previously described [34,35]. The acquisition of *bla_{CTX-M-15}* in livestock is concerning, since it is widely disseminated [36–38], especially in healthcare facilities [38–41], and can compromise the treatment of Gram-negative infections.

Regarding the analyses of the sequencing data, it is important to be aware of the limitation of databases to obtain the most accurate results. On the basis of an example from this study, cytotoxin-producing toxin (CDT) is composed of three subunits (encoded by three genes, *cdtA*, *cdtB*, and *cdtC*), which are all required for bonding to the cell's surface and for entering the cell. However, VirulenceFinder only found the *cdtB* gene, while *cdtA* and *cdtC* were also present when aligning the sequence with the reference genome from NCBI. In depth analysis of the sequencing data should consider if a virulence element is composed of different genes to be fully operative.

4. Materials and Methods

4.1. Study Design

After the identification in 2017 of an *E. coli* isolate of bovine origin harboring both *mcr-1* and *mcr-3*, the farm from where the sample was obtained was contacted by the Spanish Official Veterinary Services to follow up on the finding. This farm belonged to a private farmer and contained two separate areas. The first area was a farrow-to-finish system for pig production. At not more than a 100-m distance, and without a physical barrier, there was a multi-origin bovine fattening farm, also the property of the farmer.

The number of samples to be collected in each of the housing facilities (three housing facilities for bovine and one for swine) was calculated to allow for the detection of a prevalence of *mcr-1-mcr-3 E. coli* of at least 5%, with a 95% confidence level. Sample size calculations were carried out using the WinEpi tool (<http://www.winepi.net/uk/index.htm>, accessed on 1 March 2021). Additionally, the farmer was interviewed by the Official Veterinary Services, and the farm's treatment book was inspected to determine the antimicrobial treatments prescribed to the two animal species from 2015 to the time of sampling.

A total number of 210 fecal samples were collected: 152 from calves ($n = 501$), 57 from fattening pigs ($n = 900$), and one from the farmer ($n = 3$). Fecal samples were taken from individual animals and transported to the laboratory at 4° C on the day of sampling. The farmer sent a refrigerated fecal sample by courier within 24 h of the visit to the farm. Faces were homogenized and plated onto both MacConkey agar and MacConkey agar supplemented with colistin (2mg/L). For quality control of the colistin plates, a positive and negative control were also included. Following incubation, one presumptive colistin resistant *E. coli* isolate per positive sample was identified by PCR [42] and stored at −80 °C for further analyses. Detection of the five *mcr* genes (*mcr-1* to *mcr-5*) described at the time of sampling was performed by multiplex PCR, as described by Rebelo et al., [43].

4.2. Antimicrobial Susceptibility Testing

Minimal inhibitory concentration (MIC) was carried out for 14 antimicrobial agents (VetMIC GN-mo, Swedish National Veterinary Institute) in those isolates harboring *mcr*-genes. Antimicrobials tested were ampicillin (1 to 128 mg/L), cefotaxime (0.016 to 2 mg/L), ceftazidime (0.25 to 16 mg/L), nalidixic acid (1 to 128 mg/L), ciprofloxacin (0.008 to 1 mg/L), gentamicin (0.12 to 16 mg/L), streptomycin (2 to 256 mg/L), kanamycin (8 to 16 mg/L), chloramphenicol (2 to 64 mg/L), florfenicol (4 to 32 mg/L), trimethoprim (1 to 128 mg/L), sulfamethoxazole (8 to 1,024 mg/L), tetracycline (1 to 128 mg/L), and colistin (0.5 to 4 mg/L). Epidemiological cut-off values were those recommended by the European Committee on Antimicrobial Susceptibility Testing (EUCAST). MDR isolates were defined as resistance to at least three different antimicrobial families [44].

4.3. Whole Genome Sequencing and Data Analysis

DNA from *mcr*-positive isolates was extracted using QIAGEN DNeasy® Ultraclean Microbial Kit under manufacturer's conditions. Illumina (San Diego, CA, USA) libraries were prepared by enzymatic fragmentation and double indexing using an NGSgo kit (GenDx, Utrecht, Netherlands), according to the manufacturer's instructions. The indexed libraries were pooled, denatured, and diluted to a final concentration of 4 nM. The pooled library was sequenced on the MiSeq system (Illumina) with a 300-cycle MiSeq reagent kit v2. Illumina paired-end reads were merged into one unique file per isolate using a custom python script (<https://github.com/isovic/racon/issues/68>, accessed on 1 March 2021).

In parallel, DNA was quantified using Qubit dsDNA BR assay (Invitrogen by ThermoFisher Scientific), and sequenced using MinION sequencer (Oxford Nanopore Technologies, ONT, Oxford, UK) in two runs of 9 samples each. Two sequencing libraries were prepared using 400 ng DNA per sample with the Rapid Barcoding Kit (SQK-RBK004, ONT, Oxford, UK) according to the manufacturer's instructions. The samples were run using MinKNOW software (version 18.07.18). Fast5 files generated were basecalled and demultiplexed using Albacore v2.3. Reads classified as pass (minimum Phred score of 7) were used for further steps. A second round of demultiplexing was performed with Porechop [45], which also assisted to trim barcodes, chimeric reads, and sequencing adapters.

Nanopore fastQ files were used to perform the assembly of genomes and plasmids from the 18 isolates with Flye [46] (v2.6), specifying flags “-nano-raw”, and “-plasmids” to retrieve smaller contigs, such as plasmids. Once the assembly was finished, raw ONT reads were mapped to the contigs using minimap2 (v2.17) [47]. A first round of polishing using Racon [48] (v1.4.10) with ONT reads was performed, followed by two rounds of polishing with Medaka (v0.11.4), using the “medaka_consensus” option. A final round of polishing was performed using Illumina reads. First, Illumina reads were mapped to the ONT-polished contigs using Minimap2 (v2.17) and then a round of Racon (v1.4.10) was performed. The files obtained from this polishing step were the final assemblies and were used for the further analyses.

In order to characterize the presence of plasmid replicons, antibiotic resistance genes (ARGs) and virulence factors, Abricate [49] (v0.8.13) along with PlasmidFinder [50], CARD [51] and VFDB [52] (respectively) were applied, with a minimum identity and

coverage of 90%. Insertion sequences, phage presence, and presence of conjugative elements were analyzed using ISFinder [53], PHASTER [54], and OriTFinder [55], respectively. Gene annotation was performed with NCBI Prokaryotic Genome Annotation Pipeline (PGAP) [56] and Prokka [57] (v1.14.16). BUSCO [58] (v4.0.1) was used to assess genome completeness with the *Enterobacteriaceae* database (OrthoDb v10.1). SerotypeFinder [59], MLST [60], CSIPhylogeny [61] to call SNPs and ClermonTyping [62] were also applied.

Contigs were visualized with Bandage [63]. Plasmid annotation was visualized with BLAST Ring Image Generator [64] (BRIG) and SnapGene Viewer (v5.0.7). Finally, phylogeny was visualized with FigTree (v1.4.3) (<http://tree.bio.ed.ac.uk/software/figtree/>, accessed on 1 March 2021).

5. Conclusions

In conclusion, co-existence of *mcr-1-mcr-3* in *E. coli* from the farm could not be confirmed. Nevertheless, we isolated *mcr-1* across the farm in different *E. coli* lineages, mainly associated with plasmids of the IncX4, IncHI and IncHI2 families. The most likely mechanism for the farmer to have acquired the *mcr-1* gene was the horizontal gene transfer from the calves, since plasmids from both origins were highly similar. Additionally, *mcr-1* positive *E. coli* isolates were MDR and contained a high number of virulence genes, including *stx2*, demonstrating that food-producing animals can be a reservoir of such determinants, posing a risk for human health, especially for personnel at the farm.

Supplementary Materials: The following are available online at <https://www.mdpi.com/2079-6382/10/3/313/s1>, Figure S1: Prokaryotic Genome Annotation Pipeline (PGAP) annotation of the IncX4 plasmid from the Farmer visualized with SnapGene Viewer; Figure S2: Prokaryotic Genome Annotation Pipeline (PGAP) annotation of the IncX4 plasmid from P2_2 visualized with SnapGene Viewer. Table S1: Minimal inhibitory concentration ($\mu\text{g}/\text{mL}$) for the 14 antibiotics tested. R, resistant; WT, wild type; Table S2: Chromosomal assembly and in-silico analyses of the colistin resistant *E. coli* isolates; Table S3: Antibiotic Resistance Genes (ARGs) and Virulence Factors (VFs) described by Abricate and CARD database; Table S4: IncF-family plasmids harboring virulence factors (VF) and antibiotic resistance genes (ARGs); File 1: GBK file with the annotation of the IncI2 plasmid harbouring *mcr-1* gene from 15A_1.; File 2: GBK file with the annotation of the IncHI2 plasmid harbouring *mcr-1* gene from 15B_22.

Author Contributions: Conceptualization, L.M.-G., S.N., J.L.S.-L. and M.R.-R.; formal analysis, J.V., L.M.-G., A.C. and O.F.; data curation, J.V., L.M.-G., A.C. and O.F.; writing—original draft preparation, J.V. and L.M.-G.; writing—review and editing, J.V., L.M.-G., A.C., O.F., S.N., J.L.S.-L., M.R.-R. and J.A.; supervision, L.M.-G., A.C. and O.F.; funding acquisition, L.M.-G. and O.F. All authors have read and agreed to the published version of the manuscript.

Funding: This work was partially supported by the grant RTI2018-095586-B-C22 from the Ministerio de Economía y Competitividad (Gobierno de España), by the CERCA program from Generalitat de Catalunya, and by the Generalitat de Catalunya Industrial Doctorate Program grant 2017DI037.

Institutional Review Board Statement: Sampling was done under institutional authorization and followed good veterinary practices. According to European (Directive 2010/63/EU of the European Parliament and of the Council of 22 September 2010 on the protection of animals used for scientific purposes) and Spanish (Real Decreto 53/2013) normative. This procedure did not require specific approval by an Ethical Committee. Faecal sampling is not likely to cause pain, suffering, distress, or lasting harm equivalent to, or higher than, that caused by the introduction of a needle in accordance with good veterinary practice (Chapter I, Article 1, 5 (f) of 2010/63/EU). All experiments were performed in accordance with relevant guidelines and regulations.

Informed Consent Statement: Informed consent was obtained from all subjects involved in the study.

Data Availability Statement: Nanopore and Illumina fast Q files, genomes and plasmids sequences, and supplementary material that support the findings of this study are openly available in OSFHome at <http://doi.org/10.17605/OSF.IO/7Q2CB>, reference number 7Q2CB.

Acknowledgments: We are grateful to Patricia Pleguezuelos and Judith Gonzalez for their technical assistance.

Conflicts of Interest: The authors declare no conflict of interest.

References

- Koyama, Y.; Kurosasa, A.; Tsuchiya, A.; Takakuta, K. A new antibiotic “colistin” produced by spore-forming soil bacteria. *J. Antibiot.* **1950**, *3*, 457–458.
- Catry, B.; Cavaleri, M.; Baptiste, K.; Grave, K.; Grein, K.; Holm, A.; Jukes, H.; Liebana, E.; Navas, A.L.; Mackay, D.; et al. Use of colistin-containing products within the European Union and European Economic Area (EU/EEA): Development of resistance in animals and possible impact on human and animal health. *Int. J. Antimicrob. Agents* **2015**, *46*, 297–306. [[CrossRef](#)] [[PubMed](#)]
- Moreno, M.A. Survey of quantitative antimicrobial consumption per production stage in farrow-to-finish pig farms in Spain. *Vet. Rec. Open* **2014**, *1*, e000002. [[CrossRef](#)] [[PubMed](#)]
- Van Rennings, L.; von Münchhausen, C.; Otilie, H.; Hartmann, M.; Merle, R.; Honscha, W.; Käsbohrer, A.; Kreienbrock, L. Cross-Sectional Study on Antibiotic Usage in Pigs in Germany. *PLoS ONE* **2015**, *10*, e0119114. [[CrossRef](#)]
- Sjölund, M.; Backhans, A.; Greko, C.; Emanuelson, U.; Lindberg, A. Antimicrobial usage in 60 Swedish farrow-to-finish pig herds. *Prev. Vet. Med.* **2015**, *121*, 257–264. [[CrossRef](#)] [[PubMed](#)]
- Callens, B.; Persoons, D.; Maes, D.; Laanen, M.; Postma, M.; Boyen, F.; Haesebrouck, F.; Butaye, P.; Catry, B.; Dewulf, J. Prophylactic and metaphylactic antimicrobial use in Belgian fattening pig herds. *Prev. Vet. Med.* **2012**, *106*, 53–62. [[CrossRef](#)] [[PubMed](#)]
- European Medicines Agency. *European Medicines Agency Sales of Veterinary Antimicrobial Agents in 29 European Countries in 2014*; European Medicines Agency: London, UK, 2014.
- Informe JIACRA España. Primer Análisis Integrado del Consumo de Antibióticos y su Relación con la Aparición de Resistencia. 2018. Available online: https://resistenciaantibioticos.es/es/system/files/field/files/informe_jiacra-espana.pdf?file=1&type=node&id=410&force=0 (accessed on 17 March 2021).
- Liu, Y.-Y.; Wang, Y.; Walsh, T.R.; Yi, L.-X.; Zhang, R.; Spencer, J.; Doi, Y.; Tian, G.; Dong, B.; Huang, X.; et al. Emergence of plasmid-mediated colistin resistance mechanism MCR-1 in animals and human beings in China: A microbiological and molecular biological study. *Lancet Infect. Dis.* **2016**, *16*, 161–168. [[CrossRef](#)]
- Xavier, B.B.; Lammens, C.; Ruhel, R.; Kumar-Singh, S.; Butaye, P.; Goossens, H.; Malhotra-Kumar, S. Identification of a novel plasmid-mediated colistin-resistance gene, mcr-2, in *Escherichia coli*, Belgium, June 2016. *Euro Surveill.* **2016**, *21*, 30280. [[CrossRef](#)]
- Yin, W.; Li, H.; Shen, Y.; Liu, Z.; Wang, S.; Shen, Z.; Zhang, R.; Walsh, T.R.; Shen, J.; Wang, Y. Novel Plasmid-Mediated Colistin Resistance Gene mcr-3 in *Escherichia coli*. *MBio* **2017**, *8*. [[CrossRef](#)]
- Borowiak, M.; Fischer, J.; Hammerl, J.A.; Hendriksen, R.S.; Szabo, I.; Malorny, B. Identification of a novel transposon-associated phosphoethanolamine transferase gene, mcr-5, conferring colistin resistance in d-tartrate fermenting *Salmonella enterica* subsp. *enterica* serovar Paratyphi B. *J. Antimicrob. Chemother.* **2017**, *72*, 3317–3324. [[CrossRef](#)]
- Carattoli, A.; Villa, L.; Feudi, C.; Curcio, L.; Orsini, S.; Luppi, A.; Pezzotti, G.; Magistrali, C.F. Novel plasmid-mediated colistin resistance mcr-4 gene in *Salmonella* and *Escherichia coli*, Italy 2013, Spain and Belgium, 2015 to 2016. *Euro Surveill.* **2017**, *22*, 30589. [[CrossRef](#)]
- Wang, R.; van Dorp, L.; Shaw, L.P.; Bradley, P.; Wang, Q.; Wang, X.; Jin, L.; Zhang, Q.; Liu, Y.; Rieux, A.; et al. The global distribution and spread of the mobilized colistin resistance gene mcr-1. *Nat. Commun.* **2018**, *9*, 1179. [[CrossRef](#)]
- Hernández, M.; Iglesias, M.R.; Rodríguez-Lázaro, D.; Gallardo, A.; Quijada, N.; Miguela-Villoldo, P.; Campos, M.J.; Píriz, S.; López-Orozco, G.; de Frutos, C.; et al. Co-occurrence of colistin-resistance genes mcr-1 and mcr-3 among multidrug-resistant *Escherichia coli* isolated from cattle, Spain, September 2015. *Euro Surveill.* **2017**, *22*, 30586. [[CrossRef](#)] [[PubMed](#)]
- Partridge, S.R.; Kwong, S.M.; Firth, N.; Jensen, S.O. Mobile genetic elements associated with antimicrobial resistance. *Clin. Microbiol. Rev.* **2018**, *31*. [[CrossRef](#)]
- Bai, F.; Li, X.; Niu, B.; Zhang, Z.; Malakar, P.K.; Liu, H.; Pan, Y.; Zhao, Y. A mcr-1-Carrying Conjugative IncX4 Plasmid in Colistin-Resistant *Escherichia coli* ST278 Strain Isolated from Dairy Cow Feces in Shanghai, China. *Front. Microbiol.* **2018**, *9*, 1–9. [[CrossRef](#)]
- Zurfluh, K.; Nüesch-Inderbilen, M.; Klumpp, J.; Poirel, L.; Nordmann, P.; Stephan, R. Key features of mcr-1-bearing plasmids from *Escherichia coli* isolated from humans and food. *Antimicrob. Resist. Infect. Control* **2017**, *6*, 1–6. [[CrossRef](#)]
- Wu, R.; Yi, L.X.; Yu, L.F.; Wang, J.; Liu, Y.; Chen, X.; Lv, L.; Yang, J.; Liu, J.H. Fitness advantage of mcr-1-bearing IncI2 and IncX4 plasmids in vitro. *Front. Microbiol.* **2018**, *9*. [[CrossRef](#)] [[PubMed](#)]
- Li, R.; Xie, M.; Zhang, J.; Yang, Z.; Liu, L.; Liu, X.; Zheng, Z.; Chan, E.W.C.; Chen, S. Genetic characterization of mcr-1-bearing plasmids to depict molecular mechanisms underlying dissemination of the colistin resistance determinant. *J. Antimicrob. Chemother.* **2017**, *72*, 393–401. [[CrossRef](#)] [[PubMed](#)]
- Sun, J.; Fang, L.X.; Wu, Z.; Deng, H.; Yang, R.S.; Li, X.P.; Li, S.M.; Liao, X.P.; Feng, Y.; Liu, Y.H. Genetic Analysis of the IncX4 Plasmids: Implications for a Unique Pattern in the mcr-1 Acquisition. *Sci. Rep.* **2017**, *7*, 424. [[CrossRef](#)] [[PubMed](#)]
- Li, B.; Ke, B.; Zhao, X.; Guo, Y.; Wang, W.; Wang, X.; Zhu, H. Antimicrobial resistance profile of mcr-1 positive clinical isolates of *Escherichia coli* in China from 2013 to 2016. *Front. Microbiol.* **2018**, *9*, 1–10. [[CrossRef](#)]
- Shen, Y.; Wu, Z.; Wang, Y.; Zhang, R.; Zhou, H.W.; Wang, S.; Lei, L.; Li, M.; Cai, J.; Tyrrell, J.; et al. Heterogeneous and flexible transmission of mcr-1 in hospital-associated *Escherichia coli*. *MBio* **2018**, *9*. [[CrossRef](#)]
- Dunn, S.J.; Connor, C.; McNally, A. The evolution and transmission of multi-drug resistant *Escherichia coli* and *Klebsiella pneumoniae*: The complexity of clones and plasmids. *Curr. Opin. Microbiol.* **2019**, *51*, 51–56. [[CrossRef](#)]

25. San Millan, A. Evolution of Plasmid-Mediated Antibiotic Resistance in the Clinical Context. *Trends Microbiol.* **2018**, *26*, 978–985. [[CrossRef](#)]
26. Ludden, C.; Raven, K.E.; Jamrozny, D.; Gouliouris, T.; Blane, B.; Coll, F.; de Goffau, M.; Naydenova, P.; Horner, C.; Hernandez-Garcia, J.; et al. One Health Genomic Surveillance of *Escherichia coli* Demonstrates Distinct Lineages and Mobile Genetic Elements in Isolates from Humans versus Livestock. *MBio* **2019**, *10*. [[CrossRef](#)] [[PubMed](#)]
27. Saliu, E.-M.; Vahjen, W.; Zentek, J. Types and prevalence of extended-spectrum beta-lactamase producing Enterobacteriaceae in poultry. *Anim. Heal. Res. Rev.* **2017**, *18*, 46–57. [[CrossRef](#)] [[PubMed](#)]
28. McDaniel, C.J.; Cardwell, D.M.; Moeller, R.B., Jr.; Gray, G.C. Humans and Cattle: A Review of Bovine Zoonoses. *Vector Borne Zoonotic Dis.* **2014**, *14*, 1. [[CrossRef](#)]
29. Tomley, F.M.; Shirley, M.W. Livestock infectious diseases and zoonoses. *Philos. Trans. R. Soc. Lond. B. Biol. Sci.* **2009**, *364*, 2637–2642. [[CrossRef](#)] [[PubMed](#)]
30. Fan, R.; Shao, K.; Yang, X.; Bai, X.; Fu, S.; Sun, H.; Xu, Y.; Wang, H.; Li, Q.; Hu, B.; et al. High prevalence of non-O157 Shiga toxin-producing *Escherichia coli* in beef cattle detected by combining four selective agars. *BMC Microbiol.* **2019**, *19*, 213. [[CrossRef](#)]
31. Thomas, N.A.; Navarro-Garcia, F.; Jorge Blanco, M.; Robins-Browne, R.M.; Holt, K.E.; Ingle, D.J.; Hocking, D.M.; Yang, J.; Tauschek, M. Are *Escherichia coli* Pathotypes Still Relevant in the Era of Whole-Genome Sequencing? *Front. Cell. Infect. Microbiol.* **2016**, *1*, 141. [[CrossRef](#)]
32. Hussein, H.S.; Bollinger, L.M. Prevalence of Shiga toxin-producing *Escherichia coli* in beef cattle. *J. Food Prot.* **2005**, *68*, 2224–2241. [[CrossRef](#)]
33. Padola, N.L.; Etcheverría, A.I. Shiga toxin-producing *Escherichia coli* in human, cattle, and foods. Strategies for detection and control. *Front. Cell. Infect. Microbiol.* **2014**, *4*, 89. [[CrossRef](#)]
34. Yasui, H.; Kurosawa, Y. Measurement of recombination frequencies between two homologous DNA segments embedded in a YAC vector. *Gene* **1993**, *129*, 135–139. [[CrossRef](#)]
35. Komoda, Y.; Enomoto, M.; Tominaga, A. Large Inversion in *Escherichia coli* K-12 1485IN Between Inversely Oriented IS3 Elements Near lac and cdd. *Genetics* **1991**, *129*, 639–645. [[CrossRef](#)]
36. Cantón, R.; Coque, T.M. The CTX-M β -lactamase pandemic. *Curr. Opin. Microbiol.* **2006**, *9*, 466–475. [[CrossRef](#)]
37. Chong, Y.; Shimoda, S.; Shimono, N. Current epidemiology, genetic evolution and clinical impact of extended-spectrum β -lactamase-producing *Escherichia coli* and *Klebsiella pneumoniae*. *Infect. Genet. Evol.* **2018**, *61*, 185–188. [[CrossRef](#)] [[PubMed](#)]
38. Bevan, E.R.; Jones, A.M.; Hawkey, P.M. Global epidemiology of CTX-M β -lactamases: Temporal and geographical shifts in genotype. *J. Antimicrob. Chemother.* **2017**, *72*, 2145–2155. [[CrossRef](#)] [[PubMed](#)]
39. Boyd, D.A.; Tyler, S.; Christianson, S.; Mcgeer, A.; Muller, M.P.; Willey, B.M.; Bryce, E.; Gardam, M.; Nordmann, P.; Mulvey, M.R.; et al. Complete Nucleotide Sequence of a 92-Kilobase Plasmid Harboring the CTX-M-15 Extended-Spectrum Beta-Lactamase Involved in an Outbreak in Long-Term-Care Facilities in Toronto, Canada. *Antimicrob. Agents Chemother.* **2004**, *48*, 3758–3764. [[CrossRef](#)]
40. Yasir, M.; Farman, M.; Shah, M.W.; Jiman-Fatani, A.A.; Othman, N.A.; Almasaudi, S.B.; Alawi, M.; Shakil, S.; Al-Abdullah, N.; Ismaeel, N.A.; et al. Genomic and antimicrobial resistance genes diversity in multidrug-resistant CTX-M-positive isolates of *Escherichia coli* at a health care facility in Jeddah. *J. Infect. Public Health* **2020**, *13*, 94–100. [[CrossRef](#)] [[PubMed](#)]
41. Mehrad, B.; Clark, N.M.; Zhanel, G.G.; Lynch, J.P. Antimicrobial resistance in hospital-acquired gram-negative bacterial infections. *Chest* **2015**, *147*, 1413–1421. [[CrossRef](#)] [[PubMed](#)]
42. Heininger, A.; Binder, M.; Schmidt, S.; Unertl, K.; Botzenhart, K.; Döring, G. PCR and blood culture for detection of *Escherichia coli* bacteremia in rats. *J. Clin. Microbiol.* **1999**, *37*, 2479–2482. [[CrossRef](#)] [[PubMed](#)]
43. Rebelo, A.R.; Bortolaia, V.; Kjeldgaard, J.S.; Pedersen, S.K.; Leekitcharoenphon, P.; Hansen, I.M.; Guerra, B.; Malorny, B.; Borowiak, M.; Hammerl, J.A.; et al. Multiplex PCR for detection of plasmid-mediated colistin resistance determinants, mcr-1, mcr-2, mcr-3, mcr-4 and mcr-5 for surveillance purposes. *Euro Surveill.* **2018**, *23*. [[CrossRef](#)]
44. Schwarz, S.; Silley, P.; Simjee, S.; Woodford, N.; van Duijkeren, E.; Johnson, A.P.; Gaastra, W. Assessing the antimicrobial susceptibility of bacteria obtained from animals. *Vet. Microbiol.* **2010**, *141*, 1–4. [[CrossRef](#)] [[PubMed](#)]
45. Porechop. Available online: <https://github.com/rrwick/Porechop> (accessed on 17 March 2021).
46. Kolmogorov, M.; Yuan, J.; Lin, Y.; Pevzner, P.A. Assembly of long, error-prone reads using repeat graphs. *Nat. Biotechnol.* **2019**, *37*, 540–546. [[CrossRef](#)] [[PubMed](#)]
47. Li, H. Minimap2: Pairwise alignment for nucleotide sequences. *Bioinformatics* **2018**, *34*, 3094–3100. [[CrossRef](#)] [[PubMed](#)]
48. Vaser, R.; Sovic, I.; Nagarajan, N.; Sikic, M. Fast and accurate de novo genome assembly from long uncorrected reads. *Genome Res.* **2017**, *27*. [[CrossRef](#)]
49. Abricate. Available online: <https://github.com/tseemann/abricate> (accessed on 17 March 2021).
50. Carattoli, A.; Zankari, E.; García-Fernández, A.; Voldby Larsen, M.; Lund, O.; Villa, L.; Møller Aarestrup, F.; Hasman, H. In Silico Detection and Typing of Plasmids using PlasmidFinder and Plasmid Multilocus Sequence Typing. *Antimicrob. Agents Chemother.* **2014**, *58*, 3895–3903. [[CrossRef](#)]
51. Jia, B.; Raphenya, A.R.; Alcock, B.; Waglechner, N.; Guo, P.; Tsang, K.K.; Lago, B.A.; Dave, B.M.; Pereira, S.; Sharma, A.N.; et al. CARD 2017: Expansion and model-centric curation of the comprehensive antibiotic resistance database. *Nucleic Acids Res.* **2017**, *45*, D566–D573. [[CrossRef](#)]

52. Chen, L.; Zheng, D.; Liu, B.; Yang, J.; Jin, Q. VFDB 2016: Hierarchical and refined dataset for big data analysis—10 years on. *Nucleic Acids Res.* **2016**, *44*, D694–D697. [[CrossRef](#)]
53. Siguier, P.; Perochon, J.; Lestrade, L.; Mahillon, J.; Chandler, M. ISfinder: The reference centre for bacterial insertion sequences. *Nucleic Acids Res.* **2006**, *34*, D32–D36. [[CrossRef](#)] [[PubMed](#)]
54. Arndt, D.; Grant, J.R.; Marcu, A.; Sajed, T.; Pon, A.; Liang, Y.; Wishart, D.S. PHASTER: A better, faster version of the PHAST phage search tool. *Nucleic Acids Res.* **2016**, *44*. [[CrossRef](#)]
55. Li, X.; Xie, Y.; Liu, M.; Tai, C.; Sun, J.; Deng, Z.; Ou, H.-Y. oriTfinder: A web-based tool for the identification of origin of transfers in DNA sequences of bacterial mobile genetic elements. *Nucleic Acids Res.* **2018**, *46*, 229–234. [[CrossRef](#)]
56. Tatusova, T.; DiCuccio, M.; Badretdin, A.; Chetvernin, V.; Nawrocki, E.P.; Zaslavsky, L.; Lomsadze, A.; Pruitt, K.D.; Borodovsky, M.; Ostell, J. NCBI prokaryotic genome annotation pipeline. *Nucleic Acids Res.* **2016**, *44*, 6614–6624. [[CrossRef](#)] [[PubMed](#)]
57. Seemann, T. Prokka: Rapid prokaryotic genome annotation. *Bioinformatics* **2014**, *30*, 2068–2069. [[CrossRef](#)] [[PubMed](#)]
58. Sepey, M.; Manni, M.; Zdobnov, E.M. BUSCO: Assessing Genome Assembly and Annotation Completeness. *Methods Mol. Biol.* **2019**, *1962*, 227–245.
59. Joensen, K.G.; Tetzschner, A.M.M.; Iguchi, A.; Aarestrup, F.M.; Scheutz, F. Rapid and Easy In Silico Serotyping of Escherichia coli Isolates by Use of Whole-Genome Sequencing Data. *J. Clin. Microbiol.* **2015**, *53*, 2410–2426. [[CrossRef](#)] [[PubMed](#)]
60. Larsen, M.V.; Cosentino, S.; Rasmussen, S.; Friis, C.; Hasman, H.; Marvig, R.L.; Jelsbak, L.; Sicheritz-Ponten, T.; Ussery, D.W.; Aarestrup, F.M.; et al. Multilocus Sequence Typing of Total-Genome-Sequenced Bacteria. *J. Clin. Microbiol.* **2012**, *50*, 1355–1361. [[CrossRef](#)]
61. Kaas, R.S.; Leekitcharoenphon, P.; Aarestrup, F.M.; Lund, O. Solving the Problem of Comparing Whole Bacterial Genomes across Different Sequencing Platforms. *PLoS ONE* **2014**, *9*, e104984. [[CrossRef](#)] [[PubMed](#)]
62. Beghain, J.; Bridier-Nahmias, A.; Le Nagard, H.; Denamur, E.; Clermont, O. ClermonTyping: An easy-to-use and accurate in silico method for Escherichia genus strain phylotyping. *Microb. Genom.* **2018**, *4*. [[CrossRef](#)]
63. Wick, R.R.; Schultz, M.B.; Zobel, J.; Holt, K.E. Bandage: Interactive visualization of de novo genome assemblies. *Bioinformatics* **2015**, *31*, 3350–3352. [[CrossRef](#)] [[PubMed](#)]
64. Alikhan, N.F.; Petty, N.K.; Ben Zakour, N.L.; Beatson, S.A. BLAST Ring Image Generator (BRIG): Simple prokaryote genome comparisons. *BMC Genomics* **2011**, *12*, 402. [[CrossRef](#)] [[PubMed](#)]

Annex 5

“Dissemination of NDM-producing *Klebsiella pneumoniae* and *Escherichia coli* high-risk clones in Catalan healthcare institutions”

Dissemination of NDM-producing *Klebsiella pneumoniae* and *Escherichia coli* high-risk clones in Catalan healthcare institutions

Marta Marí-Almirall^{1†}, Clara Cosgaya^{1†}, Cristina Pitart^{2†}, Joaquim Viñes^{3,4}, Laura Muñoz¹, Irene Campo², Anna Cuscó⁴, Laura Rodríguez-Serna⁵, Gemina Santana⁵, Ana Del Río⁶, Olga Francino³, Pilar Ciruela^{7,8}, Isabel Pujol^{9,10}, Frederic Ballester¹¹, Francesc Marco^{1,2}, José Antonio Martínez⁶, Álex Soriano⁶, Jordi Vila^{1,2} and Ignasi Roca^{1*} on behalf of the MERCyCAT Study Group‡

¹Laboratory of Antimicrobial Resistance, ISGlobal, Hospital Clínic - Universitat de Barcelona, Barcelona, Spain; ²Department of Clinical Microbiology, Hospital Clínic - Universitat de Barcelona, Barcelona, Spain; ³SVGM, Molecular Genetics Veterinary Service, Universitat Autònoma de Barcelona, Bellaterra, Barcelona, Spain; ⁴Vetgenomics, PRUAB, Universitat Autònoma de Barcelona, Bellaterra, Barcelona, Spain; ⁵Department of Epidemiology and Preventive Medicine, Hospital Clínic - Universitat de Barcelona, Barcelona, Spain; ⁶Department of Infectious Diseases, Hospital Clínic - Institut d'investigacions Biomèdiques August Pi i Sunyer, Universitat de Barcelona, Barcelona, Spain; ⁷Public Health Agency of Catalonia (ASPCAT), Generalitat de Catalunya, Barcelona, Spain; ⁸CIBER de Epidemiologia y Salud Pública (CIBERESP), Instituto de Salud Carlos III, Madrid, Spain; ⁹Laboratori de Microbiologia, Hospital Universitari Sant Joan de Reus, Reus, Spain; ¹⁰Unitat de Microbiologia, Facultat de Medicina i Ciències de la Salut, IISPV, Universitat Rovira i Virgili, Reus, Spain; ¹¹Hospital Universitari Sant Joan de Reus-Laboratori de Referència del Camp de Tarragona i de les Terres de l'Ebre, Reus, Spain

*Corresponding author. E-mail: Ignasi.roca@isglobal.org

†These authors equally contributed to this work.

‡Other members of the MERCyCAT Study Group are listed in the Acknowledgements section.

Received 13 June 2020; accepted 12 October 2020

Objectives: To characterize the clonal spread of carbapenem-resistant *Klebsiella pneumoniae* and *Escherichia coli* isolates between different healthcare institutions in Catalonia, Spain.

Methods: Antimicrobial susceptibility was tested by disc diffusion. MICs were determined by gradient diffusion or broth microdilution. Carbapenemase production was confirmed by lateral flow. PCR and Sanger sequencing were used to identify the allelic variants of resistance genes. Clonality studies were performed by PFGE and MLST. Plasmid typing, conjugation assays, S1-PFGE plus Southern blotting and MinION Oxford Nanopore sequencing were used to characterize resistance plasmids.

Results: Twenty-nine carbapenem-resistant isolates recovered from three healthcare institutions between January and November 2016 were included: 14 *K. pneumoniae* isolates from a tertiary hospital in the south of Catalonia (hospital A); 2 *K. pneumoniae* isolates from a nearby healthcare centre; and 12 *K. pneumoniae* isolates and 1 *E. coli* isolate from a tertiary hospital in Barcelona (hospital B). The majority of isolates were resistant to all antimicrobial agents, except colistin, and all were NDM producers. PFGE identified a major *K. pneumoniae* clone ($n = 27$) belonging to ST147 and co-producing NDM-1 and CTX-M-15, with a few isolates also harbouring *bla*_{OXA-48}. Two sporadic isolates of *K. pneumoniae* ST307 and *E. coli* ST167 producing NDM-7 were also identified. *bla*_{NDM-1} was carried in two related IncR plasmid populations and *bla*_{NDM-7} in a conjugative 50 kb IncX3 plasmid.

Conclusions: We report the inter-hospital dissemination of XDR high-risk clones of *K. pneumoniae* and *E. coli* associated with the carriage of small, transferable plasmids harbouring *bla*_{NDM} genes.

Introduction

Carbapenem resistance has been rising very rapidly during recent decades, hence reducing the treatment options that are available to tackle infections caused by the main Gram-negative nosocomial pathogens, such as *Acinetobacter baumannii*, *Pseudomonas aeruginosa* and members of Enterobacterales, all of which are

top-priority pathogens according to the global priority list of antibiotic-resistant bacteria from the WHO.¹ The main mechanism of carbapenem resistance among these organisms is the production of carbapenem-hydrolysing β -lactamases, such as KPC, GES and OXA enzymes and MBLs (e.g. IMP, VIM and NDM).² In particular, there is great concern regarding the dissemination of

NDM-producing Gram-negative bacteria, since carriage of the *bla*_{NDM} gene is usually associated with resistance to all β -lactam antibiotics, except monobactams, plus co-resistance to additional antibiotic families, such as quinolones and aminoglycosides.^{3,4} Since the initial identification of NDM-1 in a Swedish patient of Indian origin in 2008,⁵ NDM-producing Gram-negative bacteria have been reported worldwide and up to 29 different NDM allelic variants are recorded in the NCBI reference gene catalogue (last accessed 9 June 2020).^{3,4} Among Enterobacteriales, NDM has been described in several species, but *Escherichia coli* and *Klebsiella pneumoniae* seem to be the most frequent hosts. In Spain, NDM was first described in 2011 in *E. coli* and only a few sporadic cases and outbreaks have been reported since.^{6,7} Here we have examined and characterized the clonal spread of NDM-producing *K. pneumoniae* between different healthcare institutions in Catalonia, Spain.

Materials and methods

Ethics

Bacterial samples studied here were recovered from clinical samples used for microbiological diagnosis at clinical microbiology laboratories. Informed consent was, therefore, not required. The protocol for this study was approved by the Ethics Committee on Clinical Research (CEIC) of the Hospital Clinic de Barcelona (HCB/2014/0499, HCB/2017/0923 and HCB/2017/0833).

Bacterial samples

Twenty-nine carbapenem-resistant isolates from three healthcare institutions were included: 14 *K. pneumoniae* isolates recovered from January to October 2016 from a tertiary hospital in the south of Catalonia (hospital A); 12 *K. pneumoniae* isolates and 1 *E. coli* isolate recovered from July to November 2016 at a tertiary hospital in Barcelona (hospital B); and 2 *K. pneumoniae* isolates recovered in September and October 2016, respectively, from a primary healthcare centre also in the south of Catalonia. Isolates were from surveillance and clinical samples. Identification of species was performed by MALDI-TOF MS. The clinical and microbiological data from all isolates and patients are provided in Table S1 (available as [Supplementary data](#) at JAC Online).

Susceptibility testing and resistance

Antimicrobial susceptibility was determined by disc diffusion in agar plates following EUCAST guidelines. Carbapenemase-producing Enterobacteriales were selected according to EUCAST screening cut-off values for carbapenems.⁸ Production of KPC, OXA-48-like, VIM, IMP or NDM carbapenemases was detected using NG-Test[®] CARBA 5 (NG-Biotech, France). MICs were determined by gradient diffusion (AB-bioMérieux, Sweden), except for colistin MICs, which were determined by broth microdilution.⁹ Results were interpreted according to EUCAST guidelines.¹⁰ Isolates were categorized as MDR, XDR or pan-drug resistant according to *ad hoc* definitions.¹¹ *E. coli* ATCC 25922 was used for quality control.

The presence of genes encoding carbapenemases,^{7,12} ESBLs¹³ or 16S rRNA methyltransferases (*armA* and *rmtA-rmtH*)¹⁴ was investigated by PCR and Sanger sequencing. Alleles were determined through sequence alignment against the NCBI reference gene catalogue (PRJNA313047; last accessed 9 June 2020).

Epidemiology and molecular typing

Clonality was studied by PFGE using XbaI genomic digestions and a CHEFF-DRIII system (Bio-Rad, Spain).¹⁵ Molecular patterns were analysed with

InfoQuest[™]FP-v.5.4 (Bio-Rad) and the unweighted pair group method with arithmetic mean to create dendrograms based on Dice's similarity coefficient, using bandwidth tolerance and optimization values set at 1.5% and 1.2%, respectively. Isolates were considered within the same PFGE cluster (pulsotype) if their Dice similarity index was >85%.

MLST was performed according to the Pasteur scheme for *K. pneumoniae* and the Achtman scheme for *E. coli*.^{16,17}

Plasmid analysis

Transferability of *bla*_{NDM} was studied by biparental conjugation in broth medium using azide-resistant *E. coli* J53 as the recipient. Transconjugant strains (TC1–4) were selected on LB agar plates containing 1 mg/L imipenem and 100 mg/L sodium azide. Plasmid profiling was performed by S1-nuclease digestion followed by PFGE and Southern hybridization with digoxigenin-labelled probes against *bla*_{NDM}, *bla*_{OXA-48} and *bla*_{CTX-M}.

Plasmid incompatibility groups were identified using the PBRT-2.0 kit (Diatheva, Italy).¹⁸ Classification of IncR plasmids into IncR1 or IncR2 arbitrary groups was performed by PCR using the following primers: IS26_Rev, 5'-ggcactgttgcaagtagcg-3'; ISAb125_Rev, 5'-caaacatgaggtgcgacag-3'; Tn5403Int_Fwd, 5'-ggtttgcgtgacatcactcg-3'; and Tn5403Int_Rev, 5'-ccgtgagtgtggcttagag-3'. Plasmids belonged to the IncR1 group if the PCR was negative upon using primers IS26_Rev with ISAb125_Rev, but positive when combining IS26_Rev with Tn5403Int_Rev and Tn5403Int_Fwd with ISAb125_Rev (3 and 4.3 kb, respectively). Plasmids belonged to the IncR2 group if positive to the IS26_Rev and ISAb125_Rev primer combination (1.7 kb), but negative for the other two primer pairs.

Genomic DNA extracted using the Wizard Genomic DNA purification kit (Promega, Spain) was sequenced using MinION sequencing (Oxford Nanopore, UK), in accordance with the manufacturer. Base-calling was done with Guppy-v3.0.3 and demultiplexing with qcat-v1.1.0 (<https://github.com/nanoporetech/qcat>). FASTQ files were mapped using Minimap2-v2.17 against plasmids from Enterobacteriales.¹⁹ Mapping reads were assembled with Flye-v2.5 (<https://github.com/fenderglass/Flye>). Annotation was done with Prokka-v.1.12 combined with BLASTP/BLASTN searches against the UniProtKB/Swiss-Prot and RefSeq databases.²⁰

ResFinder (<https://cge.cbs.dtu.dk/services/ResFinder/>), PlasmidFinder (<https://cge.cbs.dtu.dk/services/PlasmidFinder/>) and ISFinder (<https://www-is.biotoul.fr/>) were used to identify antimicrobial resistance genes, mobile elements and plasmid replicons. Gene organization diagrams were drawn using SnapGene[®] Viewer-v5.1.2 (<https://www.snapgene.com/>) and CGViewAdvanced-v.0.0.1.²¹ Sequence comparisons were graphically displayed using Kablammo.²²

FASTQ files of isolates HA-2, HA-3, HA-4, HB-377 and HB-536 have been deposited into the NCBI Sequence Read Archive (SRA) under accession numbers SRR11828896, SRR11828895, SRR11828894, SRR18228893 and SRR11828892, respectively; BioProject PRJNA6346391. Annotated plasmid sequences are available as [Supplementary data](#) at JAC Online.

Results

Bacterial isolation and PFGE

Overall, 24 different patients were involved in the study, being either colonized ($n = 7$) or infected ($n = 17$), and typically presented multiple comorbidities (mostly hepatic, pancreatic and cardiovascular diseases). Five of the infected patients died (29%). The most common treatment for infected patients was the administration of carbapenems together with tigecycline and/or colistin (Table S1).

In January 2016, a carbapenem-resistant NDM-producing *K. pneumoniae* isolate (HA-3) was recovered at a tertiary hospital (hospital A) in the province of Tarragona, Spain, from a urine

sample of a patient admitted to the internal medicine ward who had just been transferred from a tertiary hospital in Barcelona (hospital D). From April to June 2016, four additional NDM-producing *K. pneumoniae* isolates were recovered from the surveillance and clinical samples of three different patients admitted to the internal medicine ward of hospital A.

At the beginning of July, an NDM-positive patient from hospital A was transferred to the liver ICU of a second university hospital in Barcelona (hospital B). The patient was isolated and enhanced barrier precautions were implemented upon admission. Nevertheless, 11 additional NDM-producing *K. pneumoniae* isolates and 1 NDM-producing *E. coli* isolate were recovered from different wards from July to November.

During the same period, NDM-producing *K. pneumoniae* continued to disseminate at hospital A and eight new isolates were reported in both the internal medicine and surgery wards, two of them recovered from a newly admitted patient transferred again from hospital D. Furthermore, two additional NDM-producing *K. pneumoniae* isolates were also reported in September and October 2016, respectively, from a primary healthcare centre close to hospital A. Infection control measures and active screening of both carriers and environmental samples were intensified in all centres during this period and, at hospital B, hydrogen peroxide vaporizers were even used to decontaminate those wards involved in the outbreak. No additional isolates were recovered after November 2016 (Figure 1).

The analysis of the 28 *K. pneumoniae* isolates by PFGE revealed the presence of two different pulsotypes, A and B (Figure 2). Most of the isolates were highly related and clustered together into pulsotype A, while pulsotype B contained a single strain recovered at hospital B (HB-536). Pulsotype A could be further subdivided into clusters A1 and A2 (20 and 7 isolates, respectively), differing by only one band and sharing 96% similarity (Figure 2). Isolates from pulsotype A1 were recovered from

all three centres, while those from the A2 pulsotype were exclusively from hospital A.

Antimicrobial resistance

Antimicrobial susceptibility testing showed that 25 out of the 27 pulsotype A *K. pneumoniae* isolates were XDR, only remaining susceptible to colistin. Interestingly, the two pulsotype A1 isolates recovered from the primary healthcare centre (HC-15 and HC-16) were also susceptible to all aminoglycosides and, therefore, considered MDR. The single *K. pneumoniae* isolate from pulsotype B (HB-536), as well as the NDM-producing *E. coli* isolate (HB-543), were also MDR, remaining susceptible to either amikacin, fosfomicin and colistin, or to gentamicin, amikacin, tobramycin, fosfomicin, tigecycline and colistin, respectively (Table S1).

PCR screening confirmed carriage of *bla*_{NDM} in all *K. pneumoniae* and *E. coli* isolates, as well as *bla*_{CTX-M}-group 1 in all *K. pneumoniae* isolates. *K. pneumoniae* isolates from pulsotype A harboured the *bla*_{NDM-1} allelic variant, but both the *K. pneumoniae* isolate from pulsotype B (HB-536) and the single NDM-producing *E. coli* isolate (HB-543) carried *bla*_{NDM-7}. The β-lactamase gene *bla*_{TEM-1} was also identified in these two isolates. DNA sequencing also confirmed the *bla*_{CTX-M-15} allelic variant among *K. pneumoniae* isolates. Of note, the *rmtF* gene was detected in the 25 XDR *K. pneumoniae* isolates from pulsotype A1.

All isolates were negative for *bla*_{KPC}, *bla*_{VIM} and *bla*_{IMP}, but four *K. pneumoniae* isolates from pulsotype A2 also carried the *bla*_{OXA-48} gene, encoding a class D carbapenem-hydrolysing β-lactamase (Figure 2). Interestingly, isolates co-carrying OXA-48 and NDM were recovered at hospital A after the outbreak had been extended to hospital B, and the first patient at hospital A with NDM/OXA-48 (HA-4) represents a second referral from hospital D, the original source of the outbreak at hospital A (Figure 1).

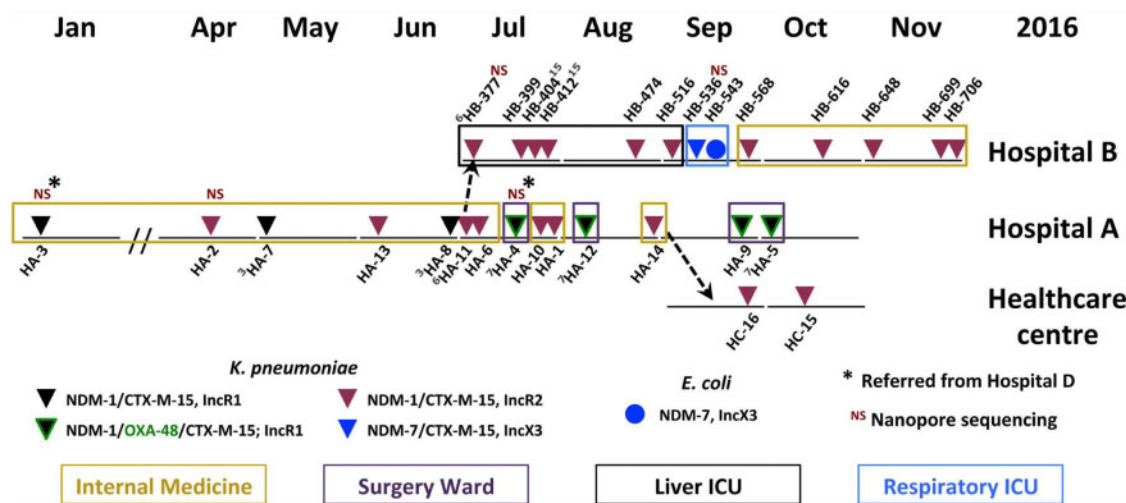


Figure 1. Temporal and spatial distribution of NDM-producing isolates recovered from patients at three healthcare institutions in Catalonia from January to November 2016. Coloured boxes show the different wards hosting the patients at the time of isolation. Bacterial isolates are represented by an inverted triangle (*K. pneumoniae*) or a circle (*E. coli*). Colour codes indicate carriage of different combinations of β-lactamases and IncR or IncX3 plasmids. Isolates recovered from patients referred from hospital D are shown with an asterisk. The transfer of patients between the three healthcare centres is represented with a dotted line. NS indicates isolates selected for Nanopore sequencing. Superscript numbers indicate isolates recovered from the same patient (Table S1). This figure appears in colour in the online version of JAC and in black and white in the print version of JAC.

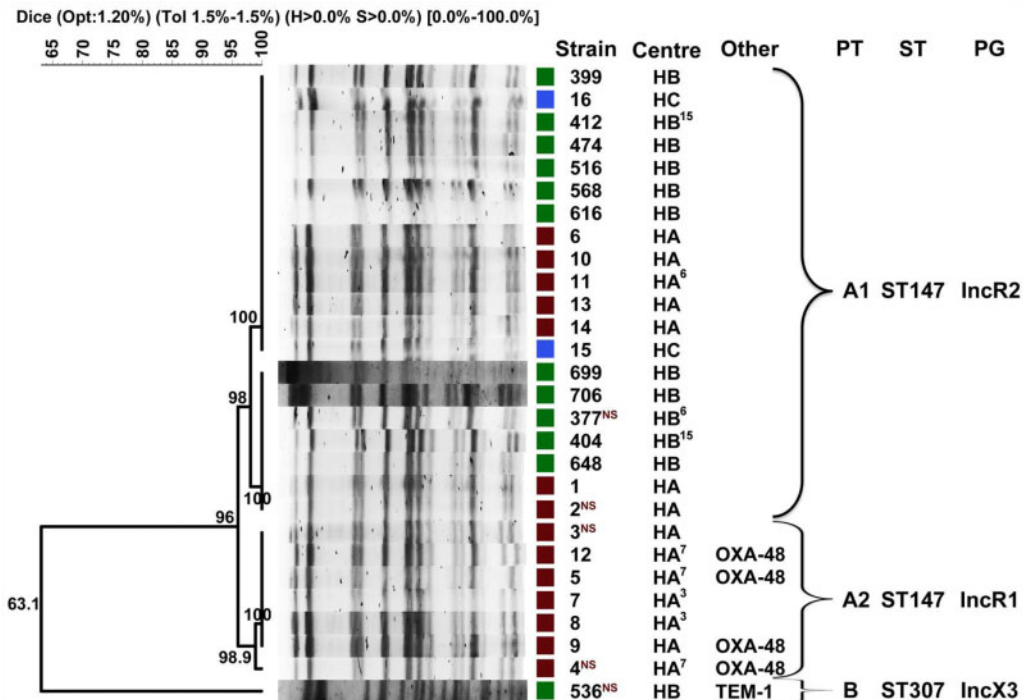


Figure 2. PFGE dendrogram of NDM-producing *K. pneumoniae* isolates from three healthcare centres in Catalonia (HA, hospital A; HB, hospital B; and HC, primary healthcare centre). Other, carriage of additional β -lactamases; PT, pulsotype; PG, plasmid incompatibility group of plasmids harbouring bla_{NDM} ; NS, isolates selected for Nanopore sequencing. Braces indicate classification to the corresponding PFGE cluster or pulsotype. Isolates were included in the same pulsotype if their Dice similarity index was $\geq 85\%$. Superscript numbers indicate isolates recovered from the same patient (Table S1). This figure appears in colour in the online version of JAC and in black and white in the print version of JAC.

Molecular typing and plasmid analysis

MLST studies identified isolates from pulsotype A as belonging to ST147, while the NDM-7-producing *K. pneumoniae* (pulsotype B) and *E. coli* isolates belonged to ST307 and ST167, respectively.

The transferability of putative plasmids harbouring bla_{NDM-1} , $bla_{CTX-M-15}$, bla_{OXA-48} and bla_{NDM-7} was analysed by conjugation using *K. pneumoniae* producing NDM-1/OXA-48 or NDM-7 as donors. Four different types of transconjugant *E. coli* strains were obtained: TC1, carrying bla_{NDM-1} , $bla_{CTX-M-15}$ and bla_{OXA-48} ; TC2, carrying bla_{NDM-1} and $bla_{CTX-M-15}$; TC3, carrying just bla_{OXA-48} ; and TC4, that only acquired bla_{NDM-7} . None of the transconjugant strains acquired the *rmtF* gene. TC1 and TC2 transconjugants acquired resistance to all β -lactam antibiotics, but not to aminoglycosides, while TC3 transconjugants only showed reduced susceptibility to β -lactams and TC4 transconjugants acquired resistance to all β -lactams, except aztreonam. The MIC values and molecular characteristics for representative isolates and transconjugant strains are shown in Table 1.

These results suggested that ST147 *K. pneumoniae* isolates carried bla_{NDM-1} and $bla_{CTX-M-15}$ in the same plasmid, while bla_{OXA-48} and *rmtF* were likely to be located in two separate plasmids. In contrast, bla_{NDM-7} and $bla_{CTX-M-15}$ were apparently located in different plasmids in the ST307 *K. pneumoniae* isolate HB-536. To corroborate these results, the location of the bla_{NDM-1} , $bla_{CTX-M-15}$, bla_{OXA-48} and bla_{NDM-7} genes was investigated by S1-PFGE and Southern blotting. As shown in Figure 3(a and b), DNA probes specific for bla_{NDM} and $bla_{CTX-M-15}$ hybridized with the same bands in

NDM-1-producing *K. pneumoniae* (ST147) isolates and the corresponding transconjugant strains (TC1 and TC2), while the same probes hybridized with different bands in the NDM-7-producing *K. pneumoniae* (HB-536) isolate and the corresponding transconjugant strain (TC4) and only the bla_{NDM} probe hybridized against the NDM-7-producing *E. coli* isolate (HB-543). In addition, DNA probes against bla_{OXA-48} hybridized with a smaller band in an isolate co-producing NDM-1/OXA-48 (HA-4) and the same band was also identified in the corresponding OXA-48 (TC3) or NDM-1/OXA-48 (TC1) transconjugant strains (Figure 3c).

PBRT showed that *K. pneumoniae* isolates producing NDM-1 or NDM-1/OXA-48 were positive for IncR and IncFII_S, or IncR, IncFII_S and IncL plasmid replicons, respectively, while the corresponding *E. coli* transconjugants presented the following plasmid replicons: TC1 (NDM-1/OXA-48), positive for IncR and IncL; TC2 (NDM-1), positive for IncR; and TC3 (OXA-48), positive for IncL. The *K. pneumoniae* isolate producing NDM-7 (HB-536) presented IncX3, IncFIB-KN and IncFII_K plasmid replicons, but only the IncX3 replicon was transferred to the *E. coli* transconjugant (TC4). Likewise, the single *E. coli* clinical isolate producing NDM-7 also harboured an IncX3 plasmid replicon (Table 1).

Plasmid sequences

K. pneumoniae isolates initially selected to characterize the plasmids harbouring bla_{NDM} and bla_{OXA-48} genes included: the first NDM-1-producing isolates at both hospital A and hospital B (HA-3 and HB-377, respectively); the first NDM-1/OXA-48-producing

Table 1. Antimicrobial susceptibility and molecular characterization of representative *K. pneumoniae* and *E. coli* isolates and their corresponding transconjugant *E. coli* strains (using azide-resistant *E. coli* J53 as the recipient)

Strain	Bacterial species	MIC (mg/L)																Pulsotype	ST	NDM	Other	rmtF	PG
		IPM	MEM	FOX	FEP	CTX	CAZ	ATM	GEN	AMK	TOB	CIP	L VX	TGC	CST ^a	FOF							
HA-3	<i>Kp</i>	>32	>32	>256	>256	>32	>256	>256	>256	>256	>256	>256	>32	2	0.25	64	A2	ST147	1	CTX-M-15	+	R1	
HA-2	<i>Kp</i>	>32	>32	>256	>256	>32	>256	>256	>256	>256	>256	>32	2	0.125	48	A1	ST147	1	CTX-M-15	+	R2		
HB-377	<i>Kp</i>	>32	>32	>256	>256	>32	>256	>256	>256	>256	>256	>32	3	0.25	48	A1	ST147	1	CTX-M-15	+	R2		
HA-4	<i>Kp</i>	>32	>32	>256	>256	>32	>256	>256	>256	>256	>256	>32	2	0.125	64	A2	ST147	1	OXA-48	+	R1/L		
																			CTX-M-15				
HC-16	<i>Kp</i>	>32	>32	>256	>256	>32	>256	2	2	6	>32	>32	4	0.25	48	A1	ST147	1	CTX-M-15	-	R2		
HB-536	<i>Kp</i>	>32	>32	>256	256	>32	>256	48	4	8	>32	>32	4	0.25	12	B	ST307	7	TEM-1	-	X3		
																			CTX-M-15				
HB-543	<i>Ec</i>	>32	>32	>256	>256	>32	>256	0.25	1	0.38	>32	>32	0.75	0.25	0.38	NA	ST167	7	TEM-1	-	X3		
TC1	<i>Ec</i>	16	4	>256	32	>32	>256	0.125	0.5	0.38	0.125	0.25	0.25	0.125	1	NA	NA	1	OXA-48	-	R1/L		
																			CTX-M-15				
TC2	<i>Ec</i>	12	2	>256	16	>32	>256	12	0.5	0.25	0.125	0.38	0.38	0.125	1	NA	NA	1	CTX-M-15	-	R1		
TC3	<i>Ec</i>	0.5	0.19	4	0.64	0.5	0.19	0.094	0.38	1.5	0.25	0.08	0.023	0.19	0.125	1	NA	NA	-	OXA-48	-	L	
TC4	<i>Ec</i>	>32	>32	>256	8	>32	>256	0.125	0.38	1.5	0.25	0.012	0.016	0.125	1	NA	NA	7	-	-	X3		
J53AZ ^R	<i>Ec</i>	0.19	0.016	4	0.023	0.016	0.047	0.125	0.064	0.75	0.094	0.008	0.016	0.094	0.125	0.094	NA	NA	-	-	-	NA	

Kp, *K. pneumoniae*; *Ec*, *E. coli*; IPM, imipenem; MEM, meropenem; FOX, ceftaxime; FEP, cefepime; CTX, ceftazidime; ATM, aztreonam; GEN, gentamicin; AMK, amikacin; TOB, tobramycin; CIP, ciprofloxacin; LVX, levofloxacin; TGC, tigecycline; CST, colistin; FOF, fosfomicin; NDM, presence of bla_{NDM-1} or bla_{NDM-7}; Other, presence of additional bla genes; rmtF, presence of the rmtF gene; PG, plasmid incompatibility group of plasmids carrying bla_{NDM} and bla_{OXA-48}; NA, not applicable.
^aColistin MICs were determined by broth microdilution.

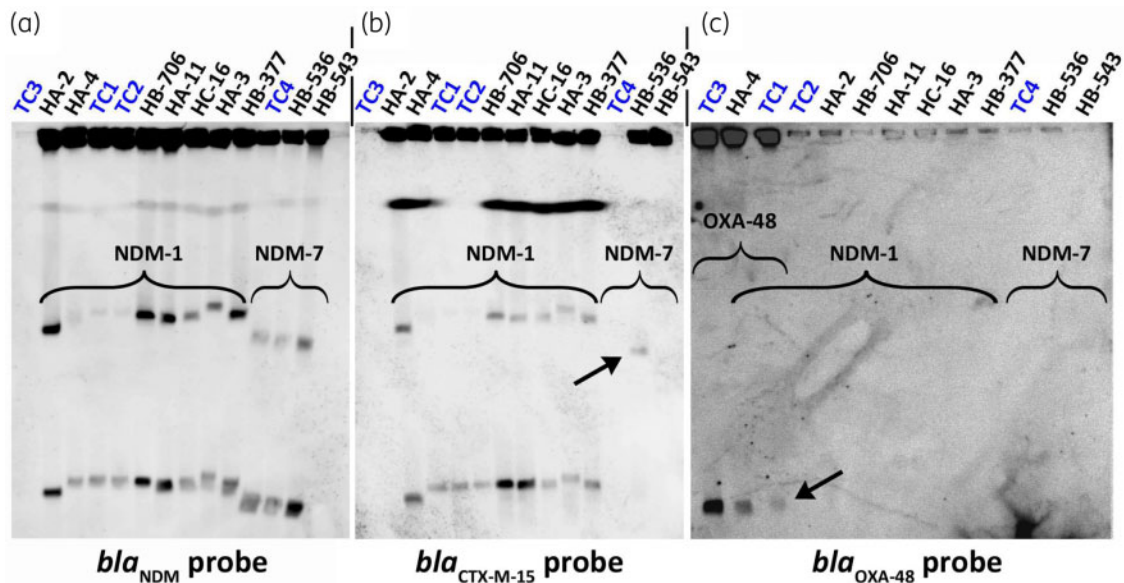


Figure 3. S1-PFGE and Southern hybridization of *K. pneumoniae* or *E. coli* isolates harbouring different combinations of β -lactamases. (a) Hybridization with the *bla*_{NDM} probe. (b) Hybridization with the *bla*_{CTX-M-15} probe. (c) Hybridization with the *bla*_{OXA-48} probe. Braces indicate molecular detection of different *bla* genes. Transconjugants are shown in blue. Arrows indicate weak bands. Of note, mirroring double bands were attributed to incomplete cleavage by the S1 nuclease so that other conformations of the plasmid rather than the linear one are also seen. This figure appears in colour in the online version of JAC and in black and white in the print version of JAC.

isolate that was recovered at hospital A (HA-4) [all three of them belonging to ST147 (Figures 1 and 2)]; and the ST307 *K. pneumoniae* isolate producing NDM-7 (HB-536).

Genomic sequencing corroborated previous results showing that ST147 *K. pneumoniae* isolates harboured both the *bla*_{NDM-1} and *bla*_{CTX-M-15} genes in a single plasmid belonging to the IncR incompatibility group (Figures S1 to S3). There were, however, some interesting differences. The HA-3 and HA-4 isolates, both recovered at hospital A from patients referred from hospital D, shared almost identical plasmids of approx. 74 kb (pNDM-HA3 and pNDM-HA4, respectively) that carried *bla*_{NDM-1} within a Tn3000 transposon. In both plasmids the upstream IS3000 element was partially replaced by a full-length Tn5403, as previously described.⁶ The Tn3000 transposon was in turn flanked by two IS26 elements in reverse orientation (Figure 4). The bulk of the remaining plasmid backbone shared high similarity (>99% average identity) with p48896_1 (CP024430), an IncR plasmid carrying *bla*_{CTX-M-15} (but not *bla*_{NDM}) that was recently recovered from an ST147 *K. pneumoniae* isolate in Pakistan.²³

Additional resistance genes included the aminoglycoside resistance gene *aph(3')-Ia*, as well as *qnrB*, involved in low-level quinolone resistance.²⁴ On the other hand, plasmid pNDM-HB377 (from the first isolate recovered at hospital B) presented a slightly smaller IncR plasmid of approx. 67 kb, also containing both *bla*_{NDM-1} and *bla*_{CTX-M-15}. The genetic structures surrounding *bla*_{NDM-1} in pNDM-HB377 were similar to those of pNDM-HA3 and pNDM-HA4, except for a 5494 bp sequence containing Tn5403 that was missing upstream of *bla*_{NDM-1} (Figure 4). In addition, pNDM-HB377 presented an inversion of a 52 kb region containing *bla*_{CTX-M-15}, the IncR *repB* gene and *mobC*, involved in plasmid mobilization. The region containing the aminoglycoside resistance gene *aph(3')-Ia* was also missing (Figure 5).

These findings suggested a slightly different plasmid population between NDM-producing *K. pneumoniae* isolates from hospitals A and B. To corroborate such differences, specific PCR primers (see the Materials and methods section) were designed to differentiate between pNDM-HA3/HA4-like plasmids (hereafter IncR1 group) and pNDM-HB377-like plasmids (hereafter IncR2 group). PCR screening showed that all NDM-1-producing *K. pneumoniae* isolates from hospitals B and C carried *bla*_{NDM-1} in a plasmid from the IncR2 group, while isolates from hospital A carried *bla*_{NDM-1} in plasmids from either group (Figure 2). Sequence analysis of yet another IncR2 plasmid (pNDM-HA2), but from an isolate at hospital A, also yielded a plasmid of roughly 67 kb, almost identical to pNDM-HB377 (Figure S4). Interestingly, isolates carrying the IncR2 group plasmid belonged to pulsotype A1, while isolates harbouring the IncR1 group belonged to pulsotype A2 (Figure 2).

The immediate genetic structures downstream of *bla*_{NDM-1} were identical in these plasmids and comprised genes commonly associated with *bla*_{NDM} genes in Enterobacteriales and *Acinetobacter* spp. (Figure 4).^{25,26}

In addition, the HA-4 isolate harboured a second plasmid of approx. 64 kb carrying *bla*_{OXA-48} and belonging to IncL (pOXA48-HA4) that was highly similar (>99% average identity and 100% query coverage) to the IncL pUR17313-1 plasmid (KP061858) sequenced in Portugal from an *Enterobacter cloacae* clinical isolate (Figure S5).²⁷ *bla*_{OXA-48} was located within Tn1999.2 (Figure 4) and no additional antimicrobial resistance genes were identified in pOXA48-HA4.²⁸

On the other hand, the ST307 *K. pneumoniae* isolate HB-536 carried *bla*_{NDM-7} (but not *bla*_{CTX-M-15}) in an IncX3 plasmid of 50.5 kb (pNDM-HB536) highly similar (>98% average identity and 99% query coverage) to the pAR_0162 plasmid recovered from *E. coli* (CP021682) (Figure S6). The sequence upstream of *bla*_{NDM-7}

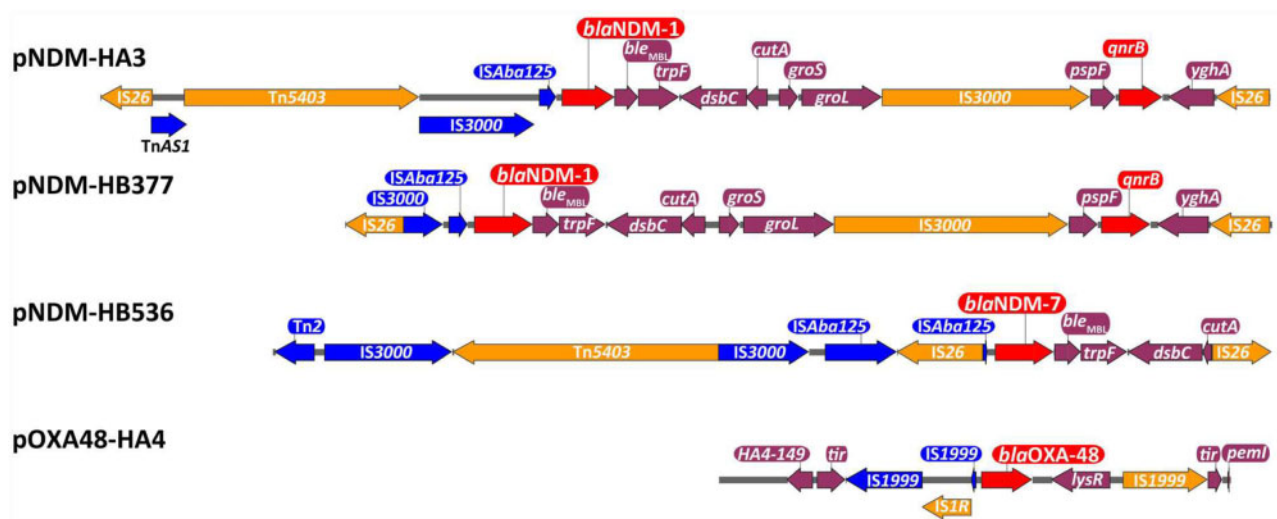


Figure 4. Schematic drawing showing the genetic elements surrounding the bla_{NDM} genes in pNDM-HA3, pNDM-HB377 and pNDM-HB536, as well as the bla_{OXA-48} gene in pOXA48-HA4. Arrows are proportional to the lengths of the genes and are orientated in the direction of transcription. Red arrows represent resistance genes, orange arrows represent full-length transposon-related genes and ISs, blue arrows represent partial or truncated transposon-related genes and ISs, and purple arrows are used for the remaining set of genes. This figure appears in colour in the online version of JAC and in black and white in the print version of JAC.

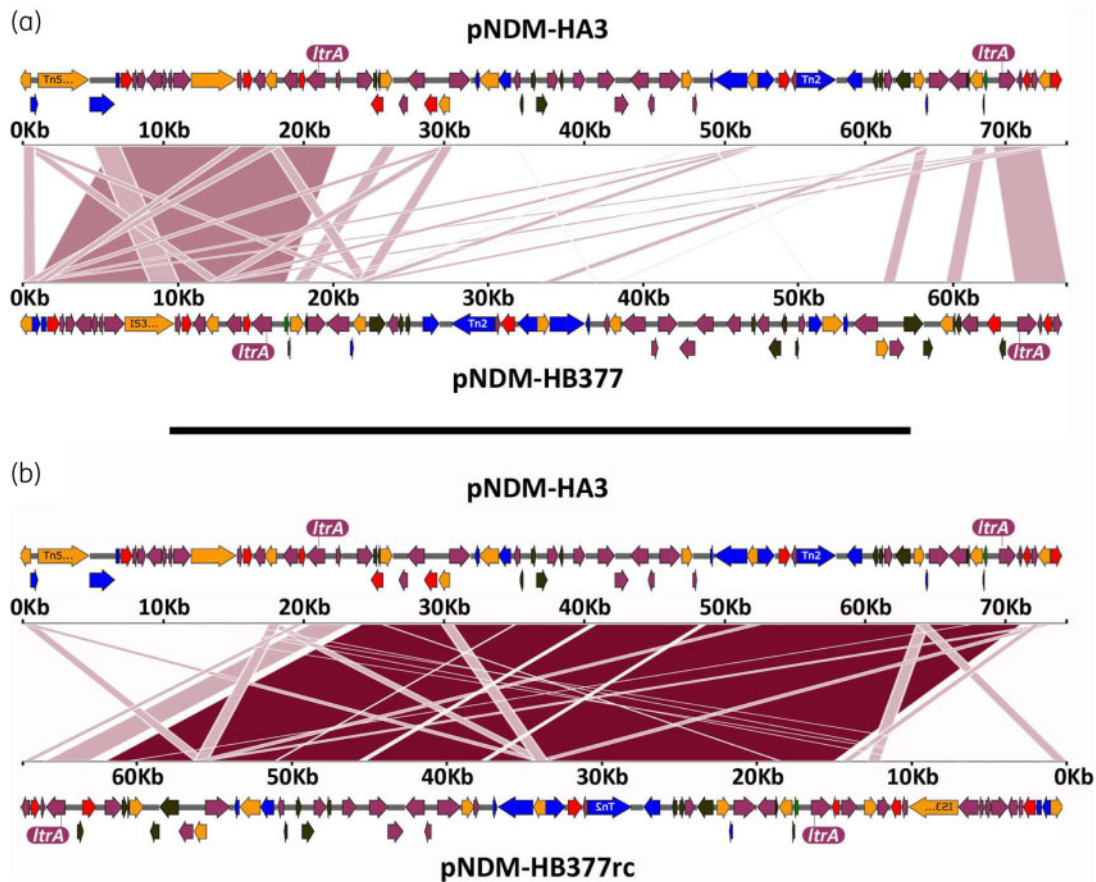


Figure 5. Graphical comparison of plasmids pNDM-HA3 and pNDM-HB377 in either: (a) parallel orientation or (b) antiparallel orientation (reverse complement sequence of pNDM-HB377). The shaded stripes show regions shared between the two plasmids. The locations of the *ItrA* sequences flanking a 52 kb inversion are shown. This figure appears in colour in the online version of JAC and in black and white in the print version of JAC.

comprised several partial or complete ISs and transposons (again Tn5403 and IS3000) among which stood out the presence of an IS_{Aba125} that was truncated by an IS5 element. The region downstream of *bla*_{NDM-7} also presented the canonical *ble*, *trpF* and *dsbC* genes, but the adjacent *cutA1* gene was partially deleted upon the insertion of an IS26 element (Figure 4). The *bla*_{NDM-7} gene was the only antimicrobial resistance gene present in plasmid pNDM-HB536.

Discussion

NDM was first reported in Spain in 2011 from an *E. coli* isolate in a Spanish traveller returning from India.⁷ Since then, NDM-producing Enterobacteriales have slowly crawled into the Spanish healthcare system, initially associated with imported sporadic cases, then autochthonous and, more recently, causing small hospital outbreaks.^{25,29-35}

A recent nationwide study comparing the genome sequences of NDM-producing *K. pneumoniae* and *E. coli* isolates in Spain also suggested the inter-hospital and inter-regional spread of a few clonal lineages.⁶

Here we report the inter-hospital dissemination of NDM-1-producing *K. pneumoniae* isolates between at least three healthcare settings in Catalonia from January to October 2016, with some isolates also co-producing OXA-48. A single clone carrying both *bla*_{NDM-1} and *bla*_{CTX-M-15} in the same transferable IncR plasmid and belonging to the high-risk clone ST147 was responsible for such dissemination. Nevertheless, three distinct populations of ST147 isolates were identified according to the number and types of plasmids carried.

The first population clustered together into pulsotype A2 was associated with the isolate from the index case patient at hospital A, probably acquired from a previous hospital admission (hospital D), and carried *bla*_{NDM-1} within an IncR1 plasmid of approx. 74 kb characterized by the presence of a Tn5403 insertion upstream of *bla*_{NDM-1} (Figure 2). The second population is a subset of the previous one, ST147 *K. pneumoniae* isolates with the IncR1 plasmid and belonging to pulsotype A2, but co-producing OXA-48 from an IncL plasmid. This population appeared at hospital A after a second patient transfer from hospital D. These two populations only disseminated among patients from hospital A (Figures 1 and 2). Interestingly, OXA-48-producing *K. pneumoniae* in Spain is commonly found in many hospitals and associated with several lineages, including ST405, ST15 and ST101, but, to our knowledge, not ST147.^{12,36} Most likely, the identification of OXA-48 associated with ST147 in this study reflects the acquisition of the IncL plasmid from OXA-48-producing strains previously circulating at hospital D, the original source of the outbreak.

The third population comprises ST147 *K. pneumoniae* isolates carrying *bla*_{NDM-1} and *bla*_{CTX-M-15} in an IncR2 plasmid of approx. 67 kb, highly similar to IncR1, except for a 52 kb inversion and the loss of a region upstream of *bla*_{NDM-1} (Figures 4 and 5).

IncR2 plasmids may have resulted from homologous recombination through *ltrA* sequences at an IncR1 plasmid that developed into this particular inversion, since *ltrA* genes were located flanking the inverted region. Isolates within this population belonged to pulsotype A1 and appeared first at hospital A, but further spread to other centres through the referral of patients (Figures 1 and 2).

K. pneumoniae ST147 is commonly associated with carbapenem resistance and is considered one of the main high-risk clones of MDR *K. pneumoniae* currently disseminating worldwide.^{37,38} In Spain, NDM-1-producing *K. pneumoniae* ST147 was first reported in 2018 causing a small outbreak at a tertiary hospital in Tenerife.³⁴ More recently, a retrospective surveillance study has reported sporadic IncR NDM-1-producing ST147 *K. pneumoniae* isolates in the south of Catalonia during the summer of 2016, as well as causing another small outbreak in Galicia in 2015.⁶ The genetic structures surrounding *bla*_{NDM-1} in those isolates matched that of IncR1 plasmids in the present study, although the plasmid was slightly larger (110 kb) and lacked *bla*_{CTX-M-15}. The index case in our study was referred from another hospital within Catalonia and, hence, it is not clear whether these ST147 isolates are related to previous outbreaks in Spain.

In our study, two sporadic isolates of *K. pneumoniae* and *E. coli* producing NDM-7 and belonging to ST307 and ST167, respectively, were identified in one of the hospitals. They were recovered from two patients that overlapped in the same ward and both carried *bla*_{NDM-7} in an IncX3 plasmid of approx. 50 kb, thus suggesting horizontal transfer. *E. coli* and *K. pneumoniae* isolates harbouring *bla*_{NDM-7} in similar IncX3 plasmids have also been described in Spain, mainly in Madrid, where they were associated with the dissemination of *K. pneumoniae* ST437 and *Enterobacter hormaechei* in 2013 and 2016, respectively.^{6,35} In Catalonia, NDM-7 has been reported twice in sporadic ST679 (2013) or ST399 (2015) *E. coli* isolates associated with IncX4 or IncX3 plasmids, respectively, both of which were recovered from patients that had just returned from Pakistan.^{29,39} In our study we could not relate either of these two patients to recent travel, although one of them was originally from Pakistan. Nevertheless, it is important to highlight that *K. pneumoniae* ST307 is also one of the main MDR *K. pneumoniae* high-risk clones and *E. coli* ST167 is considered an epidemic clone commonly associated with the worldwide dissemination of IncX3 plasmids harbouring *bla*_{NDM-5} and *bla*_{NDM-7}.^{37,40}

We acknowledge several limitations in our study. First, WGS was performed using a single Nanopore approach, while the use of a hybrid approach would have allowed for additional and more accurate comparisons with isolates from previous studies. Also, only a handful of isolates were sequenced and sequence similarity was, therefore, assumed for the remaining isolates on the basis of PFGE, MLST and conventional PCR data. Unfortunately, further WGS studies were beyond our possibilities. Finally, the index case and the spread of NDM-producing *K. pneumoniae* at hospital D was not known, although we are aware that an investigation is currently ongoing at the hospital and the results will be made available in due course.

Overall, the results presented here report the dissemination of XDR and MDR high-risk clones of *K. pneumoniae* and *E. coli* among different hospitals in Catalonia, whose success in the clinical setting is likely related to the carriage of small, transferable plasmids, harbouring *bla*_{NDM} genes that provide resistance to last-resort antimicrobials. In Spain, such XDR clones are increasingly being reported in outbreak situations and autochthonous dissemination, and our results reinforce previous findings suggesting the national spread of NDM-producing *K. pneumoniae* associated with a few clonal lineages.

Acknowledgements

We thank the team of curators of the Institute Pasteur MLST and whole-genome MLST databases for curating the data and making them publicly available at <http://bigsdb.pasteur.fr/>.

We thank the clinical and laboratory staff of the participating hospitals for obtaining clinical samples and the initial identification of microorganisms.

Other members of the MERCyCAT Study Group

Pepa Pérez Jove, Emma Padilla and Mónica Ballesteró-Téllez (Catlab, Centre analítiques Terrassa AIE), Yuliya Zboromyrska, Miguel Àngel Benítez, Raquel Clivillé, Sabina González and Iolanda Calvet (Consorci del Laboratori Intercomarcal de l'Alt Penedès, l'Anoia i el Garraf), Carmen Gallés (Corporació de Salut del Maresme i la Selva), Goretti Sauca (Hospital de Mataró), Carmina Martí-Sala and M^a Angeles Pulido (Hospital General de Granollers), Anna Vilamala (Hospital General de Vic), Araceli González-Cuevas, (Hospital General del Parc Sanitari Sant Joan de Déu), Amadeu Gené (Hospital Sant Joan de Déu de Barcelona), Gloria Trujillo and Joan Lopez Madueño (Hospital Sant Joan de Déu de Manresa), Xavier Raga (Hospital Sant Pau I Santa Tecla), Frederic Gómez, Ester Picó and Carolina Sarvisé (Hospital Universitari Joan XXIII de Tarragona) and Xesca Font (Hospital Universitari Sant Joan de Reus).

Funding

This study was supported by: Plan Nacional de I+D+i 2013–2016, Instituto de Salud Carlos III, Subdirección General de Redes y Centros de Investigación Cooperativa, Ministerio de Economía y Competitividad, Spanish Network for Research in Infectious Diseases (REIPI RD16/0016/0010); the 2017 call for Strategic Action on Health (PI17/01932), co-financed by European Development Regional Fund 'A way to achieve Europe' and the operative programme Intelligent Growth 2014–2020; and grant 2017 SGR 0809 from the Departament d'Universitats, Recerca i Societat de la Informació, of the Generalitat de Catalunya. M.M.-A. and C.C. were supported by grants FPU 14/06357 and FPU 13/02564, respectively, from the Spanish Ministry of Education, Culture and Sports. I.R. was supported by the Department of Health, Generalitat de Catalunya, grant SLT002/16/00349. We also acknowledge support from the Spanish Ministry of Science, Innovation and Universities through the 'Centro de Excelencia Severo Ochoa 2019–2023' programme (CEX2018-000806-S) and support from the Generalitat de Catalunya through the CERCA programme.

The funders had no role in the study design, data collection, analysis and interpretation of data, decision to publish or preparation of the manuscript.

Transparency declarations

None to declare.

Author contributions

All authors critically revised the manuscript for intellectual content and read and approved the final manuscript.

Supplementary data

Table S1, annotated plasmid sequences and Figures S1 to S6 are available as [Supplementary data](#) at JAC Online.

References

- Tacconelli E, Carrara E, Savoldi A *et al.* Discovery, research, and development of new antibiotics: the WHO priority list of antibiotic-resistant bacteria and tuberculosis. *Lancet Infect Dis* 2018; **18**: 318–27.
- Nordmann P, Poirel L. Epidemiology and diagnostics of carbapenem resistance in Gram-negative bacteria. *Clin Infect Dis* 2019; **69** Suppl 7: S521–8.
- Wailan AM, Paterson DL. The spread and acquisition of NDM-1: a multifactorial problem. *Expert Rev Anti Infect Ther* 2014; **12**: 91–115.
- Khan AU, Maryam L, Zarrilli R. Structure, genetics and worldwide spread of New Delhi metallo- β -lactamase (NDM): a threat to public health. *BMC Microbiol* 2017; **17**: 101.
- Yong D, Toleman MA, Giske CG *et al.* Characterization of a new metallo- β -lactamase gene, bla_{NDM-1}, and a novel erythromycin esterase gene carried on a unique genetic structure in *Klebsiella pneumoniae* sequence type 14 from India. *Antimicrob Agents Chemother* 2009; **53**: 5046–54.
- Pérez-Vázquez M, Sola Campoy PJ, Ortega A *et al.* Emergence of NDM-producing *Klebsiella pneumoniae* and *Escherichia coli* in Spain: phylogeny, resistome, virulence and plasmids encoding bla_{NDM-1}-like genes as determined by WGS. *J Antimicrob Chemother* 2019; **74**: 3489–96.
- Solé M, Pitart C, Roca I *et al.* First description of an *Escherichia coli* strain producing NDM-1 carbapenemase in Spain. *Antimicrob Agents Chemother* 2011; **55**: 4402–4.
- EUCAST. EUCAST Guidelines for Detection of Resistance Mechanisms and Specific Resistances of Clinical and/or Epidemiological Importance. Version 2.0. 2017. <http://EUCAST.org>.
- EUCAST. Recommendations for MIC Determination of Colistin (Polymyxin E) as Recommended by the Joint CLSI-EUCAST Polymyxin Breakpoints Working Group. 2016. <http://EUCAST.org>.
- EUCAST. Breakpoint Tables for Interpretation of MICs and Zone Diameters. Version 10.0. 2020. <http://EUCAST.org>.
- Magiorakos AP, Srinivasan A, Carey RB *et al.* Multidrug-resistant, extensively drug-resistant and pandrug-resistant bacteria: an international expert proposal for interim standard definitions for acquired resistance. *Clin Microbiol Infect* 2012; **18**: 268–81.
- Pitart C, Solé M, Roca I *et al.* First outbreak of a plasmid-mediated carbapenem-hydrolyzing OXA-48 β -lactamase in *Klebsiella pneumoniae* in Spain. *Antimicrob Agents Chemother* 2011; **55**: 4398–401.
- Calbo E, Freixas N, Xercavins M *et al.* Foodborne nosocomial outbreak of SHV1 and CTX-M-15-producing *Klebsiella pneumoniae*: epidemiology and control. *Clin Infect Dis* 2011; **52**: 743–9.
- Taylor E, Sriskandan S, Woodford N *et al.* High prevalence of 16S rRNA methyltransferases among carbapenemase-producing Enterobacteriaceae in the UK and Ireland. *Int J Antimicrob Agents* 2018; **52**: 278–82.
- Durmaz R, Otlu B, Koksall F *et al.* The optimization of a rapid pulsed-field gel electrophoresis protocol for the typing of *Acinetobacter baumannii*, *Escherichia coli* and *Klebsiella* spp. *Jpn J Infect Dis* 2009; **62**: 372–7.
- Diancourt L, Passet V, Verhoef J *et al.* Multilocus sequence typing of *Klebsiella pneumoniae* nosocomial isolates. *J Clin Microbiol* 2005; **43**: 4178–82.
- Wirth T, Falush D, Lan R *et al.* Sex and virulence in *Escherichia coli*: an evolutionary perspective. *Mol Microbiol* 2006; **60**: 1136–51.
- Carattoli A, Bertini A, Villa L *et al.* Identification of plasmids by PCR-based replicon typing. *J Microbiol Methods* 2005; **63**: 219–28.
- Orlek A, Phan H, Sheppard AE *et al.* A curated dataset of complete Enterobacteriaceae plasmids compiled from the NCBI nucleotide database. *Data Brief* 2017; **12**: 423–6.
- Seemann T. Prokka: rapid prokaryotic genome annotation. *Bioinformatics* 2014; **30**: 2068–9.

- 21** Stothard P, Wishart DS. Circular genome visualization and exploration using CGView. *Bioinformatics* 2005; **21**: 537–9.
- 22** Wintersinger JA, Wasmuth JD. Kablammo: an interactive, web-based BLAST results visualizer. *Bioinformatics* 2015; **31**: 1305–6.
- 23** Nahid F, Zahra R, Sandegren L. A *bla*_{OXA-181}-harbouring multi-resistant ST147 *Klebsiella pneumoniae* isolate from Pakistan that represent an intermediate stage towards pan-drug resistance. *PLoS One* 2017; **12**: e0189438.
- 24** Ruiz J. Transferable mechanisms of quinolone resistance from 1998 onward. *Clin Microbiol Rev* 2019; **32**: e00007–19.
- 25** Seara N, Oteo J, Carrillo R et al. Interhospital spread of NDM-7-producing *Klebsiella pneumoniae* belonging to ST437 in Spain. *Int J Antimicrob Agents* 2015; **46**: 169–73.
- 26** Roca I, Mosqueda N, Altun B et al. Molecular characterization of NDM-1-producing *Acinetobacter pittii* isolated from Turkey in 2006. *J Antimicrob Chemother* 2014; **69**: 3437–8.
- 27** Manageiro V, Pinto M, Canica M. Complete sequence of a *bla*_{OXA-48}-harbouring IncI plasmid from an *Enterobacter cloacae* clinical isolate. *Genome Announc* 2015; **3**: e01076–15.
- 28** Carrër A, Poirel L, Eraksoy H et al. Spread of OXA-48-positive carbapenem-resistant *Klebsiella pneumoniae* isolates in Istanbul, Turkey. *Antimicrob Agents Chemother* 2008; **52**: 2950–4.
- 29** Espinal P, Mirò E, Segura C et al. First description of *bla*_{NDM-7} carried on an IncX4 plasmid in *Escherichia coli* ST679 isolated in Spain. *Microb Drug Resist* 2018; **24**: 113–9.
- 30** Fuster B, Tormo N, Salvador C et al. Detection of two simultaneous outbreaks of *Klebsiella pneumoniae* coproducing OXA-48 and NDM-1 carbapenemases in a tertiary-care hospital in Valencia, Spain. *New Microbes New Infect* 2020; **34**: 100660.
- 31** Gil-Romero Y, Sanz RN, Almagro MM et al. [New description of a NDM-1 carbapenemase producing *Klebsiella pneumoniae* carrier in Spain]. *Enferm Infecc Microbiol Clin* 2013; **31**: 418–9.
- 32** Oteo J, Domingo-García D, Fernández-Romero S et al. Abdominal abscess due to NDM-1-producing *Klebsiella pneumoniae* in Spain. *J Med Microbiol* 2012; **61**: 864–7.
- 33** Pitart C, Solé M, Roca I et al. Molecular characterization of *bla*_{NDM-5} carried in an IncFII plasmid in *Escherichia coli* from a non traveler patient in Spain. *Antimicrob Agents Chemother* 2015; **59**: 659–62.
- 34** Sampere A, García Martínez de Artola D, Alcoba Florez J et al. Emergence of carbapenem-resistant NDM-1-producing *Klebsiella pneumoniae* high-risk sequence type 147 in a tertiary care hospital in Tenerife, Spain. *J Glob Antimicrob Resist* 2019; **17**: 240–1.
- 35** Villa J, Carretero O, Viedma E et al. Emergence of NDM-7-producing multi-drug-resistant *Enterobacter hormaechei* sequence type ST-78 in Spain: a high-risk international clone. *Int J Antimicrob Agents* 2019; **53**: 533–4.
- 36** Esteban-Cantos A, Aracil B, Bautista V et al. The carbapenemase-producing *Klebsiella pneumoniae* population is distinct and more clonal than the carbapenem-susceptible population. *Antimicrob Agents Chemother* 2017; **61**: e02520–16.
- 37** Wyres KL, Lam MMC, Holt KE. Population genomics of *Klebsiella pneumoniae*. *Nat Rev Microbiol* 2020; **18**: 344–59.
- 38** Becker L, Kaase M, Pfeifer Y et al. Genome-based analysis of carbapenemase-producing *Klebsiella pneumoniae* isolates from German hospital patients, 2008–2014. *Antimicrob Resist Infect Control* 2018; **7**: 62.
- 39** Pérez-Moreno MO, Ortega A, Pérez-Vázquez M et al. Simultaneous colonisation by ST340 *Klebsiella pneumoniae* producing NDM-5 and ST399 *Escherichia coli* producing NDM-7. *Int J Antimicrob Agents* 2016; **48**: 464–6.
- 40** Mouftah SF, Pál T, Darwish D et al. Epidemic IncX3 plasmids spreading carbapenemase genes in the United Arab Emirates and worldwide. *Infect Drug Resist* 2019; **12**: 1729–42.

